MR-Muscle Spectroscopy and Spiroergometry:
Impact of Exercise-Induced Metabolic Changes in Single Muscle on Whole-Body Physiology – A Comparison of Global and Local Physiological Parameters

Dissertation

zur Erlangung des akademischen Grades

doctor philosophiae (Dr. phil.)

vorgelegt dem Rat der Fakultät für Sozial- und Verhaltenswissenschaften

der Friedrich-Schiller-Universität Jena

von Kevin Moll

geboren 10.01.1989 in Apolda

-2017-

1. Gutachter: Prof. Dr. phil. nat. habil. Reinhard Blickhan, Jena
2. Gutachter: Prof. Dr. rer. nat. med. habil. Jürgen R. Reichenbach, Jena
3. Gutachter: PD Dr. med. habil. Christoph Anders, Jena

Tag der mündlichen Prüfung: 22.01.2018

Danksagung

An dieser Stelle möchte ich all jenen danken, die mich auf dem langen Weg unterstützt und zum Gelingen dieser Dissertation beigetragen haben.

An aller erster Stelle zu nennen sind meine beiden Betreuer und Mentoren Prof. Reinhard Blickhan und Prof. Jürgen R. Reichenbach, die mir während meiner gesamten Promotionszeit immer mit fachlichem Rat und konstruktiven Denkanstößen zur Seite standen. Prof. Blickhan gab mir bereits während meines Studiums die Möglichkeit in die Forschung hinein zu schnuppern und die Mitarbeit an diversen Projekten bestärkte mich, diesen Weg auch nach dem Studium weiter zu gehen. Leider (und wie oft üblich in der Forschung) fehlten die finanziellen Mittel für eine Promotionsstelle in der Biomechanik. Dann bot mir Prof. Reichenbach eine Stelle in seiner Arbeitsgruppe Medical Physics Group an. Trotz einer komplett neuen Thematik und umfangreichen Einarbeitungszeit unterstützten mich beide Professoren und zweifelten nie am Gelingen dieses Projektes. Dieses Vertrauen weiß ich sehr zu schätzen.

Besonderer Dank gilt Dr. Alexander Gussew, welcher mich immer wieder mit Matlab Scripten und hilfreichen Gedanken versorgte und mir immer den Rücken frei hielt. Seine Unterstützung und motivierende Art trugen maßgeblich dazu bei, dass dieses Projekt erfolgreich umgesetzt werden konnte.

Weiterhin möchte ich Dipl. Sportwiss. Maria Nisser und Dr. Steffen Derlien vom Institut für Physiotherapie des UKJ danken, die sich sofort bereiterklärten mich bei meinen letzten beiden Studien, der Probandenakquise und der Laktatleistungsdiagnostik zu unterstützen. Vielen Dank für die interessanten und aufschlussreichen Gespräche und die Hilfe bei der Planung meiner Experimente.

Dr. Norman Stutzig von der Abteilung Sport- und Bewegungswissenschaft an der Universität Stuttgart, der mir die Stelle in der MedPhys empfohlen hat. Die Zusammenarbeit für die gemeinsame Publikation und weiterführenden Projekten erweiterten stets meinen Horizont im Bereich Muskeln, NMES und Physiologie.

Ebenso möchte ich der gesamten Arbeitsgruppe MedPhys danken. Für den regelmäßigen Gang zur Mensa pünktlich um 11:25 Uhr oder zum ‚cake @ 3 pm in the kitchen' und den lustigen Grillabenden vor dem Institut.

Hier möchte ich meine Büro- und Leidensgefährtin M.Sc. (bald Dr. rer. nat.) Marianne Cleve nennen, mit der ich viele freundschaftliche Momente beim Espresso oder im Büro teilen durfte. Danke

für deine Motivation und Aufmunterung, wenn diese nötig waren ebenso für deine stets offene Art und wissenschaftliche Akribie, für die ich dich sehr schätze.
Weiterhin ist Dr. Reinhard Rzanny zu erwähnen, welcher immer einen Rat bei akuten Problemen zum muskulären Stoffwechsel und ein entsprechendes Paper bereithielt.
Dr. Martin Krämer für eine tolle Zeit auf nationalen und internationalen Konferenzen.
Dr. Andreas Deistung mit dem ich allmorgendlich die ersten Worte im Büro neben dem Wasserkocher wechselte.
Dr. Daniel Güllmar für seine Art die Sachen ruhig anzugehen und die entspannten Gespräche beim Mittag.
Dr. Karl-Heinz Herrmann für sein umfangreiches Wissen im Bereich MRT, Technik, Espresso, Indien, Tauchen, Drohnen,….
Der größte Dank gilt meiner geliebten Frau Sandra. Dafür, dass du mich stets unterstützt und unsagbar großes Verständnis für die zeitintensive Bearbeitung dieser Dissertation aufgebracht hast. Ebenso danke ich meinen Eltern. Ihr habt stets an mich geglaubt und mich bei meinem Studium unterstützt, welches den Grundstein für diese Arbeit legte. Meiner ganzen Familie möchte ich danken für die schöne und dringend benötigte „promotionsfreie“ Zeit.

Ich weiß mein Glück zu schätzen.

Abstract

In training sciences whole-body properties like oxygen consumption, lactate concentration in the blood or the heart frequency are acquired relative to the performance level to evaluate the current fitness level of athletes, while considering the activated muscle proportion. For a better understanding of global physiological parameter changes, phosphorous magnetic resonance spectroscopy (^{31}P-MRS) can be used to quantify cellular and biochemical processes in resting and exercised muscles. To characterize muscular performance, thereby obtained local metabolic values can be compared and analyzed by typical parameters of conventional performance diagnostic approaches (spirometry and blood lactate diagnostic). The aim of this thesis was to exercise the muscle complex *m. triceps surae* by using a pedal ergometer, which enables a plantar flexion under MR conditions. Exercise-induced changes in the muscular metabolism were non-invasively acquired by means of ^{31}P-MRS. Simultaneously, ventilatory values and blood lactate concentrations were measured and correlated with the local spectroscopic findings.

The thesis is organized as follows: A brief introduction of the fundamentals of muscle physiology, metabolism and measurement methods and their extracted physiological parameters is followed by the first experiment of this thesis, which describes the reproducible load of the calf muscle by means of the MR-compatible pedal ergometer inside a magnetic resonance imaging system (Chapter 2). Angle- and force sensors allowed the acquisition of important mechanical parameters, which were presented to the volunteer as a visual feedback. Repeated measurements under different load intensities demonstrated a high reproducibility of this plantar flexion exercise and were supported by small variations of mechanical and metabolic changes. In the next step this setup was extended by an adapted commercially available spirometry unit, which allows the acquisition of the oxygen uptake and carbon dioxide exhalation simultaneous to spectroscopic measurements (Chapter 3). Thereby, first correlations between local and global metabolic adaptations were presented allowing the initial comparison of local pH changes and the overshoot in exhaled carbon dioxide, which both represent important markers of the anaerobic metabolism. However, since these measured values revealed a high physiological variation among the untrained subjects, sprinters and endurance athletes with well defined inclusion criteria were subsequently investigated in a comparative study under complete exhaustion of the calf muscle (Chapter 4). Besides obvious metabolic differences between the muscles *m. soleus* and *m. gastrocnemius medialis*, distinct strategies in dealing with this exercise were identified between both athlete groups. Endurance-trained athletes partially recover their muscular PCr stores even during exercise, whereas sprinters were able to tolerate a

significantly higher muscular acidification. This was mirrored in athlete-specific global adaptations like blood lactate concentrations or the production of non-metabolic CO_2.

As part of a side project, the effect of an alternative stimulation method on muscular fatigue of the *m. gastrocnemius medialis*, the so-called neuromuscular electrical stimulation (NMES), alongside with the characterization of different muscle fiber types with ^{31}P-MRS are presented in this thesis (Chapter 5). The results suggest that the observed split of the Pi peak into three different resonances during the load is a result of heterogeneous pH kinetics, which can be ascribed to the three different muscle fiber types, i.e., type I, type IIa and type IIx, respectively. Even though these conclusions should be verified in further independent experiments, this approach might be an elegant way to assess fiber type contributions in the muscle.

In summary, the findings of this thesis contribute to a better understanding of muscular load and its impact on whole-body physiology. Moreover, exercise-limiting factors were identified together with athlete-specific strategies to cope with exhaustive exercises. This non-invasive and specific diagnostic investigation offers great potential in designing, applying and assessing training interventions but also in performance assessment of young sport talents. Finally, the comprehensive collection of physiological data with the combined approach, which is presented in this thesis, allows adding advanced information to cybernetic models.

Zusammenfassung

Für die Leistungsdiagnostik in den Trainingswissenschaften werden Ganzkörpereigenschaften wie die Sauerstoffextraktion aus der Atemluft, die Laktatkonzentration im Blut oder die Herzfrequenz und deren Abhängigkeiten vom Leistungsniveau erfasst. Hierbei wird der Einfluss der Stoffwechselaktivität auf die Ganzkörperphysiologie maßgeblich durch den relativen Anteil des Einzelmuskels an der Gesamtmuskulatur mitbestimmt. Um Änderungen globaler physiologischer Größen erfassen und gegebenenfalls besser verstehen zu können, kann die Phosphormagnetresonanzspektroskopie (^{31}P-MRS) eingesetzt werden, welche nicht-invasiv Untersuchungen zellulärer und biochemischer Prozesse sowohl im ruhenden als auch im aktiven Muskel ermöglicht. Die daraus gewonnenen lokalen Stoffwechselparameter können anschließend mit den typischen Parametern konventioneller sportwissenschaftlicher Verfahren (Spiroergometrie und Laktatdiagnostik) zur Charakterisierung der muskulären Leistungsfähigkeit verglichen und analysiert werden. Im Rahmen dieser Dissertation sollte der Muskelkomplex *m. triceps surae* mithilfe eines MR-kompatiblen Pedalergometers durch eine Plantarflexion definiert belastet werden. Dabei sollten belastungs-induzierte Änderungen des muskulären Energiestoffwechsels mittels ^{31}P-MRS nichtinvasiv erfasst werden. Parallel dazu wurden Atemgasparameter und Blutlaktatwerte als globale Größen gemessen und zusammen mit den lokalen physiologischen Parametern analysiert, statistisch ausgewertet und korreliert.

Die vorgelegte Arbeit gliedert sich wie folgt: Nach einer kurzen Einführung zu den Grundlagen der Muskelphysiologie und des Metabolismus, den eingesetzten Messmethoden und den daraus extrahierten physiologischen Parameter folgt die Vorstellung des ersten Experiments zur reproduzierbaren Belastung mit Hilfe eines im Magnetresonanztomographen eingesetzten Pedalergometers (Chapter 2). Ein Winkel- und Kraftsensor ermöglichte die Erfassung wichtiger mechanischer Größen, welche dem Probanden mittels visuellen Feedbacks präsentiert werden konnten. Durch wiederholte Messungen unter verschiedenen Belastungsstärken wurde die hohe Reproduzierbarkeit des mechanischen Aufwands demonstriert und durch geringe Variationen metabolischer Parameter untermauert. Im nächsten methodischen Schritt wurde dieser experimentelle Aufbau durch eine kommerziell erhältliche Spirometrie Einheit erweitert, welche mittels verschiedener apparativer Anpassungen, Messungen der O_2 Aufnahme und CO_2 Abgabe simultan zur Durchführung der spektroskopischen Messungen ermöglichte (Chapter 3). Dabei konnten Korrelationen zwischen lokalen und globalen metabolischen Anpassungen aufgezeigt und erstmals Anpassungen des muskulären pH Wertes mit dem Überschuss an ausgeatmeten CO_2 als wichtige Parameter des

anaeroben Stoffwechsels verglichen werden. Da die Messwerte bei den untersuchten unspezifisch trainierten Probanden allerdings eine hohe physiologische Streuung aufwiesen, wurden nachfolgend in einer Vergleichsstudie mit definierten Einschlusskriterien Sprinter und Ausdauerathleten während einer vollständigen Ausbelastung der Wade untersucht (Chapter 4). Neben eindeutigen metabolischen Unterschieden zwischen den Muskeln *m. soleus* und *m. gastrocnemius medialis* konnten darüber hinaus verschiedene Strategien im Umgang mit dieser Art der Belastung zwischen den beiden Athletengruppen ermittelt werden. So waren Ausdauersportler in der Lage, selbst während der Belastung ihre muskulären Energiespeicher teilweise wieder aufzufüllen, wohingegen Sprinter eine hohe Toleranz gegenüber muskulärer Übersäuerung aufwiesen. Auch bei globalen Anpassungen wie der Blutlaktatkonzentration oder der Produktion von überschüssigem CO_2 waren die Unterschiede zwischen beiden Gruppen deutlich erkennbar.

Im Zuge eines Nebenprojektes wurden abschließend die Auswirkungen auf die Muskelermüdung des *m. gastrocnemius medialis* mittels einer alternativen Stimulationsmethode, der sogenannten neuromuskulären elektrischen Stimulation (NMES), sowie die Möglichkeit einer Differenzierung zwischen unterschiedlichen Muskelfasertypen mit Hilfe der ^{31}P-MRS untersucht (Chapter 5). Die Ergebnisse legen nahe, dass der beobachteten Aufspaltung des Pi Signales in drei verschiedene Resonanzen im MR Spektrum während der Belastung aufgrund der resultierenden pH-Heterogenität die drei unterschiedlichen Fasertypen Typ I, Typ IIa und Typ IIx zugeschrieben werden können. Auch wenn diese Schlussfolgerung in weiteren unabhängigen Untersuchungen sicher noch überprüft werden muss, scheint es über diesen methodischen Ansatz eine elegante Möglichkeit zu geben, Fasertypenverteilungen im Muskel beurteilen zu können.

Zusammenfassend tragen die Ergebnisse der vorgelegten Arbeit zu einem verbesserten allgemeinen Verständnis muskulärer Belastung und deren Einfluss auf die Gesamtkörperphysiologie bei. Insbesondere konnten darüber hinaus leistungslimitierende Faktoren benannt und sportartspezifische Strategien zur Vermeidung von Erschöpfung beobachtet werden. Dieses große Potential einer nicht-invasiven, spezifischen Diagnostik könnte in den Sportwissenschaften bei der Planung, Anwendung und Bewertung spezifischer Trainingsinterventionen sowie bei der Feststellung der sportlichen Eignung bei Talenten genutzt werden. Letztendlich erlaubt eine umfangreiche Erhebung physiologischer Parameter mit dem hier präsentierten kombinierten Ansatz die Unterstützung kybernetischer Modelle.

Contents

List of Abbreviations

1 RM	one repetition maximum
^{1}H-, ^{31}P-MRS	proton, phosphorous magnetic resonance spectroscopy
ADC	analog to digital converter
AMARES	Advanced Method for Accurate, Robust and Efficient Spectral fitting
ATP	adenosine triphosphate
ADP	adenosine diphosphate
CK	creatine kinase
Cr	creatine
Ca	calcium
DRESS	depth-resolved surface coil MRS
FID	free induction decay
GM	*m. gastrocnemius medialis*
GUI	graphical user interface
H^{+}	proton
IAT	individual anaerobic threshold
jMRUI	java-based MR user interface
Lac	lactate
LT	lactate threshold
maxLaSS	maximal lactate steady state
MCT	monocarboxylate transporter
MRS	magnetic resonance spectroscopy
MVC	maximum voluntary contraction
MUSCLE	MUlti SliCe Localized Excitation
NMR	nuclear magnetic resonance
NMES	neuromuscular electrical stimulation
OVS	outer volume suppression
Pi	inorganic phosphate
PCr	phosphocreatine
PDE	phosphodiester
PME	phosphomonoester
ppm	parts per million

RCP	respiratory compensation point
rf	radio frequency
SNR	signal-to-noise-ratio
SOL	*m. soleus*
τ	time constant
t_A	delay time
$t_{10–90}$	response time
TE	echo time
TR	repetition time
VE	ventilation
VCO_2	carbon dioxide output
VO_2	oxygen uptake
$VO_{2,\,max}$	maximum oxygen uptake
VOI	voxel of interest
VT	ventilatory threshold

1. General Introduction

The energy metabolism in humans is a complex interplay of energy producing and consuming processes, where switching between metabolic pathways occurs depending on exercise conditions and the physical status of the subject. The latter is directly affected by different training activities or inactivity and influences the structure and function of the motors of the human body – the muscles. Muscles are responsible for our ability to perform a broad range of physiological activities, such as posture, movement, agility, blood circulation, or control of internal organs. Depending on these activities, three main muscle types with different structural and metabolic features as well as specific neuronal control regimes can be distinguished. Skeletal muscles represent the majority of the human muscles and are under conscious control, whereas the myocardium and smooth muscle tissue work completely involuntarily to maintain blood circulation and the functionality of the inner organs.

Activated skeletal muscles are the biggest energy consumer of the body. To handle their variable energy demand, the human organism provides several pathways to produce the main energy metabolite adenosine triphosphate (ATP). Anaerobic splitting of a phosphate from phosphocreatine (PCr) is the fastest way to maintain ATP synthesis during initial muscular load. Depending on the intensity and duration of the load, anaerobic glycolysis and aerobic oxidation gradually take over the ATP production. Since the efficiency of these pathways directly affects the mechanical power output, implementation of appropriate methods for monitoring the energy metabolism has always been in the focus of exercise physiology research. Generally, the connection between muscular energy output and oxygen consumption is measured with spiroergometry and usually taken as a basis of actual training status evaluations and identification of exercise-limiting factors. On the other hand, understanding the local processes underlying the development of muscular fatigue is still controversially discussed due to the methodological challenges to measure metabolic events within exercised muscles appropriately. In this context, phosphorus magnetic resonance spectroscopy (^{31}P-MRS) offers a powerful tool, because it allows direct and non-invasive observation of local high-energy metabolic adjustments. Dynamic acquisition of muscle ^{31}P-MR spectroscopic data allows monitoring PCr and pH evolutions, thus opening a wide field to investigate metabolic processes affecting muscular fatigue or training outcome. Furthermore, combining ^{31}P-MRS and '*gold standard*' sport science methods (spirometry and blood lactate measurements) is highly attractive for obtaining deeper insight into connections between local and global metabolic adaptations that take place during muscle exercise.

Against this background, the main objective of this thesis was to examine metabolic processes in muscles under exercise conditions by combining global (spiroergometry and blood lactate

diagnostic) and local (MRS) measurements. Since calf muscles are largely involved in many sports activities and locomotion, the *m. triceps surae* was selected as the main target of interest. Furthermore, muscles of the lower leg are directly affected by training-induced changes and reveal important structural and metabolic information due to the heterogeneous muscle fiber compositions known to exist between athletes exercising different sports.

The following sections provide an overarching introductory frame for chapters 2 to 5, which are the formatted and adapted versions of published or under revision, peer-reviewed international papers.

1.1. Skeletal Muscles

While responding to different conditions, like posture or performing moderate or intense exercises, skeletal muscles are the main energy consumer. In order to meet these different demands, human muscles are typically composed of three muscle fiber types with characteristic metabolic domains as reflected by their ATP activity (Pette and Staron, 1990; Schiaffino and Reggiani, 2011). First, slow-twitch or type I fibers are, as their name implies, slow in contraction, i.e., the force production per unit time is relatively low, but highly resistant against fatigue. This capability is based on the high mitochondrial density in type I fibers, allowing aerobic energy supply with triglycerides as the major storage fuel. Therefore, these fibers are mainly involved in moderate exercises over long periods of time, such as during posture tasks. Second, the fast-twitch or type II fibers have faster contraction times with very high force output but reveal lower resistance against fatigue. Type II fibers are further subdivided into fast-twitch A (or type IIA) and fast-twitch B (or type IIB) muscle fibers. Type IIA fibers show intermediate resistance against fatigue and provide sufficient energy output under higher intensities due to a high mitochondria density. Representing a bridge between the extreme cases of type I and type IIB fibers, they can utilize either glucose or fatty acids, whereas type IIB fibers mainly rely on PCr and glycogen stores as their main energy sources. Type IIB fibers provide the highest and fastest force production among all muscle fiber types, but are prone to fatigue due to low mitochondrial density, which is associated with low oxidative but high glycolytic capacity. Consequently, they are also characterized by low capillary density leading to both limited oxygen supply and removal of fatigue-promoting products, like lactate and H^+. Therefore, type IIB fibers are mostly involved in short, highly intense activities, such as sprinting or jumping.

It is well known that muscle contains different fiber types, which, as a complex, define the overall characteristics of the whole muscle. For example, within the calf muscle (*m. triceps surae*), on

which this thesis focuses, one finds type I as well as type II fibers among the *m. soleus* (~80% type I fibers) and the *m. gastrocnemius medialis* (~50% type I fibers) (Edgerton, Smith and Simpson, 1975; Kemp, Meyerspeer and Moser, 2007). This heterogeneous fiber composition enables this muscle group to cope with a broad range of muscular tasks, including moderate activity like posture, continuous contractions during locomotion, and short and high-intensity activations as they occur during running, jumping or kicking. Thus, determining muscle fiber composition in athletes is still an important focus of previous and recent studies (Takahashi *et al.*, 1996; Herda *et al.*, 2010; Stutzig *et al.*, 2017), since recruitment of muscle fibers and their training-induced alterations might allow to select the appropriate discipline for young athletes or to identify weak spots to improve training interventions. This is also of great interest for research in the field of exercise physiology, because training-induced alterations of muscle fibers and their recruitment are responsible for the different metabolic adaptations among different athletes. The '*gold standard*' method to analyze muscle fiber composition is muscle biopsy (Edgerton, Smith and Simpson, 1975; Shanely *et al.*, 2014), which requires harvesting muscle tissue. However, biopsy interventions intrude muscular integrity while producing vascular injuries and scars, both of which often lead to training interruptions. Furthermore, even in the same muscle group, fiber compositions might vary locally and inter-individually as well as between sub-muscular sections as a consequence of aging or longstanding training (Juel *et al.*, 2004). Moreover, skeletal muscles are able to rearrange their phenotypes in response to specific activities via hypertrophy or atrophy of myofibrils (Steinacker *et al.*, 2002). It is known that as a result of exercise training, especially type IIB fibers tend to transform into more oxidative type IIA and type I fibers, whereas inactivity, training interruption or zero gravity promotes development of type IIB fibers alongside with muscular atrophy (Pette and Staron, 1997). The extent of a 'slow-to-fast' transition after strength- and speed strength-related training interventions is still controversially discussed, because sprint ability is assumed to be predetermined genetically. Recent studies, however, observed increased type IIA fiber fractions without hypertrophy after resistance training (Aagaard *et al.*, 2011) and a shift from type I to type IIA fibers after combined strength training with maximal contractions (Liu *et al.*, 2003). The cause of such fiber type transitions might be related to increased neuromuscular activity and firing rates by either slow or fast motor neurons due to endurance or sprint training, respectively (Gehlert *et al.*, 2012). This leads to a reduced number of recruited fibers, but increases contraction times of the activated fibers. Muscle fiber type transitions are also expressed in shifts of the energy metabolism (Pette and Staron, 1997), which affects either oxidative or glycolytic capacities by changes in enzyme activity. In this regard, despite providing a highly precise local characterization of muscle fiber composition, biopsies are unable to continuously monitor any short term temporal changes that may, for instance, occur as a result of fiber type transitions during training interventions. Therefore, non-invasive techniques with

similar precision, but without the previously mentioned disadvantages, are needed to establish adequate monitoring of training related adjustments of muscle fibers, muscle energy metabolism and load- and training-induced adaptations.

1.2. Energy Metabolism

The human body is a complex system, which continuously produces and utilizes energy. Even during rest or total immobility skeletal muscles are one of the main consumers of energy in form of ATP, which is hydrolyzed into less energized adenosine diphosphate (ADP) and inorganic phosphate (Pi) under the production of H^+:

$$\boldsymbol{ATP \rightarrow ADP + Pi + H^+} \tag{1-1}$$

ATP can be then used by the force-generating myosin ATPase, which catalyzes the decomposition of ATP to ADP under energy release. The amount of ATP, which is stored in small concentrations within cellular vesicles (Bonora *et al.*, 2012), is the origin to provide chemical energy for muscular contractions and ATP synthesis always equals ATP demand (Kemp, 2015). Since the initially available concentration of ATP in local stores is limited, muscular work consuming this reserve is only possible for a few seconds. Consequently, ATP has to be continuously re-synthesized during the subsequent contractions. In general, there are two ways to produce ATP in muscle cells:

- *Anaerobic glycolysis*, which is the transformation of glycogen into lactate by reduction of pyruvate. This pathway provides fast and sustaining ATP production without oxygen supply and allows muscle cells to respond to immediate, high-intense exercises. Metabolization of glycogen and glucose, however, is accompanied by accumulation of lactate and protons (H^+) as reflected in the continuous pH level decline in exercised muscles. Together with other processes, such as increase in inorganic phosphate (Pi) concentration and cellular water influx, muscle acidification represents one of the most crucial exercise-limiting factor (Fitts, 1994; Keyser, 2010).
- With *aerobic glycolysis*, ATP is produced via oxidation of glucose and fatty acids. Despite being stoichiometrically more efficient compared to the anaerobic pathway, oxidative glycolysis lags behind during the initial load phase (up to 1-2 minutes) due to the delayed oxygen supply from blood (Gastin, 2001). However, once being activated, oxidative

glycolysis is able to maintain ATP synthesis for several hours since it is not associated with accumulation of lactate.

Since ATP demand can rise very quickly, while the onsets of anaerobic and aerobic ATP production take several seconds and minutes, respectively, ATP is re-synthesized by phosphorylation of intra-cellular PCr and ADP via the creatine kinase (CK) reaction to bridge these delays and to avoid crucial ATP depletion during the initial load phase by the PCr breakdown

$$\boldsymbol{PCr + H^+ \rightarrow Cr + Pi} \qquad (1\text{-}2),$$

which results in an apparent splitting of PCr with accompanying creatine (Cr) delivery and H^+ consumption, which tends to lower the cellular pH. The CK reaction catalyzes the following reaction:

$$\boldsymbol{ADP + PCr + H^+ \leftrightarrow ATP + Cr} \qquad (1\text{-}3)$$

Since the CK in skeletal muscles provides equilibrium in ATP a temporary mismatch between energy demand and supply can be met by PCr breakdown (see Equ. 1-2 and 1-3). The CK-driven ATP production is indicated by a significant decrease of intra-muscular PCr concentrations as well as distinct pH increases following exercise onset (Kemp, 2015). Although having different time regimes, none of the mentioned energy-metabolism pathways precede exclusively or independently from one another, but rather blend into each other with varying degrees in order to warrant constant ATP supply during the entire time course of muscle activity (Figure 1-1). Thus, all physical activities draw energy from all energy pathways. However, based on the physical condition the contribution of each pathway differs among subjects. Influencing factors, which lead to an overall lower energy demand in endurance athletes compared to sprinters during all-out experiments, are higher vascularity and mitochondrial density. Consequently, long-distance athletes are able to utilize oxygen more efficiently. The ability to quantify such metabolic processes under controlled exercise conditions provides deep insight into energy supply, differentiation between aerobic and anaerobic energy pathways, determination of limitations regarding fatigue as well as identification of exercise-induced adaptations. This knowledge is widely used by applying distinct approaches in the field of physiology, sports science and sports medicine therapy.

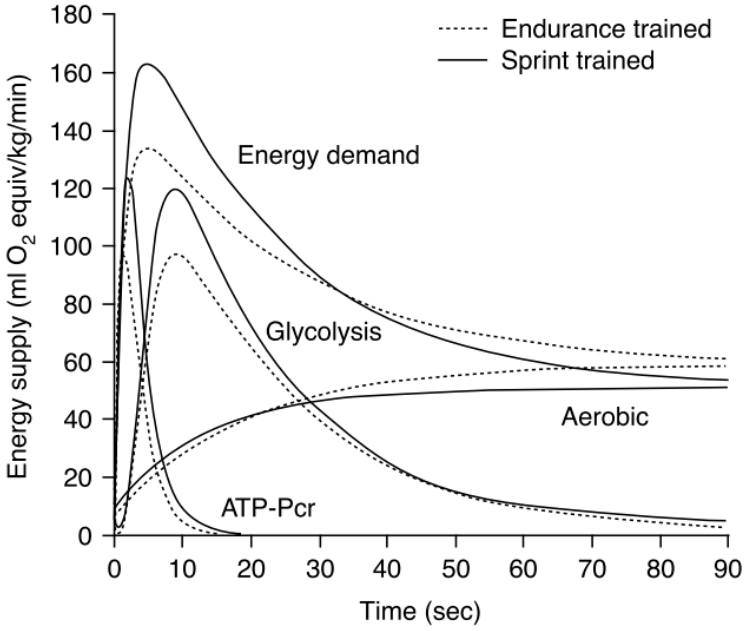

Figure 1-1 Contributions of the three main energy supply pathways to meet the total energy demand during an all-out 90 s cycle exercise (figure taken from Gastin 2001). This energy balance was determined from two differently trained groups (six male sprint-trained cyclist and eight triathletes) and is given as oxygen equivalents derived from spirometry measurements.

1.3. Quantification of energy adjustments

1.3.1. Sport Science '*Gold Standard*' methods

Respiratory gas exchange measurements, blood lactate diagnostics and neuromuscular electrical stimulation (NMES) are commonly applied in sport and exercise science as well as sports medicine to determine the multifactorial, performance limiting parameters and to assess neuronal and muscular function. Such measurements are typically conducted under standardized laboratory conditions with appropriate exercise protocols and by using ergometers (e.g. cycle-, treadmill-, rower-, hand crank- or canoe-ergometer), which mimic sport discipline-specific muscular involvements and load regimes. Usually, exercise protocols with continuously rising or incrementally increasing work rates are used to gather mechanical parameters as well as respiratory and blood lactate adjustments under maximal effort conditions or within defined load regimes. Step-wise protocols have the advantage that they allow investigation of target parameters under varying conditions and observation of possible leveling of metabolic kinetics. On the other hand, ramp protocols allow detection of thresholds and peak values in a 10-15 min exercise test (Whipp *et al.*, 1981; Burnley, Doust and Vanhatalo, 2006). Simultaneously acquired profiles of lactate and oxygen consumption

(VO_2) enable prediction of exhaustion and assessment of the performance level while determining the metabolic regime, in which the subject currently exercises.

Despite being more suited to assess muscle performance under typical sports-related conditions with appropriate ergometers, the determined performance can be subjectively affected by the volunteer's daily condition or motivation. This can introduce significant intra-individual variations in the measured parameters and complicates metabolic characterization. A more standardized activation of muscle motor units can be achieved by NMES, which provokes muscular contractions by transducing series of electric impulses to the skin surface or directly to the muscles (Maffiuletti *et al.*, 2011). With this selective activation technique it is possible to objectively assess muscular function *in vivo* independent from other muscles groups. However, to specify the spatial recruitment with NMES the investigator needs to know the specific motor points in each muscle compartment on which the electrodes have to be placed to avoid inconsistent stimulation outcomes (Gobbo *et al.*, 2014). Besides reducing or even excluding motivation bias on muscle performance, NMES also offers the advantage to achieve very fast exhaustion of the motor units due to the significantly higher stimulation frequencies compared to voluntary contraction. Furthermore, to induce comparable muscle activation among subjects, the electrical pulse frequency has to be adapted individually in order to take into account the physiologically varying skin and subcutaneous fat thicknesses as well as to consider differing training states and habituation to NMES. Another important aspect of electrical stimulation is the different activation pattern compared to voluntary contraction. Whereas physiological recruitment of motor units depends on the 'size principle', first described by Henneman *et al.* (Henneman, Somjen and Carpenter, 1965; Maffiuletti, 2010), electrical stimulation activates both fast and slow motor units even at lower intensity levels. This so called 'disordered' recruitment principle is one of the unique aspects of NMES enabling effective activation of all muscle fiber types. At the same time, it leads to accelerated fatigue of the entire muscle (Maffiuletti, 2010; Maffiuletti *et al.*, 2011). One major limitation of NMES is that it addresses only superficial muscles fibers (Maffiuletti, 2010). By exploiting these features (spatial selectivity and all-in recruitment), NMES offers a broad range of applications covering, e.g., strength training (Seyri and Maffiuletti, 2011), rehabilitation (Feil *et al.*, 2011) or post-exercise recovery (Babault *et al.*, 2011). In this thesis, NMES was applied to suppress metabolic influences of adjacent muscles, which occur with voluntary contractions, while examining the energy metabolism in a single muscle.

Spiroergometry

The spiroergometry technique enables breath-by-breath measurements of oxygen uptake (VO_2), carbon dioxide exhalation (VCO_2), respiratory frequency and ventilation (VE) by using rapidly

responding gas analyzers, such as electrochemical cells, ultrasound or flow sensors (Roecker, Prettin and Sorichter, 2005). Typically, spirometry is performed alongside with the monitoring of ergometer parameters (e.g., power output during treadmill or speed during cycling, load duration and possible step length during a step-wise protocol) and acquisition of cardiovascular data by an ECG system to assign exercise-induced respiratory adjustments to the mechanical muscle work and heart function. This allows to characterize sports-related fitness levels in athletes or to assess cardiological and pneumatological impairments in patients with altered aerobic function. To this end, several physiological parameters, like maximum oxygen uptake ($VO_{2,max}$), higher O_2 requirements during load or specific thresholds in the O_2 profile, are quantified as markers of the aerobic function in subjects (Rossiter, Ward, Howe, *et al.*, 2002; Jones *et al.*, 2010). The efficiency to maintain muscular work defined by these parameters depends on the individual training state, muscle fiber composition and local perfusion properties (Whipp *et al.*, 1981). Prior knowledge of critical thresholds that occur during the exercise may then help to characterize the intensity domains, in which the subjects are currently exercising in (Whipp and Rossiter, 2005). For example, an exponentially increasing VO_2 with subsequent steady state plateau indicates an energy supply that is dominated by the aerobic pathway and represents a typical respiratory response to moderate load intensities (Whipp and Rossiter, 2005). In contrast, heavy or extreme exercises are indicated by a more complex VO_2 kinetics showing an additional VO_2 increase. This so-called VO_2 *slow component* occurs after a substantial delay of up to 15 min into the exercise and is typically synchronized with elevating blood lactate concentrations reflecting the sustained metabolic acidosis. Exercises at a severe intensity level are usually sustained transiently, since lactate and H^+ increase persistently in the muscle tissue. Depending on the exercise intensity, the individual fatigability and the subject's endurance, VO_2 increases steadily towards $VO_{2,max}$. The latter denotes an important marker in high-performance sport, since it directly reflects oxygen utilization at a state near to exhaustion. The efficiency of oxygen utilization increases with endurance training (Scharhag-Rosenberger *et al.*, 2009). For the $VO_{2,max}$ evaluation, it is of minor significance whether a ramp or step-wise protocol is used (Midgley *et al.*, 2008), but with a sport-specific exercise it is possible to obtain information about the current aerobic performance level. Therefore, specific pulmonary thresholds are usually determined from dynamically sampled respiratory and blood lactate data in order to differentiate between whole-body metabolic states (Wasserman and McIlroy, 1964; Green *et al.*, 1983; Beaver, Wasserman and Whipp, 1985; Hollmann, 2001; Dekerle *et al.*, 2003; Westhoff *et al.*, 2013). Respiratory thresholds are detectable by distinctive changes in the VO_2 and VCO_2 slopes. The first threshold is either termed *VT1* (Westhoff *et al.*, 2013), *ventilatory anaerobic threshold* (Green *et al.*, 1983), *anaerobic threshold* (Wasserman and McIlroy, 1964) or the *point of optimum ventilatory efficiency* (Hollmann, 2001) and implies an increase of VCO_2 in relation to VO_2 due to the initial rise of blood

lactate concentration. This threshold indicates the transition from aerobic to anaerobic energy supply. The second threshold, denoted either as *VT2* (Westhoff *et al.*, 2013) or *respiratory compensation point RCP* (Dekerle *et al.*, 2003) is characterized by an excessive increase in ventilation and VCO_2 exhalation corresponding to the equilibrium between accumulation and elimination of lactate (lactate steady-state). This threshold defines the compensation of lactate increase by the ventilatory system to cope with the metabolic acidosis in order to respond to the non-metabolically accumulated CO_2 (Dekerle *et al.*, 2003). This so-called *excess CO_2* corresponds to the quantity of H^+ bound by bicarbonate and is used to define ventilatory thresholds (Roecker *et al.*, 2000). By considering the stoichiometric proportionality between the accumulating H^+ and lactate, the amount of spirometrically determined *excess CO_2* is assumed to be suited for a rough estimation of the anaerobic energy turnover fraction and represents an additional criterion of maximum exhaustion (Beaver, Wasserman and Whipp, 1985, 1986). However, whereas lactate is constantly increasing above VT2, VCO_2 is more volatile and might be additionally affected by individual influences, like hyperventilation or inter-breath fluctuations (Lamarra *et al.*, 1987). Thus, adequate characterization of anaerobic turnover relies on an additional and more direct analysis of the blood lactate time course. One crucial aspect that limits the assessment of muscle metabolism from spirometry data is the fact that global parameter evolutions represent delayed responses of local metabolic adjustments, which are additionally affected by other muscles and inner-organs (Edgerton, Smith and Simpson, 1975; Bangsbo *et al.*, 2000). As an alternatively to 'simple' visual inspections, a more reliable identification of the mentioned thresholds and better dynamic characterization can be achieved by fitting the *raw* respiratory data with appropriate mathematical models. For example, mono- or multi-exponential models have been used to parametrize exercise-induced VO_2 elevations (Barstow *et al.*, 1994; Ozyener *et al.*, 2001; Rossiter, Ward, Kowalchuk *et al.*, 2002).

The accuracy of parameter estimations crucially depends on the quality of the acquired respiration data as they might be contaminated by fluctuations due to, e.g., swallowing, coughing, yawning or unnecessary fast and deep breaths (Lamarra *et al.*, 1987). The effects of such errant breaths have great influence during the early transient of an exercise or during recovery as they can corrupt the ensuing interpretation of pulmonary results since each data point represents the amount of pulmonary change. Therefore, acquisition of spirometry data should be accompanied by precise briefing of the subjects, including a sufficiently long phase to familiarize the volunteers with the non-physiological breathing patterns due to the respiratory mask (Moll *et al.*, 2017).

In summary, spiroergometry is the method of choice for analyzing sport-related efficiency and whole-body metabolism in athletes and patients. The extracted parameters allow good assessment of the aerobic function to organize and adapt training or therapeutic interventions. However, since spiroergometry focusses on the global adjustments important information on the muscular level is

missed. Consequently, combination with other established methods to investigate energy metabolism should be considered to increase the diagnostic power.

Blood lactate diagnostics

Measuring blood lactate concentrations during an incremental exercise in hyperemic capillary blood is considered to be the most important and reliable method to determine exercise intensity (Kindermann, Schramm and Keul, 1980) and to assess endurance associated metabolic processes in athletes (Juel *et al.*, 2004; Faude, Kindermann and Meyer, 2009). Small blood samples are typically extracted during rest, load (usually at the end of each 50 W step or every 3 min on the bicycle ergometer) and recovery (up to three times) from the ear lobe or the fingertip. Thereby, spiroergometry combined with lactate diagnostics are the top-ranking tools with specialized applications in clinical and sport-related performance diagnostics. So far, both are unsurpassed since they complete the interpretation of estimated threshold concepts by sufficient characterization of the underlying metabolic events. Similar to the analysis of spirometry data, blood lactate time courses are typically parametrized in terms of characteristic thresholds, which indicate the pathway transitions between aerobic and anaerobic energy supply (Westhoff *et al.*, 2013). The first threshold, denoted as *LT1* (Westhoff *et al.*, 2013) or *LT* (Beaver, Wasserman and Whipp, 1985) corresponds to a load intensity with an initial lactate increase, whereas Kindermann *et al.* referred this threshold to a fixed point at 2 mmol/l lactate concentration (Kindermann, Simon and Keul, 1979). The second threshold, termed *LT2* (Westhoff *et al.*, 2013), *individual anaerobic threshold (IAT)* or *maximal lactate steady state maxLaSS* (Wahl, Bloch and Mester, 2009), has in some cases been referred to a fixed point of 4 mmol/l lactate concentration (Mader *et al.*, 1976) However, *lactate-steady-state* (*maxLass* or *MLSS*) corresponds to load intensities (in km/h on the treadmill or watts on the bicycle ergometer) at the equilibrium between lactate accumulation and depletion and varies among subjects depending on their ability to effectively metabolize lactate (Westhoff *et al.*, 2013). The higher the lactate-steady-state, the better is the athletes' endurance capacity (Roecker *et al.*, 1998). In the process of long-term training the typical lactate-performance curves, which are acquired during an incremental exercise on an ergometer, show a *right shift*. Highly-trained endurance athletes thus achieve distinctly higher maximum performance levels over a longer period as a consequence of improved oxygen supply, increased oxygen transport capacity of the blood and more effective aerobic metabolism together with a lower lactate production rate (Heck and Schulz, 2002; Rivera-Brown and Frontera, 2012).

As described before, lactate accumulates as an intermediate of pyruvate reduction during anaerobic glycolysis (see Chapter 1.2). In order to prevent cellular acidification, lactate is actively

transported via the fiber type-specific membrane transmitter monocarboxylate transporter (MCT) (Juel, 1997, 2004) and metabolized in adjacent or remote tissues, including the heart and other skeletal muscles (Van Hall, 2010). Type I fibers are known to metabolize lactate up to four times faster than type II fibers, making them more resistant against acidification (Juel, 1997). However, as a consequence of this active metabolization and peripheral distribution of lactate the measured blood lactate concentrations are distinctly lower than in the active muscles and reveal significant delays in their time courses. Thus, the peak lactate value is typically not observed at the end of exercise, but only a few minutes into the post-load period (Stegmann, Kindermann and Schnabel, 1981).

Even though blood lactate diagnostics provides good insight into the overall whole-body performance, blood flow-induced dilution, metabolization in surrounding tissues and spatially differing locations of lactate origin and lactate concentration measurements prevent accurate assessment of this important anaerobic parameter. Moreover, peripheral lactate measurements do not allow muscle-specific considerations regarding the contribution to the lactate production of a single muscle to the finally measured value. Therefore, an approach enabling to determine lactate or the accompanying grade of acidification in the muscle would be beneficial for better understanding the role of lactate as an exercise-limiting factor and metabolic surrogate marker.

1.3.2. NMR Spectroscopy

Obtaining insight into the local energy metabolic processes in muscles remains one of the most exciting challenges in current muscle physiology research. Usually this requires invasive approaches, like muscle biopsies (Shanely *et al.*, 2014), blood lactate diagnostics (Van Hall, 2010) or isotope labeling (Rennie, 1999). Histologic characterizations of muscle tissue rely on the extraction of muscle samples, which were immediately frozen in liquid nitrogen and stored at -80°C. Analytical techniques for detecting specific proteins allow to measure muscle membrane proteins and fiber determination. After freeze-drying the probe can be used for pH and lactate determination (Juel *et al.*, 2004). For blood lactate diagnostics small blood samples taken from the hyperemic earlobe or fingertip were examined with a photometric method after being hemolyzed to determine the lactate concentration (Weippert *et al.*, 2008). Isotopic labelling techniques are ideal to describe the characteristics of metabolic rates and changes through a reaction or metabolic pathway. Therefore, the reactant is labeled by replacing specific atoms by their isotope, which is then allowed to undergo the reaction. While measuring the position of the isotope a determination of the metabolic sequence in the metabolic pathway, which was followed by the isotope, is possible (Rennie, 1999). All these methods, however, focusing on the investigation of aging effect, diseases or exercise

physiology-related metabolic adjustments, are challenging and bear residual risks. In contrast, magnetic resonance spectroscopy (MRS) is a much more favorable technique for metabolic studies, since it allows quantitative and simultaneous monitoring of different metabolic processes non-invasively without any radiation exposure (Boesch, 2007; Kemp, Meyerspeer and Moser, 2007; Kemp, 2015; Kemp *et al.*, 2015; Valkovič, Chmelík and Krššák, 2017).

Similar to MR imaging, MRS relies on the nuclear magnetic resonance (NMR) phenomenon, which is described in detail in the work of de Graaf (de Graaf, 2007). Nuclear magnetic resonance comprises the interaction between atomic nuclei in a strong static magnetic field and alternating radiofrequency (RF) (electro-)magnetic fields (B_1), whose radiofrequency (ω_{RF}) matches the so-called precession or *Larmor* frequency (ω_0) of the selected nuclei. This resonance frequency ω_0 depends directly on the nucleus type as well as on the strength of the static magnetic field (B_0) of the MR scanner. An appropriate RF pulse-mediated energy transduction to the nuclei containing magnetized sample generates non-equilibrium macroscopic magnetization, which rotates with the frequency ω_0 in the plane orthogonal to the axis of the static magnetic field. This rotating magnetization induces an electric current in the receiver coil, which is located close to the sample. The number of nuclei contributing to the macroscopic magnetization can be determined from the signal amplitude revealing the nuclei concentration within the sample. In addition, the type of the nuclei can be identified by the frequency of the measured signal. Another important feature of the detected time signal is its exponential decay (FID: free induction decay), which starts immediately after the RF excitation and depends on the spatial B_0 inhomogeneity within the sample. The corresponding frequency spectrum of such an FID, which can be calculated by applying the Fourier Transform, comprises (in the simplest case) a Lorentzian shaped peak at the frequency ω_0. The peak intensity and the peak linewidth (spectral width at half height of the peak maximum) are proportional to the time signal amplitude and to the inverse value of the FID decay time constant, respectively. Besides being proportional to the B_0 field strength, the *Larmor* frequency of the same nuclei type (e.g., protons) can slightly vary due to magnetic shielding effects at the site of the nuclei, which is mediated by the surrounding electrons. Since electron constellations are intrinsically determined by the bonds in molecules, the shielding strength depends on the nuclei arrangement in a molecule (Haacke *et al.*, 1999). This so-called chemical shift of resonance frequencies allows the distinction between nuclei in different molecules and thus enables to identify different metabolites by their characteristic peaks or peak multiplets in a spectrum (Figure 1-2). For practical reasons, the chemical shift is introduced as the difference ($\Delta\omega$ in Hz) between the Larmor frequency of a nucleus in the molecular site of interest and the Larmor frequency of the same isotope in a reference substance (e.g., TMS), normalized by the latter frequency (ω_{ref}) and is given in relative units (*part per million*, ppm):

$$\boldsymbol{\delta\,[ppm] = 10^6 \cdot \frac{\Delta\omega}{\omega_{ref}}} \qquad (1\text{-}4)$$

Although being less relevant for *in vitro* NMR measurements of homogeneous samples, the attribution of the acquired MR spectra to specific tissues or tissue regions (localization) becomes one of the most crucial steps for *in vivo* experiments. Such spatial localizations can be realized by using surface transmitter/receiver coils, whose RF penetration and signal transmit sensitivity profiles depend on the coil radius. More advanced and more accurate localization methods rely on applying transient linear magnetic field gradients in addition to the permanent B_0 field, which induce a spatially linear resonance frequency dispersion within the sample. Applying these field gradients simultaneously with frequency selective RF pulses, nuclei within a tissue slice can be selectively excited. For a fixed spectral bandwidth of the RF pulse, the slice position and thickness are defined by the center frequency of the RF pulse and the gradient magnitude, respectively. The final step in MRS is then the quantitation of metabolites from the spectra. Although spectral peak intensities depend on the metabolite concentrations, they are also affected by numerous technical factors, such as, e.g., spatial homogeneity of the RF excitation or coil sensitivities. In order to compensate for these influences, the quantified peak intensities are typically normalized by the intensity of a reference metabolite, which has to be measured under identical conditions and whose concentration is assumed to be constant or ideally known. For example, for *in vivo* muscle ^{31}P-MR spectra, the peak intensities are normalized by the intensity of ATP, which is assumed to remain constant in the resting state and during load (Kemp, Meyerspeer and Moser, 2007). A typical ^{31}P-MR spectrum of a muscle at rest is displayed in Figure 1-2 and contains, aside from the singlets of PCr (0 ppm) and Pi (5.02 ppm), three multiplets of ATP (γ-ATP doublet at –2.48 ppm, α-ATP doublet at –7.52 ppm and β-ATP triplet at –16.26 ppm).

The chemical shift of the Pi resonance (relative to the PCr resonance) enables to extract the intra-cellular pH value, because the former is determined by the equilibrium concentration ratio between both dissociation forms of phosphoric acid ($H_2PO_4^-$ and HPO_4^{2-}) (Heerschap *et al.*, 1999):

$$\boldsymbol{pH = pK_A + log\frac{(\delta_{HA}-\delta)}{(\delta-\delta_A)}} \qquad (1\text{-}5)$$

where $pK_A = 6.75$ is the dissociation constant of Pi, $\delta_{HA} = 3.27$ is the chemical shift of the protonated and $\delta_A = 5.63$ is the chemical shift of the non-protonated form of Pi, respectively.

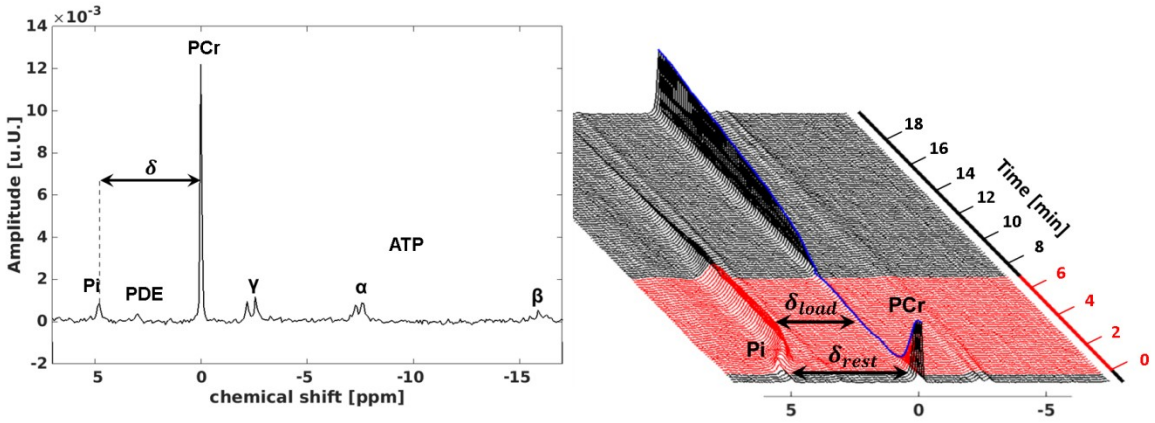

Figure 1-2 ^{31}P-MR spectrum of a human calf muscle acquired at 3 T under resting state conditions showing peaks of PCr, Pi, ATP and phosphodiester (PDE). The α-, β- and γ-ATP peaks correspond to the three phosphoryl groups of the ATP molecule and show different chemical shifts due to the specific magnetic shielding of the ^{31}P nuclei. The frequency difference (δ) between the Pi and PCr peaks is determined by the equilibrium ratio between $\mathbf{H_2PO_4^-}$ and $\mathbf{HPO_4^{2-}}$ and provides the possibility to quantitate the intra-cellular pH value (see Equ. 1-5). *Right*: 'Stack plot' of ^{31}P-MR spectra from the same calf muscle. The red spectra were acquired during an intense exercise showing depleted PCr and increasing Pi intensities as well as distinct Pi frequency shifts (δ_{rest} and δ_{load}), indicating time-variant reductions in intracellular pH.

Acquiring a series of ^{31}P-MR spectra prior to, during and after muscle load allows then to monitor metabolic processes, such as exercise-induced PCr depletion or PCr recovery during the post-load phase. The initial PCr depletion directly reflects the ATP synthesis rate and immediate ATP demand for that exercise (Kemp, 2015). Moreover, the post-exercise PCr re-synthesis is a function of mitochondrial ATP production, where the rate constant of PCr recovery is proportional to muscle mitochondrial oxidative capacity (Prompers *et al.*, 2014) and provides indirect information about the muscle's composition of glycolytic and oxidative muscle fibers (Vandenborne *et al.*, 1993; Gwenael Layec *et al.*, 2013; Stutzig *et al.*, 2017). Even though the muscle fiber contribution is mostly unknown, these spectroscopy-based data may nevertheless unravel typical working domains of type I and type II fibers and thus enable at least indirectly muscle fiber characterization. Monitoring pH allows assessment of H^+ accumulation, which is associated with lactate production during anaerobic glycolysis and provides information about processes directly affecting muscle fatigue (Juel, 1997; Allen, Lamb and Westerblad, 2008; Keyser, 2010). More detailed descriptions of the underlying physiologic processes that can be examined by means of ^{31}P-MRS *in vivo* are given elsewhere

(Kemp, Meyerspeer and Moser, 2007; Kemp, 2015; Kemp *et al.*, 2015; Valkovič, Chmelík and Krššák, 2017).

In contrast to ^{31}P-MRS, proton MR-spectroscopy (^{1}H-MRS) is better suited to monitor the intramyocellular lipid infiltration (Boesch *et al.*, 1997), but is less frequently used to investigate energy metabolism of muscles. Nevertheless, ^{1}H-MRS has been previously applied to measure directly exercise-induced lactate alterations in order to characterize the anaerobic energy turnover (Hsu and Dawson, 2000; Gladden, 2004; Ren, Sherry and Malloy, 2013). However, due to the overlap of the lactate resonances with the strong lipid peaks in ^{1}H-MR spectra, their detection remains challenging and typically requires additional suppression of the interfering signals by using advanced spectral editing techniques (Kmiecik *et al.*, 1997; Meyerspeer *et al.*, 2007).

All in all, ^{31}P-MRS is a powerful tool to examine exercise-induced adjustments of muscular energy metabolism and offers a wide range of applications in physiology, exercise science, sports medicine and muscle pathology research areas. Moreover, in combination with the previously described global analytic approaches of spiroergometry or blood lactate diagnostics, it is predestined to expand the current knowledge about regulation of local energy turnover and muscle function, including oxygen supply, perfusion or intermediate recycling, all of which are modulated by sport-specific training interventions. Therefore, ^{31}P-MRS has great potential for a comprehensive determination of muscle physiology on a molecular level, especially in combination with other techniques for metabolic measurements.

1.3.3. Combined acquisition of metabolic parameters

As described in the previous sections the different methods, which were applied in this thesis, are highly specific approaches to collect various information about energy metabolism under different aspects. In order to provide an overview, Figure 1-3 schematically illustrates the basic energy supply mechanisms in muscle together with the available measurement techniques for monitoring the underlying metabolic processes. Isolated application of a particular technique severely limits adequate characterization of the multiple, global and local processes and their consequences on muscle function or endurance. Although spiroergometry and blood lactate diagnostics provide comprehensive insight into whole-body metabolic adjustments during an exercise, they only reflect diluted and temporally delayed conditions of the loaded muscles, making characterization of local metabolic turnover difficult. On the other hand, dynamic ^{31}P-MRS allows the examination of local metabolic processes in single muscles, but does not provide information about the whole-body concomitants, which predefine or at least affect muscular performance based on the underlying muscular structure and fiber configuration.

These respective limitations of complementary state-of-the-art techniques make their combination highly attractive in order to achieve a more accurate approximation of the many factors determining fatigue physiology. The practical implementation, however, comes along with crucial methodological challenges, including, e.g., the need to adapt the spirometric system to allow performing viable measurements inside an MR scanner or to realize muscle exercises within the MR-scanner via an suitable ergometer to mimic physiological exercise situations under different load intensities. Reproducible activation of specific muscle groups should avoid involvement of other muscle groups whose energy demand might affect global measurements. Finally, such an implementation also requires proper communication between the different modalities (MR scanner, ergometer, spiroergometry system etc.) in order to ensure correct temporal assignments of the acquired data-time-courses.

Fusion of local and peripheral information has already been the focus of current and recent research (Hunter and Borg, 2003; Hunter *et al.*, 2010; Edwards *et al.*, 2013). Since the human body is a complex system, which always reacts to the weakest unit, athletes pursuing the goal to obtain optimum performance during a competition should focus their training on these parts. Consequently, improving our knowledge of exercise-induced metabolism in a single muscle as the smallest unit of muscle fibers to generate force and movement, and the impact of fatigue and training interventions on the local muscular level, should be highly valuable. Having available a combined setup including spirometry, blood lactate diagnostics and MRS should enable differentiation between energy providing systems during a well-defined load regime. Such a comprehensive approach

certainly benefits the understanding about the dependency of global metabolic changes on local muscular demands, which in turn may help to identify multi-parametric exercise-limiting processes, fatigue and training-induced adaptation processes.

Combined approaches have been also used to monitor associations between load induced VO_2 adaptations and metabolic changes derived from dynamic ^{31}P-MRS (Barstow *et al.*, 1994; Grassi *et al.*, 1996; McCreary *et al.*, 1996; Whipp *et al.*, 1999; Rossiter *et al.*, 1999, 2000; Rossiter, Ward, Kowalchuk, 2002; Layec *et al.*, 2012; Cannon *et al.*, 2013, 2014). These studies reported positive correlations between post-load PCr recovery rates and VO_2 slopes confirming the assumption of aerobically driven PCr re-synthesis. In addition, Rossiter and colleagues were able to directly link VO_2 and PCr changes during load and recovery by simultaneous spiroergometry and ^{31}P-MRS measurements, taking into account the muscle-to-lung transit VO_2 time delay (Rossiter, Ward, Howe, 2002; Rossiter, Ward, Kowalchuk, 2002). They demonstrated that PCr kinetics reveal the most consistent correlation to pulmonary VO_2 supporting the assumption that VO_2 kinetics are determined by intramuscular mechanisms. However, most of the referenced studies were based on repeated measurements with MRS performed inside and spirometry outside the MR scanner. Thus, comparability of local and global findings relies on the assumption that the physiological responses to the exercise are reproducible between both measurements in the same subject. Even with simultaneous spirometry and MRS, these studies focused mainly on VO_2 during the load phase, while omitting the whole respiration profile as well as VCO_2 and blood lactate kinetics, where both of the latter contain important information of acidification driven by anaerobic glycolysis and allow more comprehensive insight into the processes affecting muscle function.

From the perspective of sports science, the findings accumulated by combining muscle specific ^{31}P-MRS with '*gold standard*' analysis methods (spiroergometry and blood lactate diagnostics) benefit a deeper understanding of the dependency of global metabolic changes on muscular demands, which is expected to help to resolve highly debated circumstances of fatigue development and exercise-limiting processes. In addition, such a combined approach should further motivate the usage of physiological models to characterize local metabolic processes from global measurements without invasive procedures or costly spectroscopic measurements. This again would improve evaluations of training interventions or even help to assess possible youth sport talents in a non-invasive but specific, individualized way.

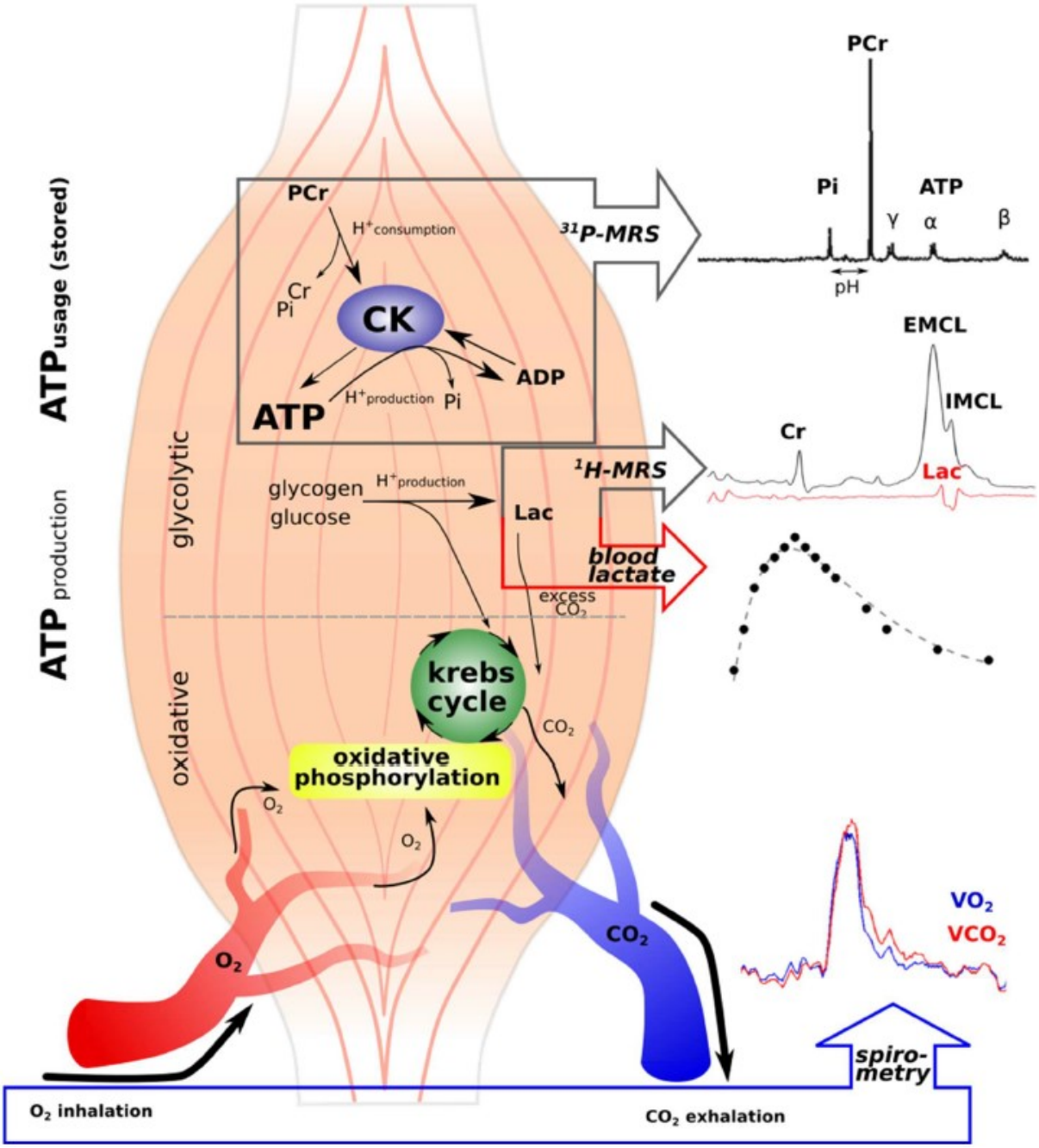

Figure 1-3 Simplified scheme of muscle energy metabolism to illustrate the demand and supply of ATP as it can be characterized by parameters measured with ^{31}P-MRS, ^{1}H-MRS (both gray boxes), blood lactate diagnostics (red box) and spirometry (blue box). At the fastest instance energy demand is compensated by the creatine kinase (CK) reaction with the splitting of PCr to balance ATP consumption. Such changes in high energy metabolites can be detected by ^{31}P-MRS together with cellular acidification. Exercise-induced alterations in lactate concentrations are observable with adapted ^{1}H-MR sequences. Whereas the latter allows direct quantification within the muscle, blood lactate measurements represent lactate formation and metabolization in the periphery. Gas exchange with O_2 inspiration and CO_2 expiration can be measured by spirometry.

1.4. Objectives and structures of the thesis

Against this background laid out above, the primary objective of this thesis was to set up and evaluate dynamic *in vivo* ^{31}P-MRS in the human calf muscle in combination with well-established spiroergometry and blood lactate measurements. According to the previously mentioned methodological challenges, this main objective was separated into the following sub-goals.

The first milestone (see Chapter 2) was to set up an MR-compatible pedal ergometer system to perform graded and dynamic plantar flection exercises, which were selected to exercise the human calf muscle. The main focus was to establish a methodical frame for comparable exercises under restricted conditions within an MR-scanner. In addition, the ergometer system had to be equipped with mechanical sensors enabling online monitoring via a graphical user interface and allowing interactive adjustments of load conditions. The setup was evaluated by repetitive *in vivo* ^{31}P-MR measurements during graded loads of the human calf muscle.

The third chapter covers the adaptation of a commercial spirometry system in order to perform gas exchange measurements within the MR scanner during human calf exercises. The modified spirometry system was applied in examinations with non-specifically trained subjects. It was hypothesized, that the measured global changes of several respiratory parameters correlates with local, high-energy adaptations in the exercised muscle.

Following its successful implementation and testing, the complete setup (exercise, pulmonary data and ^{31}P MR spectra acquisition) was used to investigate in two different athlete groups, whether the expected, sport-specific energy supply regimes can be identified from the simultaneously acquired MR spectroscopic, pulmonary and blood lactate data (see Chapter 4). This study was performed by furthermore applying a novel MR spectroscopic technique, allowing simultaneous monitoring of metabolic data in multiple muscles.

Chapter 5 summarizes ^{31}P-MR spectroscopic measurements performed in the human calf muscles in volunteers during neuromuscular electrical stimulation (NMES). In contrast to the subject-dependent, voluntary mechanical muscle exercise, NMES was assumed to be better suited to objectively evaluate energy turnover. It was hypothesized that fatigue induced by NMES allows detection of different pH compartments reflecting the load responses of different muscle fiber types.

Chapter 6 summarizes the results of the performed experiments alongside with a critical discussion and references to research findings from the fields of medical physics and exercise physiology. The last chapter (chapter 7) provides conclusions and an outlook for future studies. Finally, the appendix provides the supplementary material of chapter 4 and 5, respectively.

Chapter 2

2. MR-compatible Pedal Ergometer for Reproducible Exercising of the Human Calf Muscle

Medical Engineering and Physics; 2014; 36(7) 933-937

Tschiesche K.
Rothamel M.
Rzanny R.
Gussew A.
Hiepe P.
Reichenbach JR.

Abstract

A pneumatic MR-compatible pedal ergometer was designed to perform dynamic contraction exercises of the human calf muscle in a whole-body 3T MR scanner. The set-up includes sensors for monitoring mechanical parameters, such as pedal angle, cadence as well as applied force and power. Actual parameter values during the exercise were presented to the volunteer as a visual feedback to enable real-time self- adjustment of pedal deflection and cadence to the target reference value. Time-resolved dynamic ^{31}P-MR spectroscopic measurements of phosphocreatine (PCr), inorganic phosphate (Pi) and pH were performed in a pilot experiment before, during, and after the exercise by a single volunteer. Two different load strengths were applied in these experiments (15% and 25% of the maximum voluntary contraction, MVC). As expected, mechanical and metabolic parameters differed for the two load levels. Small variations of the cadence, power and metabolic changes (time constants of PCr depletion and Pi accumulation) during the experiments demonstrate a highly reproducible mechanical output by the volunteer mediated by the ergometer.

2.1.Introduction

Monitoring muscle exercising with functional ^{31}P-magnetic resonance spectroscopy (^{31}P-MRS) is an important method that is often used for quantitative estimation of dynamic metabolic parameters, such as load induced changes of phosphocreatine (PCr), inorganic phosphate (Pi) or pH (Yoshida, 1988; Rzanny *et al.*, 2006; Kemp, Meyerspeer and Moser, 2007). The method enables non-invasive assessment of physiological information about muscle fatigue (Tonson *et al.*, 2010),

monitoring and potentially quantifying training effects (Rzanny *et al.*, 2009), analyzing pathological states (Barnes *et al.*, 1997) or assessing exercise-induced metabolic changes (Rzanny *et al.*, 2006). Dedicated MR-compatible ergometers, specifically adapted to the limited available space in the bore of an MR scanner, are typically used to apply defined muscular loads. Several different MR-compatible ergometers have been already developed in the past to perform isometric contractions (Bangsbo *et al.*, 1993) and dynamic exercises(Wilson *et al.*, 1988; Ryschon *et al.*, 1995; Jeneson *et al.*, 2010; Hosseini Ghomi *et al.*, 2011). Defined loads are applied by using, e.g., force transfer beams in combination with a wheel (Francescato and Cettolo, 2001; Layec *et al.*, 2008), elastic cords (Francescato and Cettolo, 2001) or pneumatic force control (Raymer *et al.*, 2006; Sinha *et al.*, 2012).

So far, only few of these ergometers monitor mechanical parameters during the exercise (Francescato and Cettolo, 2001; Meyerspeer *et al.*, 2005; Raymer *et al.*, 2006; Sinha *et al.*, 2012) that can be used as feedback information to the volunteer or patient to adjust the current activity to the intended examination protocol. A missing feedback, however, may lead to unintended deviations in the exercise performance which, in turn, may limit the accuracy of the results of functional muscle measurements.

Against this background, the aim of our work was to design a pneumatic MR-compatible pedal ergometer, which allows precise adjustment of the muscular load of the human calf muscle (*m. triceps surae*, including the *m. gastrocnemius medialis/lateralis* and the *m. soleus*) as well as monitoring of mechanical parameters, including pedal angle, cadence, applied force and power. Cadence and pedal angle are used for the visual feedback for real-time self-adjustment of exercise conditions. Dynamic ^{31}P-MRS before, during, and after calf muscle exercise was applied to verify the reliability of the extracted metabolic changes.

2.2. Materials and Methods

Ergometer Design

Figure 2-1 shows the ergometer designed to perform standardized MR measurements of exercising human calf muscles in a clinical whole-body 3 T MR scanner (MAGNETOM Tim Trio, Siemens, Germany). The foot pedal (Figure 2-1) is made of polyamide and polyurethane and mounted on a wooden plate (49 cm × 71 cm). It permits ankle deflections up to 35° and can be used with the left or the right leg. A pneumatic cylinder, which connects the pedal to a compressed-air tank (air pressure range: 0 - 10 bar) via an air hose (ø 9 mm), generates defined forces that counteract the plantarflexion. Two handle pieces with adaptable length provide footholds for the volunteer during the exercise. A second, slightly tilted wooden panel (49 cm × 190 cm) is fitted to the patient table of the MR scanner which suppresses any movement of the ergometer during

exercise and includes an additional lower leg frame. The latter enables flexible positioning of different types of RF surface coils, which can be placed above the *m. triceps surae*. During the measurements the upper leg and the foot are fixed using Velcro fasteners.

Pedal deflections and forces applied to the pedal during the exercise are continuously monitored. Forces are measured by using a hydraulic transducer, which is located beneath the pedal (Figure 2-1b)and connected to a piezoresistive pressure transducer (located outside the scanner room, see Figure 2-1c for a more detailed experimental set up) via a liquid filled hose line (CTE8000/CTU8000 Series, Sensortechnics, hose line 10 m, diameter: 4 mm). Pedal deflections are determined by means of a rotary potentiometer (3310 – 9 mm Square Sealed Panel Control, Bourns, California) mounted on the pedal axis (Figure 2-1b) that creates electrical potential differences in response to the motion. Following amplification, all sensor data are digitized with a 12 bit ADC (1208FS ME-RedLab, Meilhaus Electronic, Germany) and transferred to an external computer via an USB interface. A self-written MATLAB program (The Mathworks, Inc., USA) reads the voltage values from the force sensor (U_{sensor}) and potentiometer (U_{pot}) and calculates the force and deflection angle values by using the following equations, respectively:

$$\boldsymbol{F = c \cdot \left(U_{sensor} - U_{offset}\right)}, \tag{2-1}$$

$$\boldsymbol{\alpha = \frac{35^\circ}{U_{35^\circ} - U_{0^\circ}} \cdot \left(U_{pot} - U_{0^\circ}\right)}, \tag{2-2}$$

The constant *c* (190.8 $N \cdot V^{-1}$) in Eq. 2-1 was determined during an initial calibration experiment, in which changes of U_{sensor} induced by different defined graded weights were measured. The mean power (P) is calculated during each deflection from the mean force per cycle($\bar{F}$) and cadence (f_{cad}) according to

$$\boldsymbol{P = \pi \cdot r \cdot \frac{\Delta\alpha}{180^\circ} \cdot \bar{F} \cdot f_{cad}}, \tag{2-3}$$

where r and Δα denote the rotation radius and actual deflection angle span, respectively.

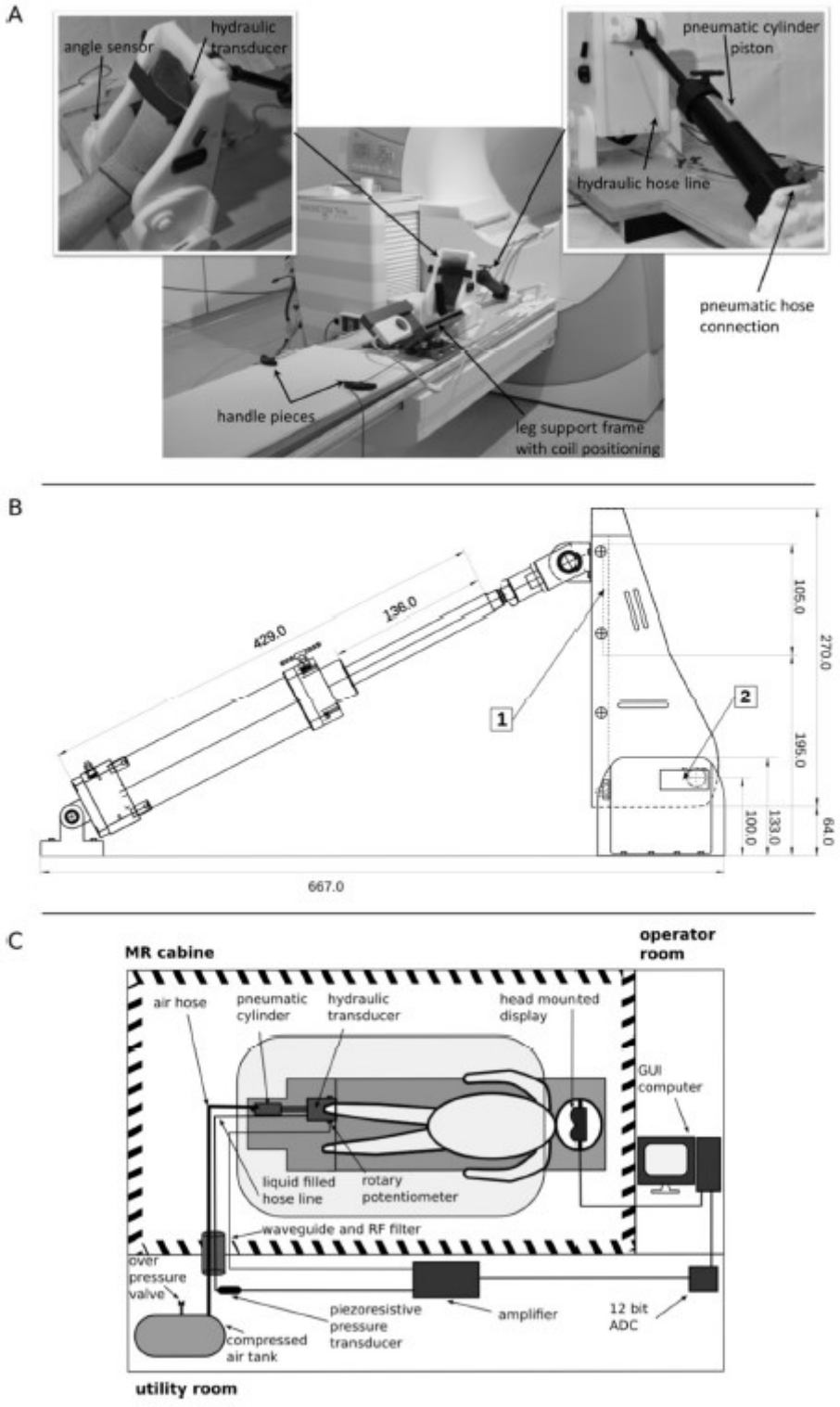

Figure 2-1 (A) Ergometer and experimental set up consisting of the leg support frame with the MR surface coil, the foot pedal with angle sensor and hydraulic transducer (located beneath the tread), the pneumatic cylinder piston and the adapter plate with two handle pieces. (B) Functional CAD drawing of the pedal and the cylinder in side view with the most important construction dimensions. The numbers represent the location of [1] the pressure transducer beneath the tread and [2] the angle sensor. (C) Schematic drawing of the experimental set up with individual components.

The time courses of the forces and deflections are recorded and visualized in real time using a dedicated MATLAB graphical user interface (GUI). The actual deflection maximum, cadence and remaining exercise time are presented to the subject in the scanner by means of a MR-compatible head-mounted display (VisuaStim XGA, Resonance Technology, USA). This visual feedback enables interactive adjustment for self-controlling the exercise conditions (Figure 2-2).

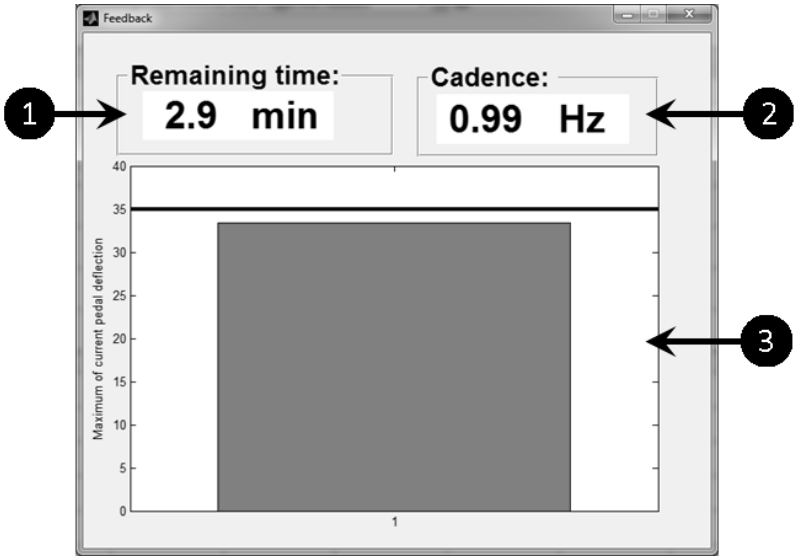

Figure 2-2 Feedback-window, which is presented to the subject via projecting goggles and displays the remaining exercise time [min] (1), the cadence [deflection/sec] (2) and the deflection angle [°] of the pedal (3).

Exercise protocol

One healthy 21-year-old male subject participated in this initial study after informed written consent was obtained. The examination protocol was approved by the local Ethics Committees. ^{31}P-MR spectra were acquired in the left calf muscle before, during and after the exercise using the ergometer. During the 3 min exercise period, the volunteer was asked to deflect the pedal by 35° with a cadence of 1 Hz. The complete exercise and measurements were repeated six times at different days within five weeks. The load intensity was normalized to the individual maximum voluntary contraction (MVC) (Kemmler *et al.*, 2006). To this end, MVC was determined prior to the first examination by asking the volunteer to push the locked pedal at 0° with maximum effort (isometric exercise over 5 s). The pedal was locked by using a pressure of 4 bar and an additional Velcro fastener was used to avoid foot shifts on the pedal. The maximum force exerted during this load period was set to 100% of F_{MVC}. For graded loads, as applied in this work, the air pressure in the compressor was adjusted to 15% or 25% of F_{MVC} (determined using the rule of three). Overall, both load strengths were applied in three of six repetitions of the experiment.

Dynamic ^{31}P-MRS

All MR measurements were performed in a clinical whole-body 3 T MR scanner (MAGNETOM Tim Trio, Siemens, Germany) by using a double-tuned loop coil for RF excitation and signal detection (^{1}H/^{31}P, ø 8 cm, Rapid Biomedical GmbH, Germany). The MR coil was positioned under the left calf using reference markers on the lower leg frame. Prior to MRS, manual shimming was performed to adjust the magnetic field homogeneity in the *m. gastrocnemius medialis*. ^{31}P-MR spectra were measured with an FID sequence without additional volume selection (512 sampled complex FID data points, sampling bandwidth 2 kHz, TR = 5 s). A dynamic series containing 70, 36 and 196 spectra (rest, load and recovery) were acquired prior, during and after the 3 min load, respectively.

All spectroscopic data were first corrected for zero- and first-order phase errors, frequency shifts as well as baseline distortions by using a self-written MATLAB program, followed by quantitative analysis with the AMARES routine (Advanced Method for Accurate, Robust and Efficient Spectral fitting) (Vanhamme, van den Boogaart A and Van Huffel S, 1997) in the jMRUI 4.0 software (www.mrui.uab.es). PCr and Pi peaks were fitted as single Lorentzians, whereas γ- and α-ATP signals were fitted as Lorentzian doublets and β-ATP as a triplet. Appropriate prior knowledge was used for the ATP multiplets as described previously (Stubbs *et al.*, 1996). All ^{31}P-MR peaks were normalized to the mean PCr-intensity during rest I_{PCr}^{0}.

To quantify the dynamics of the load-induced metabolic changes, the time constants of the PCr decrease and Pi increase (T_{PCr} and T_{Pi}) during load were estimated by mono-exponential fitting of the corresponding signal-time-courses:

$$\boldsymbol{I_{PCr}(t) = \left(I_{PCr}^{0} - I_{PCr}^{full\ load}\right) \cdot e^{-\frac{t}{T_{PCr}}} + I_{PCr}^{full\ load},} \qquad (2\text{-}4)$$

$$\boldsymbol{I_{Pi}(t) = (I_{Pi}^{full\ load} - I_{Pi}^{0}) \cdot \left(1 - e^{-\frac{t}{T_{Pi}}}\right) + I_{Pi}^{0},} \qquad (2\text{-}5)$$

The constants I_{PCr}^{0}, I_{Pi}^{0}, $I_{PCr}^{full\ load}$ and $I_{Pi}^{full\ load}$ denote the resting PCr, resting Pi and maximum load PCr and Pi intensity, respectively. In addition, the pH difference (ΔpH) between the mean pH during rest (pH_{rest}) and pH at the end of the exercise (pH_{load}) was calculated by determining the chemical shift (δ) between the PCr and Pi peaks and inserting it into the Henderson-Hasselbalch equation (Heerschap *et al.*, 1999). All results are expressed as mean (range).

2.3. Results

All metabolic and mechanical parameters are summarized in Table 2-1. The actual mean cadences at 15% F_{MVC} (0.92 Hz within the range of 0.91 - 0.94 Hz) and 25% F_{MVC} (0.95 Hz within the range of 0.94 – 0.97 Hz) are both close to the intended target cadence of 1 Hz. The values of the mean power P (see Eq. 2-3) are different between both load levels, as expected. PCr and Pi time courses are demonstrated in Figure 2-3 for both load levels. At the higher load (25% F_{MVC}), the distinctly faster PCr decrease (T_{PCr} = 23.5 s within the range of 19.3 – 25.9 s at 25% *vs.* T_{PCr} = 56.2 s within the range of 49.5 – 61.1 s at 15%) leads to complete consumption of PCr after approximately 1.5 min muscle stress. In contrast to this with 15% F_{MVC} there is still remaining PCr signal observable at the end of the exercise. The increase in Pi also occurs faster and is larger for the higher load (T_{Pi} = 25.0 s within the range of 23.9 – 26.3 s at 25% *vs.* T_{Pi} = 43.6 s within the range of 36.7 – 49.1 s at 15%). Averaged over three examinations, the mean ΔpH was 0.16 at 15% F_{MVC} and 0.37 at 25% F_{MVC}.

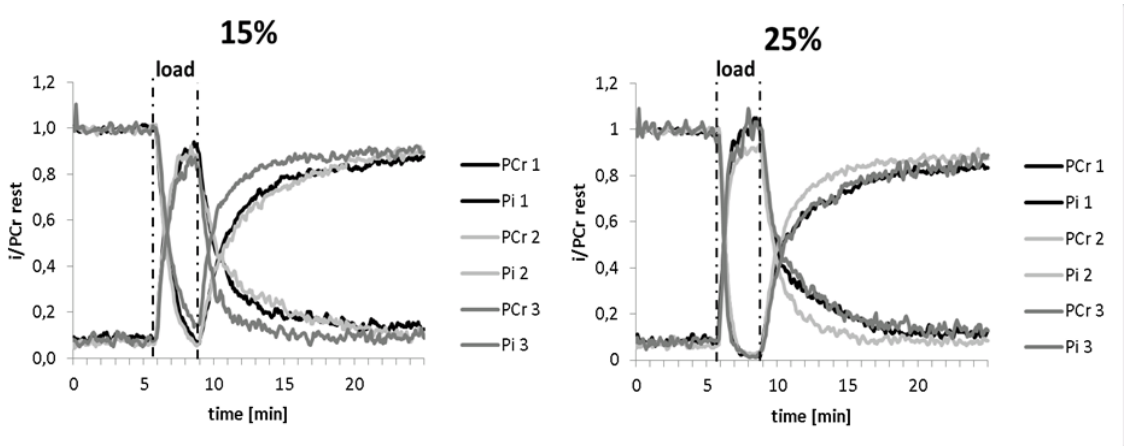

Figure 2-3 Time courses of PCr and Pi intensities for 15% and 25% F_{MVC}. Each data curve represents a complete single dynamic exercise measurement.

Table 2-1 Results of parameters mean (range) obtained for 15% and 25% F_{MVC}.

	15% F_{MVC}	**25% F_{MVC}**
power [W]	15.5 (14.4 – 16.5)	21.8 (21.5 – 22.2)
cadence [Hz]	0.92 (0.91 – 0.94)	0.95 (0.94 – 0.97)
pH_{rest}	6.93 (6.93 – 6.97)	6.92 (6.87 – 6.92)
pH_{load}	6.77 (6.77 – 6.84)	6.55 (6.51 – 6.59)
T_{PCr} [s]	56.2 (49.5 – 61.1)	23.5 (19.3 – 25.9)
T_{Pi} [s]	43.6 (36.7 – 49.1)	25.0 (23.9 – 26.3)

2.4.Discussion

This technical note describes the design of a muscle ergometer which was customized for the use in a clinical whole-body 3 T MR scanner. The ergometer allows standardized exercises of the calf muscle while ^{31}P-MRS measurements can be simultaneously performed to quantify exercise-induced metabolic changes. Isometric and dynamic exercises using defined stress intensities (based on the individual maximum force, F_{MVC}) can be performed by adapting the pressure of the pneumatic air system (0.01 bar steps).

The lower leg frame provides a constant foothold of the calf and, thus, ensures correct positioning of the surface coil over the region-of-interest. The reproducibility of the mechanical output by the volunteer was demonstrated, and low variations of the measured cadence (up to 3%) and mean power (up to 9%) were obtained between three repeated measurements at two different load levels. Key to this was the application of a visual feedback to the exercising volunteer. This feedback allows the subject to interactively adjust his physical output to the target reference values of pedal deflection and cadence. The strong association between metabolic results and mechanical output further indicates the reliability of the measured metabolic changes caused by the graded loads.

The presented ergometer set up has several advantages compared to alternatively proposed ergometers (Wilson *et al.*, 1988; Bangsbo *et al.*, 1993; Ryschon *et al.*, 1995; Francescato and Cettolo, 2001; Meyerspeer *et al.*, 2005; Raymer *et al.*, 2006; Layec *et al.*, 2008; Jeneson *et al.*, 2010; Hosseini Ghomi *et al.*, 2011; Sinha *et al.*, 2012). Instead of using bulky space occupying force transfer beams in combination with wheels (Francescato and Cettolo, 2001; Layec *et al.*, 2008) or servo motors, which require substantial distance from the magnet bore to avoid unwanted forces of attraction or interferences with the acquired MR signal (Wilson *et al.*, 1988; Ryschon *et al.*, 1995), our proposed ergometer separates physically the ergometer frame and additional MR-incompatible components, like the air compressor, electronic amplifiers and analog-digital converters which are all placed outside the MR scanner room. Due to the use of lightweight materials (12 kg pedal, 20 kg patient table) our ergometer can be easily installed and modified to switch between the left and right calf. Furthermore, the applied materials are cost-efficient and easy to procure.

One minor current limitation of the ergometer is a slight residual friction of the pneumatic cylinder (additional force of 21.6 N, which corresponds to approximately 8% of the applied study conditions), which was determined by calibration measurements with gauged weights. However, this resistance is small enough to enable even measurements of subjects with low pedal effort, like children or patients with reduced muscle mass. Nevertheless, this issue may affect metabolic turnover parameters for defined loads and, thus, care of periodically greasing has to be taken.

Furthermore, due to the leg support frame, applications are currently limited to investigations of the *m. triceps surae* whereas the *m. tibialis anterior* or the *m. quadriceps femoris* were examined in other studies (Kreis *et al.*, 1999; Francescato and Cettolo, 2001).

For future studies, we plan to implement additional acoustic triggering using gradient pulses within the FID sequence (Quistoroff *et al.*, 1990; González de Suso *et al.*, 1993) to further improve the reliability of the feedback tool. With these improvements additional studies using the proposed ergometer to assess exercise-induced ischemic effects, oxygen consumption or PCr recovery kinetics, which mainly reflects mitochondrial function (G Layec *et al.*, 2013), should be conveniently addressable.

Acknowledgements

We thank Günter Ditze and his team of the Central Research Workshop of the Friedrich Schiller University Jena for their support in the construction and assembly of the ergometer. This work was supported by the Competence Center for Interdisciplinary Prevention (KIP) at the Friedrich Schiller University Jena and the German Professional Association for Statutory Accident Insurance and Prevention in the Foodstuffs Industry and the Catering Trade (BGN). K.T. acknowledges support from a PhD stipend provided by KIP (ID 1.1.7.13). The study was also supported by the German Research Foundation (Deutsche Forschungsgemeinschaft, DFG, Rz 10/5-1). We have no relevant financial interests to disclose with regard to this study. The examination protocol, which was applied in this study, was approved by the local Ethics Committee (Ethics committee ID: 2478-02/09).

Chapter 3

3. Combined Spiroergometry and ^{31}P-MRS of Human Calf Muscle during High-Intensity Exercise

NMR Biomed; 2017; 30(7):e3723

Moll K.
Gussew A.
Hein C.
Stutzig N.
Reichenbach JR.

Abstract

Simultaneous measurements of pulmonary oxygen consumption (VO_2), carbon dioxide exhalation (VCO_2) and phosphorus magnetic resonance spectroscopy (^{31}P–MRS) are valuable in physiological studies to evaluate muscle metabolism during specific loads. Therefore, the aim of this study was to adapt a commercially available spirometric device to enable measurements of VO_2 and VCO_2 whilst simultaneously performing ^{31}P–MRS at 3T. Volunteers performed intense plantar flexion of their right calf muscle inside the MR scanner against a pneumatic MR-compatible pedal ergometer. The use of a non-magnetic pneumotachograph and extension of the sampling line from 3 m to 5 m to place the spirometric device outside the MR scanner room did not affect adversely the measurements of VO_2 and VCO_2. Response and delay times increased, on average, by at most 0.05 s and 0.79 s, respectively. Overall, we were able to demonstrate a feasible ventilation response (VO_2 = 1.05 ± 0.31 L/min; VCO_2 = 1.11 ± 0.33 L/min) during the exercise of a single calf muscle, as well as a good correlation between local energy metabolism and muscular acidification ($\tau_{PCr\ fast}$ and pH; $R^2 = 0.73$, $p < 0.005$) and global respiration ($\tau_{PCr\ fast}$ and VO_2; $R^2 = 0.55$, $p = 0.01$). This provides improved insights into aerobic and anaerobic energy supply during strong muscular performances.

3.1.Introduction

The determination of the kinetics of oxygen uptake (VO_2) and carbon dioxide production (VCO_2), commonly measured by spiroergometry, is important to evaluate the pulmonary performance during exercise. It is well known that the adaptation of ventilation not only reflects workload intensity (Ozyener *et al.*, 2001; Whipp, Rossiter and Ward, 2002) and the training status of athletes

(Millet *et al.*, 2002; Layec *et al.*, 2012) but may also be used in the assessment of pulmonary diseases (Celli, 2000; Palange *et al.*, 2007). The recording and analysis of individual ventilation responses to exercise, such as treadmill or bicycle tests, yields insights into muscle bioenergetics, which is not only relevant for the sustainment and limitation of exercise, but may also play a role in gender- and age-specific functional alterations of the muscle system (Kohrt *et al.*, 1985; Grey *et al.*, 2014). When performing high-intensity exercise, even small affected muscle groups (e.g. quadriceps, gastrocnemius) can cause adaptations in VO_2 (McCreary *et al.*, 1996; Rossiter *et al.*, 1999; Whipp *et al.*, 1999; Cannon *et al.*, 2013; Richardson *et al.*, 2015) which are assumed to be related to locally increased high energy metabolic demands. However, the link between local muscle function and global respiration is so far only poorly understood.

Phosphorus magnetic resonance spectroscopy (^{31}P–MRS) is a particularly important tool for obtaining direct insights into local metabolic adjustments as it enables the non-invasive quantification of changes in high-energy metabolites, such as phosphocreatine (PCr) and inorganic phosphate (Pi), in loaded muscles (Boesch, 2007; Kemp, Meyerspeer and Moser, 2007). Therefore, a combination of spiroergometry and ^{31}P–MRS offers the unique possibility to perform multimodal analyses of both global and local alterations of the aerobic and anaerobic energy supply during exercise, thus providing different views on the mitochondrial capacity, which is characterized by the rate of mitochondrial adenosine triphosphate (ATP) synthesis. The latter can be determined from the aerobic PCr re-synthesis slope of post-load ^{31}P–MR spectra (Kemp *et al.*, 2015).

Several groups have combined exercise-induced kinetics of ventilation with metabolic adaptations in single muscles using ^{31}P–MRS (Barstow *et al.*, 1994; McCreary *et al.*, 1996; Whipp *et al.*, 1999; Roecker *et al.*, 2000; Rossiter *et al.*, 2000; Ozyener *et al.*, 2001; Rossiter, Ward, Howe, 2002; DiMenna *et al.*, 2010; Bringard *et al.*, 2012; Layec *et al.*, 2012; Richardson *et al.*, 2015). The most crucial technical challenge to overcome to perform viable spirometric measurements inside an MR scanner is related to the high static magnetic field and the radiofrequency electromagnetic fields with their harmful effects on the electronic parts of the spirometry unit. In the past, some researchers have performed repeated measurements with the same exercise protocol inside and outside the MR scanner (Barstow *et al.*, 1994; McCreary *et al.*, 1996; DiMenna *et al.*, 2010). This approach requires the additional effort of performing measurements twice with the same subjects and may suffer from daily physiological changes or motivation from one measurement to the other. Recently, several groups have performed simultaneous ^{31}P–MRS and spiroergometry measurements (Whipp *et al.*, 1999; Rossiter *et al.*, 2000; Rossiter, Ward, Howe, *et al.*, 2002; Layec *et al.*, 2012) to investigate VO_2 kinetics and to relate it to local, load-induced metabolic changes to find strong correlations between mitochondrial energy supply and global respiration. Using modified

spirometry equipment with long respiratory sampling lines (6.5 – 13.5 m), these studies demonstrated successfully the feasibility of valid spirometric measurements inside the MR scanner. Despite having access to a broad range of spirometric parameters, these studies mostly focused on the analysis of load-induced VO_2 adaptations, whereas investigations of the associations between metabolic measures and VCO_2 dynamics were mostly neglected. However, as the load-induced non-linearly increasing and excessive CO_2 output indicates the transition to an anaerobic energy supply (Roecker *et al.*, 2000), it appears promising to analyze pH alterations in exercised muscles.

Against this background, the aim of this work was to establish an experimental set-up to enable combined spirometric and ^{31}P–MRS measurements in humans during local loads of specific muscles. To this end, a commercial gas exchange system was adapted for dynamic evaluation of pulmonary ventilation during muscle exercise inside a whole-body MR scanner. The functionality was tested in healthy volunteers by the evaluation of the dynamic changes in high-energy phosphate metabolites and monitoring of the concomitant alterations in pulmonary parameters (oxygen and carbon dioxide volume flows) during exercise of the calf muscle.

3.2.Experimental

Set up

The set up used is schematically illustrated in Figure 3-1 Besides the 3 T whole-body MR scanner (Magnetom PRISMA fit, bore size 60 cm, Siemens Healthcare, Erlangen, Germany), it consists of a previously described MR-compatible pedal ergometer (Tschiesche *et al.*, 2014) and a commercially available spirometric system *PowerCube* (Ganshorn, Medizin Electronic GmbH, Niederlauer, Germany). Whereas the former has been designed to perform defined dynamic loads in human calf muscles, the latter allows continuous measurements of oxygen, carbon dioxide and expiratory volumes (VO_2 and VCO_2 in L/min, sampling rate: 100 Hz) by using an electrochemical cell, an ultrasound sensor and a flow sensor, respectively. To ensure proper working of the spirometric system in the magnetic field environment, the following modifications were employed:

- replacement of the metal clips adhering the pneumotachograph membrane in the respiration mask by non-magnetic synthetic screws
- extension of the original 3 m gas sampling line to 5 m for placement of the *PowerCube* analyzer device outside of the MR scanner room to avoid interactions and interferences between all sensitive hardware parts and static and radiofrequency magnetic fields, respectively.

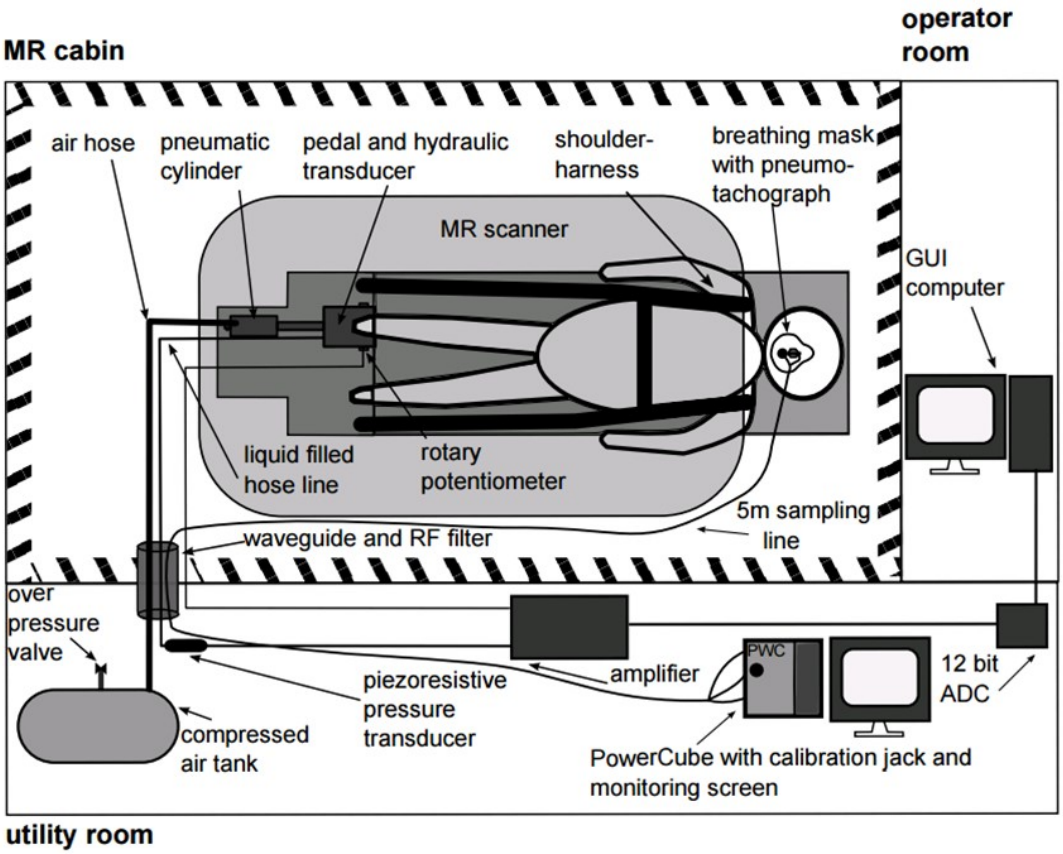

Figure 3-1 Scheme of the experimental (MR)-compatible ergometer and spirometer set up. The MR cabin, the operator room and the utility room are outlined together with several salient components including the ergometer and parts of the spirometer inside the cabin. The main spirometer device (*PowerCube-PWC*) is placed outside of the MR-scanner cabin. ADC, analog to digital converter; GUI, graphical user interface; RF, radio frequency.

To assess the effect of the longer sampling line five calibration measurements of the delay and response time (t_A and t_{10-90}) were performed with both the original line of 3 m and the extended line of 5 m. The delay time is the time required for the gases (O_2 and CO_2) to reach their analyzers, whereas the response time represents the time required to record 10-90% of an expected maximum change in gas concentration (Roecker, Prettin and Sorichter, 2005). In order to take into account the extended line length, the system's intrinsically stored delay time was adjusted from 1.25 s to 2 s in the spirometer operating software (*LF8*). This adjustment did not affect the effectively measured values. Additionally, resting state values of VO_2 and VCO_2 as well as exercise induced gas volume adaptation were performed with either 3 m or 5 m sampling lines in two healthy male subjects outside the MR scanner by applying the same exercise protocol as in the main study. For all measurements the gas analyzers were calibrated with ambient air (20.95% O_2 and 0.03% CO_2) and a gas mixture of known composition (16% O_2 and 5.02% CO_2). The calibration protocols consisted of volume adjustment with a 1 L syringe and gas flow synchronization was included in the vendor specific *LF8* software.

In vivo validation

Ten healthy male volunteers (age 29 ± 5 years) participated in the study after having signed an informed consent. The examination protocol was approved by the local Ethics Committee (Ethics committee ID: 2478-02/09). None of the subjects were specifically trained. All volunteers abstained from intense physical activity and alcohol consumption the day before and on the day of measurement.

The exercise (3 min) was performed in supine position as a series of highly intense, unilateral plantar flexions of the right calf muscle by pushing the right foot against a 0.6 bar pedal resistance with a frequency of 80 bpm (mean peak force of 163 ± 23 N). A metronome assisted the subjects in maintaining the proper pedal frequency. During load, verbal instructions were given to the volunteers to maintain constant pedal deflection of 25°. To minimize additional energy loss from movements of the whole upper body, an individually adaptable shoulder harness was applied to keep the subject in position and to provide a passive foothold for the volunteer during exercise. In addition, the exercising lower leg was stabilized by three Velcro straps placed over the ankle, upper knee and hip to reduce counter movements.

The experiment was separated into three phases (rest: 10 min, load: 3 min and recovery: 20 min) during which spirometric and MR spectroscopic data were acquired simultaneously (Figure 3-2). During rest, acquisition of pulmonary ventilation data started first to familiarize the subjects with the breathing mask and to avoid an unusual breathing pattern due to the small breathing resistance of the pneumotachograph membrane. Verbal instructions were given to the volunteers to breathe in a normal way and to prevent hyperventilation, coughing or yawning.

MR data were sampled by using a double-tuned ($^{1}H/^{31}P$) flexible surface coil with an integrated phosphorous loop (Ø 11 cm; RAPID Biomedical, Rimpar, Germany). The coil was wrapped around the right lower leg and fixed on the ergometer frame. Prior to MRS, the spectroscopic volume was selected in the *m. gastrocnemius medialis* by means of localizer MR images (see Figure 3-2). Manual shimming (first and second order) was performed to tune the magnetic field homogeneity across the spectroscopic volume. Localized, time resolved ^{31}P-MR spectroscopic measurements within the calf muscles were performed with a DRESS sequence (depth-resolved surface coil MRS), which was previously introduced by Valkovič et al. and implemented (Valkovič *et al.*, 2014). By using this technique, dynamic series of ^{31}P MR spectra were collected with time resolution of 5 s in a 15 mm thick slice, which was oriented parallel to the leg in order to cover the *m. gastrocnemius medialis* (TR/TE = 5000/1.3 ms), since it provides the largest action during plantar flexion (Schmid *et al.*, 2014). Twenty-four spectra were measured during the rest phase followed by the

acquisition of 36 spectra during load and 240 spectra during the recovery (see data acquisition protocol in Figure 3-2).

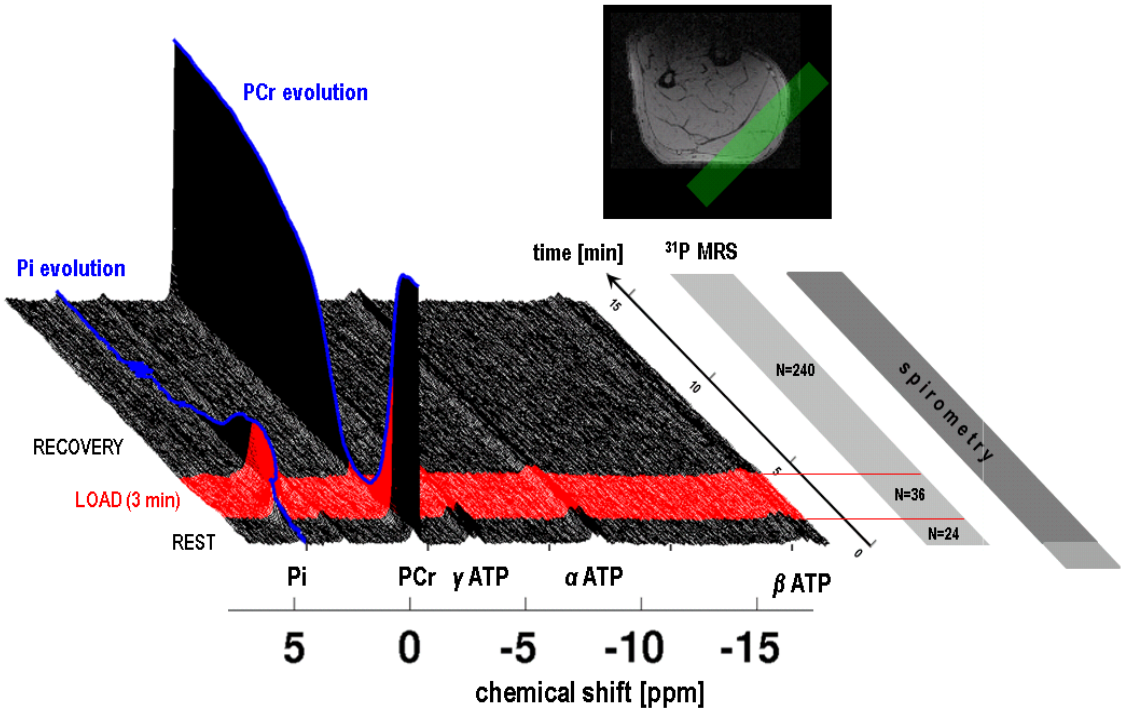

Figure 3-2 Representative 'stack plot' of dynamic ^{31}P magnetic resonance (MR) spectra from the right *m. gastrocnemius medialis*. The red spectra (N = 36) were acquired during the 3 min load phase followed by the recovery phase. The blue lines indicate the inorganic phosphate (Pi) and phosphocreatine (PCr) evolutions during all three phases. Spirometry measurements (gray) started prior to the MRS to familiarize the subjects to the breathing mask. ATP, adenosine triphosphate

Data analysis

Vendor-specific software was used to resample the raw spirometric data to a temporal resolution of 10 s and to extract the time courses of VO_2 and VCO_2. In order to account for the low time resolution and physiological variations, the VO_2 and VCO_2 curves were fitted in sections by three different functions representing rest ($t < T_{start}$), load ($T_{start} \leq t < T_{rec}$) and recovery ($t \geq T_{rec}$) phases, respectively.

$$y(t) = offset + \begin{cases} 0, & t < T_{start} \\ A \cdot \left(1 - e^{-\frac{t - T_{start}}{\tau_{inc}}}\right), & T_{start} \leq t < T_{rec} \\ A \cdot \left(1 - e^{-\frac{T_{rec} - T_{start}}{\tau_{inc}}}\right) \cdot \left(f_{vent} \cdot e^{-\frac{t - T_{rec}}{\tau_{fast}}} + \left(1 - f_{vent}\right) \cdot e^{-\frac{t - T_{rec}}{\tau_{slow}}}\right), & t \geq T_{rec} \end{cases} \quad (3\text{-}1)$$

The 'offset' denotes the resting value during pre-exercise, whereas A is the magnitude of the exponential VO_2 or VCO_2 increase during the load phase, which is characterized by a time constant τ_{inc}. The recovery function is expressed by a weighted sum of a fast (τ_{fast}, weighting factor f_{vent}) and a slowly (τ_{slow}, weighting factor 1- f_{vent}) decreasing component. Besides the extraction of the time constants of gas volume recovery slopes, the resulting fit was also used to estimate the CO_2 over-shoot over the O_2 volume (excess CO_2, see Figure 3-4), which was determined by integrating the differences between the fitted VO_2 and VCO_2 curves.

All MR spectra were corrected for zero- and first-order phase errors, frequency shifts as well as baseline distortions by using a self-written MATLAB script and were quantified with an AMARES (Advanced Method for Accurate, Robust and Efficient Spectral Fitting) routine included in the jMRUI 4.0 software (Java-Based MR User Interface; www.jmrui.eu). PCr and Pi peaks were fitted as single Lorentzians. In addition, the pH value was calculated by determining the chemical shift between the PCr and Pi peaks and inserting it into the Henderson-Hasselbalch equation (Heerschap *et al.*, 1999):

$$\boldsymbol{pH = 6.7 + log\frac{(3.27-\delta)}{(\delta-5.63)}}, \qquad (3\text{-}2)$$

where δ is the observed chemical shift of Pi. Finally, the PCr time course during recovery, which is a sensitive index of muscle oxidative capacity (G Layec *et al.*, 2013), was fitted with a bi-exponential function:

$$\boldsymbol{PCr(t) = a_{PCr}\cdot\left(f_{PCr}\cdot\left(1-e^{-\frac{t}{\tau_{PCr_{fast}}}}\right)+(1-f_{PCr})\cdot\left(1-e^{-\frac{t}{\tau_{PCr_{slow}}}}\right)\right)+offset} \qquad (3\text{-}3)$$

where $\tau_{PCr\ fast}$, $\tau_{PCr\ slow}$ and a_{PCr} denote the time constants and magnitude, respectively. The fast and slow components of the sum equation are weighted with the factor f_{PCr} and 1-f_{PCr}, respectively.

3.3.Results

Calibration measurements

Table 3-1 summarizes the mean results of the five calibration measurements performed with two different lengths of the gas sampling line. Compared to the original 3 m sampling line the response time (t_{10-90}, O_2 and CO_2) increased on average by at most 0.05 s for the 5 m line. Similarly, the mean delay time (t_A, O_2 and CO_2) was increased by 0.79 s for the 5 m line. These changes are

comparable to the findings of other studies (Roecker, Prettin and Sorichter, 2005; Bringard *et al.*, 2012). The additional in vivo measurements outside the MR scanner yielded similar resting state VO_2 and VCO_2 values as well as comparable kinetics of load induced gas exchange adaptations for the 3 m and 5 m sampling lines, indicating that the line extensions had no significant effects on the spirometric measurements (Figure 3-3a).

Table 3-1 Mean t_A and t_{10-90} values of the five initial calibration measurements of the sampling lines (mean ± standard deviation).

	3 m sampling line		**5 m sampling line**	
	O_2	**CO_2**	**O_2**	**CO_2**
Response time t_{10-90} [s]	0.288 ± 0.019	0.163 ± 0.025	0.307 ± 0.031	0.212 ± 0.007
Delay time t_A [s]	1.285 ± 0.124	1.173 ± 0.129	2.075 ± 0.01	1.96 ± 0.012

In vivo measurements

Metabolic parameters derived from the ^{31}P-MRS and parameters of the gas exchange dynamics from the spiroergometry measurements are summarized in Table 3-2. Figure 3-4 shows representative PCr and pH time courses obtained with the rest-load-recovery protocol, whereas the corresponding VO_2 and VCO_2 results are illustrated in Figure 3-3b.

Table 3-2 Mean metabolic and pulmonary parameters determined by means of combined ^{31}P magnetic resonance spectroscopic and spirometric measurements during rest, exercise and recovery of the applied protocol (mean ± standard deviation).

^{31}P-MRS	
pH_{rest}	7.03 ± 0.02
pH_{load}	6.45 ± 0.22
$\tau_{PCr\ fast}$ [s]	93 ± 39
$\tau_{PCr\ slow}$ [s]	460 ± 241
f_{PCr}	0.71 ± 0.1
Spirometry	
f_{VO2}	0.93 ± 0.13
f_{VCO2}	0.86 ± 0.15
$VO_{2\ rest}$ [l/min]	0.28 ± 0.05
$VCO_{2\ rest}$ [l/min]	0.22 ± 0.05
$VO_{2\ load}$ [l/min]	1.05 ± 0.3
$VCO_{2\ load}$[l/min]	1.11 ± 0.33
VE_{rest} [l/min]	7.6 ± 1.8
VE_{load} [l/min]	29.8 ± 8.1
excess CO_2 [l]	2.24 ± 1.67
$VO_2\ \tau_{fast}$ [s]	56 ± 10
$VO_2\ \tau_{slow}$ [s]	330 ± 153
$VCO_2\ \tau_{fast}$ [s]	86 ± 33
$VCO_2\ \tau_{slow}$ [s]	260 ± 105

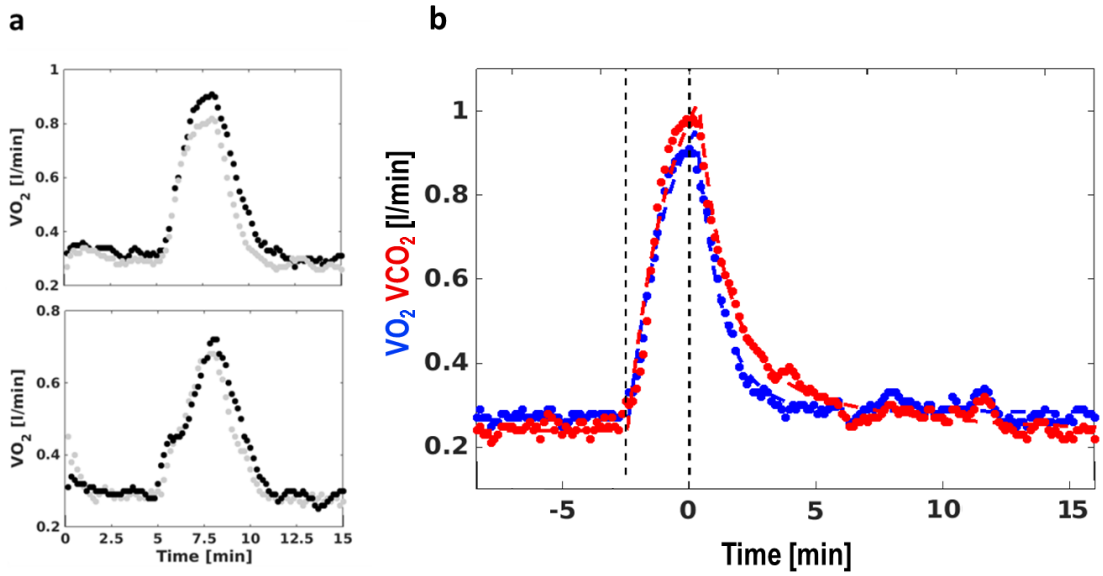

Figure 3-3 (a) Signal-time-courses of VO_2 measured in two subjects with 3 m (gray dots) and 5 m (black dots) sampling lines. (b) Representative signal-time-courses of VO_2 (blue) and VCO_2 (red) during rest, exercise (vertical black broken lines), and recovery as measured in the MR scanner. The colored dashed lines are the corresponding fits. Both VO_2 and VCO_2 show steep increases during load. Increased VCO_2 levels above the VO_2 levels during exercise and recovery correspond to the so-called excess CO_2. The latter was calculated from the difference between the integrals of the area under the VO_2 and VCO_2 fit time curves.

The attained O_2 consumption (1.05 ± 0.3 L/min) and CO_2 exhalation (1.11 ± 0.33 L/min) during load both indicate high pulmonary adaptation when considered against the small loaded muscle group (<15% of the whole muscle mass). For all subjects, VO_2 reached its peak value after a short delay of approximately 10 s after the end of the exercise, before it decreased which, however, may be due to the low temporal sampling resolution (10 s) and should be investigated in further measurements with breath-by-breath data sampling. The weighting factor of the bi-exponential function (f = 0.93 ± 0.13) showed a distinct weighting towards the fast component and a rather negligible impact of the slower component. For all subjects, the integrated area under the VCO_2 curve was higher than the integrated area under the VO_2 curve indicating accumulation of non-metabolic CO_2. Averaged over all subjects, the excess CO_2 value was 2.24 ± 1.67 l.

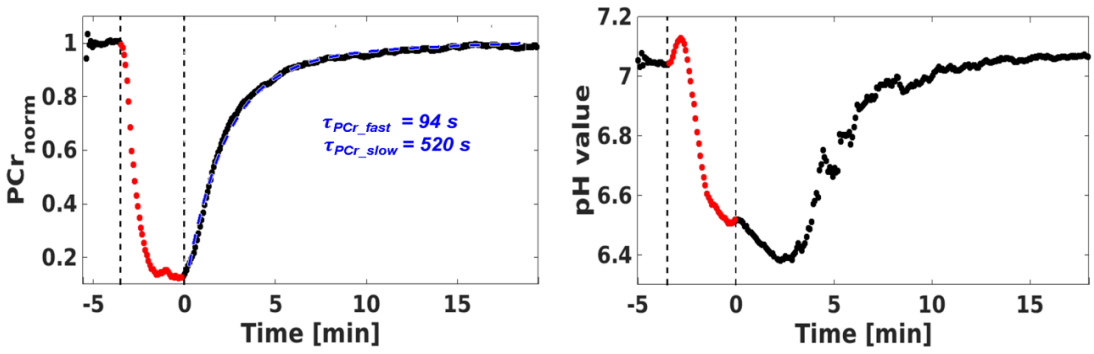

Figure 3-4 Representative PCr (left) and pH (right) signal-time courses during rest, exercise (between broken vertical lines) and the recovery phase of the experiment. During the load phase, PCr shows a fast depletion below 20% of its initial level followed by the recovery phase. The blue broken line represents the bi-exponential recovery fit with an extracted fast and slow time constant of 94 s and 520 s, respectively. The muscular pH value drops further after the end of the load due to PCr re-synthesis, before it starts to rise again towards its resting value.

All subjects showed a strong initial PCr depletion below 20% of its resting state level after less than 70 s into the exercise, indicating a stressful work rate. Following the end of the exercise, PCr recovered to pre-exercise levels with a mean fast and slow time constant of 93 ± 39 s and 460 ± 241 s, respectively. This relatively slow kinetics goes with the high metabolic and acid responses in the wake of the exercise (pH_{load} = 6.45 ± 0.22). As indicated by its relatively high weighting factor of 0.71 ± 0.1 (f_{PCr}, see Eq. 3-3), the fast PCr recovery component dominated the PCr intensity evolution after the exercise. In five subjects, the signal of Pi decreased during recovery towards or even below the noise level, and thus became unidentifiable after 6 - 12 min over a period of up to 6 min (4.2 ± 1.6 min).

Figure 3-5a shows a scatter plot of the τ_{PCr_fast} time constants of the bi-exponential fit against the individual post-load pH values for all ten subjects revealing a strong negative correlation (R^2 = 0.73, $p < 0.005$). The time constant of the fast VO_2 recovery component ($VO_{2\,\tau\,fast}$) was positively, albeit more weakly correlated with τ_{PCr} (R^2 = 0.55, p = 0.01, Figure 3-5b). Except for one subject with an unusually high difference of 0.4 l/min between the peak values of VO_2 and VCO_2 on the one hand and a relatively low pH_{load} = 6.6 (see the red dot in Figure 3-5c) on the other hand, the excess CO_2 revealed a significant negative correlation to the pH value at the end of the exercise (R^2 = 0.65, $p < 0.01$).

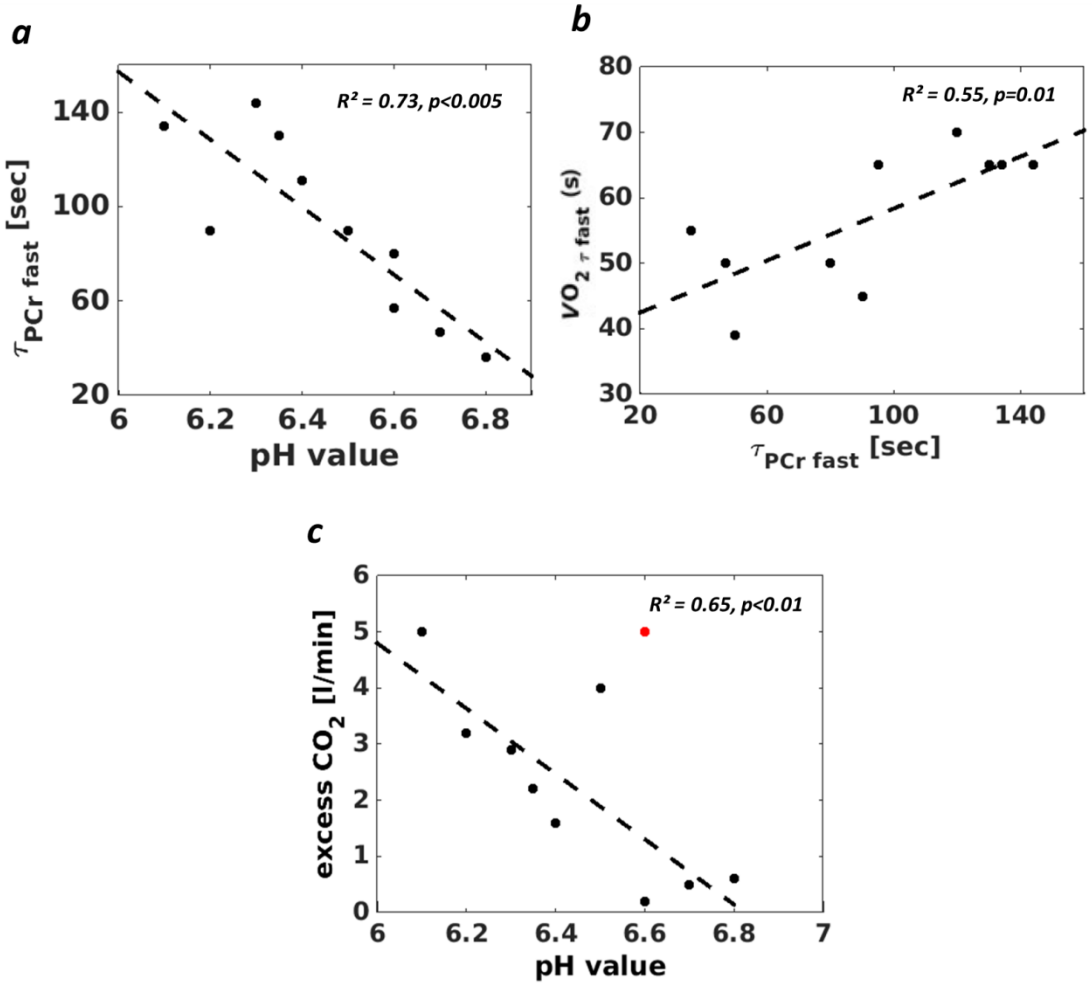

Figure 3-5 (a) Scatter plot of PCr recovery time constants ($\tau_{PCr\ fast}$) of the bi-exponential fit against individual end-exercise pH values, together with the linear regression line, indicating a strong negative correlation between the two quantities. (b) Scatter plot of the time constants of the fast component of VO_2 decrease during recovery against the corresponding PCr recovery rate constants ($\tau_{PCr\ fast}$) of the bi-exponential fit. The broken line represents the linear regression line indicating the positive correlation between both time constants. (c) Scatter plot of the individual excess CO_2 and end-exercise pH values, showing a significant negative association between bicarbonate buffering-related CO_2 overshoot and pH. The red dot represents one subject with a high amount of exhaled CO_2 due to hyperventilation, which was excluded from this correlation analysis.

3.4.Discussion

This work describes simultaneously performed spirometric and functional ^{31}P–MRS measurements in vivo using an appropriately adapted commercial spirometry system. By extending the sampling line, the spirometer could be placed outside of the MR scanner room to avoid any adverse electromagnetic interference between the scanner and the spirometer. This extension affected the VO_2 and VCO_2 data acquisition by an increase in the response and delay times (see Table 3-1). The

latter is in accordance with the system's generic delay time, which was manually increased from 1.25 to 2 s directly in the software. These changes in delay time are in line with values measured in previous studies (Whipp *et al.*, 1999; Rossiter *et al.*, 2000; Rossiter, Ward, Howe, *et al.*, 2002; Bringard *et al.*, 2012; Layec *et al.*, 2012). A crucial point in spirometry measurements is the high breathing frequency above 1 s^{-1}, in which flow and gas signals are not synchronized because of overlapping breath analyses, resulting in an overestimation of the pulmonary VO_2 uptake. However, with regard to the moderate maximum breathing frequencies in our study (< 0.5 s^{-1}), even a long response time of 0.3 s for O_2 had no effect on the accuracy of the VO_2 determination in consecutive breathing cycles. This was also demonstrated in our preliminary in vivo measurements with 3 m and 5 m sampling lines, which yielded no significant differences between the two line lengths.

Interestingly, we observed large respiratory changes in all subjects, despite stressing less than 15% of their whole muscle mass (see $VO_{2\,load}$ and $VCO_{2\,load}$ in Table 3-2). We presume that these respiratory responses are mainly related to the calf muscle load, as we reduced the participation of other muscles in oxygen consumption to the greatest possible extent by using a shoulder harness, which effectively suppresses whole-body movements during the exercise. For the analysis of post-exercise VO_2 dynamics, we applied a bi-exponential model proposed by Özyener et al. (Ozyener *et al.*, 2001), which comprises fast and slow gas volume depletion components. The fast component describes the oxygen supply for aerobic refilling of the cellular stores of PCr andO_2, whereas the slow component is related to the depletion of accumulated lactate (Wahl, Bloch and Mester, 2009). In our study, both time constants showed high inter-individual variations, especially for the long time constant, which was also reported by Özyener et al. (Ozyener *et al.*, 2001). during a whole-body exercise and linked to physiological breath-by-breath fluctuations and individual endurance or strength training orientation (Ozyener *et al.*, 2001; Wahl, Bloch and Mester, 2009). The breath-by-breath noise affects the estimation of kinetic parameters, such as the time constants of VO_2 and VCO_2, and occurs with different intensities among subjects (Lamarra *et al.*, 1987). Nonetheless, because of the clear domination of the fast component ($f_{VO2} = 0.93 \pm 0.13$), the second (slow) compartment shows negligible contribution. Therefore, physiological comparisons were limited to the short time constants.

In all subjects, we observed an overshoot of CO_2 during load and recovery (so-called excess CO_2; see Table 3-2). This excess CO_2 corresponds to non-metabolic CO_2, which is formed during exercise as a result of buffering of high H^+ concentrations with bicarbonate, and is thus stoichiometrically related to the acidification of muscle and blood (Wahl, Bloch and Mester, 2009). Moreover, in the work of Roecker et al. (Roecker *et al.*, 2000), the time point of initial CO_2 increase was used to determine the so-called anaerobic threshold, which indicates the initial increase in lactate

concentration in blood. However, this relation between excess CO_2 respiration and lactic acid buffering to evaluate the amount of anaerobic energy supply is controversial, even for whole-body exercises (Roecker *et al.*, 2000).

In this study, the intense muscle loads were reflected in strong pH decreases at the end of exercise. Furthermore, our study revealed higher, but compatible, PCr time constants compared with other studies (Vandenborne *et al.*, 1991; Schmid *et al.*, 2014), again reflecting the intensity of the exercise. Vandenborne et al. (Vandenborne *et al.*, 1991) also reported similar low pH values with a slowed recovery towards resting pH after a repeated plantar flexion exercise over 2 min with 30% maximum voluntary contraction (MVC) and maximum frequency. Previously, negative correlations between pH values at the end of exercise and PCr recovery times have been reported in finger, plantar flexor muscles, quadriceps muscles and calf muscles (Vandenborne *et al.*, 1991; Poole *et al.*, 1994; Lodi *et al.*, 1997; van den Broek *et al.*, 2007; Gwenael Layec *et al.*, 2013). This association was confirmed in our in vivo cohort (see Figure 3-5 a), and reflects the alterations in inhibited mitochondrial respiration as a result of H^+ accumulation and release in muscles.

As stated previously, five subjects showed a slowly disappearing Pi peak during the recovery phase without an obvious frequency shift, followed by a re-emerging peak at the resting resonance frequency. The disappearing Pi peak may be attributed to a physiological process first described by Bendahan et al. (Bendahan *et al.*, 1990). These authors suggested a trapping of Pi in the glycogenolytic pathway and a build-up in phosphomonoester at very high load intensities (Rossiter, Ward, Howe, *et al.*, 2002). This effect still remains unclear and requires further and more detailed investigation using repeated measurements of single subjects, as well as higher field strengths for better signal-to-noise ratio (SNR) and spectral resolution.

The high adaptation of VO_2 seems to be indirectly associated with the oxidatively driven PCr recovery. This link between global and local respiration has also been shown previously by Rossiter et al. (Rossiter *et al.*, 1999). However, it should be taken into account that global VO_2 does not directly represent local O_2 supply in muscles. Therefore, verification of the interrelation between local and global parameters (PCr recovery and O_2 supply) requires additional parameters, which describe, for example, the influence of lactate accumulation and metabolic acidosis (Wasserman, Hansen and Sue, 1991) on the efficiency of oxygen release from oxyhemoglobin. We assume that exercise-induced inhibitions of H^+ efflux and lactate depletions are also reflected in VO_2 and VCO_2 kinetics, and that these effects can be assessed by means of combined ^{31}P–MRS, ^{1}H–MRS and spirometric measurements, providing better insight into anaerobic metabolism. In our study, we observed a significant negative correlation between excess CO_2 and pH values at the end of exercise, as indicated by an overshoot of the exhaled carbon dioxide (Roecker *et al.*, 2000). This

association might be ascribed to a source of lactate and H^+ from the loaded calf muscle. One subject revealed a relatively large amount of excess CO_2, but a moderate pH drop at the end of the exercise (see red data point in Figure 3-5c), which may indicate a load-induced hyperventilation leading to unusually high CO_2 exhalation. Such non-physiological breathing patterns during exercise complicate the assessment of anaerobic metabolism. For this reason, the subject was excluded from this part of the analysis. Nonetheless, using spirometry to assess VCO_2 and the amount of excess CO_2 could be worthwhile to gain a better insight into anaerobic metabolism.

In summary, this study has successfully demonstrated combined measurements of global respiratory parameters and muscular energy metabolites. The set-up was applied to healthy volunteers to investigate load-induced changes in pulmonary and metabolic data, thus enabling a more detailed view on the physiological processes that occur when muscular function is adjusted during sustained loads.

Acknowledgements

This work was supported by the Competence Centre for Interdisciplinary Prevention (KIP) at the Friedrich Schiller University Jena and the German Professional Association for Statutory Accident Insurance and Prevention in the Foodstuffs Industry and the Catering Trade (BGN). K.M. is supported by a graduate scholarship of the Friedrich-Schiller-University Jena (Landesgraduiertenstipendium). K.M. also acknowledges support by the German Academic Exchange Service (DAAD) for a short-term international scholarship at the University of Liverpool (57044996). The authors declare to have no relevant financial interests to disclose with regard to this study.

Chapter 4

4. Comparison of metabolic adaptations between endurance- and sprint-trained athletes after an exhaustive exercise in two different calf muscles using a multi-slice ^{31}P-MR spectroscopic sequence

NMR Biomed; 2017; Revision in progress

Moll K.
Gussew A.
Nisser M.
Derlien S.
Krämer M.
Reichenbach JR.

Abstract

Measurements of exercise-induced metabolic changes, like oxygen consumption, carbon dioxide exhalation or lactate concentration, are important indicators for assessing the current performance level of athletes in training science. With exercise limiting metabolic processes occurring in loaded muscles, ^{31}P-MRS represents a particularly powerful modality to identify and analyze corresponding training-induced alterations. Against this background, the current study aimed to analyze metabolic adaptations after an exhaustive exercise in two calf muscles (*m. soleus – SOL* and *m. gastrocnemius medialis - GM*) of sprinters and endurance athletes by using localized dynamic ^{31}P-MR spectroscopy. In addition, the respiratory parameters VO_2 and VCO_2 as well as blood lactate concentrations were monitored simultaneously to assess the effects of local metabolic adjustments in the loaded muscles on global physiological parameters. Besides noting obvious differences between the *SOL* and the *GM* muscles, we were also able to identify distinct physiological strategies in dealing with the exhaustive exercise by recruiting two athlete groups with opposing metabolic profiles. Endurance athletes tended to use the aerobic pathway in the metabolism of glucose, whereas sprinters produced a significantly higher peak concentration of lactate. These global findings go along with locally measured differences, especially in the main performer *GM*, with sprinters revealing a higher degree of acidification at the exercise end (pH 6.29 ± 0.20 *vs.* 6.57 ± 0.21). Endurance athletes were able to partially recover their PCr stores during the exhaustive exercise and seemed to distribute

their metabolic activity more consistently over both investigated muscles. In contrast, sprinters mainly stressed type II muscle fibers, which corresponds more to their training orientation preferring the glycolytic energy supply pathway. In conclusion, we were able to analyze the relation between specific local metabolic processes in loaded muscles and typical global adaptation parameters, conventionally used to monitor the training status of athletes, in two cohorts with different sports orientation.

4.1.Introduction

The ability to maintain muscular exercise depends on several factors including utilization of oxygen (O_2), continuous production of high-energy metabolites, and the capacity to cope with exercise-limiting variables, such as energy depletion or acidification. Different orientations in sports lead to muscle fiber adaptations to meet the performance requirements of the specific discipline and thus the ability to either produce extreme high peak forces within a short time or to sustain submaximal intensities for long time periods up to several hours (Johansen and Quistorff, 2003). Usually, all-out types of exercise performed on bicycle ergometers, treadmills or rowing machines are commonly applied methods to evaluate the exhaustion of athletes within their individual time period (Broxterman *et al.*, 2017). To do so, several physiological parameters, like maximum oxygen uptake ($VO_{2,max}$), higher O_2 requirements (slow component of O_2 during load) alongside with the inefficiency of force production (Rossiter, Ward, Howe, 2002), thresholds of O_2 consumption and initial lactate increases (Faude, Kindermann and Meyer, 2009), or the critical power as the maximal work rate in a state of aerobic balance (Jones *et al.*, 2010), are commonly quantified as representatives of the individual aerobic function and performance efficiency, which are monitored during the execution of exhaustive protocols to evaluate training status and exercise tolerance (Broxterman *et al.*, 2017). Apart from these global physiological parameters, it is well known that differently trained athletes, e.g., sprinters and endurance athletes, also show distinct variations of several local muscular quantities related to constitutional, metabolic and biomechanical aspects as well as different perfusion patterns and different muscle fiber composition even in a single muscle complex, such as the calf muscle (Edge *et al.*, 2006; Pesta *et al.*, 2013). Several authors suggested an association between changes in global whole-body parameters, like ventilation, and local, high-energy metabolic adaptations (Rossiter *et al.*, 1999; Whipp *et al.*, 1999), but also between exercise termination and accumulation of fatigue-related intramuscular metabolites as a result of different muscle fiber constellations (Hureau *et al.*, 2014). Therefore, a more comprehensive characterization of metabolite kinetics during muscular performance with non-invasive histochemical interventions has always been an important aim of sport science studies (Gastin, 2001; Johansen and Quistorff, 2003).

Against this background, localized phosphorous MR spectroscopy (^{31}P-MRS) appears to be an ideal modality in not only monitoring spatially-resolved, exercise-induced changes of high-energy metabolites non-invasively, such as phosphocreatine (PCr), inorganic phosphate (Pi) and adenosine-triphosphate (ATP), but also in resolving the ATP re-synthesis related proton accumulation and consumption in muscles (pH value) (Kemp, 2015). The latter issue is particularly important, as proton (H^+) accumulation directly impairs muscle fiber contraction (Maassen and Böning, 2008; Grassi, Rossiter and Zoladz, 2015). Exercise-limiting effects, like acidification and increase in lactate concentration, might be reduced with continuous, long-term training interventions that may either elevate perfusion and oxidative capacity due to a higher content of type I muscle fibers for endurance sports or elevate the acidosis resistance by improving the inter-muscular H^+ buffer capacity in type II muscle fibers for short and high intense exercises, which are typical for the sprint disciplines (Johansen and Quistorff, 2003; Edge *et al.*, 2006; Pesta *et al.*, 2013).

Therefore, the aim of this study was to investigate global (whole-body) adaptations in combination with local, muscle-specific changes in two groups of differently trained athletes. Both athlete groups performed an exhausting all-out calf exercise, while localized ^{31}P-MRS data of two calf muscle groups were continuously acquired together with spirometry data and blood lactate concentrations. We tested triathletes and runners with long-term endurance training, which is associated with an elevation of the proportion of oxidative type I fibers in muscle tissue (Coyle *et al.*, 1992; Mogensen *et al.*, 2006) to sustain muscular load below or at the anaerobic steady state for up to several hours. For the second group, we tested sprinters with a high proportion of type II muscle fibers (Baguet *et al.*, 2011) that are known to provide explosive muscular power. Series of dynamic ^{31}P-MR spectra were acquired in two *m. triceps surae* muscle groups, i.e., *m. soleus* (*SOL*) and *m. gastrocnemius medialis* (*GM*). These muscles were selected because they are mainly involved in plantar flexion and may both be affected by specialized training orientations (Costill *et al.*, 1979; Coyle *et al.*, 1992). Due to their different fiber composition we presumed contributions to both metabolic pathways, which are assessable by spirometry and blood lactate diagnostics. Whereas the *SOL* is composed predominately by slow twitch type I fibers utilizing the aerobic cellular respiration as the main pathway for ATP production, the *GM* exhibits a higher amount of fast twitch type II fibers, for which anaerobic glycolysis represents the main pathway (Edgerton, Smith and Simpson, 1975; Kemp, Meyerspeer and Moser, 2007). Thus, we hypothesized different metabolic adaptations between the *SOL* and *GM* muscles as well as training specific differences in the metabolic outcome between the two athlete groups when performing an exercise.

4.2.Experimental

In vivo set-up

In total, 21 male subjects practicing either sprint sports (100 m, long- and high jump, hurdles, n = 11, median age 23 years (range 18-26 yrs.) or endurance sports (triathlon and long distance runners, n = 10, median age 28 years (range 24-35 yrs.) participated in this study (see Table 4-1). All subjects performed their respective discipline for at least 5 years with regular training during that time (at least 3 days per week). In both groups, the athletic abilities ranged from state to national level. None of the endurance athletes had been involved in regular sprint-type training, but had performed continuously exercises over long distances below the lactate threshold. The sprint sport athletes had undergone regular skill and agility training as well as sprint type training and specific weight training.

Table 4-1 Subject demographics, mechanical parameter derived from the initial MVC force test and duration of exercise in the MR scanner during the main study. All parameters are presented as median values with the corresponding 25th and 75th percentile limits in brackets.

	sprint-trained athletes	**endurance-trained athletes**
Age [years]	23 (20, 26)	28 (26, 33)
Height [cm]	182 (179, 189)	183 (180, 186)
Weight [kg]	82 (78,84)	73 (71, 79)
estimated 100% MVC pedal resistance [bar]	4.8 (4.5, 5.3)	4.2 (3.7, 4.5)*
load duration (main study) [min]	7.2 (5.8, 9.3)	6.7 (5.1, 9.7)

*Significantly different from the sprint-trained group ($p \leq 0.01$)

The examination protocol of the whole study was approved by the local Ethics Committee (ID: 2478-02/09). All participants abstained from intense physical activity of the lower extremities and alcohol consumption on the day before and on the day of measurements. Prior to the main MR examination, all subjects familiarized themselves with the in-house, MR-compatible pedal ergometer (Tschiesche *et al.*, 2014), which was exploited to determine the individual maximum voluntary contraction force (MVC) of the right calf muscle. After three warming-up sets, each consisting of

12 low resistance repetitions, the pedal counter-pressure was adjusted to a submaximal resistance between 3.2 bar and 4.2 bar according to the individual level of the subjects. Next, the subjects had to deflect the pedal as often as possible through its full angular range (25°) until the point of muscular failure was reached. The number of performed deflections as well as the pedal counter-force were then used to estimate the *one repetition maximum* (1 RM) corresponding to 100% MVC by using prediction equations summarized by Mayhew *et al.* (Mayhew *et al.*, 2008). To ensure reliable accuracy of these 1 RM estimates, muscular fatigue had to occur within 10 repetitions, otherwise the exercise was repeated with a higher pedal resistance after at least 15 min of rest (Mayhew *et al.*, 2008).

The MR measurements were performed within one week after these initial MVC tests. The exercises consisted of a series of unilateral plantar flexions performed in supine position with 20% of the subject's individual MVC (corresponding to 20% of the pedal counter pressure at 1 RM) and with a frequency of 0.8 Hz. Subjects were assisted in maintaining the proper pedal frequency by a metronome. Angulation magnitudes and pedal frequencies were monitored by means of a graphical user interface hooked up to the ergometer (Tschiesche *et al.*, 2014). During load, subjects were encouraged to sustain the exercise as long as possible and verbal instructions were given to ensure constant load conditions until total fatigue of the calf muscle was reached. The latter was defined as an inability to maintain the prescribed maximum angulation magnitude or the proper pedal frequency for more than 5 s. A recovery phase of up to 25 min (depending on the individual load period) followed with released pedal position to ensure proper recovery of the muscle fibers (Moll, Gussew and Reichenbach, 2017) during which MRS data were still acquired.

Figure 4-1 illustrates the protocol of the multi-modal data acquisition (total duration: 30 min), which consisted of a rest phase (2 min), a load phase (3 - 15 min) and a recovery phase after the exercise (up to 25 min). Dynamic series of ^{31}P-MR spectra were acquired continuously on a clinical 3 T whole-body MR scanner (Magnetom PRISMA fit; bore size, 60 cm; VE11B, Siemens Healthcare, Erlangen, Germany) by using a double-tuned (^{1}H/^{31}P) transmit/receive flexible surface coil with an integrated phosphorous loop (Ø = 11 cm with an approximate penetration depth of 6 cm; RAPID BioMedical; Rimpar, Germany). The coil was fixated on the leg support frame of the ergometer and wrapped around the right lower leg.

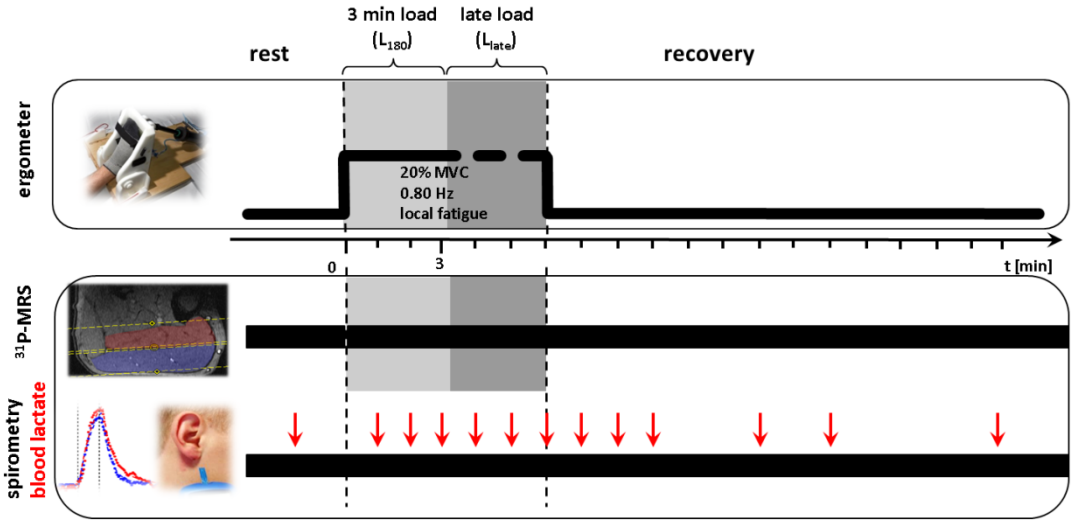

Figure 4-1 Scheme of the calf muscle exercise (20% MVC) showing the time regimes of ^{31}P-MRS (*SOL* and *GM*), spirometry, and blood lactate samplings (red arrows). The experiment consisted of three successive phases ('rest', 'load' and 'recovery') with individually variable load period depending on the time until complete muscular exhaustion was reached. For the analysis of the local metabolic changes of PCr and pH the load period was separated into an initial (L_{180}, first 3 min, lighter gray zone) and a late load phase (L_{late}, darker gray zone). The initial load phase (L_{180}) was mastered by all subjects, whereas the duration of the late phase (L_{late}) varied between the subjects.

An in-house developed ^{31}P-MRS pulse sequence, dubbed MUSCLE (MUlti SliCe Localized Excitation (Gussew *et al.*, 2017); TR = 5000 ms; flip angle: 50°; acquisition delay between excitation RF pulse and acquisition: 1.3 ms; excitation pulse duration: 1600 µs), was used to acquire series of 360 single ^{31}P-MR spectra in two parallel, 16 mm thick slices covering the *GM* and *SOL* muscle, respectively (see Figure 4-2b for slice positions). The sequence combines slice selective excitation with fast spectroscopic FID data sampling and enables interleaved measurements in multiple, spatially shifted slices (see Figure 4-2a for the sequence scheme). With an excitation pulse bandwidth of 2.45 kHz and a slice thickness of 16 mm, the maximum chemical shift displacement was 2.5 mm (between the Pi and γ-ATP specific slices). This leads to a relative slice overlap of 85% and 95% for Pi *vs.* γ-ATP and PCr *vs.* γ-ATP slices, respectively. In addition, up to four localized, outer volume suppression (OVS) bands with individually adjusted thicknesses were applied with each excitation to suppress the intra-slice magnetization in adjacent muscles (e.g., in *m. gastrocnemius lateralis*) and to improve the volume-of-interest selections within *SOL* and *GM* (see criss-crossed bands in Figure 4-2b).

Slice and OVS positions were selected based on 3D T_1-weighted gradient-echo MR images (TR/TE = 10/6.15 ms) acquired with 1 mm isotropic spatial resolution prior to ^{31}P-MRS. Automatic and manual shimming (1st and 2nd order) was performed across a volume covering both muscles of interest. For each spectroscopic slice, 24 spectra were measured during rest (2 min), followed by the acquisition of 36 to 180 spectra during load (3 - 15 min), and up to 300 spectra during recovery (25 min) (see Figure 4-1). Since the number of spectra acquired during and after load varied depending on the subject-specific exercise duration, the entire load period was subdivided into an initial phase with a constant duration of 3 min (L_{180}), which was managed by all subjects, and an individually variable, late load phase (L_{late}) (marked as lighter and darker gray zones, respectively, in Figure 4-1). This division of the load phase allowed illustrating the PCr and pH kinetics of the two subject groups during the first 3 min for all participants in a single figure. Prior to acquiring the dynamic MRS data, additional, four fully recovered resting state spectra (*reference spectra*) were collected with TR of 15 s for absolute quantitation of metabolite concentrations in *SOL* and *GM* by using the intensity of the γ-ATP peak at –2.5 ppm as internal reference (Kemp, Meyerspeer and Moser, 2007).

Oxygen uptake (VO_2 in l/min) and carbon dioxide production (VCO_2 in l/min) were monitored continuously by using a spirometry system *PowerCube* (LF8, Ganshorn, Medizin Electronic GmbH, Niederlauer, Germany), which had been adapted to enable measurements in the MR scanner (Moll *et al.*, 2017). The acquisition of the respiratory data started immediately after placing the subject into the scanner to allow habituation to the breathing mask and to avoid unusual breathing patterns due to the small breathing resistance of the pneumotachograph membrane.

Small blood samples were collected once during rest, every minute during the exercise and at 1, 2, 3, 4, 5, 8, 10 and 15 min during the recovery phase by stitching the earlobe with safety lancets (Extra 18G/ Penetration Depth 1.8 mm, Sarstedt AG&Co, Nürmbrecht, Germany). The skin was cleaned before with an antiseptic solution and slightly massaged to increase the local blood flow. Blood lactate concentrations were immediately quantified with a portable lactate SCOUT unit (EKF Diagnostics GmbH; Cardiff, UK).

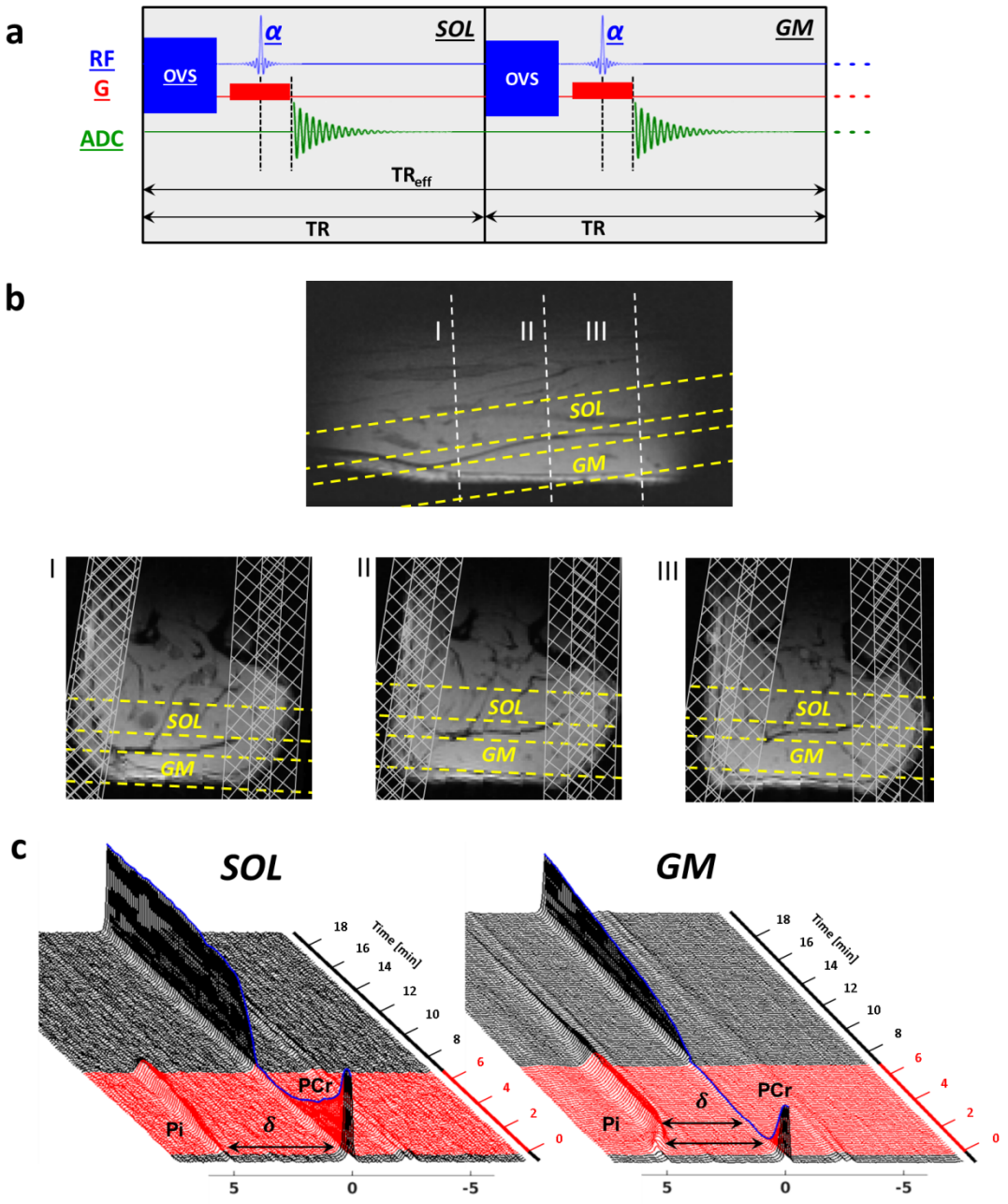

Figure 4-2 (a) Scheme of the MUSCLE pulse sequence enabling interleaved measurements in multiple, spatially shifted slices. For each slice, the effective repetition time TR_{eff} is defined by the duration of a single excite-acquire event TR multiplied by the slice number. Each event also includes a preparation period of the OVS bands. (b) Sagittal GRE image onto which the two MRS slices along the FH axis are indicated. The dashed white lines indicate positions of three orthogonal image slices, illustrating MRI cross-sections of the selected MRS slices and the muscles of interests at three different layers of the calf. The criss-crossed areas indicate the OVS bands, which were applied to suppress signal contributions from adjacent tissue. (c) Representative 'stack plots' of dynamic ^{31}P-MR spectra series of a sprint-trained athlete for the two muscles. The red areas indicate the load phase. The *SOL* series (left chart) shows a slow PCr decrease with no apparent frequency shift of the Pi peak (δ) due to pH changes. In contrast, the *GM* series (right chart) exhibits a distinct Pi frequency shift due to a strong pH decrease as well as a fast and strong reduction of the PCr intensity, which reaches its minimum approximately 60 s into the load phase.

Data analysis

All MR spectra were corrected for zero- and first-order phase errors, frequency shifts as well as baseline distortions by using an in-house MATLAB script and were quantified with an AMARES routine with prior knowledge for linewidth, frequency and peak shape (Vanhamme, van den Boogaart A and Van Huffel S, 1997) included in the jMRUI 5.2 software (www.jmrui.eu). Whereas the PCr and Pi peaks (at 0 ppm and 5.02 ppm, respectively) were each fitted as a single Lorentzian line, the α-ATP (at -7.52 ppm) and γ-ATP (-2.48 ppm) doublets and β-ATP triplets (-16.26 ppm) were quantified with pre-constrained linear combinations of two and three Lorentzian lines, respectively. While the peak linewidths were allowed to vary between 5 Hz 20 Hz, the signal phases were fixed at zero degree. Absolute metabolite concentrations were determined from the fully recovered reference spectra by normalizing the peak intensities (I_{met}) with the γ-ATP intensity ($I_{\gamma\text{-}ATP}$) and assuming a resting state muscle ATP concentration of 8.2 mmol/l (C_{met} = 8.2 mmol/l × $I_{met}/I_{\gamma\text{-}ATP}$) (Kemp, Meyerspeer and Moser, 2007). The intra-muscular pH values prior to the load onset (pH_{rest}), at the end of the initial load phase L_{180} (pH_{180}) as well as at the end of the ergometer exercise (pH_{end}) were calculated by inserting the corresponding chemical shifts between the PCr and Pi peaks (δ) into the Henderson-Hasselbalch equation (Heerschap *et al.*, 1999):

$$\boldsymbol{pH = 6.7 + log\frac{(3.27-\delta)}{(\delta-5.63)}} \qquad (4\text{-}1)$$

In addition, the potential pH increase during the L_{late} phase, indicated by ΔpH, was calculated as the difference between pH_{end} and the lowest pH value during the load phase (Figure 4-3b, lower chart). Figure 4-3a and b illustrate two representative PCr and pH time courses of the *GM* of a sprint- and an endurance-trained athlete, respectively, and also indicate the different metabolic parameters that were determined and used in the analysis. During L_{180}, the decreasing pH values, typically occurring after the short initial alkaline increase, were fitted with a mono-exponential decaying function in the *GM* to determine the acidification time constant (τ_{pH_d}). Fitting of the corresponding values in the *SOL* was dispensed, as the latter revealed distinctly lower pH drops compared to *GM*.

The PCr time courses, *PCr(t)*, were fitted in four sections including a constant term A_{rest} for the pre-load level, an initially decaying mono-exponential function (time constant τ_{PCr_d}), a mono-exponential increasing function for the partial recovery during the subsequent load phase (time constant τ_{PCr_i}) and, finally, a bi-exponential function described by a weighted sum of fast (time constant τ_{PCr_f}) and slow (time constant τ_{PCr_s}) PCr recovery during the post-load phase:

$$PCr(t) = \begin{cases} A_{rest}, & t \le t_1 \\ (PCr(t_1) - offset) \cdot e^{-\frac{t-t_1}{\tau_{PCr\_d}}} + offset, & t_1 < t \le t_2 \\ A_{init} \cdot \left(1 - e^{-\frac{t-t_2}{\tau_{PCr\_i}}}\right) + PCr(t_2), & t_2 < t \le t_3 \\ A_{rec} \cdot \left(f_{PCr}\left(1 - e^{-\frac{t-t_3}{\tau_{PCr\_f}}}\right) + (1 - f_{PCr})\left(1 - e^{-\frac{t-t_3}{\tau_{PCr\_s}}}\right)\right) + PCr(t_3), & t_3 < t \end{cases} \quad \text{(4-2)}$$

The terms A_{init} and A_{rec} denote the amplitude of the initial partial PCr increase within the ($t_3 - t_2$)-interval and the post-load PCr increase starting at t_3 until the end of data acquisition, respectively. The parameters, t_1, t_2 and t_3, indicate the time point of the onset of load, the time point of the initial partial PCr recovery during the load phase, and the time point of the end of load, respectively. The parameters f_{PCr} and (1-f_{PCr}) are the weighting factors of the fast and slow component of the bi-exponential PCr recovery during the post load phase. The *offset* in Eq. [4-2] reflects the residual PCr intensity after depletion of the PCr stores during the initial load phase.

Interestingly, the majority of sprint-trained athletes (n = 9, both muscles) and only few endurance-trained athletes (n = 2, both muscles) did not reveal a detectable increase of the PCr concentration during the load phase, whereas the majority of endurance-trained athletes (n = 8) and a minority of sprinters (n = 2) did indeed show such an increase (see Figure 4-3). The potential presence of PCr increase during the load phase was inferred prior to performing the fits by comparing the local minimum PCr concentration after load onset during the load phase (mean value of at least five successive PCr minima) and the PCr concentration at the end of the exercise. The difference between these two levels was then chosen as the starting value for the parameter A_{init} in the fit function of Eq. [4-2]. A compilation of the PCr and pH time courses for all subjects can be found in the Supplementary Material (Figures S4-1 and S4-2).

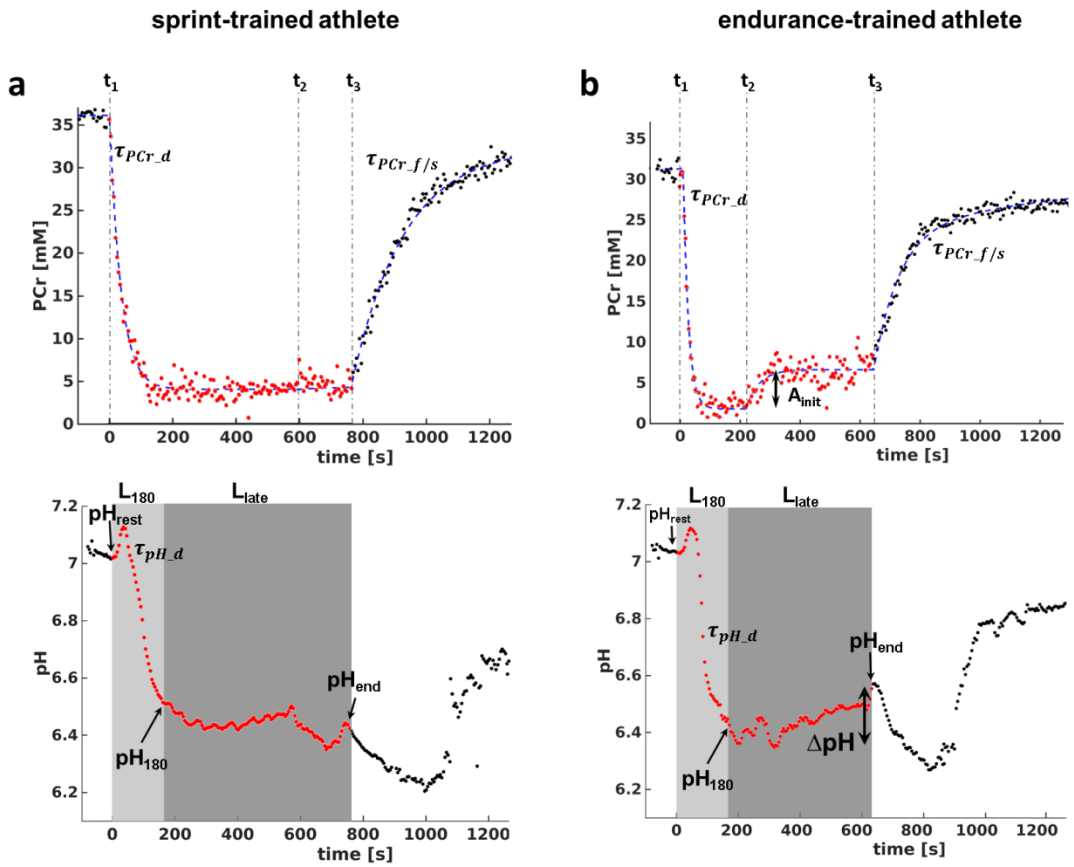

Figure 4-3 Representative PCr (upper charts) and pH (lower charts) time courses in the *GM* of a sprint-trained (a) and an endurance-trained (b) athlete during rest, load (red dots) and recovery. From the fitted PCr time course (blue dashed lines, see text for details and Eq. [4-2]), time constants of PCr decrease during load (τ_{PCr_d}) and PCr increase during recovery ($\tau_{PCr\_f/s}$) were extracted. The time points, t_1, t_2 and t_3, indicate onset of load, beginning of the partial recovery of PCr during the load phase, and end of load, respectively. The parameters pH_{rest}, pH_{180} and pH_{end} indicate the pH levels prior to load onset, at the end of the L_{180} phase, and at the end of the L_{late} phase, respectively. The L_{180} and L_{late} phases are marked as lighter and darker gray areas, respectively. For the GM data, the time constant of the pH decrease (τ_{pH_d}) during the L_{180} phase was determined from a mono-exponential fit. (a) The sprint-trained athlete shows fast PCr decrease after load onset, which levels off to a stable PCr level with no apparent partial recovery during the later load phase, L_{late}. This is paralleled by permanently low pH values or even further decreasing values towards the final pH_{end} value. (b) For the endurance-trained athlete, PCr depletes quickly below 5 mM before starting to recover partially at t_2. This is paralleled by a rapid drop of the pH value, followed by alkalization ($\Delta pH > 0$) during the L_{late} phase towards the end-exercise value pH_{end}.

Post-processing of the respiratory data has been described in detail in our previous work (Moll *et al.*, 2017). In brief, the raw spirometric data were resampled to a temporal resolution of 10 s by the vendor software. Time courses of VO_2 and VCO_2 were again fitted in sections by three different functions representing rest (constant offset), load (mono-exponential increase, τ_{VO2_i}) and recovery (bi-exponential decrease, $\tau_{VO2\_f/s}$, $\tau_{VCO2\_f/s}$) phases. Similar to the bi-exponential PCr kinetic, the

spirometric recovery during the post-load phase was weighted to assess the impact of the fast and slow component, respectively (f_{VO2}, f_{VCO2}). Besides determining the time constants during load and recovery, the resulting fit data were also used to assess the resting state (VO_{2_r} and VCO_{2_r}) and peak (VO_{2_p} and VCO_{2_p}) gas volume rates as well as the exercise-induced over-shoot of CO_2 over the O_2 volume (*excess CO_2* in l), which was determined from the difference between the areas under the superimposed fitted VO_2 and VCO_2 curves during load and recovery. In order to consider the inter-individual offsets between VO_2 and VCO_2 levels, the fitted curves were co-aligned with respect to their resting state levels prior to the calculation of the accumulated amount of excess CO_2.

Finally, the blood lactate evolutions were modelled using a simple kinetic model based on pharmacokinetic theory and was fitted to the following equation, which describes the lactate release from the muscle into the blood compartment as well as the lactate elimination due to dilution and oxidative depletion (Francaux, Jacqmin and Sturbois, 1989):

$$\boldsymbol{Lac(t) = A_{lac} \cdot \left(\frac{\tau_{depl}}{\tau_{depl} - \tau_{rel}}\right) \cdot \left(e^{-\frac{t}{\tau_{depl}}} - e^{-\frac{t}{\tau_{rel}}}\right) + offset} \qquad (4\text{-}3)$$

The term A_{lac} denotes the amplitude of lactate increase and τ_{rel} and τ_{depl} are the time constants of lactate release and depletion, respectively. The *offset* denotes the constant blood lactate concentration at rest (Lac_{rest}), which is defined by the equilibrium between lactate release and elimination.

Statistical analysis

All values are reported as median values with the corresponding 25th and 75th percentiles, calculated separately for *SOL* and *GM* muscles and for both athlete groups. To compare between the athlete groups and the calf muscles, the two-sided Wilcoxon rank sum was used. Data were analyzed with an α-level of 0.05 to determine statistical significance in all tests. The *p*-values from the two-sided Wilcoxon rank sum test, which were calculated by testing the differences between the athlete groups and the calf muscles, were adjusted by applying the Bonferroni-Holm procedure as a post-hoc test for correcting for multiple comparisons (Holm, 1979). Therefore, parameters were subdivided into groups corresponding to the same metabolic processes i.e., the PCr values prior to the load, a group containing the load related PCr decreases and the corresponding time constants; a group containing the pH values after 180 s, the pH values after the end of the exercise and the time constant of pH decrease; a group containing the time constants of the VO_2 increase during load, peak values of VO_2 and VCO_2 and excess CO_2; the lactate values during rest; and a group containing changes in lactate concentration and the time constants in lactate release and depletion.

Estimated *p*-values (p_1, p_2 …pk) were then ordered from the highest to the lowest and corrected as follows:

$$\boldsymbol{p_{corr\_k} = \frac{p_k}{n+1-k}} \qquad (4\text{-}4)$$

where *k* is the index of each *p*-value and *n* is the number of parameters within each group. Corrected *p*-values are stated in Table 4-2 and Table 4-3. The associations between muscle-related and global metabolic changes were quantified by using the Spearman's correlation coefficient.

4.3. Results

Sprint-trained athletes were able to overcome significantly higher counter pressures during the initial MVC measurement compared to endurance-trained athletes (see Table 4-1; estimated 1 RM and 100% MVC counter pressure, sprinters: 4.8 (4.5, 5.3) bar *vs.* endurance athletes: 4.2 (3.7, 4.5) bar; $p \leq 0.01$). Both groups showed similar but inter-individually strongly varying exercise durations during the measurements in the MR scanner (see Table 4-1, load duration, sprinters: 7.2 (5.8, 9.3) min; endurance athletes: 6.7 (5.1, 9.7) min; range: 3 – 15 min). The scatter of the achieved load durations is illustrated in the Supplementary Material (Figures S4-1 and S4-2) where the individual time courses of PCr concentration and pH value are presented for all subjects.

^{31}P-MRS

Prior to the load, mean linewidths of PCr were 5.4 ± 0.9 Hz and 5.8 ± 1.1 Hz in *SOL* and *GM*, respectively (see Figure 4-4 for representative resting state and load phase spectra). During the exercise, the PCr peaks broadened to 8.6 ± 3.9 Hz (*SOL*) and 9.9 ± 4.8 Hz (*GM*). Table 4-2 summarizes the median values of metabolic parameters derived from the ^{31}P-MR spectra series in *GM* and *SOL*. No significant differences in absolute resting state PCr concentrations were observed between both athlete groups neither in *SOL* nor in *GM* muscle, although a slightly higher, but insignificant PCr concentration was seen in the *GM* of sprinters compared to the endurance athletes. On the other hand, in the sprinter group resting state PCr concentrations were significantly higher in *GM* compared to *SOL* ($p = 0.03$), but not in the endurance athlete group. Figure 4-2c illustrates two representative 'stack-plots' of dynamic ^{31}P-MR spectra series from the *SOL* and *GM* of a sprint-trained volunteer. During load, distinctly weaker exercise-induced PCr depletions and smaller Pi frequency shifts are seen in *SOL* compared to *GM*, which, in turn, shows a faster and stronger PCr decrease as well as a strongly pronounced acidification. These individual observations can also be carried over to both athlete groups (see Table 4-2).

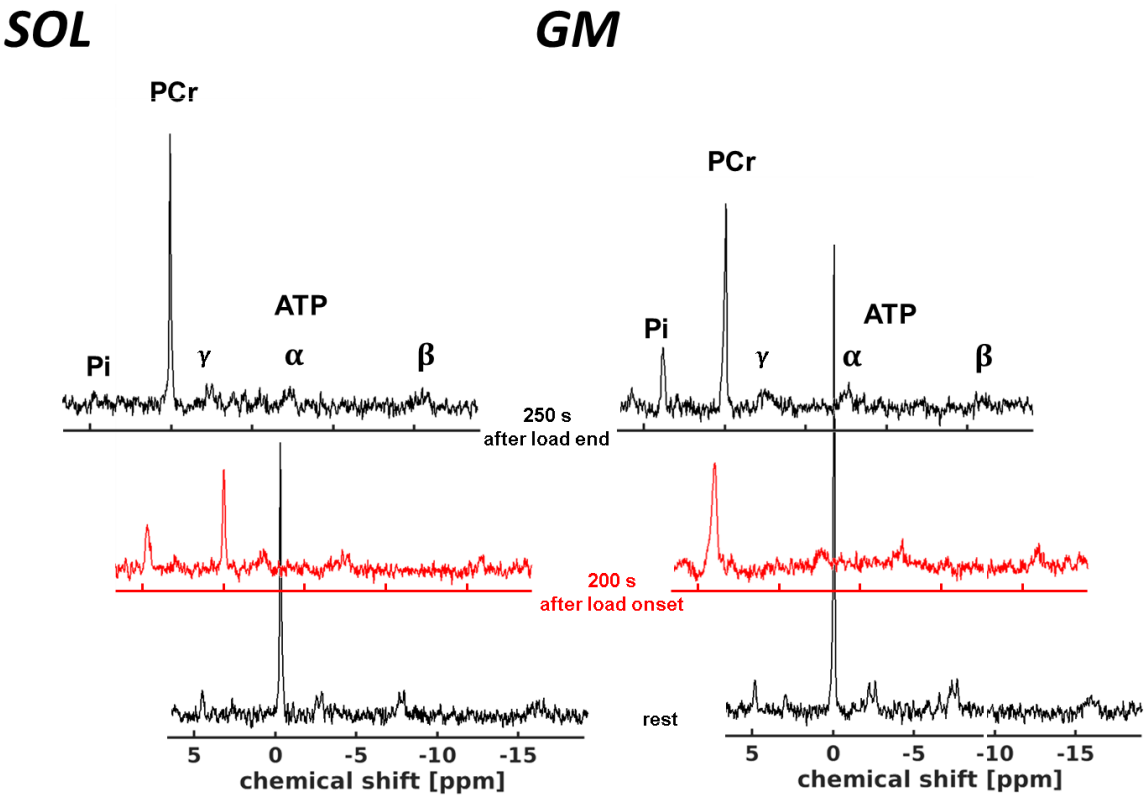

Figure 4-4 Representative ^{31}P-MR spectra acquired in *SOL* (left chart) and in *GM* (right chart) during rest (lower black graphs), 200 s after load onset (middle red graphs) and 250 s after load end.

Figure 4-5 shows the dynamics of the mean (normalized) PCr levels and mean pH values for both muscles and athlete groups during the L_{180} phase. Endurance-trained subjects revealed distinctly higher PCr depletion in the *SOL* (35 (15, 45) % of the normalized PCr level in rest) compared to sprinters with 48 (23, 57) % (Figure 4-5a, left chart). In the *GM*, almost full PCr depletion occurred in all subjects; however significantly longer PCr decay time constants were determined in the sprinter group compared to the endurance group ($\tau_{PCr\,d}$, sprinter: 29 (25, 41) s *vs.* endurance: 20 (14, 22) s; p = 0.03, see Figure 4-5a, right chart).

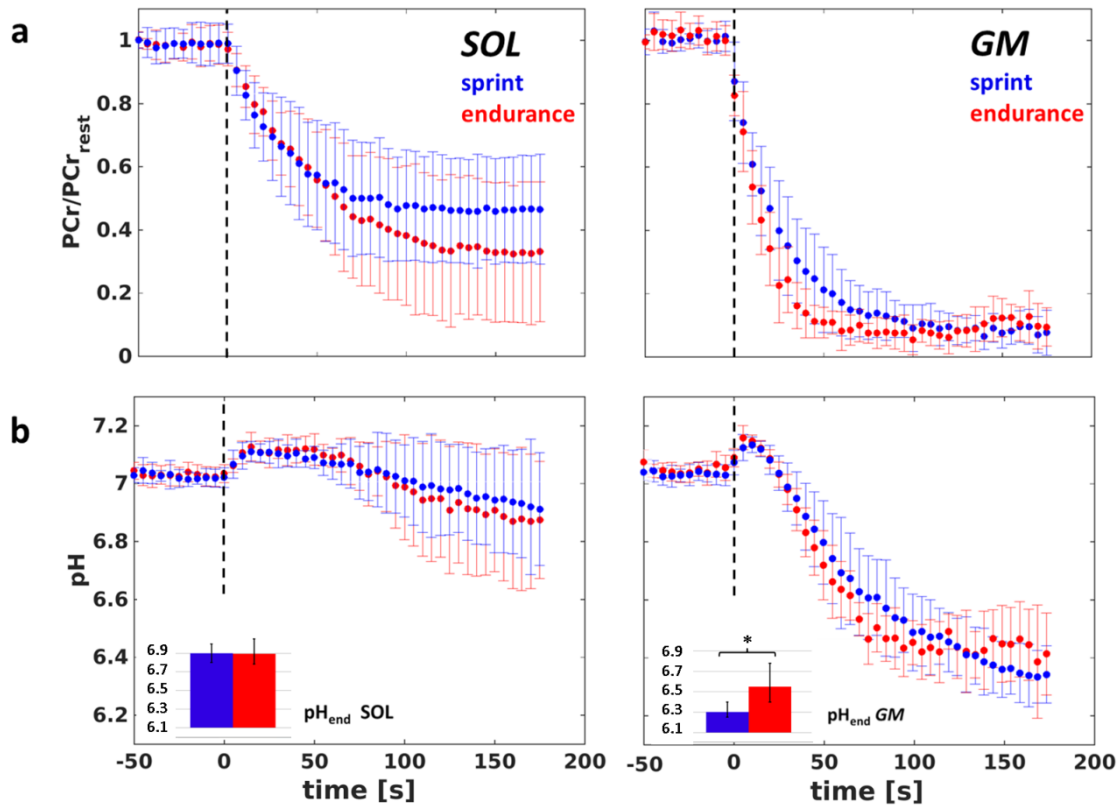

Figure 4-5 Mean kinetics of (normalized) PCr (a) and pH (b) during rest and the L_{180} phase for both muscles (*SOL*: left charts, *GM*: right charts) and both athlete groups (sprinters: blue dots, triathletes: red dots). The vertical dashed black lines represent load onset (time point t_1). The error bars indicate the standard deviations of the calculated mean metabolic parameters. (a) Compared to the endurance athletes, sprinters reveal less PCr depletion in the *SOL* and a slower PCr decay in *GM*. (b) Whereas the pH kinetics in the *SOL* is similar for both groups, it differs for the *GM*: in the sprinter group: pH decreases continuously, particularly towards the end of L_{180} phase, whereas in the endurance-trained group pH levels off approximately 70 s after load onset. The bar plots show the median values (with 25th and 75th percentiles, respectively) of pH at the end of the total load phase, pH_{end}, which were significantly different in the *GM* between the two groups.

The pH kinetics in the *SOL* represents the typical evolution for a moderately intense exercise in both athlete groups, starting with a slow alkaline shift due to H^+ consumption (creatine kinase) followed by a plateau at pH ≈ 7.1, which lasts for approximately 50 s, before starting to decrease slightly (pH_{180}, sprinter: 6.95 (6.80, 7.0) *vs.* endurance: 6.95 (6.73, 7.0); p = 0.91, see Figure 4-5b, left chart). In contrast, the pH kinetics in the *GM* reflects an intense exercise by starting with a steep increase to a alkaline pH of approximately 7.15 due to the fast PCr breakdown during the first 10 s of the exercise, followed by a monotonous drop to similar pH values for both groups at the end of the L_{180} phase (pH_{180}, sprinter: 6.35 (6.3, 6.45) *vs.* endurance: 6.4 (6.37, 6.44); p = 0.10, see Figure

4-5b, right chart). However, compared to the sprinter group showing a continuous pH decrease, the endurance athletes revealed a significantly faster pH drop in the *GM,* which levelled off approximately 70 s after load onset (τ_{pH_d}, sprinter: 53 (42, 95) s *vs.* endurance: 28 (24, 35) s; p = 0.03).

Table 4-2 Muscle- and athlete group-specific metabolic parameters extracted from the ^{31}P-MR spectra series. PCr_{dec} represents the maximum percentage drop in PCr concentration during the load phase normalized to rest. All parameters are presented as median values (25th and 75th percentile limits in brackets) with corresponding *p*-values, which were corrected by the applying the post-hoc Bonferroni-Holm procedure among subgroups and separated by gray lines. Significant differences between *SOL* and *GM* are marked with an asterisk (*); significant group differences with $p < 0.05$ are marked in bold.

	sprint-trained athletes		**endurance-trained athletes**		**p-value**	
	SOL	***GM***	***SOL***	***GM***	***SOL***	***GM***
PCr_{rest} [mmol/l]	32 (31, 35)*	36 (35, 38)*	32 (30, 33)	32 (31, 36)	0.39	0.18
PCr_{dec} [%]	48 (23, 57)*	95 (91, 95)*	35 (15, 45)*	94 (91, 95)*	0.18	-
τ_{PCr_d} [s]	45 (35, 57)	29 (25, 41)	57 (41, 70)*	20 (14, 22)*	0.28	**0.03**
τ_{pH_d} [s]	-	53 (42, 95)	-	28 (24, 35)	-	**0.03**
pH_{180}	6.95 (6.8, 7,0)*	6.35 (6.3, 6.45)*	6.95 (6.73, 7.0)*	6.4 (6.37, 6.44)*	0.91	0.10
pH_{end}	6.9 (6.8, 7.0)*	6.3 (6.2, 6.35)*	6.89 (6.73, 7.0)*	6.55 (6.4, 6.78)*	1.0	**0.04**
τ_{PCr_f} [s]	47 (41, 77)*	115 (98, 142)*	45 (23, 84)*	88 (48, 115)*	0.75	**0.04**
τ_{PCr_s} [s]	362 (210, 464)	898 (433, 915)	221 (203, 370)	662 (314, 990)	-	-
f_{PCr}	0.8 (0.8, 0.9)	0.7 (0.6, 0.9)	0.9 (0.8, 1.0)	0.8 (0.7, 1.0)	-	-

Extending the inspection of the PCr time courses beyond the L_{180} phase by including the subsequent L_{late} phase resulted in interesting findings that depended on the overall load duration subjects were able to uphold. For load durations up to approximately 350 s both athlete groups revealed similar PCr patterns showing a distinct PCr depletion during the load phase followed by recovery during the post-load phase (see upper charts of Figure 4-6). For load durations >350 s, predominantly endurance athletes (n = 8, both muscles) but only few sprinters (n = 2, both

muscles) showed a biphasic PCr profile with a partial PCr increase starting at t_2 = 200 (195, 245) sec (see lower charts of Figure 4-6 and Supplementary Figures S4-1 and S4-2).

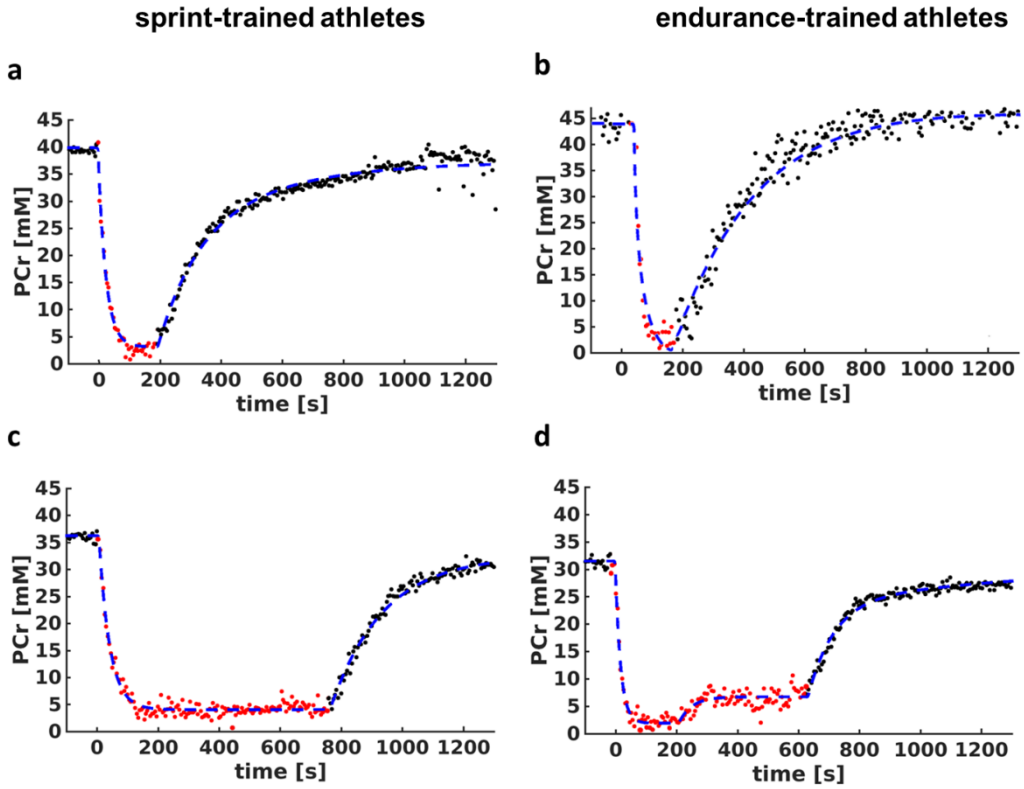

Figure 4-6 Representative PCr time courses in the *GM* of two sprint-trained (a, c) and two endurance-trained athletes (b, d). The load phase is indicated by red dots, whereas the blue dashed lines indicate the fit results (cf. Eq [4-2]). In contrast to athletes with short exercise durations (< 350s, (a),(b)), who showed similar PCr kinetics, specifically endurance-trained athletes (but also two of the sprint-trained athletes) with longer exercise periods (> 350 s, (c),(d)) revealed distinctly different PCr evolutions during the later load phase, L_{late}. As seen in (d), partial PCr recovery occurs approximately 200 s after load onset in this endurance athlete, which is not seen for the sprint-trained athlete in (c) (see text for details and Supplementary Material).

In the *GM,* this was usually accompanied by a pH increase of ΔpH = 0.25 (0.20, 0.3) among the endurance-trained athletes and a ΔpH of up to 0.2 in both sprint-trained athletes. This pH increase was less pronounced in the *SOL* (sprinters: ΔpH ≈ 0; endurance athletes: ΔpH up to 0.1). The partial recovery of PCr and the increase of pH during the later load phase L_{late} were stronger pronounced in the endurance group. Finally, comparing the pH values at the end of the exercise revealed significantly lower pH_{end} values in sprinters compared to endurance athletes in the *GM* (pH_{end}, sprinter: 6.30 (6.20, 6.35) *vs.* endurance: 6.55 (6.40, 6.78); p = 0.04, see Figure 4-5b, right chart, small bar-plot at the bottom part in the right pH chart). Figure 4-7 shows the time courses of normalized PCr concentrations obtained in both athlete groups and in both muscles during the post-load phase. For both groups, the short component of the PCr recovery was significantly faster

in the *SOL* compared to *GM* (τ_{PCr_f}, median over all subjects *SOL*: 47 (32, 77) s *vs.* median over all subjects *GM*: 101 (80, 124) s; $p < 0.001$). Comparing the results between the groups, the *GM* of endurance athletes revealed a significantly shorter recovery time constant τ_{PCr_f} compared to sprinters (τ_{PCr_f}, sprinters: 115 (98, 142) s *vs.* endurance athletes: 88 (48, 115) s; $p = 0.04$) but no significantly different results in the *SOL* (τ_{PCr_f}, sprinters: 47 (41, 77) s *vs.* endurance athletes: 45 (23, 84) s; $p = 0.75$).

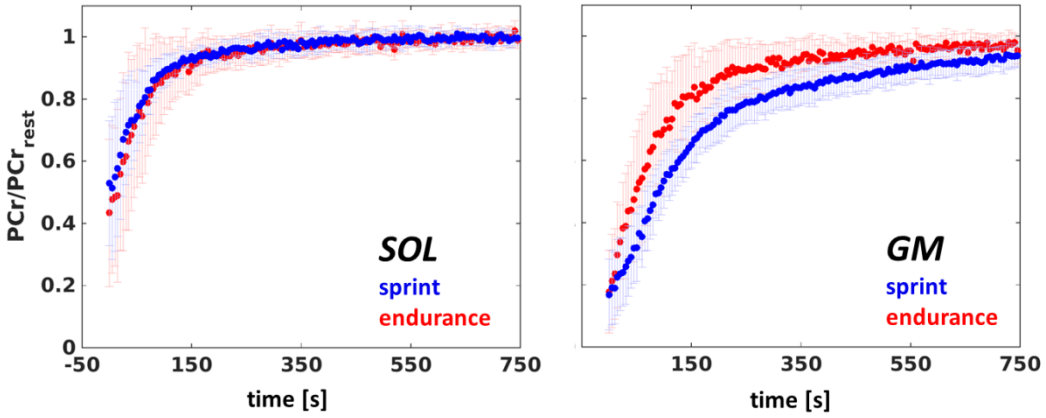

Figure 4-7 Normalized mean post-load PCr kinetics in *SOL* (a) and *GM* (b) for sprinters (blue dots) and endurance athletes (red dots). The error bars represent the corresponding standard deviations. PCr recovery is similar in the *SOL* for both groups, whereas endurance-trained athletes show a faster PCr recovery in the *GM* compared to sprinters.

Spirometry and blood lactate

Figure 4-8 displays representative time courses of respiratory and blood lactate data for one sprinter (left charts (a)) and one endurance athlete (right charts (b)). Median group values of gas volume rates and lactate concentrations obtained from the spiroergometry and blood lactate measurements, respectively, are summarized in Table 4-3. During load, both groups revealed consistent exercise-induced pulmonary changes with slightly higher VO_2 peak levels in sprinters (VO_{2_p}, sprinters: 1.1 (1.07, 1.31) l/min *vs.* endurance athletes: 0.98 (0.82, 1.08) l/min; $p = 0.28$). The sprinters also showed shorter VO_2 time constants during load (τ_{VO2_i}, sprinters: 320 (240, 410) s *vs.* endurance athletes: 440 (370, 510) s; $p = 0.33$). After the exercise, VO_2 decreased instantly for both groups, with the time constant τ_{VO2_f} for the fast component of the bi-exponential decay being shorter in endurance athletes (τ_{VO2_f}, sprinter: 60 (55, 65) s *vs.* endurance: 48 (45, 59) s; $p = 0.16$). The weighting factors of the bi-exponential function (f_{VO2} and f_{VCO2}) showed a distinct weighting towards the fast component and a rather negligible impact of the slower component (Moll *et al.*, 2017).

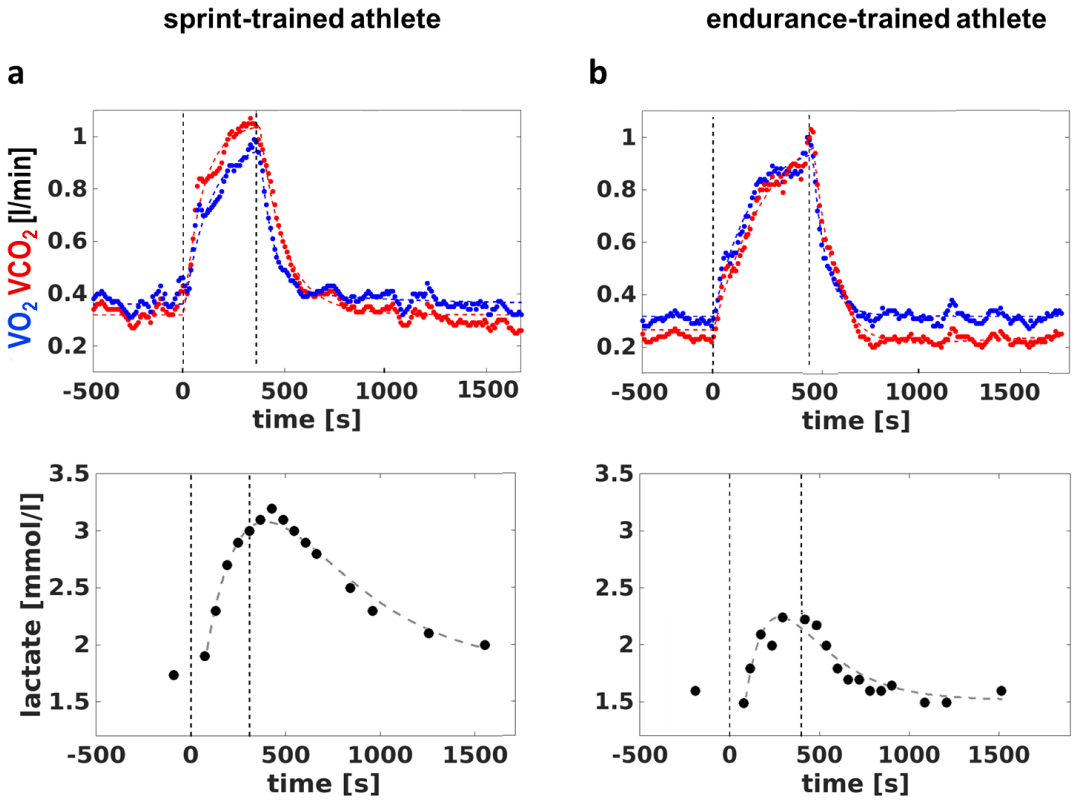

Figure 4-8 Representative VO_2 (blue) and VCO_2 (red) time courses (upper charts) and corresponding blood lactate concentration evolutions (lower charts) in a sprint-trained (a) and an endurance-trained athlete (b) prior to, during (marked by vertical dashed lines) and after the exercise. The dashed lines overlaying the parameter evolutions are the corresponding fits. The sprinter (a) shows a steeper increase of the gas volume rates and a larger overshoot of CO_2 (the area enclosed by VO_2 and VCO_2 curves during and after the load), which is mirrored in significantly higher peak lactate concentrations. The endurance-trained athlete (b) reveals a lower peak lactate level as well as a faster lactate clearance during the recovery phase.

The difference between the areas under the VCO_2 and VO_2 curves during the load and post-load phases was positive for all subjects, indicating high accumulation of non-metabolic CO_2 (*excess* CO_2, sprinter: 3.3 (2.0, 4.0) l *vs.* endurance: 1.9 (1.7, 2.9) l; p = 0.12). These anaerobic adaptations were mirrored in considerable individual blood lactate increases, which were measured within the first minutes of the post-load phase. The lactate release rates (τ_{rel}, sprinter: 499 (424, 593) s *vs.* endurance: 432 (410, 513) s; p = 0.97) were similar for both groups; however, sprinters had a higher median lactate change A_{Lac} (cf. Eq. [4-3]) (A_{Lac}, sprinters: 1.8 (1.4, 2.2) mmol/l *vs.* endurance: 1.3 (0.7, 1.5) mmol/l; p = 0.14). During the post load phase, clearance of lactate dominated over the release, with concentration depletion in sprinters being significantly slower compared to endurance athletes (τ_{depl}, sprinter: 573 (496, 681) s *vs.* endurance: 313 (234, 488) s; p = 0.03).

Table 4-3 Group-specific pulmonary parameters and lactate values derived from the spirometric and blood lactate measurements during rest, exercise and recovery phases presented as median values (25th and 75th percentile limits in brackets) and corresponding p-values, which were corrected by the applying the post-hoc Bonferroni-Holm procedure among subgroups and separated by gray lines. Significant group differences with $p < 0.05$ are marked in bold.

	sprint-trained athletes	endurance-trained athletes	p-value
τ_{VO2_i} [s]	320 (240, 410)	440 (370, 510)	0.33
VO_{2_p} [l/min]	1.1 (1.07, 1.31)	0.98 (0.82, 1.08)	0.28
VCO_{2_p} [l/min]	1.07 (0.92, 1.23)	0.96 (0.86, 1.03)	0.27
excess CO_2 [l]	3.3 (2,0 4.0)	1.9 (1.7, 2.9)	0.12
τ_{VO2_f} [s]	60 (55, 65)	48 (45, 59)	0.16
f_{VO2}	0.9 ± 0.1	0.9 ± 0.1	-
f_{VCO2}	0.8 ± 0.2	0.9 ±0.1	-
Lac_{rest} [mmol/l]	1.3 (1.3, 1.7)	1.3 (1.1, 1.5)	-
A_{Lac} [mmol/l]	1.8 (1.4, 2,2)	1.3 (0.7, 1.5)	0.14
Lac τ_{rel} [s]	499 (424, 593)	432 (410, 513)	0.97
Lac τ_{depl} [s]	573 (496, 681)	313 (234, 488)	**0.03**

Associative data analysis

In the sprint-trained group, the intra-muscular pH values in the *GM* at the end of the ergometer exercise, pH_{end}, showed a positive correlation with the load duration (sprinter, pH_{end} *vs.* load duration, R = 0.68; p = 0.02; endurance: pH_{end} *vs.* load duration, R = 0.521; p = 0.11), a trend for a positive correlation with the blood lactate changes, A_{Lac}, (sprinters: pH_{end} *vs.* A_{Lac}, R = 0.561; p = 0.06; endurance athletes: pH_{end} *vs.* A_{Lac}, R = 0.470; p = 0.17), and a negative correlation with the *excess* CO_2 levels (sprinters: pH_{end} *vs. excess* CO_2, R = -0.726; p = 0.01; endurance athletes: pH_{end} *vs. excess* CO_2, R = -0.543; p = 0.10).

Both athlete groups revealed significantly positive correlations between changes in lactate concentrations, A_{Lac}, and *excess* CO_2 levels (sprinters: A_{Lac} *vs. excess* CO_2, R = 0.548; p = 0.052; endurance athletes: Lac_{peak} *vs. excess* CO_2, R = 0.605; p = 0.038). In the sprinters, the time constants of the post-load lactate depletion, τ_{depl}, were also positively associated with the time constants of the VO_2 decay, τ_{VO2_f} (τ_{depl} *vs.* τ_{VO2_f}, R = 0.706; p = 0.02).

4.4.Discussion

In this work, a comprehensive analysis of metabolic adaptations in all-out exercised calf muscles of two differently trained athlete groups was performed by using localized dynamic ^{31}P-MR spectroscopy. Respiratory parameters VO_2 and VCO_2 as well as blood lactate concentrations were monitored simultaneously to the spectroscopic measurements in order to assess the effects of local metabolic adjustments in the loaded muscles on global physiologic parameters, which are typically used in sport science studies to evaluate the training state and fatigue resistance of athletes (Poole *et al.*, 1988; Grey *et al.*, 2014). By recruiting two opposing athlete groups we intended to differentiate the impact of specific metabolic energy supply pathways, whose kinetics are assumed to be affected by specific training orientations. Applying an advanced ^{31}P-MRS sequence with time-resolved spectra acquisition in multiple slices enabled interleaved tracking of the metabolic time courses in two different calf muscle parts.

The locally measured metabolic parameters in the current study allow separation between different training orientations with sport-specific regimes of energy supply pathways. Specifically, endurance-trained athletes showed a higher grade of metabolic adjustments, especially in the *SOL,* in terms of PCr depletion halfway through the final part of the L_{180} phase. During the first 60 s both athlete groups revealed similar PCr depletions, indicating comparable energy demands and degrees of mechanical workload (see Figure 4-4a, left chart). The subsequent plateau phase implies a leveling-off between consumption and re-synthesis of PCr, where the former is obviously more pronounced in endurance athletes. In addition, both groups showed a steady, but smooth decrease of pH as a consequence of the H^+-producing anaerobic glycolysis. However, since pH drops only to 6.9 on average, the impact of the anaerobic pathway seems to be small in the *SOL*.

In contrast to endurance athletes, sprinters showed a slower PCr decrease in *GM*, which indicates lower energy demand. Furthermore, sprinters presented with continuous pH decrease during the entire L_{180} phase, which goes along with recent findings of Pesta et al., who also demonstrated a higher grade of acidification in sprint-trained subjects and ascribed this to lower oxidative capacity and higher contractile costs of activated motor units (Pesta *et al.*, 2013). In contrast, the more distinct pH plateau, which levels off in endurance athletes during the second half of the L_{180} phase (see Figure 4-4b, right chart), indicates a reduced grade of anaerobic glycolysis compared to the sprinters. This assumption of higher efficiency of the aerobic pathway in the *GM* of endurance athletes is further supported by the significantly faster PCr recovery during the post-load phase, which again, may indicate an overall higher oxidative capacity as a result of a higher amount of type I fibers (S. C. Forbes *et al.*, 2009). The absence of a pH plateau during the L_{180} phase in sprinters' *GM* is a good marker for a continuously high anaerobic energy production leading to severe

mean acidification up to 6.3 at the end of the exercise. In contrast, the energy supply of the endurance athletes seems to be more aerobic as supported also by the lower pH drop, even though the initial decrease (τ_{pH_d}) was faster than in the sprinters. However, since the chosen exercise was fairly intense in this study compared to the usual exercising domain of endurance athletes, their long-term aerobic metabolism might have been delayed and had to be initially supported by the anaerobic pathway. This, in turn, explains the steeper acidification in the endurance athletes at the beginning of the exercise. Overall, our findings suggest a more evenly distributed metabolic activation among both muscles in endurance athletes with a higher impact of the supporter muscle *SOL* halfway through the L_{180} phase compared to sprinters who rely mostly on the main contributor *GM*. As mentioned before, this could be an indicator of different fatigue-avoiding strategies as both groups showed similar mean load durations.

An interesting, even unexpected finding of our study was the apparent different PCr and pH kinetics, which was observed in both muscles during the L_{late} phase in athletes exceeding a load duration of 350 s. Sprinters showed a constantly decreasing pH value in conjunction with fully (*GM*) or partly (*SOL*) drained PCr stores, whereas most of the endurance athletes revealed a partial PCr recovery during the load phase (see Figure 4-3). This indicates that the *GM* of sprinters utilized the anaerobic pathway to a greater extent, whereas the endurance athletes were obviously able to switch to the aerobic pathway and thus oxygenate lactate, which led to diminished PCr turnover and partial elevation of the PCr concentration (Juel, 1997). Support for this interpretation comes from the pH values, which increased in the endurance athletes despite the H^+ production of the PCr re-synthesis, thus indicating a switch towards the H^+-neutral and oxidative metabolic pathway (Kemp, 2015; Fiedler *et al.*, 2016). As a consequence, the H^+ efflux dominates the H^+ production of the anaerobic pathway. A partial PCr recovery in the muscles of endurance athletes due to a reduced energy demand can be excluded, since the load conditions in our study were kept constant during the entire exercise period by constantly checking the monitored pedal frequency and angulation. Alternatively, as indicated by similar findings in the literature, the fractional PCr and pH recoveries might also be related to the recruitment of additional motor units with a lower energy demand enabling to spread the work load over or to reduce the impact on muscle compartments (Pesta *et al.*, 2013). Because such findings were made in a professional cyclist, the occurrence of such metabolic recovery behaviors represents the effectiveness of the metabolism in highly-trained athletes. Long-term aerobic training is also known to increase fatigue resistance and selective recruitment of muscles and motor units in endurance athletes might be a way of dealing with the particular exercise type of our study (Enoka and Stuart, 1992). In agreement with findings of Pesta *et al.*, we also observed significantly faster PCr recovery kinetics (shorter τ_{PCr_f}) in the *GM* of endurance trained athletes, which indicates a higher oxidative capacity due to a larger type I fiber fraction,

higher mitochondrial density and perfusion (Pesta *et al.*, 2013). Since muscular perfusion is more elevated in endurance athletes than in sprinters, the phenomenon of fractional PCr and pH recovery may reflect an increased vasodilatory response (Duteil *et al.*, 2004). Besides the autonomic nervous system, which causes vasodilation in the first place, perfusion and blood flow are closely related to tissue metabolic activity e.g., high CO_2, lactate concentrations as well as decreased pH values, which are, however, usually more prominent in sprint-trained athletes. Thus, severe changes in the metabolism may also support an enhanced perfusion alongside with an adequate oxygen supply of the tissue.

It is well known that sport orientation-driven adaptations in the muscular metabolism, such as changes in mitochondrial density, oxygen turnover or muscle fiber fractions, are accompanied by further metabolic adjustments, including changes in perfusion, efficiency of capillary gas exchange or intermediate turnover rates (Millet *et al.*, 2002; Rivera-Brown and Frontera, 2012; Grey *et al.*, 2014). Consequently, it was not surprising to find distinctly different respiration and blood lactate characteristics between our investigated athlete groups as indicated, e.g., by the almost twice as large *excess* CO_2 levels in sprinters, which are related to the elevated anaerobic energy supply and are also mirrored in distinctly higher amounts of accumulated lactate in the blood. This association was confirmed by significant correlations between *excess* CO_2 and blood lactate peak values in both groups. As an intermediate, lactate limits muscle performance and is buffered by bicarbonate, causing the production of non-metabolic CO_2 (Beaver, Wasserman and Whipp, 1986; Roecker *et al.*, 2000). The connection between these markers of anaerobic metabolism can be explained by the fact that formation of lactic acid is directly related to the accumulation of an equimolar amount of H^+, which both lead to a pH reduction forcing bicarbonate buffering and the production of non-metabolic CO_2 during high intense exercises (Juel, 1997). Interestingly, sprint-trained athletes revealed a correlation between local acidification and *excess* CO_2 as well as between local acidification and blood lactate peaks, which implies that pH might be a good indicator for anaerobic metabolism.

According to their slower VO_2 increases (τ_{VO2_i}) during the L_{180} phase (see Figure 4-7), endurance athletes tend to demand lower O_2 amounts to sustain the mechanical output. This slow VO_2 kinetic is reflected in a faster PCr depletion (τ_{PCr_d}) in the *GM* (Jones and Poole, 2005), assuming a higher rate of anaerobic glycolysis during the L_{180} phase. In addition, the lower VO_2 rates in endurance athletes might also be associated with more efficient muscle perfusion and O_2 release by oxyhemoglobin, as is common for muscles with elevated type I proportion (Wasserman, Hansen and Sue, 1991; Yoshida, Abe and Fukuoka, 2013). However, without having access to perfusion related measures or blood oxyhemoglobin concentrations these particular effects could not be differentiated directly in the present study.

The pH leveling-off, as observed in the *GM* of the endurance group throughout the L_{180} phase, suggests an accelerated aerobic energy supply, which also explains the lower accumulation of lactate in the blood. As mentioned above, the endurance-trained athletes had distinctly lower Lac_{peak} values and lactate changes (A_{Lac}) as well as significantly faster depletion of blood lactate (lower τ_{depl}), which can be ascribed to a typical *right-shift* of the lactate-performance curve often observed in highly-trained athletes as a result of their endurance training (Heck and Schulz, 2002; Rivera-Brown and Frontera, 2012). In addition, the faster blood lactate decrease might also be promoted by a high amount of type I fibers, which are not only supposed to make up a larger fraction in the *GM* of endurance athletes but also known to metabolize lactate up to four times faster than type II fibers (Juel, 1997). Overall, the changes in the global parameters seem to be majorly driven by the distinctly more pronounced metabolic adaptations of the *GM* muscle, which acts as the main contributor of force generation in our plantar flexion setup (Price *et al.*, 2003). In contrast, the *SOL* plays a supporting role and affects the global adjustments to a lesser extent than the *GM,* as also reflected in its distinctly lower metabolic changes.

These metabolic differences between *SOL* and *GM* found in this study are in accordance with recent findings from the literature (Allen *et al.*, 1997; Valkovič *et al.*, 2014; Fiedler *et al.*, 2016; Niess *et al.*, 2017). Using a similar plantar flexion exercise setup, a considerably stronger exercise-induced PCr depletion and acidification was observed in the *GM* compared to the *SOL*. The breakdown of PCr during the initial load phase is directly linked to ATP demand and turnover, since the former acts as the sole phosphate buffer for the ATP re-synthesis (Kemp, 2015). Thus, slower initial PCr depletion in the *SOL* indicates distinctly lower activation compared to the *GM*. A reduced energy demand of the *SOL* confirms the different working domains of both muscles, which is also evident from the higher exercise-induced acidification in the *GM*. The mono-articular *SOL* acts as a supporter in the specific form of plantar flexion applied in our study with an extended knee and usually reveals constant activation to cover posture tasks. In contrast, the poly-articular main contributor *GM* is able to generate higher forces (Sale *et al.*, 1982). According to these pre-conditioned performance tasks, Allen *et al.* assumed different fiber compositions with higher amount of type I fibers in the *SOL* and higher amount of type II fibers in the *GM* (Edgerton, Smith and Simpson, 1975). This, in turn, could affect the preference of either aerobic or anaerobic energy supply in the *SOL* and *GM*, respectively (Allen *et al.*, 1997; Price *et al.*, 2003). Furthermore, the mainly oxidative metabolic contribution is reflected in the present experiment by exercise-induced pH levels around 7.0 in the *SOL* of athletes with exercise durations > 350 s (Fiedler *et al.*, 2016). Other authors confirmed the assumption of different metabolic domains, in which both muscles are working (Forbes *et al.*, 2009; Fiedler *et al.*, 2015). Thus, based on the conclusions drawn from recent findings, the pH and PCr kinetics measured in the present study indicate that the *GM* is characterized by higher

activation, higher acidification as well as a presumably higher impact of glycolytic energy supply in contrast to the *SOL*. Activation of the supportive *SOL* was more heterogeneous, especially among the endurance athletes, who tend to use it to a greater extent. This, in turn, may represent an adaptive strategy to cope with this unusual, stressful exercise.

This heterogeneous activation of *GM* and *SOL* muscles restricts the direct and objective comparison of exercise-induced metabolic changes in separate calf muscle groups. Therefore, more advanced exercise protocols, e.g., with angled knees, might be better suited to induce a more balanced activation of both muscles, and thus allow better characterization of the *SOL's* contributions to the global adjustments. Furthermore, applying an exercise protocol with multiple MVC increments could assess a broader range of metabolic adaptations in differently trained athletes and would allow a more comprehensive characterization of training-induced adjustments of energy supply as well as exercise-limiting factors. Last but not least, previously mentioned assumptions, like training-induced varying perfusion patterns and vasodilatory changes require further verification, which could be done by, e.g., additional arterial spin labeling measurements in the investigated muscle region, to characterize vasodilating effects of CO_2 on metabolic changes.

In summary, our present study demonstrates the capability of *in vivo* ^{31}P-MRS to resolve effects of different training strategies by simultaneous monitoring of exercise-induced changes of pH values and high energy phosphates in multiple muscle groups, which contribute to the mechanical output to different extents. It has been shown that training orientation leads to heterogeneous metabolic adaptations, which might be assigned to appropriate muscle fiber distributions as they make it possible to deal with different load domains during exhaustive exercises. In addition, by combining local MRS measurements with acquisition of respiratory and blood lactate data we were able to link metabolic processes in the loaded muscles with global physiological adaptations, which are commonly used to monitor the training status of athletes. Therefore, the results of the present work might be useful for setting up further studies, which focus on a comprehensive evaluation of training interventions by supporting the sport science golden standard methods with knowledge of local adjustments in trained muscles.

Chapter 5

5. The pH Heterogeneity in Human Calf Muscle During Neuromuscular Electrical Stimulation

Magnetic Resonance in Medicine; 2016; 77(6):2097-2106

Stutzig N.
Rzanny R.
Moll K.
Gussew A.
Reichenbach JR.
Siebert T.

Abstract

Purpose: The aim of the study was to examine pH heterogeneity during fatigue induced by neuromuscular electrical stimulation (NMES) using phosphorus magnetic resonance spectroscopy (^{31}P-MRS). It is hypothesized that three pH components would occur in the ^{31}P-MRS during fatigue, representing three fiber types.

Methods: The medial gastrocnemius of eight subjects was stimulated within a 3-Tesla whole body MRI scanner. The maximal force during stimulation (F_{stim}) was examined by a pressure sensor. Phosphocreatine (PCr), adenosintriphosphate, inorganic phosphate (Pi), and the corresponding pH were estimated by a nonvolume-selective ^{31}P-MRS using a small loopcoil at rest and during fatigue.

Results: During fatigue, F_{stim} and PCr decreased to 27% and 33% of their initial levels, respectively. In all cases, the Pi peak increased when NMES was started and split into three different peaks. Based on the single Pi peaks during fatigue, an alkaline (6.76 ± 0.08), a medium (6.40 ± 0.06), and an acidic (6.09 ± 0.05) pH component were observed compared to the pH (7.02 ± 0.02) at rest.

Conclusion: It is suggested that NMES is able to induce pH heterogeneity in the medial gastrocnemius, and that the single Pi peaks represent the different muscle fiber types of the skeletal muscle.

5.1. Introduction

It is well known that human skeletal muscles consist of different muscle fiber types (Brooke and Kaiser, 1970), which adapt under physical training (Andersen, Klitgaard and Saltin, 1994), age

(Lexell, 1995), or inactivity (Häkkinen, Alén and Komi, 1985; Andersen and Aagaard, 2000). Muscle fiber types are commonly classified into type I, type IIa, and type IIx based on ATPase (adenosine triphosphatase) activity (Pette and Staron, 1990). Type IIx fibers have the highest ATPase activity and accordingly the highest contractile speed (Siebert *et al.*, 2014), which is associated with high ATP costs during contraction. These fibers show a high anaerobic glycolytic potential (Pette, Peuker and Staron, 1999). In contrast, type I fibers have the lowest ATPase activity and the lowest ATP costs during contraction, and thus a high aerobic oxidative potential. The golden standard for analyzing muscle fiber types is based on histochemistry and therefore requires extraction of muscle tissue from a muscle. Extracting muscle tissue, however, may entail several complications, including pain, training cancelation, scars on skin, or even vascular injuries. Various noninvasive methods (e.g., surface electromyography (Kupa *et al.*, 1995; Farina, 2008), mechanomyography (Herda *et al.*, 2010), force-time curves (Tidow and Wiemann, 1993), muscle properties (Ranatunga and Thomas, 1990; Siebert *et al.*, 2007, 2015), and phosphorus magnetic resonance spectroscopy (^{31}P-MRS) (Takahashi *et al.*, 1996; Mäurer *et al.*, 1999) have been applied to determine muscle fiber types. However, until now a noninvasive method that is able to replace invasive methods does not exist.

^{31}P-MRS is a promising approach to determine muscle fiber types noninvasively by means of their different biochemical properties. The difference between the pH dependent chemical shift of inorganic phosphate (Pi) and the largely unaffected shift of phosphocreatine (PCr) can be used to estimate pH values in vivo (Moon and Richards, 1973; Kemp and Radda, 1994). During high-intensity dynamic exercises, decreasing pH values have been observed, as well as a split of the Pi peak in different detectable components (Park *et al.*, 1987; Achten *et al.*, 1990; Vandenborne *et al.*, 1993). So far, however, it is unknown why this pH heterogeneity occurs during fatigue. Different explanations exist, including signal contamination by another muscle (Meyerspeer *et al.*, 2011), proton fluctuations in interstitial space (MacLean, Imadojemu and Sinoway, 2000; Street, Bangsbo and Juel, 2001), or active muscle fibers with different glycolytic activity (Tesch, Thorsson and Fujitsuka, 1989; Vandenborne *et al.*, 1993; Yoshida and Watari, 1993). Two Pi peaks may be expected if the signal is contaminated by a second muscle with different pH or if pH differences exist between interstitial and intracellular space. Some studies observed even three Pi peaks, which cannot be explained by the aforementioned rationales (Vandenborne *et al.*, 1991). One possible explanation for the pH heterogeneity is the presence of different, activated muscle fiber types in the examined muscle. This effect might then be used for determining muscle fiber types. It is furthermore assumed that the peak with the highest pH value represents fiber type I with the lowest glycolytic activity, whereas the peak with the lowest pH value corresponds to fiber type IIx with the highest glycolytic activity.

Thus far, there exist some methodological limitations examining pH heterogeneity by using ^{31}P-MRS. Splitting of the Pi peak was only observed during high-intensity voluntary exercise until fatigue. However high-intensity voluntary exercise with progressive fatigue is associated with activity of different muscles and increased body movement to maintain the effort. To avoid or at least reduce the latter, Velcro stripes (Velcro Company, Manchester, NH) are commonly used to maintain the subject's position. Nevertheless, the quality (reliability and validity) of the measurements will decrease with increasing effort. Furthermore, voluntary contraction enables examination of only few muscles and always requires construction of an MRI-suitable ergometer. Consequently, an alternate method would be beneficial to control the process of muscle fatigue without voluntary contraction, which can be furthermore applied to various muscles. Neuromuscular electrical stimulation (NMES) is a common tool to induce fatigue selectively to one specific muscle without voluntary influences (Gregory and Bickel, 2005; Maffiuletti, 2010). Neuromuscular electrical stimulation uses electrical current to activate skeletal muscle and to facilitate contractions (Gregory and Bickel, 2005; Stutzig and Siebert, 2015b). In contrast to voluntary muscle activation, the recruitment order of the motor units of NMES-activated muscle fibers does not follow the size principle and is nonselective (for review see Gregory and Bickel, 2005; Maffiuletti, 2010). Furthermore, the activated muscle area depends on the stimulation intensity, that is, electric current (Adams *et al.*, 1993; Vanderthommen *et al.*, 2000). Because NMES is able to fatigue a single muscle selectively (Akima *et al.*, 2002; Stutzig and Siebert, 2015a), it appears attractive to see whether NMES produces a threefold Pi split, and thus three different pH components in the investigated muscle. To the authors' knowledge, no study exists so far that has examined NMES protocols with respect to pH heterogeneity. Therefore, the aim of our study was to apply NMES to examine the issue of pH heterogeneity. It was hypothesized that fatigue induced by NMES leads to pH heterogeneity and that 1) a three-fold peak split appears, 2) all three pH components shift significantly from baseline value at rest, and 3) the Pi peaks appear concurrent.

5.2.Methods

Subjects

Eight healthy subjects (male: 7, female: 1; age: 33.6 ± 11.2 year; height: 178.0 ± 6.7 cm; weight: 76.3 ± 13.2 kg; body mass index: 24.0 ± 3.1) participated in this study. All of them were informed about the aims and risks of the study and gave their written consent before the experiments started. The study was approved by the ethical committee of the University Hospital of Jena, Germany.

Experimental Protocol

The subjects were placed supine on a bench with their left calf put into a leg support frame of a MR-compatible pedal ergometer (Tschiesche *et al.*, 2014) and slid into the magnet bore feet first. They performed a standardized warm-up consisting of 10 submaximal isometric plantar flexions. After 2 min of rest, subjects performed two maximal voluntary contractions (MVC) separated by 1 min (Figure 5-1). If the registered MVC forces differed by more than 5%, a third MVC was performed. Prior to the measurements, MR adjustments were performed (see subsection MRS). The experiment started with ^{31}P-MRS measurements at rest for 30 s. Afterward, the medial gastrocnemius was electrically stimulated for 160 s (see subsection neuromuscular electrical stimulation), followed by a recovery phase of 510 s.

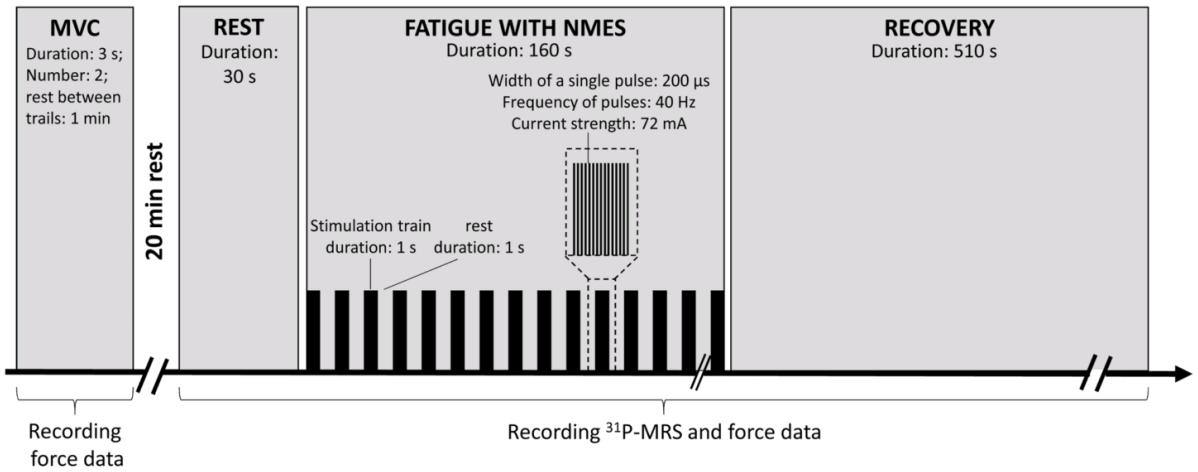

Figure 5-1 Experimental set up. The gray blocks show the conducted measurements, whereas the arrow represents the time line. MVC, maximal voluntary contraction; NMES, neuromuscular electrical stimulation.

Neuromuscular Electrical Stimulation

To fatigue the medial gastrocnemius, two carbonized rubber electrodes (size: 5 cm x 5 cm) coated with conductive gel were fixed with tape on the skin above the muscle. One electrode was placed medially, approximately 4 cm below the popliteal fossa, and the second electrode was placed on the motor point of the medial gastrocnemius. Electrical stimulations were delivered with a high-voltage stimulator (Digitimer DS7AH, Welwyn Garden City, Hertfordshire, UK). The muscle was stimulated using a pulse frequency of 40 Hz, pulse width of 200 ms, stimulation train duration of 1 s, rest time between trains of 1 s, and current strength of 72 mA. The stimulation parameters were chosen based on literature. The largest PCr depletion and pH changes within a human muscle have been observed at stimulation frequencies above 30 Hz (Matheson *et al.*, 1992) by using on–off cycles of 1:1 (Bergström and Hultman, 1988) and train durations of 0.8 s (Matheson *et al.*, 1992). The current was set at the maximal tolerated level by the subjects (Adams *et al.*, 1993; Maffiuletti, 2010; Stutzig and Siebert, 2015a).

To avoid signal MR artifacts due to interference with the NMES equipment, the high voltage stimulator was placed outside the scanner room, and shielded wires were used inside. To block radio frequency interferences (RFI), the incoming electrical pulses passed RF filters (BLP-10.7þMini-Circuits, Brooklyn, NY) that are mounted on a special filter plate of the RF shielding of the MR cabin.

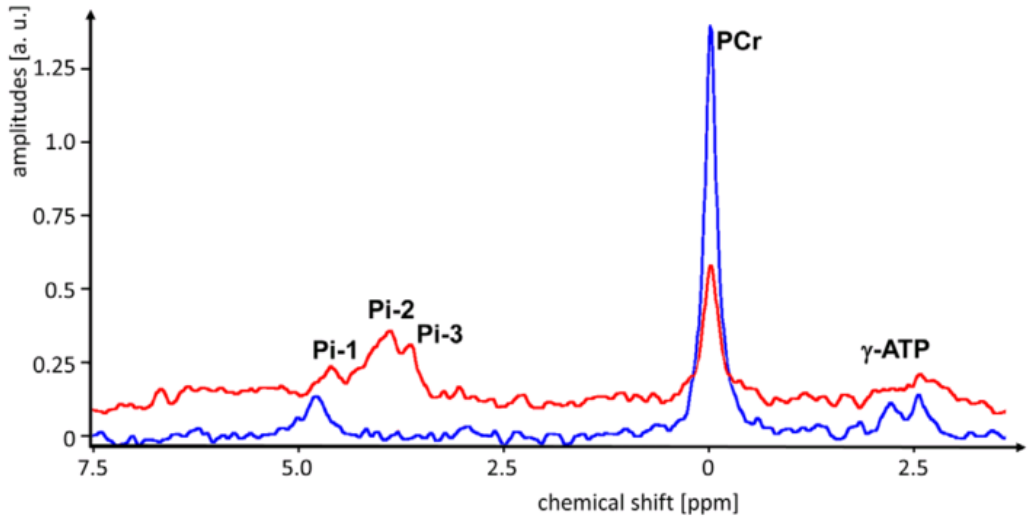

Figure 5-2 Demonstration of the peak split by a spectra prior to exercise (blue line) and 80 s after starting the exercise (red line), indicating three Pi components with corresponding pH values of 6.90 (Pi_1), 6.41 (Pi_2), and 6.04 (Pi_3). Pi, inorganic phosphate.

^{31}P Magnetic Resonance Spectroscopy

All MR measurements were performed with a 3 Tesla whole body scanner (Magnetom TIM TRIO, Siemens Healthcare, Erlangen, Germany) by using a double-tuned ^{1}H/^{31}P transmit/receive loop coil (a single wire ring for both frequencies with a diameter of 7 cm at an internal bore diameter of 6 cm; Biomedical Rapid GmbH, Würzburg, Germany), which was positioned on the most prominent bulge of the medial gastrocnemius and fixed with Velcro stripes (Velcro Company) around the calf. The position of the coil, shim volume, and coil-sensitivity profile were controlled by five T1-weighted, radio frequency (rf)-spoiled gradient echo images (repetition time (TR)/echo time (TE)/α = 6/20/90°) for each of the three orthogonal spatial planes. Spectroscopic measurements were performed by using a ^{31}P-free induction decay sequence (without gradient mediated volume selection, consisting of a block pulse followed by the signal acquisition of 1,024 data points with a dwell time of 0.5 ms, whereby the reference amplitude was adapted to a maximal signal yield) provided by the manufacturer. After shimming and frequency adjustment, two dynamic series of measurements (TR = 5 s, no averaging) were started, one for the resting measurements and a second for the stimulation and recovery phase.

Force Measurements

The force output of the plantar flexors was measured by using a hydraulic transducer, which was integrated in the pedal beneath the ball of the foot. The hydraulic transducer provides an electrical signal, which was amplified and recorded (sampling rate 200 Hz) during the experiment. The measurement system was calibrated prior to each experiment, and the obtained voltage was converted in force units (Newton). Because time data were also captured, the assignment between force and spectroscopic data was possible. The mean of the two highest MVC forces was calculated (Figure 5-1). Furthermore, the maximal force output of the first NMES train and the last NMES train was determined.

Data Analyses

Spectra were post-processed and quantified by using jMRUI (http://www.mrui.uab.es/). Post-processing included phase correction (zero- and first-order) and frequency-adjustment shifting the PCr signal to 0 ppm. Phase correction was performed by using manually estimated phase shifts of the accumulated resting spectra. Frequency shifts due to homogeneity or temperature effects were automatically corrected and manually controlled. Quantitation was performed with the advanced method for accurate, robust, and efficient spectral fitting (AMARES) (Vanhamme, van den Boogaart A and Van Huffel S, 1997) by using prior knowledge of constant intensity ratios within

the ATP multiplets (Schröder, Schmitz and Bachert, 2005). Equal line widths were assumed within the same multiplet and for the Pi components, respectively. Complete time series were inspected to estimate the splitting of the Pi signal into different pH components. By comparing consecutive spectra, the time when a peak splits into two components and their frequency time course becomes apparent. The number of detected pH components is based on those spectra with the most significant separation between two adjacent peaks, in which the components are well resolved (the signal goes down clearly between two adjacent peaks but at least by 20% [Rayleigh criterion (Rayleigh, 1880)]). However, the number of signals fitted by AMARES was already extended by a new Pi peak when one of the Pi components starts to split, and the difference between measured and fitted spectra indicates a residual signal present in the following spectra. Frequency shifts of the Pi signal caused by pH changes were considered by adapting the start values of the new fit to the results of the previous fit. The peak distances between Pi and PCr were estimated to calculate the corresponding pH values by means of the Henderson–Hasselbalch equation (Taylor *et al.*, 1986). A Pi-split into three components is demonstrated in Figure 5-2 by the comparison of spectra prior to exercise and 45 s after beginning the exercise. In the PCr recovery analysis, more than one component with different time constants was accepted by using a multi-exponential model

$$\boldsymbol{Y^{PCr}(t) = A - \sum_{j=1}^{N} B_j * exp\left(-t/\tau_j\right)}, \qquad (5\text{-}1)$$

where $Y^{PCr}(t)$ indicates the PCr signal at time t that had elapsed since the end of the exercise. The constant A represents the PCr intensity asymptotically reached at the end of the recovery ($t \rightarrow \infty$), and B_j indicates the fraction of component j with specific time constant τ_j with the condition $A \geq B_j$. To obtain an overview of the number of components with different recovery times, a NNLS analysis (Whittall *et al.*, 1997) was performed for the time series of each subject, which resolves the number of exponential components, their time constant, and their distribution without prior knowledge and has been widely used to evaluate NMR T_2 relaxometry (MacKay *et al.*, 2006). Fast and slow fractions of recovery time (B_1, B_2) correspond to muscle fiber type I and II, respectively (SC. Forbes *et al.*, 2009). The goodness of the mono- and bi-exponential fit was estimated by using the sequential quadratic programming approach of the nonlinear least square fit procedures of SPSS (SPSS 16.0 for Windows, SPSS Inc., Chicago, IL).

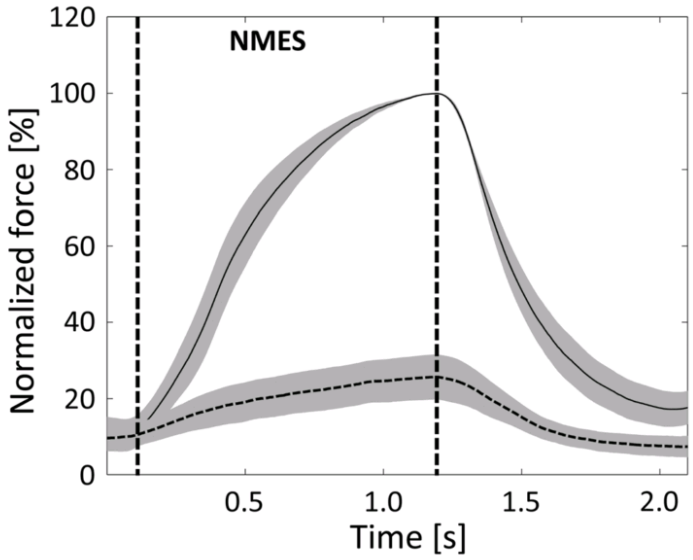

Figure 5-3 Mean (black solid line) and standard error (gray area) of the force during the first (solid line) and last NMES (dashed line) train. Data are averaged over all subjects (n = 8). The data are normalized to the maximum force of the first NMES train. NMES, neuromuscular electrical stimulation.

Statistical Analyses

Ordinary statistical analyses like means and standard error (SE) were calculated. All data were tested for normal distribution using the Kolmogorov-Smirnov test with Lilliefors correction. To test for differences between force data prior to and at the end of fatigue, a paired Student *t* test was performed. The effect size (dz) for paired *t* tests was calculated:

$$\boldsymbol{dz} = \frac{\boldsymbol{\mu_{x-y}}}{\boldsymbol{\sigma_{x-y}}}, \tag{5-2}$$

where μ_{x-y} is the difference between the means, and σ_{x-y} is the standard deviation of the mean differences. The effect sizes were classified as low (dz = 0.2), medium (dz = 0.5), and large (dz = 0.8). A one-way analysis of variance (ANOVA) for repeated measures was calculated for the pH data (pH rest vs. pH alkaline vs. pH medium vs. pH acidic), and partial eta squared (η_P^2) was used as a measure for effect size

$$\boldsymbol{\eta_P^2} = \frac{\boldsymbol{SS_{between}}}{\boldsymbol{SS_{between}+SS_{error}}}, \tag{5-3}$$

where $SS_{between}$ denotes the sum of squares of the interesting effect and SS_{error} the sum of squares of the error term of the interesting effect. The effect sizes were classified as low ($\eta P2$ = 0.01), medium

($\eta P2 = 0.06$), and large ($\eta P2 = 0.14$). In case of significant differences, a post hoc test (Bonferroni) was calculated. The level of significance was set at P = 0.05. All statistical analyses were performed using IBM SPSS Statistics for Windows (Version 22.0, IBM Corp., Armonk, NY).

5.3.RESULTS

Force Data

The mean MVC force of the subjects was 175.0 ± 11.4 N. The maximum stimulation force of the first NMES train was 40% of the MVC force. Figure 5-3 presents the mean force-time traces of the first trains and the last trains at the end of the stimulation, respectively. The data are normalized to the maximal force of the initial train. The force decreased significantly (P =0.000, $T_{1,7} = 6.62$, 95% confidence intervals: lower limit = 29.3; upper limit = 62.0, dz = 2.33) from 62.7 ± 8.2 N to 17.1 ± 4.3 N at the end of stimulation (Figure 5-4).

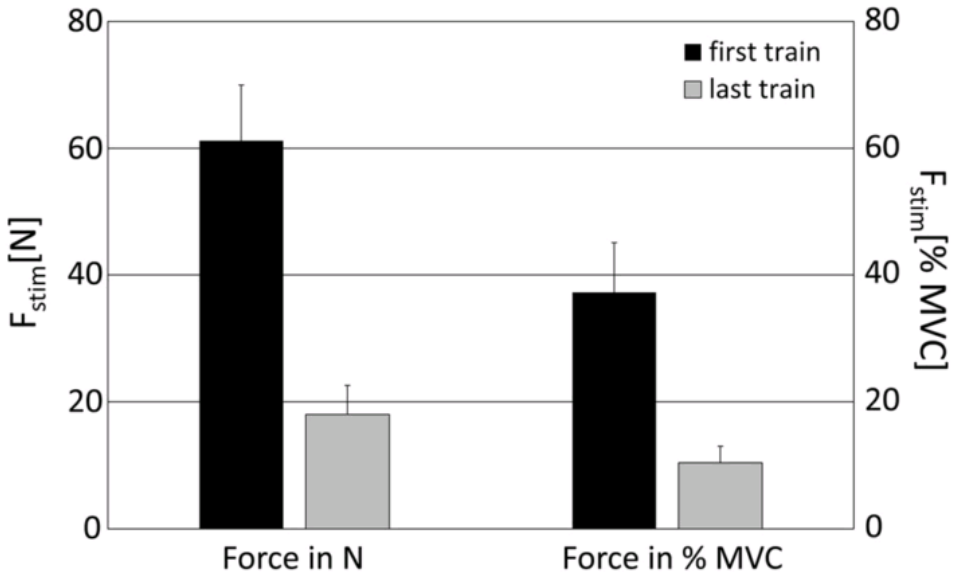

Figure 5-4 Mean and standard error of the F_{stim} at the beginning (black bars) and at the end (gray bars) of the stimulation. The axes on the left and right side of the figure represent absolute measured values (force in N) and values normalized to the maxi- mal voluntary contraction (force in % MVC), respectively. F_{stim}, maximal force during stimulation; MVC, maximal voluntary contractions.

Metabolic Data

Figure 5-5 shows the mean PCr curve during rest, NMES, and recovery. During the first third of NMES, PCr decreased to approximately 33% of its baseline value and remained constant until NMES was stopped. The analysis of the PCr kinetics during recovery revealed two recovery time constants: τ_1 = 25 ± 6 s and τ_2 = 163 ± 40 s, with corresponding fractions *B1* and *B2* of 25 ± 9% and 75 ± 9%, respectively.

During fatigue, three Pi peaks (Pi_1(left) = high pH peak, Pi_2(medium) = medium pH peak, and Pi_3(right) = low pH peak) were observed in all subjects (Fig S5-1–S5-8) based on which the corresponding pH values were calculated, and the mean pH value of the subjects were plotted (Figure 5-6). Starting from a pH value of 7.02 ± 0.02 at rest, an alkaline component (Pi_1), a medium component (Pi_2), and an acidic component (Pi_3) evolved during stimulation.

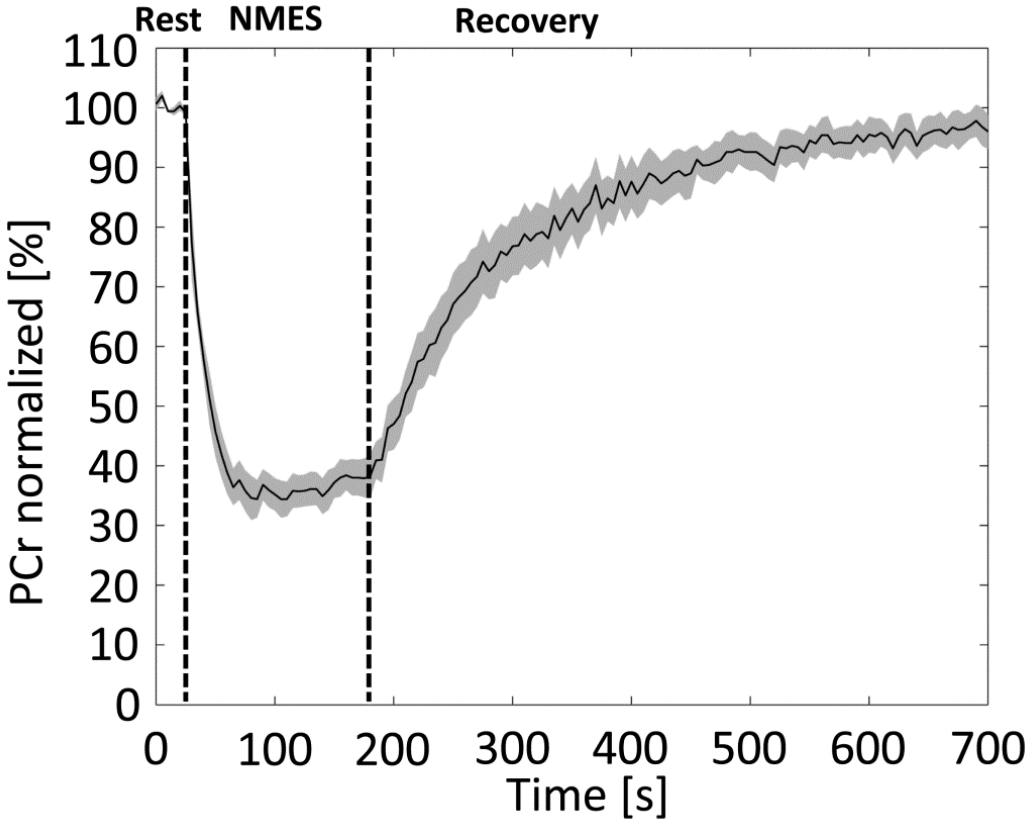

Figure 5-5 Mean (black solid line) and standard error (gray area) of PCr during rest, NMES, and recovery over eight subjects. PCr is normalized to the mean pre-fatigue value. NMES, neuromuscular electrical stimulation; PCr, phosphocreatine.

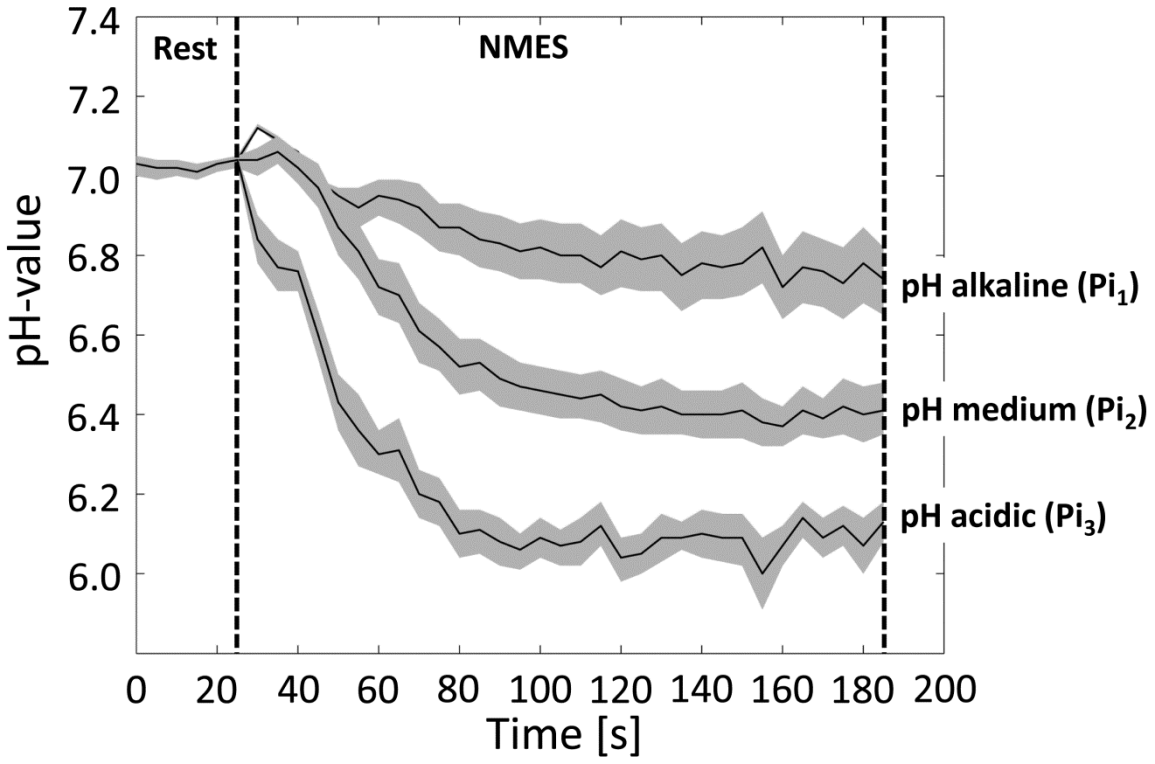

Figure 5-6 Mean (black solid line) and standard error (gray area) of the pH values during rest and NMES over eight subjects. NMES, neuromuscular electrical stimulation.

The analysis of the pH values during the last third of NMES resulted in 6.76 ± 0.08 for the alkaline, 6.40 ± 0.06 for the medium, and 6.09 ± 0.05 for the acidic component. The ANOVA for repeated measures revealed a significant main effect ($F_{1,3}$ = 143.3, P = 0.000, η_P^2 = 0.95). The post hoc test revealed differences between pH rest and pH medium (P = 0.000), as well as between pH rest and pH acidic (P = 0.000). Furthermore, there was a significant difference between pH medium and pH acidic (P = 0.000), pH alkaline and pH medium (P = 0.000), and pH alkaline and pH acidic (P = 0.000), but no significant difference between pH rest and pH alkaline (P = 0.052) (Figure 5-7).

The determination of the Pi onsets revealed that in six out of eight subjects, Pi_2 occurred first, followed by Pi_3 and then Pi_1. In one subject, all three Pi peaks occurred simultaneously after NMES was started, whereas in another subject Pi_2 and Pi_3 occurred simultaneously, followed by Pi_1. The calculation of the average Pi peak onsets for Pi_2, Pi_3, and Pi_1 revealed 0 s, 14.4 ± 13.3 s, and 23.1 ± 15.3 s, respectively. Figure 5-6 shows the mean ± SE of the pH values over all subjects. Due to the fact that in one subject all Pi peaks appeared simultaneously after NMES was started, it is not possible to identify the different onsets from Figure 5-6. The Pi areas of the single Pi peaks during the last third of stimulation were Pi_1 = 366.5 ± 108.6 arbitrary unit (a.u.),

Pi_2 = 774.4 ± 112.5 a.u., and Pi_3 = 363.5 ± 66.8 a.u. Based on the Pi areas of the single Pi peaks, the percentage distribution was calculated: Pi_1 23.464.3%, Pi_2 51.065.0%, and Pi_3 25.663.8%. Closer inspection of the Pi peak time courses revealed that in general Pi_2 appeared first, followed by Pi_3(14.46 4.3 s) and at last by Pi_1(23.865.7 s). In one subject, all three Pi components appeared simultaneously at the beginning of stimulation; in one other case, Pi_1 and Pi_2 appeared simultaneously, followed by Pi_3. To deduce for motion-induced signal changes, the total measured phosphate (Pi + PCr + ATP + PME + PDE) at rest and during stimulation were calculated. As indicated by Figure 5-8a, no substantial signal changes as sign of motion-induced shifts of the detected muscle area can be observed. The time course of the summed PCr + Pi intensity reveals a significant decrease during the first half of fatigue but increased during the second half of stimulation and remained unaltered (compared to the baseline values) until the end of fatigue. This indicates no Pi trapping occurred during the second half of fatigue.

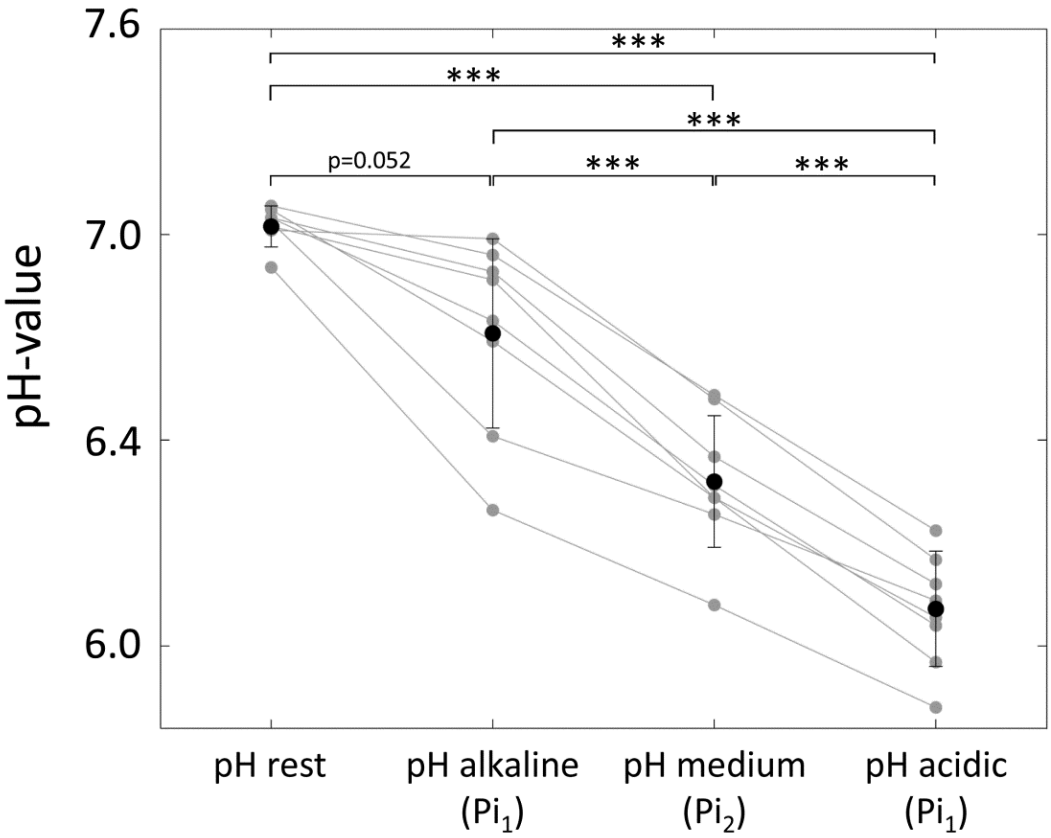

Figure 5-7 Mean (black circle), standard error (black lines), and the single subject's values (gray circles) of the pH at rest and during fatigue. Three different pH components were observed during fatigue (pH alkaline, pH medium, and pH acidic). ***P<0.001)

Imaging Data

Immediately before and after spectroscopic measurements, pre- and post-exercise T_2-weighted images were acquired using a $^{1}H/^{31}P$ loop coil. A region of increased post-fatigue intensity in the medial gastrocnemius muscle is apparent in all cases (Figure 5-9a, e and Fig S5-9–S5-12). Based on Figure 5-9e, it seems that the dividing line between stimulated and non-stimulated muscle area follows the border between the medial gastrocnemius and the soleus muscle. However, due to the non-uniform signal distribution caused by the B_1-characteristic of the surface coil, the exact boundary line of the transition between the stimulated and non-stimulated muscle area cannot be established with sufficient certainty. To reduce influences of the coil sensitivity profile on the signal intensity distribution, two NMES experiments were repeated using a flexible surface coil. The T_2^* - weighted images (Figure 5-9g and Sup. Figures S9–12) clearly demonstrate a contrast change within the medial gastrocnemius during fatigue but no or slightly changes within the soleus and lateral gastrocnemius. It is limited possible to conclude from the spatial contribution of image brightness on the distribution of ^{31}P-signal intensity in muscle tissue. Furthermore, the signal intensity from deeper muscle regions contributes to the recorded spectra. However, the absence of T_2, and T_2^* changes indicate an absence of substantial muscle activity and an absence of pH shifts of the Pi signal for these signal contributions.

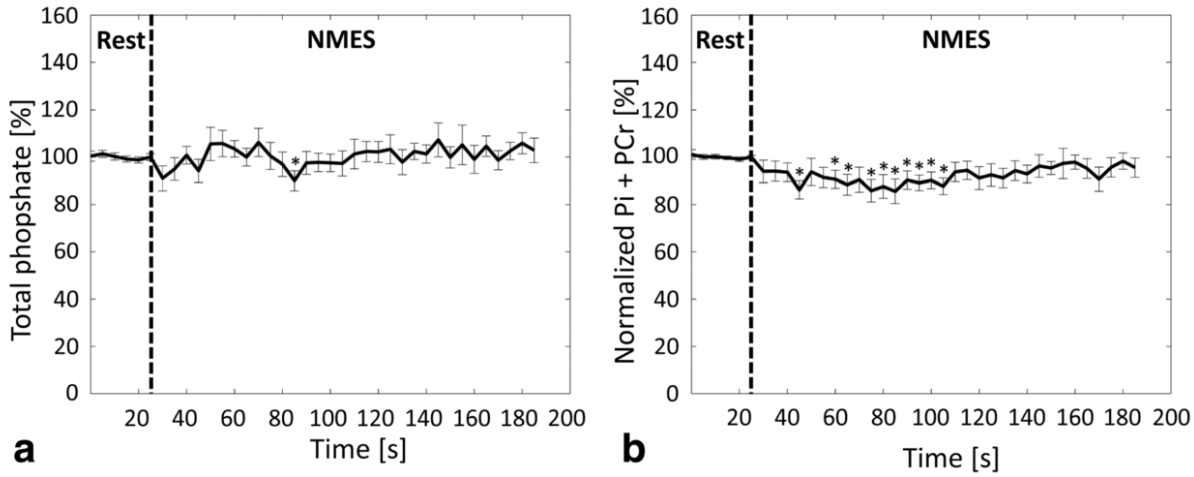

Figure 5-8 Normalized mean and standard errors of the (A) sum (total Pi + PCr) and (B) total measured phosphate (Pi + PCr + ATP + PME + PDE) during rest and fatigue (NMES). *Significant difference ($P<0.05$) compared to rest. ATP = adenosine triphosphate; NMES, neuromuscular electrical stimulation; PCr, phosphocreatine; Pi, inorganic phosphate; PME, phosphomonoester; PDE, phosphodiester.

5.4.DISCUSSION

The main purpose of the study was to investigate the possibility to induce different pH components in the medial gastrocnemius of subjects during fatigue by using NMES. Applying an on–off cycle of 1 s stimulation and 1 s rest for 160 s provoked the appearance of three different pH components in all subjects. The results suggest that the alkaline, medium, and acidic pH components represent the fiber types I, IIa, and IIx, respectively. Thus, we conclude that NMES is an appropriate means to examine fiber type distributions based on pH heterogeneity.

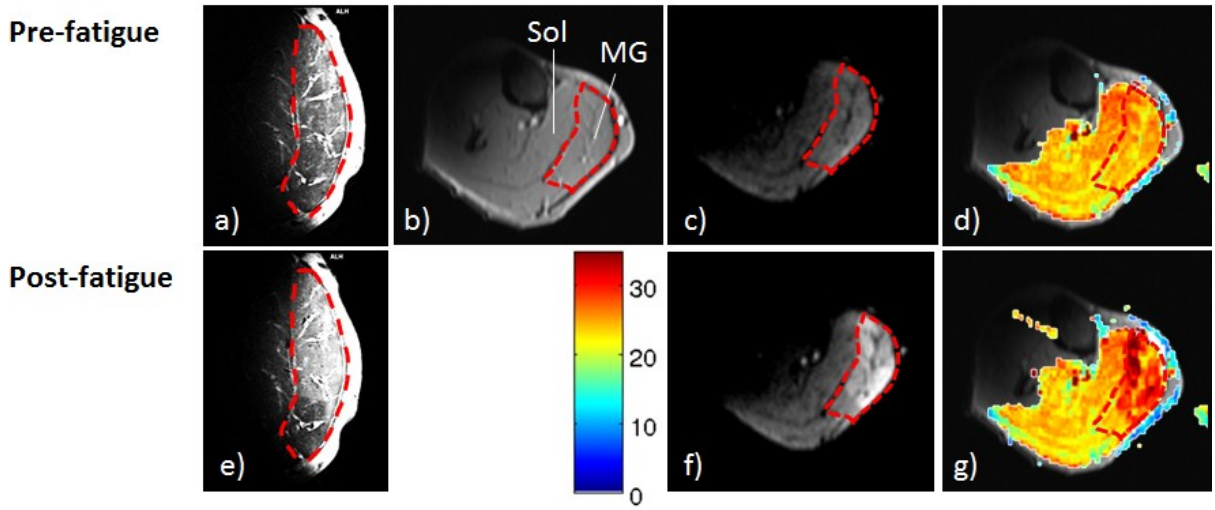

Figure 5-9 Visualization of the stimulated muscle area by signal changes between pre- and post-fatigue T_2^*-weighted gradient-echo images (a, e), and in the T_2^*-weighted multiple gradient echo-planar images using the flex coil (c, f) as well as by the T_2^* differences in the calculated T_2^* maps (d, g). The morphological structures are visualized by a T_1 image of the same slice (b).

NMES Fatigue Protocol

Pi-splitting has previously been reported to occur only with high-intensity exercises until complete muscle fatigue (Park *et al.*, 1987; Vandenborne *et al.*, 1993); therefore, a stimulation protocol was chosen that aimed to induce high metabolic demands. Because it is known that metabolic demands induced by NMES depend on the stimulation parameters (Matheson *et al.*, 1992), we selected a current pulse frequency of 40 Hz with pulse width of 200 ms to maximize this metabolic cost. Furthermore, because induced fatigue with continuous stimulation of this frequency leads to decreased propagation of the action potentials on the muscle fiber membranes, and thus decreased force without metabolic involvement, we applied an intermittent stimulation of several on (muscle activity) and off (muscle relaxation phase) cycles. A work-rest-ratio of 1:1 is appropriate to avoid partial recovery of PCr and Pi. To summarize, intermittent stimulations with the given parameters

resulted in strong fatigue (decrease of muscle pH to 6.10 ± 0.15), with PCr and force being decreased to 33.5 ± 3.7% and 25.8 ± 5.9% of their baseline values, respectively. Further fatigue might be induced by longer pulse widths.

pH Heterogeneity Induced by Fatigue

The occurrence of different pH components during muscular fatigue has been reported previously. In particular, the appearance of two distinctive Pi peaks—and thus, two pH components—has been reported (Yoshida and Watari, 1993, 1994), which were ascribed to the intracellular and interstitial space, respectively (MacLean, Imadojemu and Sinoway, 2000). However, because the interstitial pH is more alkaline at rest and has been observed to decrease from 7.38 to 7.04 during fatigue (25), whereas the highest pH value that was observed during fatigue was distinctly lower (6.76 ± 0.23) (Figure 5-7), we conclude that an interstitial space component is not contributing to our signals. Furthermore, the amount of Pi in the interstitial space is most likely too small to be visible in the spectrum. Meyerspeer et al., on the other hand, compared localized and non-localized dynamic spectroscopy to shed more light on the pH heterogeneity (Meyerspeer *et al.*, 2012). In their non-localized spectrum, they observed a split in two Pi peaks when subjects performed a plantar flexion exercise, during which the acidic peak decreased to pH of 6.68 at the end of the exercise, whereas the other pH value remained unaltered at 7.03. Interestingly, in the localized spectrum they did not find a split, but the single Pi peak decreased to a pH of 6.73. Based on their findings, the authors concluded that the non-localized spectrum was contaminated by another, more weakly used muscle. In our study, however, in contrast to Meyerspeer et al. (Meyerspeer *et al.*, 2012), we observed a threefold splitting of the Pi peak, with two peaks being shifted significantly and one trended to shift toward PCr, resulting in decreased pH. The force output at the beginning of NMES was 37.3 ± 8.3% of the MVC, which is in good agreement with expectation when assuming that the whole medial gastrocnemius was activated because the anatomical cross-sectional area accounted on average to 32% of the triceps surae (Albracht, Arampatzis and Baltzopoulos, 2008). Assuming unwanted contamination by the unfatigued soleus or lateral gastrocnemius, which is located below or lateral to the medial gastrocnemius, an unchanged pH component (i.e., pH approximately 7.00) would have been expected. Indeed, our results revealed no significant difference ($P = 0.052$) between the Pi rest and the alkaline Pi peak, which supports the assumption that the alkaline Pi peak represents unfatigued muscles (soleus or lateral gastrocnemius). However, considering the P value and the fact that in seven out of eight subjects the pH value decreased from Pi rest to Pi alkaline (Figure 5-7), we can state that the pH value at rest showed a tendency to decrease to 6.76 for the alkaline Pi peak. Furthermore, contamination from the unfatigued soleus or lateral

gastrocnemius would explain two different Pi peaks during NMES but not the three pH components that we observed in our study. Thus, signal contamination of other muscles might influence the results, but it does not explain the observed pH heterogeneity completely. A further explanation of pH heterogeneity during NMES might be the kind of muscle activity triggered by NMES. The current activates the nerve branches located closest to the electrodes; that is, the higher the current, the deeper nerve branches—and thus deeper muscle tissues will be activated. We observed that deep muscle regions were not activated or were slightly activated (Sup. Figure S9). The current intensity was not changed throughout the measurement; that is, the stimulated spatial muscle regions did not change. Thus, it might be possible that the alkaline Pi peak represents the unfatigued deep muscle region and the acidic Pi peak the fatigued muscle region. This would also explain the tendency of pH decrease in Pi_1 peak, which could be based on proton exchange between muscle cells within the MG. The explanation of pH heterogeneity based on fatigued and unfatigued muscle regions within the MG would explain two different Pi peaks but not three, as found in our study. In summary, it can be assumed that the acidic and the medium Pi peak results from different muscle fibers types, whereas the alkaline Pi peak represents either an unfatigued muscle region, another muscle, or a third muscle fiber type.

Table 5-1 Mean and SE of the Distribution of Pi Contents

	Pi_1 (or fiber type I) mean ± SE(%)	**Pi_2+ Pi_3 (or fiber type II) mean ± SE(%)**	**Pi_2 (or fiber type IIa) mean ± SE(%)**	**Pi_3 (or fiber type IIx) mean ± SE(%)**
Pi: fractions expected	49	51	33	18
Pi: fractions measured	23 ± 4	77 ± 4	51 ± 5	26 ± 4
Pi: fractions corrected	49 ± 3	51 ± 3	34 ± 3	17 ± 3
PCr: recovery	25 ± 25	75 ± 24	-	-

The Pi distributions are shown based on 1) the theoretical calculations (Pi: split expected), 2) measured Pi values (Pi split), 3) PCr-corrected Pi distributions, and 4) PCr recovery.

PCr, Phosphocreatine; Pi, inorganic phosphate; SE, standard error.

Fiber type-specific metabolic concentrations are known from invasive, single fiber-type analysis (Sant'Ana Pereira *et al.*, 1996). Assuming that the Pi peaks represent different muscle fiber types, we estimated the Pi fractions (expected Pi fractions) of the different muscle fiber types based on

1) an average fiber distribution in the medial gastrocnemius of normal active people; 2) the PCr content in different muscle fiber types, and 3) the assumption that PCr was completely used during fatigue—and we compared the distribution with the measured Pi fractions. From literature, it is known that the human m. gastrocnemius of normal active subjects consists of 51% type I, 31% type IIa, 14% type IIx fibers, and 3% type I/IIa fibers (Widrick *et al.*, 1996). We simplified the calculations by neglecting the mixed type I/IIa fraction. The PCr content in type I, IIa, and IIx has been specified with 66, 72, and 90 μmol (g dry matter)$^{-1}$, respectively (Sant'Ana Pereira *et al.*, 1996). During fatigue, Pi increases nearly stoichiometrically to the PCr decrease. Consequently, the Pi fractions formed by complete PCr consumption is 49%, 33%, and 18% for type I, IIa, and IIax muscle fiber types, respectively (Table 5-1, row 1). However, we observed a different Pi ratio of 23% (Pi_1), 51% (Pi_2), and 26% (Pi_3) (Table 5-1, row 2). It is suggested that the single Pi components represent the type I (Pi_1), type IIa (Pi_2), and type IIx (Pi_3) fibers, respectively. The extracted PCr recovery time components were similar (τ_1: 25 ± 25%, τ_2: 275 ± 24%) (Table 5-1, row 4). It is assumed that τ_1 and τ_2 represents muscle fiber type I and II, respectively. A possible explanation for the differences between expected and measured Pi ratio might be based on unused PCr in our experiments. Subsequently, we provide a hypothetical calculation that assigns the unused PCr to fiber types.

We observed that PCr did not decrease completely; for example, approximately 33% of the PCr baseline value was not used. It is assumed that the remaining PCr is mainly derived from deep muscle regions because the muscle activation depends on the stimulation strength, and this current originates from the electrodes on the skin and goes inward into the muscle. Thus, the deepest muscle regions will be activated less than superficial regions (Adams *et al.*, 1993; Vanderthommen *et al.*, 2000). Moreover, due to the sensitivity profile of the used loop coil, the signal contributions decreases with increasing distance from the coil plane; consequently, the superficial regions (near to the coil plane) are higher weighted than deeper regions. The deepest muscle regions are mainly composed of type I fibers, whereas the fascicle borders mainly composed of type II fibers (Pernus and Erzen, 1991; Sjöström, Lexell and Downham, 1992). Furthermore, invasive single fiber type analysis (Sant'Ana Pereira *et al.*, 1996) not only detected a different resting concentration of PCr in different fiber types but also different changes during exercise. Despite the lower resting concentrations, type I fibers of the fatigued muscles in the experiment of Sant'Ana Pereira et al. (Sant'Ana Pereira *et al.*, 1996) exhibit approximately two times more unused PCr than the type IIa or type IIx fibers. Thus, we assume that the remaining PCr originates mostly from type I muscle fibers. We added the remaining PCr to the Pi fraction of muscle fiber type I and observed a ratio of 49%, 34%, and 17% (Table 5-1, row 3). The distribution of Pi fractions is similar to the expected Pi

fractions that we calculated at the beginning (Table 5-1, row 1). This explanation must be interpreted with caution because our calculation contains assumptions that cannot be proven.

The assumption that the remaining PCr refers to non-fatigued type I fibers of the medial gastrocnemius might be supported by the results of PCr recovery. Our results coincide with respect to the PCr recovery analysis performed by Forbes et al (SC Forbes *et al.*, 2009) for low-intensity voluntary exercise of plantar flexors (τ_1 = 30 ± 3 s; τ_2 = 163 ± 18 s), but differ regarding the amplitudes. Whereas the PCr recovery by Forbes et al. (SC Forbes *et al.*, 2009)is dominated by the shorter τ_1 amplitude (95 ± 2%), in our experiment the slower fraction of τ_2 dominates the PCr recovery (75 ± 24%). Because type I fibers have the highest oxidative capacity— and type IIx have the lowest—the PCr recovery analysis indicates that more type II fibers were activated by NMES in our experiment compared to the voluntary activation in the experiment of Forbes et al. (SC Forbes *et al.*, 2009), and that a high content of the not used end-exercise PCr might be associated with type I fibers. We suppose that the differences between the studies are based on the kind of contraction (voluntary contraction vs. NMES). It is known that the muscle fiber recruitment for voluntary contraction is different than NMES (Maffiuletti, 2010). For voluntary contractions, there exists a fixed recruitment order from slow muscle fibers to fast muscle fibers; thus, one can conclude that the residual PCr might belong to unused PCr in muscle fiber type II in the study of Forbes et al. (SC Forbes *et al.*, 2009). The recruitment order during NMES goes from the muscle surface into the deep muscle regions. The deepest regions are dominated by type I fibers, which we did not stimulate (due to the used current of 72 mA). This would explain the differences between the contrary results of Forbes et al. and our study and supports the assumption that the remaining PCr refers to non-fatigued type I fibers of the medial gastrocnemius.

Temporal Appearance of Different Pi Peaks

In previous studies with voluntary muscle activation, it was found that the Pi peaks appear in fixed order, that is, at first Pi_1 and then Pi_2 (Vandenborne et al., 1991; Yoshida & Watari, 1994; Meyerspeer et al., 2012). In our study, however, the Pi_2 peak generally appeared first, followed by Pi_3 (approx. 14.4 ± 13.5 s) and then Pi_1 (23.1 ± 15.3 s). This may be explained by differences in the recruitment of motor units between NMES and voluntary muscle activation. A fixed order such as Pi_1, Pi_2, and Pi_3 is consistent with a recruitment order that follows the size principle of motor units. The recruitment order of muscle fibers with NMES, however, is not selective with respect to the fiber type and is spatially fixed (Maffiuletti, 2010). Given that all muscle fiber types would be stimulated simultaneously, it can be expected that PCr decreases slower in type I fibers because the PCr consumption is slower in type I fibers than in type II fibers (Sant'Ana Pereira *et al.*, 1996). Thus,

the Pi_1 signal would appear at last. A further explanation is based on different Pi areas. The Pi_1 and Pi_3 areas are smaller than the Pi_2 area, which means that Pi_1 and Pi_3 remains longer within the signal-to-noise ratio and can be detected as single Pi peaks later than Pi_2.

Moreover, due to the unequal distribution of fiber types in the muscle (type II fibers are mainly at the border of the fascicle, whereas type I fibers are mainly in the muscle center) (Sjöström, Lexell and Downham, 1992), it can be expected that type II fibers will be recruited and fatigued first; thus, the Pi_2 peak appears first. Both experimental findings support our assumption that the Pi peaks represent the different amounts of Pi that are present in the different muscle fiber types.

Limitations

One limitation of our study is that we used non-localized dynamic ^{31}P-MRS. Consequently, we cannot exclude the possibility of signal contamination due to contributions from outside the stimulated muscle region in the medial gastrocnemius. Another limitation is that a fixed current strength of 72 mA was applied to fatigue the medial gastrocnemius and that it was not adjusted to the muscle volume. Consequently, PCr was not consumed completely, as observed experimentally. On the other hand, the applied current strength corresponded to the maximum pain tolerated by the subjects.

5.5. CONCLUSION

To summarize, we observed and investigated pH heterogeneity during fatigue of the medial gastrocnemius induced by NMES. The force output decreased to 20% of its baseline. In all subjects, the single resting Pi peak split into three different Pi peaks during stimulation, resulting in three different pH components. In conclusion, NMES is an appropriate method to examine pH heterogeneity in stimulated muscles. The pH heterogeneity might be based on different sources (e.g., fatigued and non-fatigued muscle regions within the MG, signal contamination by other muscles, muscle fiber types). Based on the threefold split of Pi in combination with the consecutive appearance of the different Pi peaks, we conclude that these Pi components represent the amounts.

Chapter 6

6. General Discussion

The major aim of this thesis was to establish a methodological framework for simultaneous ^{31}P-MR spectroscopic, respiratory and blood lactate measurements, which enables combined investigations of exercise-induced changes of energy-metabolic parameters in the human calf muscle and corresponding global adjustments of pulmonary parameters and blood lactate concentrations. It was assumed that dynamic ^{31}P-MR muscle spectroscopy is suited to determine local energy metabolism adaptations, which differ according to the subject's training status and are thought to be associated with global physiological parameters typically monitored in sport science to evaluate muscle function and athlete performance. The results of this fundamental research provide a coherent picture of human metabolism in muscle and its regulatory mechanisms, exercise-limiting factors, muscle fiber composition and muscular fatigue.

The thesis was subdivided into separate milestones, including first the development of appropriate experimental equipment (see Chapters 2 and 3), and second, applying the developed setup to *in vivo* measurements in healthy subjects (see Chapter 3) and to subject groups with opposing training conditions (see Chapter 4). In a last step, the crucial point of exercise-induced movements in the MR-scanner was evaded by applying NMES to activate solely the calf muscle to study the feasibility to indirectly distinguish between different muscle fiber compartments (see chapter 5). In the following, these single work packages will be discussed by considering the specific main findings and outlining the conclusions, which can be drawn with respect to the main objective of this thesis.

MR-compatible pedal ergometer

The pedal ergometer was developed for performing graduated exercises of the *m. triceps surae* muscle complex within a clinical whole-body 3 T MR-scanner. Besides being suited to apply and monitor different load regimes (isometric, dynamic, graduated loads), the ergometer can be used in combination with MR spectroscopy or MR imaging by using appropriate RF surface coils, such as rigid ring coils or flexible coils. It also allows interactive adjustment of the physical output for reproducible exercising due to the simultaneous monitoring of mechanical parameters. The setup was tested by applying graded load intensities in two *in vivo* measurement series, which resulted in similar PCr, Pi and pH evolutions as well as distinct load-dependency of the metabolic changes. Despite being able to achieve an almost isolated activation of the *m. triceps surae* muscle complex, there was still considerable activation of supportive and stabilizing muscles, like the *m. quadriceps*

femoris or the ischiocrural muscles. Such activations substantially affect the mechanical output and performance of the plantar flexion and can induce additional non-systematic variability into the sampled metabolic parameters. Consequently, for the studies presented in this thesis, Velcro straps were placed over the hip, knee and ankle in order to reduce the impact of other muscles as much as possible (e.g. González de Suso *et al.*, 1993; Kemp *et al.*, 2001; Allen *et al.*, 2013; Cannon *et al.*, 2014). However, accompanying movements cannot be avoided completely, even by fixating the leg or using handle pieces as was the case here (see chapter 2). The handle pieces led in fact to an isometric effort in the shoulder and arm muscles, which were both activated while the subject aimed to hold a stable position during the exercise. Although being less relevant regarding the analysis of local muscular metabolic changes, this additional effort might have affected global adaptations, like respiratory and blood lactate time courses. Therefore, the hand grips were substituted with a shoulder harness in the subsequent experiments.

The placement of the RF-coil can also affect metabolic changes. Since activated muscle cells swell due to water influx (Allen, Lamb and Westerblad, 2008), a too tightly wrapped flexible coil may induce partial ischemia by impairing blood circulation. In own preliminary experiments, constant pain as well as visible pressure marks occurred in regions, which were covered by the coil, and were reported by the subjects during and after the exercise. A similar phenomenon associated with increased muscular fiber tension due to a fixed pedal position after performing the plantar flexion exercise, was also observed (Fitts, 2008). Therefore, additional *in vivo* experiments were conducted with fixated as well as released pedal positions to investigate these tension-related impairments of oxygen supply and H^+ efflux on the PCr and pH kinetics during the post-load phase (Moll, Gussew and Reichenbach, 2017). An upright pedal position with roughly 90° angle of the ankle relative to the leg was associated with impaired tissue perfusion, which was reflected in significantly delayed PCr and pH post-load recoveries compared to the released pedal position (Figure 6-1). Partial ischemia-associated delays of oxygen supply and metabolic byproduct removal can corrupt the analysis of the underlying metabolic processes because the degree of muscular tension-related impairments differs between subjects depending on the inter-individually varying tissue flexibility of the lower legs (Youdas *et al.*, 2003). Consequently, in all following experiments the pedal was released prior and after the exercise in order to avoid muscle fiber tensions.

All in all, plantar flexion exercises can be reliably performed with the ergometer and activation of multiple *m. triceps surae* compartments can be studied. Even though other muscle groups comprise larger muscle masses and offer higher flexibility regarding planning and locating the spectroscopic region-of-interest, the calf muscle has structural advantages compared to, e.g., the *m. quadriceps femoris*. Since the mono-articular *SOL* consists mainly of type I fibers, whereas the poly-articular *GM* has a higher type II fiber fraction, these calf muscles can cope with different biomechanical

tasks (Edgerton, Smith and Simpson, 1975). This, however, offers the opportunity to spectroscopically analyze exercise-induced metabolic adjustments in two muscles with distinctly heterogeneous fiber composition, which, in turn, predefine the metabolic regimes. Therefore, a specialized ^{31}P-MRS sequence (MUSCLE) was developed and successfully implemented to observe metabolic parameters in spatially-shifted slices covering both muscles in an interleaved manner. As already mentioned in the introduction section (Chapter 1.3.2), this sequence enables tracking of metabolic changes in multiple muscle regions.

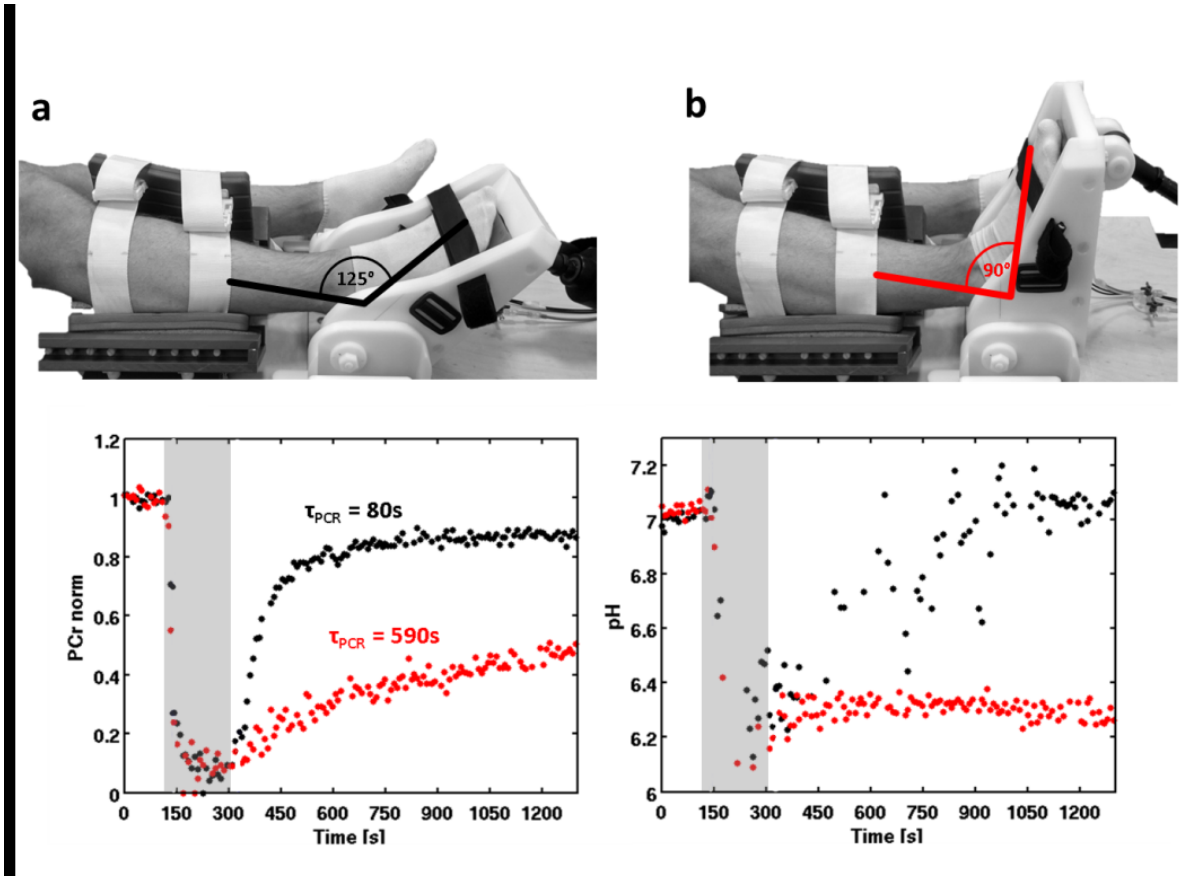

Figure 6-1 Released (a) and fixated (b) pedal positions after the exercise with 125° and 90° angles of the ankle relative to the leg, respectively. The bottom graphs show the time courses of PCr (left) and pH (right) in the *m. gastrocnemius medialis* of the same subject during rest, load (gray area) and recovery for 125° (black dots) and 90° (red dots) ankle angulations. In the fixated case, the inhibited oxygen supply as well as the reduced H^+ efflux is indicated by significantly delayed PCr and pH recoveries compared to the flexed leg showing physiologically more reasonable PCr and pH kinetics.

Furthermore, MR-compatible ergometers can be improved under various aspects. The most important point is the appropriate activation of isolated muscle regions and the reduction of concomitant movement of adjacent muscles. In the case of the plantar flexion the activation of the muscles in the upper leg and the hip can be reduced by flexing the knee. However, the limiting

space of the magnet bore has to be considered. Another option in improving MR-compatible ergometers is the positioning of the subject to guarantee a physiological load, which simulates daily routines and physiological training conditions. To do so and to reduce additional movement NMES might be a good method to stimulate selected muscle regions. Despite revealing several advantages, especially considering the limited space of the magnet bore, NMES might affect ^{31}P-MR spectroscopic findings, which will be discussed later in the thesis.

Combined spiroergometry and ^{31}P-MRS

As a next methodological step a commercially available spirometry device was adapted to perform respiratory measurements inside the bore of the MR scanner during continuous acquisition of ^{31}P-MR spectra in loaded calf muscles. This adaptation was accomplished in close collaboration with an internationally leading manufacturer in respiratory diagnostics (Ganshorn; Medizin Electronic GmbH, Niederlauer, Germany), who supplied and modified one of their state-of-the-art systems, the *PowerCube*. Since this unit had to be located outside the MR scanner cabin, the sampling lines connecting the gas analyzers with the subject's breathing mask were prolonged while maintaining, as demonstrated in preliminary calibration experiments, the system's functionality without any impairment in analyzing respiratory parameters under MR-conditions.

Additionally, a mathematical model was extended to fit retrospectively the time courses of the measured pulmonary parameters VO_2 and VCO_2. In contrast to recently introduced approaches, which are typically applied to analyze the exercise-specific data segments (e.g., the VO_2 evolution during the load phase) and to detect characteristic thresholds or peak values, this approach allows fitting of the entire VO_2 and VCO_2 time courses and provides parametrization of the resting state condition as well as the respiratory adjustments during the load and recovery phases of the experiment. Besides being able to determine all relevant respiratory parameters (resting state and load peak values of VO_2 and VCO_2) and time constants of exercise-induced increases and post-load phase recoveries, the fitting routine also integrates the area under the entire data curves to quantify the exercise-induced accumulations of non-metabolic CO_2 (*excess CO_2*).

The combined spirometric and ^{31}P-MR spectroscopic measurements were first conducted in non-specifically-trained healthy subjects, which performed intense, dynamic loads of the calf muscle, to extract associations between global pulmonary changes and local adjustments of energy metabolism parameters. Besides confirming the already known correlation between VO_2 and PCr kinetics during exercise (Whipp *et al.*, 1999; Rossiter *et al.*, 2000, 2003; Rossiter, Ward, Kowalchuk, *et al.*, 2002; Cannon *et al.*, 2013, 2014), the analysis was extended to study also the relation between the acidification in the exercised calf muscles and the non-metabolic CO_2 (*excess CO_2*). Since the

intra-muscular pH decrease reflects the activation of the anaerobic energy supply pathway, the identified interrelation between acidification and *excess CO_2* reinforces the common assumption that exercise-induced overshoots of CO_2 relative to VO_2 rely on buffering accumulated H^+ by bicarbonate. Intramuscular pH and *excess CO_2* showed a significant, physiologically determined relation, as this represents the compensation of H^+ and lactate accumulation by the respiratory system. Thus, the amount of *excess CO_2* together with spectroscopically measured muscular acidification might act as an appropriate marker for anaerobic energy supply in loaded muscles. However, since this relation is still controversially discussed in the literature (Roecker *et al.*, 2000; Robergs, Ghiasvand and Parker, 2004; Péronnet and Aguilaniu, 2006), it has to be confirmed by monitoring lactate concentration changes in the blood or directly within the loaded muscle. Finally, the pure oxidative-driven PCr recovery in the muscle was mirrored in global post-load oxygen supply. Even though muscle VO_2 is affected by several factors, such as, e.g., perfusion, acidification or efficiency in O_2 release from oxyhemoglobin, this correlation between VO_2 and PCr recovery represents a link between local and global respiration as already shown by others (Rossiter *et al.*, 1999; Crowther and Gronka, 2002).

An additional important finding of the experiments was that due to the supine position of the subjects respiration and breathing frequencies were lowered due to reduced gravitational impact alongside with a smaller muscle perfusion pressure (Jones and Burnley, 2005). This directly resulted in longer time constants of the VO_2 increase compared to values obtained when exercising on a treadmill or bicycle ergometer. Despite showing similar values in the VO_2 steady state a direct comparison of both exercising positions presented by Convertino et al. revealed a significantly higher total VO_2 with a significantly reduced VO_2 recovery (Convertino, Goldwater and Sandler, 1984). Moreover, the usual resting VO_2 is between 0.20-0.45 l/min during rest (Scharhag-Rosenberger, 2010), whereas the oxygen uptake acquired in the supine position rarely exceeded 0.25 l/min. The unusual position in the magnet bore might have prevented entirely relaxed breathing in some subjects. However, with moderate pedal frequencies unwanted high breathing rates can easily be avoided.

Metabolic adaptions in athletes

Up to that point, only non-specifically-trained subjects had been investigated as described in chapters 2 and 3. However, the broad distributions of the sampled local and global metabolic parameters, such as varying PCr recovery rates during the post-load phase, different pH drops or inter-individually varying *excess CO_2*, implied, as already mentioned, different fitness levels among the subjects. To verify the potential link between such characteristic metabolic changes and

corresponding training-induced muscular conditions, two opposing athlete groups were investigated, who performed a fully exhaustive calf muscle exercise during simultaneous acquisition of spirometric and blood lactate data as well as ^{31}P-MR spectra in *GM* and *SOL* muscles. Generally, metabolic differences between sprint- and endurance-trained athletes are mainly on the basis of heterogeneous muscle phenotypes. This enables various strategies in dealing with exhaustive exercises like producing higher peak forces as a result of a higher fast fiber proportion alongside with a higher availability of PCr stores in sprinters. Endurance athletes on the other side reveal faster PCr recovery kinetics, a higher mitochondrial density and capillarization allowing them, on the one hand, to perform exercises for a very long time and, on the other hand, providing them to recover significantly faster than other athletes (Johansen and Quistorff, 2003). Other authors expect different patterns of muscle enzyme activities in endurance athletes, which enhances the rate of ATP resynthesis (Pesta *et al.*, 2013). The same authors assumed the ability in highly trained long distance athletes to spread the workload across the pool of motor units based on a selective recruitment by the central nervous system. Furthermore, higher muscle buffer capacities enable to tolerate higher lactate concentrations without a concomitant increase in H^+, which is typically occurring in team sport athletes (Edge *et al.*, 2006).

Triathletes and sprinters were selected in this thesis, as they were expected to reveal extreme and contrary states regarding athletic skills and abilities as well as muscle histology and biochemical and metabolic local and global characteristics as a consequence of their specialized training orientation, i.e. endurance and speed strength training, respectively (Millet *et al.*, 2002; Johansen and Quistorff, 2003; Edge *et al.*, 2006; Aagaard *et al.*, 2011; Pesta *et al.*, 2013). Both athlete groups had different training scopes, training volumes and intensities. Whereas, in general, endurance-trained athletes perform long-term workouts below the anaerobic threshold, sprinters focus on short and high intense exercises for maximum intramuscular coordination supporting explosive energy output. However, so far, investigations under exhaustive, MVC-based exercise conditions of athlete-specific strategies to provide energy on the muscular level together with accompanying respiratory and lactate changes have been rarely performed. Therefore, the aim was to close this gap. The *GM* and *SOL* muscles were selected since they predominantly generate the force during plantar flexion and typically reveal distinctly different muscle fiber compositions. They were thus assumed to yield characteristic, specific energy supply kinetics. Similar to the applied fitting procedure of the pulmonary data the entire profiles of exercise-induced and post-load PCr changes were again fitted in sections to analyze the underlying metabolic adaptations by extracting the slopes of PCr during load and recovery.

As expected both athlete groups revealed different respiration and lactate characteristics under the applied all-out exercise conditions, even though less than 10% of the whole-body muscle mass

was activated by the exercise. Endurance athletes revealed significantly smaller changes in blood lactate concentrations compared to sprinters that went along with almost twice as large *excess* CO_2 values but also with faster VO_2 increases after exercise onset in the short distance athletes. The latter observation indicates more efficient oxygen turnover to sustain the mechanical output by the endurance athletes. Based on higher *excess* CO_2 and blood lactate levels, the anaerobic pathway obviously plays a more dominant role in sprinters than in endurance athletes. Interestingly, even though both investigated groups showed different sport-specific global physiological behaviors and were assumed to reveal different structural preconditions, the mean exercise time until exhaustion of the calf muscle was comparable between the athlete groups. Besides different peak forces during the MVC test no obvious differences were noticeable between the exercise protocols of both athlete groups.

^{31}P-MRS was thus assumed to provide further explanations about the different fatigue-avoiding strategies or athlete-specific alterations. The measurements revealed indeed obvious metabolic differences between *SOL* and *GM* in accordance to recent findings from the literature (Allen *et al.*, 1997; Valkovič *et al.*, 2014; Niess *et al.*, 2017). The *SOL* revealed less pronounced metabolic adaptations and lower activation compared to the *GM*. This goes along with findings of Price et al., who reported stable activation of the *SOL* independent from knee flexion measured with EMG (Price *et al.*, 2003). Thus, a supportive contribution of the *SOL* during the applied exhaustive exercise cannot be entirely ruled out. Assuming a high type I fiber fraction in the *SOL* muscle, endurance-trained athletes might use this muscle group to a greater extent since their favored metabolic working regime benefits from the aerobic-dominated and prolonged performance of these muscle fibers.

On the other hand, the main performer *GM* revealed a higher degree of acidification at the end of the exercise. Interestingly, some of the short distance athletes were able to exercise over several minutes with severe pH drops down to level of 6.1, which are considered to be a major cause of muscular fatigue. Decreases in intracellular pH during intense exercises are usually reported at ~0.5 pH units leading to inhibited muscle performance due to water influx and reduced electrolyte concentrations (Allen, Lamb and Westerblad, 2008). Acidification was thus distinctly stronger in the present work, especially among sprinters, although both groups exercised on a normalized intensity. This suggests a higher ratio of anaerobic energy production in sprinters, but also the ability to deal with accumulated H^+ and lactate without or only slightly reduced impairment of metabolic and contractile processes over long time periods. All in all, sprinters revealed a higher exercise tolerance under critical metabolic conditions, which was previously also shown in team sport athletes, whose training contains alternating sprints and recovery periods leading obviously to a higher capacity to buffer H^+ (Edge *et al.*, 2006).

Interestingly, almost all endurance athletes showed partial recovery of their PCr stores during the exhaustive exercise. Short distance athletes, on the other hand, revealed constantly depleted PCr stores in both muscles except for two subjects with one athlete irregularly attending decathlon competitions. Thus, this metabolic recovery phenomenon might occur in athletes, who generally perform long-term exercises for many years. Even though this observation seems physiologically useful and plausible in endurance-trained athletes, it is barely described in the literature. Under stable exercise conditions a partial PCr recovery could be related to an increased contractile efficiency or a higher energy supply compared to the energy demand, which is possible for both the glycolytic as well as the oxidative energy synthesis. On the one hand, a surplus production could be described either by higher production rates or the ability of the stressed muscles to recruit more fibers. The latter would explain the greater participation of the *SOL* among the endurance group. On the other hand, the observed partial pH recovery implies either an increased H^+ efflux or reduced glycogenesis, which is not supported by the ATP overshoot. However, a shift from anaerobic towards mainly aerobic energy supply with negligible H^+ accumulation explains both the continued and somehow increased PCr production as well as the recovered pH values. At the whole muscle level, these metabolic alterations may result from varying contributions by different muscle fiber types. The hypothesis of oxidative ATP synthesis implies increased recruitment of oxidative fibers, which is suspected in endurance athletes. However, it is difficult to evaluate different recruitment patterns in terms of muscular and metabolic efficiency. Another strongly influencing factor and possible indicator for a partial PCr recovery is the local perfusion and changes in blood flow, especially at such high exercise intensity. Increased blood flow might lead to increased H^+ efflux and more economic oxygen delivery, which is common in endurance-trained athletes showing elevated capillarity and enhanced mitochondrial density (Kubukeli, Noakes and Dennis, 2002). Another hint might be the ability of highly endurance-trained athletes to spread the workload across other muscles, which reduces the requirement on a given motor unit leading to a possible recreation of stressed muscles fibers. This selective recruitment is controlled by the central nervous system and occurred during submaximal exercises (Enoka and Stuart, 1992). Another form of PCr overshoot above the resting state value during recovery was demonstrated by several studies (Kushmerick, Meyer and Brown, 1992; Sahlin *et al.*, 1997; Pesta *et al.*, 2013). This finding has been reported for both oxidative and glycolytic muscle fibers after intense exercise and appeared several minutes after the termination of exercise with sustained visibility in some cases still after one hour. The cause of this molecular adaption is still unclear, but seems to be independent from muscular acidification (Korzeniewski and Zoladz, 2005). Regulation of the oxidative phosphorylation by calcium ions was considered as a main mechanism at least after the load onset, which would explain the connection between higher oxygen consumption in muscles with high mitochondria density as

they store Ca^{2+} (Pozzan *et al.*, 1994). This leads to the assumption that elevated activation of oxidative phosphorylation and thus energy production during load or recovery is also the result of muscle training, especially with endurance training. However, neither sprint- nor endurance-trained athletes revealed significant post-load PCr overshoots after the exhaustive exercise.

The preference of anaerobic energy supply in sprinters was demonstrated by high lactate concentrations alongside with lower pH values. Endurance-trained athletes on the other side avoided excessive accumulation of blood lactate and H^+ and were able to recover their energy storages significantly faster at the end, but also during the exercise. The ability to recover PCr significantly faster than other athletes characterizes highly trained endurance athletes as a result of high-volume training leading to cardiovascular adaptations, elevated capillarity and enhanced mitochondrial density (Kubukeli, Noakes and Dennis, 2002). Furthermore, muscle specific findings can be related to heterogeneous muscle fiber compositions, which, in turn, affect the preference of either aerobic or anaerobic energy supply and are observable by spirometry and blood lactate measurements. Since the latter measures are commonly used to monitor the training status of athletes, they can profoundly reflect a subject's physical condition, which can be improved by muscle-specific observations. Spectroscopic measurements might be able to identify the differences between an outstanding and an excellent athlete based on the associated metabolic changes. Specialized training interventions can be directly and non-invasively assessed thanks to the deeper specific insight into muscular adaptation processes.

In conclusion, the observed differences in metabolic adaptations between both athlete groups point to heterogeneous muscle fiber contributions as a result of the highly specialized training stimuli over several years. These findings were supported by standardized approaches adopted from the sport science and indicated different strategies in dealing with the applied exhaustive exercise protocol. It was shown that the measured values were closely related to the physical performance level of the studied athlete groups. Thus, localized ^{31}P-MRS appears to be a uniquely suited, non-invasive tool for quantifying metabolic adaptations in trained and untrained individuals and to resolve effects of different training strategies in multiple muscle groups with different muscle fiber distributions. This again could improve the evaluation of applied training interventions, which might also helps in performance assessment of young sport talents. However, compared to other diagnostic methods in sports medicine or training science (e.g., spiroergometry, electromyography or force measurement) MRS is a very costly approach. Another promising link is the creation of physiological models, which can utilize the comprehensive assessment of PCr and VO_2 kinetics with the presented fitting approaches. Such cybernetic models might help to understand the connection of regulatory systems in single motor units and allow a simulation and transfer to other muscle groups or the whole-body.

Muscle fiber assessment by pH heterogeneity

Besides performing dynamic ^{31}P-MRS under voluntary contraction, muscle energy metabolism was also investigated during isolated and fully exhausting activation of the *m. gastrocnemius medialis* by using neuromuscular electrical stimulation (NMES). Assuming simultaneous and maximum activation of all muscle fibers within the stimulated muscle, it was hypothesized that different muscle fiber fractions yield different Pi frequency shifts in the ^{31}P-MR spectra. This hypothesis relies on the different oxidative capacities of muscle fiber types (see Chapter 1.1), which determines the efficiency of oxidative energy supply and thus the impact of anaerobic glycolysis and consequently the amount of accumulated H^+ and lactate. Therefore, different muscle fibers should show characteristic pH evolutions, which in turn should manifest in distinct Pi peak splittings in ^{31}P-MR spectra series acquired during the exercise (Rossiter, Ward, Howe, *et al.*, 2002). However, since a reliable application of this approach requires NMES of a single muscle, activation in adjacent muscles has to be monitored. Therefore, the applied measurement protocol also included acquisitions of T_2-weighted transversal MR images in the lower leg of the examined subjects prior and after the stimulation. Since muscle activation is associated with increasing tissue water T_2 relaxation time constants, the stimulated muscles can be visually identified by enhanced signal intensities on T_2-weighted images (Bendahan, Giannesini and Cozzone, 2004). Although the full set of mechanisms influencing the T_2 increases in activated muscles is currently not fully understood, the osmotically driven water shifts from the extra- into intra-cellular spaces have been reported as being important determinants in response to the intra-muscular accumulation of H^+ or alternatively increasing blood flow (Ababneh *et al.*, 2008). In preliminary experiments, apparently elevated image intensity in T_2 weighted MR images and consequently higher activation was identified in the *GM* alongside with distinctly lower involvement of the surrounding tissue, which allows assuming that ^{31}P-MR spectroscopically measured metabolic changes during NMES derive only from the *GM* muscle. During the exhaustive stimulation a distinct three-fold Pi split was observed in all subjects in association with three different pH values, which is ascribable to heterogeneous H^+ accumulation kinetics during the load phase. These splits remained during the whole exercise in all subjects, suggesting alkaline, medium and acidic pH components. The latter was associated with severe pH drops to levels down to 6.1, which was also seen in the *GM* muscles of sprinters (see Chapter 4). This implies a connection between pH decrease and the amount of type II fibers, because sprint-trained athletes are assumed to have higher contributions of these muscles with high anaerobic glycolytic potential. Thus, the measured spectroscopic signal and the three Pi peaks might result from two different muscles fiber types represented by the acidic and intermediate peak, whereas

the alkaline peak then represents a less fatigued muscle or a third muscle fiber type. A quantitative estimation of the volume fractions of the three muscle fiber types may be made by the integrated area under the specific Pi signal. Further experiments need to be performed in order to verify this hypothesis, but can only be confirmed by invasive histological characterization.

Despite being a promising tool to induce maximum, spatially isolated and comparable muscle fatigue, NMES, however, is able to provoke muscle damage and can impair muscle function (Nosaka *et al.*, 2011). Highly frequent and maximum eccentric contractions, as possible with NMES, are known to induce small ruptures in the Z-lines of the myofibrils, also known as delayed onset muscle soreness (DOMS) (Cheung, Hume and Maxwell, 2003). This muscle damage is immediately followed by an acute inflammatory response and impairs muscular respiration. ATP production becomes inhibited and cell homeostasis is disturbed, which affects metabolic conditions observable by ^{31}P-MRS (Cheung, Hume and Maxwell, 2003). Some authors also reported increased plasma CK activity even few days after applying NMES (Mackey *et al.*, 2011), which could influence subsequent measurements of high-energy metabolite kinetics. Taken together, the risk of potential muscle damage has to be carefully considered when planning NMES experiments to investigate exercise-induced metabolic changes.

In summary, local electrical muscle stimulation seems to be an excellent method, especially to suppress the influences of undesirable motion. Further NMES applications can be combined with measurements of blood lactate or pulmonary changes. Since electrical stimulation does not rely on specific ergometers other muscle groups can be considered for investigations with such combined approaches.

7. Conclusion and Outlook

This work demonstrated successfully the ability to perform valid and reproducible loads of the calf muscle complex alongside with continuous ^{31}P-MR spectroscopic measurements in exercised skeletal muscles as well as simultaneous measurement of whole-body respiratory parameters (O_2 uptake and CO_2 exhalation) and blood lactate concentrations. The correlation of these global markers with muscle-specific findings suggested that activity of a single muscle influences the whole-body metabolism, which is reflected by certain well known markers, like oxygen uptake and peak concentrations of lactate. This multimodal approach allowed differentiation between the main energy providing systems (aerobic and anaerobic) on a cellular and peripheral level. Moreover, by applying experiments to carefully selected athletes with opposing metabolic profiles, it was possible to detect athlete-specific energy-providing processes, which were interpreted as adaptive strategies to cope with the stressful exercise. In summary, the aerobic pathway was more efficient in endurance athletes, whose calf muscles are not only expected to have higher type I muscle fiber fractions with higher oxidative capacities, but also to show reduced H^+ accumulation during load as well as significantly faster PCr recoveries during the post-load phase. These characteristic local metabolic adjustments were mirrored in moderate blood lactate accumulations and distinctly lower amounts of *excess CO_2* and slower VO_2 increases during load. In contrast, greater importance of the anaerobic metabolism was seen in sprint-trained athletes as reflected by severe pH drops and slower PCr recoveries. This was further substantiated by distinctly higher blood lactate concentrations, *excess CO_2* values and the assumption of a higher type II proportion.

In addition to these findings, sport-specific activation patterns were identified in both examined muscles (*GM* and *SOL*), which reflect characteristic athlete-specific strategies to cope with long lasting and exhaustive plantar flexion exercises. Most surprisingly, the experiments revealed systematic partial recoveries of muscular PCr pools even during the performance of the exercise. Being primarily observed in endurance-trained athletes, this observation might reflect surplus ATP synthesis due to more efficient oxidative glycolysis and thus represent a specific strategy to deal with long lasting muscular loads. However, in order to provide more comprehensive understanding of this particular behavior, additional studies are required including graded loads. Targeting on the quantitation of muscle fiber composition, the experiments performed with NMES allowed differentiation between multi-compartment pH kinetics and thus at least qualitative identification of different muscle fiber types in calf muscle.

However, there are some limitations of the work in this thesis, which have to be mentioned. The locomotor system usually acts as a unit, especially under exercise conditions. Consequently, it

might be difficult or even questionable to transfer results acquired in an isolated calf muscle to other muscles in order to evaluate exercise-associated adjustments of the whole-body energy metabolism. Therefore, systematic ^{31}P-MRS measurements in other participating muscles need to be performed in subsequent studies while using well defined and graded load regimes. This also requires the availability of dedicated ergometers to apply appropriate muscle loads under MR conditions. Furthermore, although muscle pH values appear to be a good marker for anaerobic energy supply, they are also affected by other interrelating factors, including the balance between anaerobic and aerobic ATP synthesis, H^+ buffer capacity, perfusion-related efficiency of H^+ efflux, or regulatory enzyme activities, which, however, are difficult to quantify by MRS (Kemp et al., 2001; Kemp, 2015). Direct measurement of lactate changes in the exercised muscle would be highly valuable for a more reliable characterization of the anaerobic metabolism. Several authors have indeed either used different MR spectroscopic approaches to directly measured lactate (Pan *et al.*, 1991; Jouvensal, Carlier and Bloch, 1997; Hsu and Dawson, 2000; Meyerspeer *et al.*, 2007; Ren, Sherry and Malloy, 2013), or have indirectly calculated lactate concentrations by assuming the H^+ kinetics (Boska, 1994; Conley et al., 1997; Kemp et al., 2001). However, since the accuracy of such calculations relies on prior knowledge of multiple input parameters (e.g. constant buffer capacity and stoichiometric assumptions), the direct ^{1}H-MR spectroscopy-based lactate measurement approach appears more promising. Associated challenges, however, include the complete overlapping of low intensity lactate resonances by large lipid signals, which have to be suppressed by using, e.g., spectral editing techniques (Meyerspeer et al., 2007) or magnetization inversion approaches (Lindeboom et al., 2017). A first step in this direction of measuring intramuscular lactate has already been undertaken in the context of this thesis (Tschiesche *et al.*, 2015). Based on these findings additional preliminary experiments were performed allowing to monitor depleting lactate concentrations after an intensive exercise in the *GM* muscle of healthy subjects by applying the so-called ^{1}H-MEGA-PRESS sequence (see Figure 7-1), which is a spectral editing technique, typically applied to quantify small quantities of brain neurotransmitters (Mullins *et al.*, 2014). Similar to the suppression of contaminating metabolites in ^{1}H-MR brain spectra, the MEGA-PRESS sequence proved also suited to suppress the lipid resonances in ^{1}H-MR muscle spectra appropriately, allowing isolated quantitation of the lactate signal at 1.3 ppm. Averaged over all preliminary examined subjects ($N = 14$), a mean lactate concentration of 25.2 ± 11.7 mmol/l (relative to the Cr signal measured by ^{1}H-MRS, which was assumed to be 44 mmol/l) was obtained in the *GM* muscle at the end of the plantar flexion exercise. These locally measured values revealed a positive correlation with blood lactate samples from the earlobe (3.3 ± 0.9 mmol/l; $R = 0.73$, $p < 0.005$). Data sampling was, however, only possible prior to and after the exercise since the calf movement prevented lactate quantitation during the load phase.

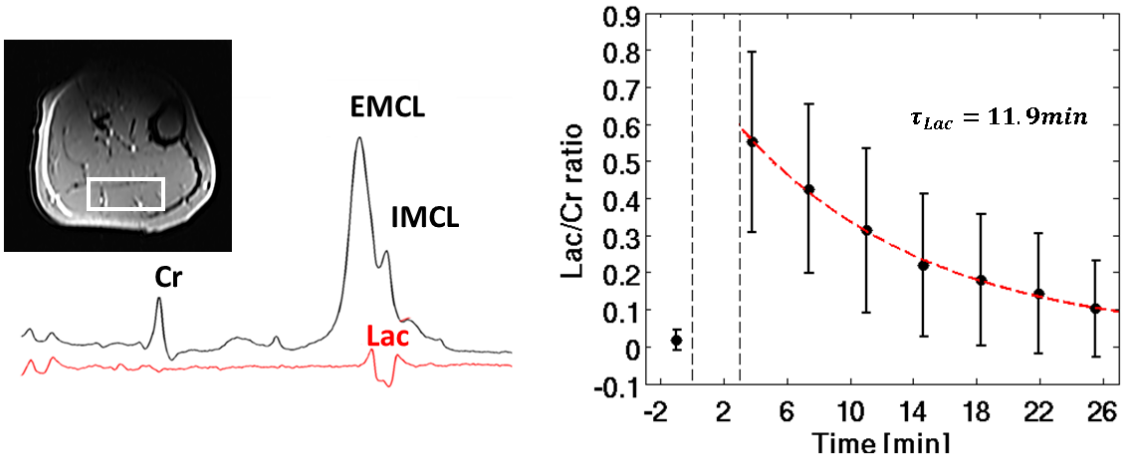

Figure 7-1 *Left:* ^{1}H-MR muscle spectra with intra- and extra-myocellular lipid signals (IMCL and EMCL), overlapping the lactate doublet at 1.3 ppm. *Right:* Mean values of exponentially decreasing lactate to creatine ratios acquired during rest and the post-load recovery phase (Cr was assumed to be 44 mmol/l). A reliable acquisition of ^{1}H-MR spectra was not possible during the exercise due to movement.

Future developments should thus involve adapted MR sequences that allow the acquisition of lactate also during load. Once successfully implemented, this should then shed light on differences in the concentration of muscle lactate and blood lactate in the periphery. Unfortunately, simultaneous acquisition of ^{1}H- and ^{31}P-MRS is currently not possible, causing therefore a tradeoff to either measure lactate or high-energy metabolites (PCr, Pi and ATP) because they all reveal fast kinetics during load and recovery. Acquiring ^{1}H- and ^{31}P-MRS data in an interleaved mode would lead to a loss of important metabolic information.

The combined approach developed during the work of this thesis allows a comprehensive and, even more importantly, non-invasive insight into muscle and exercise physiology with the perspective to be applied in follow-up studies with a broad range of research questions. Since fatigability is one of the most relevant fitness and health indicators in athletes, healthy subjects and patients, its examination is expected to contribute significantly to the sport science and sports medicine research, targeting on the characterization of muscle function and endurance. The data collected with the presented approach might also be used to add advanced information to physiological models (Hunter and Borg, 2003; Hunter, 2004) that focus on the characterization of exercise-induced alterations by considering metabolic processes within the muscle cells as well as on the whole-body level. As such models require detailed consideration of other biological sub-systems, including the circulatory, respiratory, musculoskeletal, central nervous and endocrine system, as well as a comprehensive assessment of muscles, nerves, blood or cell structure proteins, dynamic

^{31}P-MR muscle spectroscopy can be an important contributor to this endeavor to provide comprehensive information about the human motor units during rest and load to be able to accurately simulate exercise-induced metabolism, fatigue and muscle failure under different exercise conditions. The methods described in this thesis can also be applied in longitudinal studies to monitor training interventions (Kent-Braun, McCully and Chance, 1990; Sahlin, 2014). More specifically, possible metabolic weaknesses in specific muscle groups of an athlete (e.g. too fast PCr decrease, severe acidification, too slow PCr recovery) could then be detected and adjusted by means of appropriate training interventions (Kubukeli, Noakes and Dennis, 2002).

From a more clinical perspective, the lower back muscles should be an important target for future studies since inactivity as well as aging are associated with muscle fiber transitions from type I to type IIB (Pette and Staron, 1997), which can be indirectly observed with MR approaches based on a reduced energy metabolism, perfusion and a prevalently occurring fat infiltration. All these factors lead to increased fatigability of the lumbar extensors and impaired spine integrity. Due to the associated higher injury risk, these degenerative impairments can lead to chronic low back pain in the long term, which represents one of the major public health problems in western countries (Wand and O'Connell, 2008). ^{31}P-MRS-based assessment of muscle fiber-related metabolic markers in the back muscles may help with regard to early stage identification of such degenerative dysfunctionalities or monitoring the success of therapeutic interventions. The potential of such investigations has already been demonstrated in recent studies of healthy subjects by combining dynamic ^{31}P-MRS in isometric loaded back muscles with other advanced MR imaging techniques (Hiepe *et al.*, 2014, 2015) and EMG (Rzanny *et al.*, 2004, 2009), which disclosed age-related changes in muscle metabolism, structure and function. Further clinical applications could include spectroscopic measurements in patients with metabolic disorders, like McArdle disease (Vorgerd and Zange, 2007), which is associated with impaired anaerobic glycolysis leading to continuously increasing pH levels up to 7.3 and rapidly decreasing ATP concentrations during load,
or other myotonic dystrophies (Crowther *et al.*, 2003; Tonon, Gramegna and Lodi, 2012).

References

Aagaard, P., Andersen, J. L., Bennekou, M., Larsson, B., Olesen, J. L., Crameri, R., Magnusson, S. P. and Kjær, M. (2011) 'Effects of resistance training on endurance capacity and muscle fiber composition in young top-level cyclists', *Scandinavian Journal of Medicine and Science in Sports*, 21(6), pp. 298–307.

Ababneh, Z. Q., Ababneh, R., Maier, S. E., Winalski, C. S., Oshio, K., Ababneh, A. M. and Mulkern, R. V. (2008) 'On the correlation between T2 and tissue diffusion coefficients in exercised muscle: Quantitative measurements at 3T within the tibialis anterior', *Magnetic Resonance Materials in Physics, Biology and Medicine*, 21(4), pp. 273–278.

Achten, E., Van Cauteren, M., Willem, R., Luypaert, R., Malaisse, W. J., Van Bosch, G., Delanghe, G., De Meirleir, K. and Osteaux, M. (1990) '^{31}P-NMR spectroscopy and the metabolic properties of different muscle fibers.', *Journal of Applied Physiology*, 68(2), pp. 644–649.

Adams, G. R., Harris, R. T., Woodard, D. and Dudley, G. A. (1993) 'Mapping of electrical muscle stimulation using MRI.', *Journal of Applied Physiology*, 74(2), pp. 532–537.

Akima, H., Foley, J. M., Prior, B. M., Dudley, G. A. and Meyer, R. A. (2002) 'Vastus lateralis fatigue alters recruitment of musculus quadriceps femoris in humans.', *Journal of Applied Physiology*, 92(2), pp. 679–84.

Albracht, K., Arampatzis, A. and Baltzopoulos, V. (2008) 'Assessment of muscle volume and physiological cross-sectional area of the human triceps surae muscle in vivo.', *Journal of Biomechanics*, 41(10), pp. 2211–2218.

Allen, D. G., Lamb, G. D. and Westerblad, H. (2008) 'Skeletal muscle fatigue: cellular mechanisms', *Physiological reviews*, 88(1), pp. 287–332.

Allen, P. S., Matheson, G. O., Zhu, G., Gheorgiu, D., Dunlop, R. S., Falconer, T., Hochachka, P. W. and Stanley, C. (1997) 'Simultaneous ^{31}P MRS of the soleus and gastrocnemius in Sherpas during graded calf muscle exercise', *American Journal of Physiology. Regulatory, Integrative and Comparative Physiology*, 273, pp. 999–1007.

Andersen, J. L. and Aagaard, P. (2000) 'Myosin heavy chain IIX overshoot in human skeletal muscle.', *Muscle & Nerve*, 23(7), pp. 1095–1104.

Andersen, J. L., Klitgaard, H. and Saltin, B. (1994) 'Myosin heavy chain isoforms in single fibres from m. vastus lateralis of sprinters: influence of training.', *Acta Physiologica Scandinavica*, 151(2), pp. 135–142.

Babault, N., Cometti, C., Maffiuletti, N. A. and Deley, G. (2011) 'Does electrical stimulation enhance post-exercise performance recovery?', *European Journal of Applied Physiology*, 111(10), pp. 2501–2507.

Baguet, A., Everaert, I., Hespel, P., Petrovic, M., Achten, E. and Derave, W. (2011) 'A new method for non-invasive estimation of human muscle fiber type composition.', *PloS one*, 6(7), p. e21956.

Bangsbo, J., Johansen, L., Quistorff, B. and Saltin, B. (1993) 'NMR and analytic biochemical evaluation of CrP and nucleotides in the human calf during muscle contraction NMR and analytic biochemical evaluation of CrP and nucleotides in the human calf during muscle contraction', *Journal of Applied Physiology*, 74, pp. 2034–2039.

Bangsbo, J., Krustrup, P., González-Alonso, J., Boushel, R. and Saltin, B. (2000) 'Muscle oxygen kinetics at onset of intense dynamic exercise in humans.', *American Journal of Physiology. Regulatory, Integrative and Comparative Physiology*, 279(3), pp. R899-906.

Barnes, P. R., Kemp, G. J., Taylor, D. J. and Radda, G. K. (1997) 'Skeletal muscle metabolism in myotonic dystrophy A ^{31}P magnetic resonance spectroscopy study.', *Brain*, 120, pp. 1699–1711.

Barstow, T. J., Buchthal, S., Zanconato, S. and Cooper, D. M. (1994) 'Muscle energetics and pulmonary oxygen uptake kinetics during moderate exercise.', *Journal of Applied Physiology*, 77(4), pp. 1742–1749.

Beaver, W. L., Wasserman, K. and Whipp, B. J. (1985) 'A new method for detecting anaerobic threshold by gas exchange', *Journal of Applied Physiology*, 60(6), pp. 2020–2027.

Beaver, W. L., Wasserman, K. and Whipp, B. J. (1986) 'Bicarbonate buffering of lactic acid generated during exercise.', *Journal of Applied Physiology*, 60(2), pp. 472–478.

Bendahan, D., Confort-Gouny, S., Kozak-Reiss, G. and Cozzone, P. J. (1990) 'Pi trapping in glycogenolytic pathway can explain transient Pi disappearance during recovery from muscular exercise. A ^{31}P NMR study in the human.', *FEBS Letters*, 269(2), pp. 402–405.

Bendahan, D., Giannesini, B. and Cozzone, P. (2004) 'Functional investigations of exercising muscle: A noninvasive magnetic resonance spectroscopy-magnetic resonance imaging approach', *Cellular and Molecular Life Sciences*, 61(9), pp. 1001–1015.

Bergström, M. and Hultman, E. (1988) 'Energy cost and fatigue during intermittent electrical stimulation of human skeletal muscle.', *Journal of Applied Physiology*, 65(4), pp. 1500–1505.

Boesch, C. (2007) 'Musculoskeletal spectroscopy.', *Journal of Magnet Resonace Imaging*, 25(2), pp. 321–338.

Boesch, C., Slotboom, J., Hoppeler, H. and Kreis, R. (1997) 'In Vivo Determination of Intra-Myocellular Lipids in Human Muscle by Means of Localized ^{1}H-MR Spectroscopy', *Magnetic Resonance in Medicine*, 37(4), pp. 484–493.

Bonora, M., Patergnani, S., Rimessi, A., De Marchi, E., Suski, J. M., Bononi, A., Giorgi, C., Marchi, S., Missiroli, S., Poletti, F., Wieckowski, M. R. and Pinton, P. (2012) 'ATP synthesis and storage.', *Purinergic Signalling*, 8(3), pp. 343–357.

Boska, M. (1994) 'ATP Production rates as a Function of Force level in the Human Gastrocnemius/Soleus Using ^{31}P MRS', *MRM*, 32(1), pp. 1–10.

Bringard, A., Layec, G., Micallef, J. P., Bendahan, D. and Perrey, S. (2012) 'Gas exchange measurements within a magnetic environment: Validation of a new system', *Respiratory Physiology & Neurobiology*, 182(1), pp. 37–46.

van den Broek, N. M. A., De Feyter, H. M. M. L., de Graaf, L., Nicolay, K. and Prompers, J. J. (2007) 'Intersubject differences in the effect of acidosis on phosphocreatine recovery kinetics in muscle after exercise are due to differences in proton efflux rates.', *American Journal of Physiology. Cell Physiology*, 293(1), pp. C228–C237.

Brooke, M. H. and Kaiser, K. K. (1970) 'Muscle fiber types: how many and what kind?', *Archives of Neurology*, 23(4), pp. 369–379.

Broxterman, R. M., Layec, G., Hureau, T. J., Amann, M. and Richardson, R. S. (2017) 'Skeletal muscle bioenergetics during all-out exercise: mechanistic insight into the oxygen uptake slow component and neuromuscular fatigue', *Journal of Applied Physiology*, 122(5), pp. 1208–1217.

Burnley, M., Doust, J. H. and Vanhatalo, A. (2006) 'A 3-min all-out test to determine peak oxygen uptake and the maximal steady state', *Medicine and Science in Sports and Exercise*, 38(11), pp. 1995–2003.

Cannon, D. T., Bimson, W. E., Hampson, S. a., Bowen, T. S., Murgatroyd, S. R., Marwood, S., Kemp, G. J. and Rossiter, H. B. (2014) 'Skeletal muscle ATP turnover by ^{31}P magnetic resonance spectroscopy during moderate and heavy bilateral knee extension', *The Journal of Physiology*, 592(23), pp. 5287–5300.

Cannon, D. T., Howe, F. A., Whipp, B. J., Ward, S. A., McIntyre, D. J., Ladroue, C., Griffiths, J. R., Kemp, G. J. and Rossiter, H. B. (2013) 'Muscle metabolism and activation heterogeneity by combined ^{31}P chemical shift and T2 imaging, and pulmonary O_2 uptake during incremental knee-extensor exercise.', *Journal of Applied Physiology*, 115(6), pp. 839–849.

Celli, R. B. (2000) 'The importance of the differential diagnosis of COPD and asthma', *Chest*, 117(2), p. 15S–19S.

Cheung, K., Hume, P. and Maxwell, L. (2003) 'Delayed Onset Muscle Soreness', *Sports Medicine*, 33(2), pp. 145–164.

Conley, K. E., Blei, M. L., Richards, T. L., Kushmerick, M. J. and Jubrias, S. a (1997) 'Activation of glycolysis in human muscle in vivo.', *The American journal of physiology*, 273(1 Pt 1), pp. C306–C315.

Convertino, V., Goldwater, D. and Sandler, H. (1984) 'Oxygen Uptake Kinetics of Constant-Load Work: Upright vs. Supine Exercise.', *Aviation, Space and Environmental Medicine*, 55(6), pp. 501–506.

Costill, D. L., Coyle, E. F., Fink, W. F., Lesmes, G. R. and Witzmann, F. A. (1979) 'Adaptations in skeletal muscle following strength training.', *Journal of Applied Physiology: Respiratory, Environmental and Exercise Physiology*, 46(1), pp. 96–99.

Coyle, E. F., Sidossis, L. S., Horowitz, J. F. and Beltzt, J. D. (1992) 'Cycling Efficiency is Related to the Percentage of Type I Muscle Fibres', *Medicine and Science in Sports and Exercise*, 24(7), pp. 782–788.

Crowther, G. J. and Gronka, R. K. (2002) 'Fiber recruitment affects oxidative recovery measurements of human muscle in vivo.', *Medicine and Science in Sports and Exercise*, 34(11), pp. 1733–7.

Crowther, G. J., Milstein, J. M., Jubrias, S. A., Kushmerick, M. J., Gronka, R. K. and Conley, K. E. (2003) 'Altered energetic properties in skeletal muscle of men with well-controlled insulin-dependent (type 1) diabetes.', *American Journal of Physiology. Endocrinology and Metabolism*, 284(4), pp. E655-62.

Dekerle, J., Baron, B., Dupont, L., Vanvelcenaher, J. and Pelayo, P. (2003) 'Maximal lactate steady state, respiratory compensation threshold and critical power.', *European Journal of Applied Physiology*, 89(3–4), pp. 281–288.

DiMenna, F. J., Fulford, J., Bailey, S. J., Vanhatalo, A., Wilkerson, D. P. and Jones, A. M. (2010) 'Influence of priming exercise on muscle [PCr] and pulmonary O_2 uptake dynamics during "work-to-work" knee-extension exercise', *Respiratory Physiology & Neurobiology*, 172(1–2), pp. 15–23.

Duteil, S., Bourrilhon, C., Raynaud, J. S., Wary, C., Richardson, R. S., Leroy-Willig, A., Jouanin, J. C., Guezennec, C. Y. and Carlier, P. G. (2004) 'Metabolic and vascular support for the role of myoglobin in humans: a multiparametric NMR study.', *American Journal of Physiology. Regulatory, Integrative and Comparative Physiology*, 287(6), pp. R1441-9.

Edge, J., Bishop, D., Hill-Haas, S., Dawson, B. and Goodman, C. (2006) 'Comparison of muscle buffer capacity and repeated-sprint ability of untrained, endurance-trained and team-sport athletes', *European Journal of Applied Physiology*, 96(3), pp. 225–234.

Edgerton, V. R., Smith, J. L. and Simpson, D. R. (1975) 'Muscle fibre type populations of human leg muscles', *Histochemical Journal*, 7(3), pp. 259–266.

Edwards, L. M., Kemp, G. J., Dwyer, R. M., Walls, J. T., Fuller, H., Smith, S. R. and Earnest, C. P. (2013) 'Integrating muscle cell biochemistry and whole-body physiology in humans:(31)P-MRS data from the InSight trial.', *Scientific Reports*, 3, p. 1182.

Enoka, R. and Stuart, D. (1992) 'Neurobiology of muscle fatigue', *Journal of Applied Physiology*, 72(5), pp. 1631–1648.

Farina, D. (2008) 'Counterpoint: spectral properties of the surface EMG do not provide information about motor unit recruitment and muscle fiber type.', *Journal of Applied Physiology*, 105(5), pp. 1673–1674.

Faude, O., Kindermann, W. and Meyer, T. (2009) 'Lactate threshold concepts: how valid are they?', *Sports Medicine*, 39(6), pp. 469–490.

Feil, S., Newell, J., Minogue, C. and Paessler, H. H. (2011) 'The effectiveness of supplementing a standard rehabilitation program with superimposed neuromuscular electrical stimulation after anterior cruciate ligament reconstruction: a prospective, randomized, single-blind study.', *The American Journal of Sports Medicine*, 39(6), pp. 1238–1247.

Fiedler, G. B., Meyerspeer, M., Schmid, A. I., Goluch, S., Schewzow, K., Laistler, E., Mirzahosseini, A., Niess, F., Unger, E., Wolzt, M. and Moser, E. (2015) 'Localized semi-LASER dynamic ^{31}P magnetic resonance spectroscopy of the soleus during and following exercise at 7 T', *Magnetic Resonance Materials in Physics, Biology and Medicine*, 28(5), pp. 493–501.

Fiedler, G. B., Schmid, A. I., Goluch, S., Schewzow, K., Laistler, E., Niess, F., Unger, E., Wolzt, M., Mirzahosseini, A., Kemp, G. J., Moser, E. and Meyerspeer, M. (2016) 'Skeletal muscle ATP synthesis and cellular H(+) handling measured by localized (31)P-MRS during exercise and recovery.', *Scientific reports*, 6, p. 32037.

Fitts, R. H. (1994) 'Cellular mechanisms of muscle fatigue', *Physiological Reviews*, 74(1), pp. 49–94.

Fitts, R. H. (2008) 'The cross-bridge cycle and skeletal muscle fatigue.', *Journal of Applied Physiology*, 104(2), pp. 551–558.

Forbes, S. C., Paganini, A. T., Slade, J. M., Towse, T. F. and Meyer, R. a (2009) 'Phosphocreatine recovery kinetics following low- and high-intensity exercise in human triceps surae and rat posterior hindlimb muscles.', *American Journal of Physiology. Regulatory, Integrative and Comparative Physiology*, 296(1), pp. R161–R170.

Forbes, S., Paganini, A. T., Slade, J. M., Towse, T. F. and Meyer, R. A. (2009) 'Phosphocreatine recovery kinetics following low- and high-intensity exercise in human triceps surae and rat posterior hindlimb muscles.', *American Journal of Physiology. Regulatory, Integrative and Comparative Physiology*, 296(1), pp. R161–R170.

Forbes, S., Slade, J. M., Francis, R. M. and Meyer, R. A. (2009) 'Comparison of oxidative capacity among leg muscles in humans using gated ^{31}P 2-D chemical shift imaging.', *NMR in Biomedicine*, 22(10), pp. 1063–71.

Francaux, M. A., Jacqmin, P. A. and Sturbois, X. G. (1989) 'Simple kinetic model for the study of lactate metabolic adaptation to exercise in sportsmen routine evaluation.', *Archives Internationales de Physiologie et de Biochimie*, 97(3), pp. 235–245.

Francescato, M. P. and Cettolo, V. (2001) 'Two-pedal ergometer for in vivo MRS studies of human calf muscles.', *Magnetic Resonance in Medicine*, 46(5), pp. 1000–1005.

Gastin, P. B. (2001) 'Energy system interaction and relative contribution during maximal exercise.', *Sports Medicine*, 31(10), pp. 725–741.

Gehlert, S., Weber, S., Weidmann, B., Gutsche, K., Platen, P., Graf, C., Kappes-Horn, K. and Bloch, W. (2012) 'Cycling exercise-induced myofiber transitions in skeletal muscle depend on basal fiber type distribution', *European Journal of Applied Physiology*, 112(7), pp. 2393–2402.

Gladden, L. B. (2004) 'Lactate metabolism: a new paradigm for the third millennium.', *The Journal of Physiology*, 558(Pt 1), pp. 5–30.

Gobbo, M., Maffiuletti, N. A., Orizio, C. and Minetto, M. A. (2014) 'Muscle motor point identification is essential for optimizing neuromuscular electrical stimulation use.', *Journal of Neuroengineering and Rehabilitation*, 11(1), p. 17.

González de Suso, J. M., Bernús, G., Alonso, J., Alay, A., Capdevila, A., Gili, J., Prat, J. a and Arús, C. (1993) 'Development and characterization of an ergometer to study the bioenergetics of the human quadriceps muscle by 31P NMR spectroscopy inside a standard MR scanner.', *Magnetic Resonance in Medicine*, 29(4), pp. 575–81.

de Graaf, R. (2007) *In vivo NMR spectroscopy: principles and techniques*. 2nd Edition. John Wiley & Sons, Ltd.

Grassi, B., Poole, D. C., Richardson, R. S., Knight, D. R., Erickson, B. K. and Wagner, P. D. (1996) 'Muscle O_2 uptake kinetics in humans: implications for metabolic control.', *Journal of applied physiology*, 80(3), pp. 988–998.

Grassi, B., Rossiter, H. B. and Zoladz, J. a. (2015) 'Skeletal Muscle Fatigue and Decreased Efficiency', *Exercise and Sport Sciences Reviews*, 42(2), pp. 75–83.

Green, H. J. J., Hughson, R. L., Orr, G. W. and Ranney, D. A. (1983) 'Anaerobic threshold, blood lactate, and muscle metabolites in progressive exercise.', *Journal of Applied Physiology. Respiratory, Environmental and Exercise Physiology*, 54(4), pp. 1032–1038.

Gregory, C. M. and Bickel, C. S. (2005) 'Recruitment patterns in human skeletal muscle during electrical stimulation.', *Physical Therapy*, 85(4), pp. 358–364.

Grey, T. M., Spencer, M. D., Belfry, G. R., Kowalchuk, J. M., Paterson, D. H. and Murias, J. M. (2014) 'Effects of age and long-term endurance training on VO_2 kinetics', *Medicine and Science in Sports and Exercise*, 47(2), pp. 289–298.

Gussew, A., Krämer, M., Moll, K. and Reichenbach, J. R. (2017) 'MUSCLE: MUlti SliCe Localized Excitation ^{31}P-MRS', in *Proceedings of the 25th Annual Meeting ISMRM*. Honolulu.

Haacke, E., Brown, R., Thompson, M. and Venkatesan, R. (1999) *Magnetic Resonance Imaging - Physical Principles and Sequence Design*. 1st ed. John Wiley & Sons, Ltd.

Häkkinen, K., Alén, M. and Komi, P. V (1985) 'Changes in isometric force- and relaxation-time, electromyographic and muscle fibre characteristics of human skeletal muscle during strength training and detraining.', *Acta Physiologica Scandinavica*, 125(4), pp. 573–585.

Van Hall, G. (2010) 'Lactate kinetics in human tissues at rest and during exercise', *Acta Physiologica*, 199(4), pp. 499–508.

Heck, H. and Schulz, H. (2002) 'Methoden der anaeroben Leistungsdiagnostik', *Deutsche Zeitschrift für Sportmedizin*, 53(7–8), pp. 202–212.

Heerschap, A., Houtman, C., in 't Zandt, H. J., van den Bergh, a J. and Wieringa, B. (1999) 'Introduction to in vivo ^{31}P magnetic resonance spectroscopy of (human) skeletal muscle.', *The Proceedings of the Nutrition Society*, 58(4), pp. 861–870.

Henneman, E., Somjen, G. and Carpenter, D. (1965) 'Functional Significance of Cell Size in Spinal Motorneurons', *Journal of neurophysiology*, 28, pp. 560–80.

Herda, T. J., Housh, T. J., Fry, A. C., Weir, J. P., Schilling, B. K., Ryan, E. D. and Cramer, J. T. (2010) 'A noninvasive, log-transform method for fiber type discrimination using mechanomyography.', *Journal of Electromyography and Kinesiology*, 20(5), pp. 787–794.

Hiepe, P., Gussew, A., Rzanny, R., Anders, C., Walther, M., Scholle, H. C. and Reichenbach, J. R. (2014) 'Interrelations of muscle functional MRI, diffusion-weighted MRI and ^{31}P-MRS in exercised lower back muscles', *NMR in Biomedicine*, 27(8), pp. 958–970.

Hiepe, P., Gussew, A., Rzanny, R., Kurz, E., Anders, C., Walther, M., Scholle, H.-C. and Reichenbach, J. R. (2015) 'Age-related structural and functional changes of low back muscles.', *Experimental Gerontology*, 65, pp. 23–34.

Hollmann, W. (2001) '42 years ago--development of the concepts of ventilatory and lactate threshold.', *Sports Medicine*, 31(5), pp. 315–520.

Holm, S. (1979) 'A Simple Sequentially Rejective Multiple Test Procedure', *Scandinavian Journal of Statistics*, 6(2), pp. 65–70.

Hosseini Ghomi, R., Bredella, M. a, Thomas, B. J., Miller, K. K. and Torriani, M. (2011) 'Modular MR-compatible lower leg exercise device for whole-body scanners.', *Skeletal Radiology*, 40(10), pp. 1349–1354.

Hsu, A. C. and Dawson, M. J. (2000) 'Accuracy of ^{1} H and ^{31}P MRS Analyses of Lactate in Skeletal Muscle', *Magnetic Resonance in Medicine*, 44, pp. 418–426.

Hunter, P., Coveney, P. V, de Bono, B., Diaz, V., Fenner, J., Frangi, A. F., Harris, P., Hose, R., Kohl, P., Lawford, P., McCormack, K., Mendes, M., Omholt, S., Quarteroni, A., Skår, J., Tegner, J., Randall Thomas, S., Tollis, I., Tsamardinos, I., van Beek, J. H. G. M. and Viceconti, M. (2010) 'A vision and strategy for the virtual physiological human in 2010 and beyond.', *Philosophical Transactions. Series A, Mathematical, Physical, and Engineering Sciences*, 368(1920), pp. 2595–2614.

Hunter, P. J. (2004) 'The IUPS Physiome Project: a framework for computational physiology.', *Progress in Biophysics and Molecular Biology*, 85(2–3), pp. 551–569.

Hunter, P. J. and Borg, T. K. (2003) 'Integration from proteins to organs: the Physiome Project.', *Nature Reviews. Molecular Cell Biology*, 4(3), pp. 237–243.

Hureau, T. J., Olivier, N., Millet, G. Y., Meste, O. and Blain, G. M. (2014) 'Exercise performance is regulated during repeated sprints to limit the development of peripheral fatigue beyond a critical threshold.', *Experimental Physiology*, 99(7), pp. 951–963.

Jeneson, J. a L., Schmitz, J. P. J., Hilbers, P. a J. and Nicolay, K. (2010) 'An MR-compatible bicycle ergometer for in-magnet whole-body human exercise testing.', *Magnetic Resonance in Medicine*, 63(1), pp. 257–261.

Johansen, L. and Quistorff, B. (2003) '^{31}P-MRS characterization of sprint and endurance trained athletes', *International Journal of Sports Medicine*, 24(3), pp. 183–189.

Jones, A. M. and Burnley, M. (2005) 'Effects of exercise modailty on VO_2 kinetics', in Jones, A. M. and Poole, D. C. (eds) *Oxygen Uptake Kinetics in Sport, Exercise and Medicine*. London and New York: Routledge, pp. 95–114.

Jones, A. M. and Poole, D. C. (2005) 'Introduction to oxygen uptake kinetics and historical development of discipline', in Jones, A. M. and Poole, D. C. (eds) *Oxygen Uptake Kinetics in Sport, Exercise and Medicine*. London and New York: Routledge, pp. 3–35.

Jones, A., Vanhatalo, A., Burnley, M., Morton, R. and Poole, D. (2010) 'Critical power: implications for determination of VO_{2max} and exercise tolerance.', *Medicine and Science in Sports and Exercise*, 42(10), pp. 1876–1890.

Jouvensal, L., Carlier, P. G. and Bloch, G. (1997) 'Low visibility of lactate in excised rat muscle using double quantum proton spectroscopy', *Magnetic Resonance in Medicine*, 38(5), pp. 706–711.

Juel, C. (1997) 'Lactate-proton cotransport in skeletal muscle.', *Physiological reviews*, 77(2), pp. 321–358.

Juel, C. (2004) 'Laktattransport im Skelettmuskel: Trainingsinduzierte Anpassung und Bedeutung bei koerperlicher Belastung. / Lactate transport in skeletal muscle: Training-induced adaptation and significance in physical exercise', *Deutsche Zeitschrift für Sportmedizin*, 55(6), pp. 157–160.

Juel, C., Klarskov, C., Nielsen, J. J., Krustrup, P., Mohr, M. and Bangsbo, J. (2004) 'Effect of high-intensity intermittent training on lactate and H^+ release from human skeletal muscle.', *American Journal of Physiology. Endocrinology and Metabolism*, 286(2), pp. E245–E251.

Kemmler, W. K., Lauber, D., Wasserman, A. and Mayhew, J. L. (2006) 'Predicting Maximal Strength In Trained Postmenopausal Woman', *Journal of Strength and Conditioning Research*, 20(4), pp. 838–842.

Kemp, G. J. (2015) 'Muscle Studies by ^{31}P MRS', *eMagRes*, 4(1), pp. 525–534.

Kemp, G. J., Ahmad, R. E., Nicolay, K. and Prompers, J. J. (2015) 'Quantification of skeletal muscle mitochondrial function by (31) P magnetic resonance spectroscopy techniques: a quantitative review.', *Acta Physiologica*, 213(1), pp. 107–144.

Kemp, G. J., Meyerspeer, M. and Moser, E. (2007) 'Absolute quantification of phosphorus metabolite concentrations in human muscle in vivo by ^{31}P MRS: a quantitative review', *NMR Biomedicine*, 20(6), pp. 555–565.

Kemp, G. J. and Radda, G. K. (1994) 'Quantitative interpretation of bioenergetic data from ^{31}P and 1H magnetic resonance spectroscopic studies of skeletal muscle: an analytical review.', *Magnetic Resonance Quarterly*, 10(1), pp. 43–63.

Kemp, G. J., Roussel, M., Bendahan, D., Le Fur, Y. and Cozzone, P. J. (2001) 'Interrelations of ATP synthesis and proton handling in ischaemically exercising human forearm muscle studied by ^{31}P magnetic resonance spectroscopy', *Journal of Physiology*, 535(3), pp. 901–928.

Kent-Braun, J., McCully, K. K. and Chance, B. (1990) 'Metabolic effects of training in humans: a ^{31}P-MRS study.', *Journal of Applied Physiology*, 69(3), pp. 1165–1170.

Keyser, R. E. (2010) 'Peripheral fatigue: high-energy phosphates and hydrogen ions.', *PM&R*, 2(5), pp. 347–358.

Kindermann, W., Schramm, M. and Keul, J. (1980) 'Aerobic performance diagnostics with different experimental settings.', *Int J Sports Med*, 1(3), pp. 110–114. doi: 10.1055/s-2008-1034644.

Kindermann, W., Simon, G. and Keul, J. (1979) 'The significance of the aerobic-anaerobic transition for the determination of work load intensities during endurance training.', *European Journal of Applied Physiology and Occupational Physiology*, 42(1), pp. 25–34.

Kmiecik, J. A., Gregory, C. D., Liang, Z.-P., Hrad, D. E., Lauterbur, P. C. and Dawson, M. J. (1997) 'Quantitative lactate-specific MR imaging and ^{1}H spectroscopy of skeletal muscle at macroscopic and microscopic resolutions using a zero-quantum/double-quantum coherence filter and SLIM/GSLIM localization', *Magnetic Resonance in Medicine*, 37(6), pp. 840–850.

Kohrt, W. M., Malley, M. T., Coggan, A. R., Spina, R. J., Ogawa, T., Ehsani, A. A., Bourey, R. E., Martin, W. H. and Holloszy, J. O. (1985) 'Effects of gender , age , and fitness level on response in 60-71 yr olds', *Journal of Applied Physiology*, 71(5), pp. 2004–2011.

Korzeniewski, B. and Zoladz, J. A. (2005) 'Some factors determining the PCr recovery overshoot in skeletal muscle.', *Biophysical Chemistry*, 116(2), pp. 129–136.

Kreis, R., Jung, B., Slotboom, J., Felblinger, J. and Boesch, C. (1999) 'Effect of exercise on the creatine resonances in ^{1}H MR spectra of human skeletal muscle.', *Journal of Magnetic Resonance*, 137(2), pp. 350–357.

Kubukeli, Z., Noakes, T. and Dennis, S. (2002) 'Training Techniques to Improve Endurance Exercise Performances', *Sports Medicine*, 32(8), pp. 489–509.

Kupa, E. J., Roy, S. H., Kandarian, S. C. and De Luca, C. J. (1995) 'Effects of muscle fiber type and size on EMG median frequency and conduction velocity.', *Journal of Applied Physiology*, 79(1), pp. 23–32.

Kushmerick, M. J., Meyer, R. a and Brown, T. R. (1992) 'Regulation of oxygen consumption in fast- and slow-twitch muscle.', *The American Journal of Physiology*, 263(3 Pt.1), pp. C598-606.

Lamarra, N., Whipp, B. J., Ward, S. A. and Wasserman, K. (1987) 'Effect of interbreath fluctuations on characterizing exercise gas exchange kinetics.', *Journal of Applied Physiology*, 62(5), pp. 2003–2012.

Layec, G., Bringard, A., Vilmen, C., Micallef, J.-P., Fur, Y. Le, Perrey, S., Cozzone, P. J. and Bendahan, D. (2008) 'Accurate work-rate measurements during in vivo MRS studies of exercising human quadriceps.', *Magnetic Resonance Materials in Physics, Biology, and Medicine*, 21(3), pp. 227–235.

Layec, G., Bringard, A., Yashiro, K., Le Fur, Y., Vilmen, C., Micallef, J.-P., Perrey, S., Cozzone, P. J. and Bendahan, D. (2012) 'The slow components of phosphocreatine and pulmonary oxygen uptake can be dissociated during heavy exercise according to training status', *Experimental Physiology*, 97(8), pp. 955–969.

Layec, G., Haseler, L. J., Hoff, J., Hart, C. R., Liu, X., Le Fur, Y., Jeong, E.-K. and Richardson, R. S. (2013) 'Short-term training alters the control of mitochondrial respiration rate before maximal oxidative ATP synthesis.', *Acta Physiologica Scandinavica*, 208(4), pp. 376–386.

Layec, G., Malucelli, E., Le Fur, Y., Manners, D., Yashiro, K., Testa, C., Cozzone, P. J., Iotti, S. and Bendahan, D. (2013) 'Effects of exercise-induced intracellular acidosis on the phosphocreatine recovery kinetics: a ^{31}P MRS study in three muscle groups in humans.', *NMR in Biomedicine*, 26(11), pp. 1403–1411.

Lexell, J. (1995) 'Human aging, muscle mass, and fiber type composition.', *The Journals of Gerontology. Series A, Biological Sciences and Medical Sciences*, 50 Spec No, pp. 11–16.

Lindeboom, L., Bruls, Y. M. H., van Ewijk, P. A., Hesselink, M. K. C., Wildberger, J. E., Schrauwen, P. and Schrauwen-Hinderling, V. B. (2017) 'Longitudinal relaxation time editing for acetylcarnitine detection with ^{1}H-MRS', *Magnetic Resonance in Medicine*, 77(2), pp. 505–510.

Liu, Y., Schlumberger, A., Wirth, K., Schmidtbleicher, D. and Steinacker, J. M. (2003) 'Different effects on human skeletal myosin heavy chain isoform expression: strength vs. combination training', *Journal of Applied Physiology*, 94(6), pp. 2282–2288.

Lodi, R., Kemp, G. J., Iotti, S., Radda, G. K. and Barbiroli, B. (1997) 'Influence of cytosolic pH on in vivo assessment of human muscle mitochondrial respiration by phosphorus magnetic resonance spectroscopy.', *Magma*, 5(2), pp. 165–171.

Maassen, N. and Böning, D. (2008) 'Physiologische "Nebenwirkung" der Milchsäure', *Deutsche Zeitschrift für Sportmedizin*, pp. 292–296.

MacKay, A., Laule, C., Vavasour, I., Bjarnason, T., Kolind, S. and Mädler, B. (2006) 'Insights into brain microstructure from the T2 distribution.', *Magnetic Resonance Imaging*, 24(4), pp. 515–25.

Mackey, A. L., Brandstetter, S., Schjerling, P., Bojsen-Moller, J., Qvortrup, K., Pedersen, M. M., Doessing, S., Kjaer, M., Magnusson, S. P. and Langberg, H. (2011) 'Sequenced response of extracellular matrix deadhesion and fibrotic regulators after muscle damage is involved in protection against future injury in human skeletal muscle.', *The FASEB Journal*, 25(6), pp. 1943–1959.

MacLean, D. A., Imadojemu, V. A. and Sinoway, L. I. (2000) 'Interstitial pH, K(+), lactate, and phosphate determined with MSNA during exercise in humans.', *American Journal of Physiology. Regulatory, Integrative and Comparative Physiology*, 278(3), pp. R563-71.

Mader, A., Liesen, H., Heck, H., Philippi, H., Rost, R., Schuerch, P. and Hollmann, W. (1976) 'Zur Beurteilung der sportartspezifischen Ausdauerleistungsfähigkeit im Labor', *Deutsche Zeitschrift für Sportmedizin*, 27(4), pp. 80–112.

Maffiuletti, N. A. (2010) 'Physiological and methodological considerations for the use of neuromuscular electrical stimulation.', *European Journal of Applied Physiology*, 110(2), pp. 223–234.

Maffiuletti, N. A., Minetto, M. A., Farina, D. and Bottinelli, R. (2011) 'Electrical stimulation for neuromuscular testing and training: state-of-the art and unresolved issues.', *European Journal of Applied Physiology*, 111(10), pp. 2391–2397.

Matheson, G. O., McKenzie, D. C., Gheorghiu, D., Ellinger, D. C., Quinney, H. A. and Allen, P. S. (1992) '^{31}P NMR of electrically stimulated rectus femoris muscle: an in vivo graded exercise model.', *Magnetic Resonance in Medicine*, 26(1), pp. 60–70.

Mäurer, J., Konstanczak, P., Söllner, O., Ehrenstein, T., Knollmann, F., Wolff, R., Vogl, T. J. and Felix, R. (1999) 'Muscle metabolism of professional athletes using ^{31}P-spectroscopy.', *Acta Radiologica*, 40(1), pp. 73–77.

Mayhew, J., Johnson, B., LaMonte, M., Lauber, D. and Kemmler, W. (2008) 'Accuracy of Prediction Equations for Determining one Repetition Maximum Bench Press in Women Before and After Resistance Training', *Journal of Strength and Conditioning Research*, 22(5), pp. 1570–1577.

McCreary, C. R., Chilibeck, P. D., Marsh, G. D., Paterson, D. H., Cunningham, D. a and Thompson, R. T. (1996) 'Kinetics of pulmonary oxygen uptake and muscle phosphates during moderate-intensity calf exercise.', *Journal of Applied Physiology*, 81(3), pp. 1331–1338.

Meyerspeer, M., Kemp, G. J., Mlynárik, V., Krssák, M., Szendroedi, J., Nowotny, P., Roden, M. and Moser, E. (2007) 'Direct noninvasive quantification of lactate and high energy phosphates simultaneously in exercising human skeletal muscle by localized magnetic resonance spectroscopy.', *Magnetic Resonance in Medicine*, 57(4), pp. 654–660.

Meyerspeer, M., Krssák, M., Kemp, G. J., Roden, M. and Moser, E. (2005) 'Dynamic interleaved ^{1}H/^{31}P STEAM MRS at 3 Tesla using a pneumatic force-controlled plantar flexion exercise rig.', *Magnetic Resonance Materials in Physics, Biology and Medicine*, 18(5), pp. 257–262.

Meyerspeer, M., Robinson, S., Nabuurs, C. I., Scheenen, T., Schoisengeier, A., Unger, E., Kemp, G. J. and Moser, E. (2012) 'Comparing localized and nonlocalized dynamic ^{31}P magnetic resonance spectroscopy in exercising muscle at 7 T.', *Magnetic Resonance in Medicine*, 68(6), pp. 1713–1723.

Meyerspeer, M., Scheenen, T., Schmid, A. I., Mandl, T., Unger, E. and Moser, E. (2011) 'Semi-LASER localized dynamic ^{31}P magnetic resonance spectroscopy in exercising muscle at ultra-high magnetic field', *Magnetic Resonance in Medicine*, 65(5), pp. 1207–1215.

Midgley, A. W., Bentley, D. J., Luttikholt, H., McNaughton, L. R. and Millet, G. P. (2008) 'Challenging a dogma of exercise physiology: does an incremental exercise test for valid $VO_{2\ max}$ determination really need to last between 8 and 12 minutes?', *Sports Medicine*, 38(6), pp. 441–447.

Millet, G. P., Jaouen, B., Borrani, F. and Candau, R. (2002) 'Effects of concurrent endurance and strength training on running economy and .VO(2) kinetics.', *Medicine and Science in Sports and Exercise*, 34(8), pp. 1351–1359.

Mogensen, M., Bagger, M., Pedersen, P. K., Fernström, M. and Sahlin, K. (2006) 'Cycling efficiency in humans is related to low UCP3 content and to type I fibres but not to mitochondrial efficiency.', *Journal of Physiology*, 571(Pt 3), pp. 669–681.

Moll, K., Gussew, A., Hein, C., Stutzig, N. and Reichenbach, J. R. (2017) 'Combined spiroergometry and ^{31}P-MRS of human calf muscle during high-intensity exercise.', *NMR in Biomedicine*, 30(7), p. e3723.

Moll, K., Gussew, A. and Reichenbach, J. R. (2017) 'Influence of muscle fiber tension on ^{31}P MRS recovery parameter after intense exercise', in *Proceedings of the 25th Annual Meeting ISMRM*. Honolulu.

Moon, R. B. and Richards, J. H. (1973) 'Determination of intracellular pH by ^{31}P magnetic resonance.', *The Journal of Biological Chemistry*, 248(20), pp. 7276–7278.

Mullins, P. G., McGonigle, D. J., O'Gorman, R. L., Puts, N. a J., Vidyasagar, R., Evans, C. J., Cardiff Symposium on MRS of GABA and Edden, R. a E. (2014) 'Current practice in the use of MEGA-PRESS spectroscopy for the detection of GABA.', *NeuroImage*, 86, pp. 43–52.

Niess, F., Fiedler, G. B., Schmid, A. I., Goluch, S., Kriegl, R., Wolzt, M., Moser, E. and Meyerspeer, M. (2017) 'Interleaved multivoxel ^{31}P MR spectroscopy', *Magnetic Resonance in Medicine*, 77(3), pp. 921–927.

Nosaka, K., Aldayel, A., Jubeau, M. and Chen, T. C. (2011) 'Muscle damage induced by electrical stimulation.', *European Journal of Applied Physiology*, 111(10), pp. 2427–2437.

Ozyener, F., Rossiter, H. B., Ward, S. A. and Whipp, B. J. (2001) 'Influence of exercise intensity on the on- and off-transient kinetics of pulmonary oxygen uptake in humans.', *The Journal of Physiology*, 533(3), pp. 891–902.

Palange, P., Ward, S. A., Carlsen, K.-H., Casaburi, R., Gallagher, C. G., Gosselink, R., O'Donnell, D. E., Puente-Maestu, L., Schols, a M., Singh, S. and Whipp, B. J. (2007) 'Recommendations on the use of exercise testing in clinical practice.', *The European Respiratory Journal*, 29(1), pp. 185–209.

Pan, J. W., Hamm, J. R., Hetherington, H. P., Rothman, D. L. and Shulman, R. G. (1991) 'Correlation of Lactate and pH', *Magnetic Resonance in Medicine*, 20, pp. 57–65.

Park, J. H., Brown, R. L., Park, C. R., McCully, K., Cohn, M., Haselgrove, J. and Chance, B. (1987) 'Functional pools of oxidative and glycolytic fibers in human muscle observed by ^{31}P magnetic resonance spectroscopy during exercise.', *Proceedings of the National Academy of Sciences of the United States of America*, 84(24), pp. 8976–80.

Pernus, F. and Erzen, I. (1991) 'Arrangement of fiber types within fascicles of human vastus lateralis muscle.', *Muscle & Nerve*, 14(4), pp. 304–309.

Péronnet, F. and Aguilaniu, B. (2006) 'Lactic acid buffering, nonmetabolic CO_2 and exercise hyperventilation: A critical reappraisal', *Respiratory Physiology and Neurobiology*, 150(1), pp. 4–18.

Pesta, D., Paschke, V., Hoppel, F., Kobel, C., Kremser, C., Esterhammer, R., Burtscher, M., Kemp, G. and Schocke, M. (2013) 'Different Metabolic Responses during Incremental Exercise Assessed by Localized ^{31}P MRS in Sprint and Endurance Athletes and Untrained Individuals', *International Journal of Sports Medicine*, 34(8), pp. 669–675.

Pette, D., Peuker, H. and Staron, R. S. (1999) 'The impact of biochemical methods for single muscle fibre analysis.', *Acta Physiologica Scandinavica*, 166(4), pp. 261–277.

Pette, D. and Staron, R. S. (1990) 'Cellular and molecular diversities of mammalian skeletal muscle fibers.', *Reviews of Physiology, Biochemistry and Pharmacology*, 116, pp. 1–76.

Pette, D. and Staron, R. S. (1997) 'Mammalian skeletal muscle fiber type transitions.', *International Review of Cytology*, 170, pp. 143–223.

Poole, D. C., Gladden, L. B., Kurdak, S. and Hogan, M. C. (1994) 'L-(+)-lactate infusion into working dog gastrocnemius: no evidence lactate per se mediates VO_2 slow component.', *Journal of Applied Physiology*, 76(2), pp. 787–792.

Poole, D. C., Ward, S. a, Gardner, G. W. and Whipp, B. J. (1988) 'Metabolic and respiratory profile of the upper limit for prolonged exercise in man.', *Ergonomics*, 31(9), pp. 1265–1279.

Pozzan, T., Rizzuto, R., Volpe, P. and Meldolesi, J. (1994) 'Molecular and cellular physiology of intracellular calcium stores', *Physiological Reviews*, 74(3), pp. 595–636.

Price, T. B., Kamen, G., Damon, B. M., Knight, C. A., Applegate, B., Gore, J. C., Eward, K. and Signorile, J. F. (2003) 'Comparison of MRI with EMG to study muscle activity associated with dynamic plantar flexion', *Magnetic Resonance Imaging*, 21(8), pp. 853–861.

Prompers, J. J., Wessels, B., Kemp, G. J. and Nicolay, K. (2014) 'MITOCHONDRIA: investigation of in vivo muscle mitochondrial function by ^{31}P magnetic resonance spectroscopy.', *The International Journal of Biochemistry & Cell Biology*, 50, pp. 67–72.

Quistoroff, B., Nielsen, S., Carsten, T., Jensen, E. K. and Henriksen, O. (1990) 'A simple calf muscle ergometer for use in a standrad whole-body MR Scanner', *Magnetic Resonance in Medicine*, 449(13), pp. 444–449.

Ranatunga, K. W. and Thomas, P. E. (1990) 'Correlation between shortening velocity, force-velocity relation and histochemical fibre-type composition in rat muscles.', *Journal of Muscle Research and Cell Motility*, 11(3), pp. 240–250.

Rayleigh, L. (1880) 'Investigations in Optics, with special reference to the Spectroscope', *Monthly Notices of the Royal Astronomical Society*, 40, p. 254.

Raymer, G. H., Allman, B. L., Rice, C. L., Marsh, G. D. and Thompson, R. T. (2006) 'Characteristics of a MR-compatible ankle exercise ergometer for a 3.0 T head-only MR scanner.', *Medical Engineering & Physics*, 28(5), pp. 489–94.

Ren, J., Sherry, A. D. and Malloy, C. R. (2013) 'Noninvasive monitoring of lactate dynamics in human forearm muscle after exhaustive exercise by 1 H-magnetic resonance spectroscopy at 7 tesla', *Magnetic Resonance Imaging*, 70, pp. 610–619.

Rennie, M. J. (1999) 'An introduction to the use of tracers in nutrition and metabolism', *Proceedinggs of the Nutrition Society*, 58(4), pp. 935–944.

Richardson, R. S., Wary, C., Walter Wray, D., Hoff, J., Rossiter, H., Layec, G. and Carlier, P. G. (2015) 'MRS Evidence of Adequate O_2 Supply in Human Skeletal Muscle at the Onset of Exercise.', *Medicine and Science in Sports and Exercise*, 47(11), pp. 2299–307.

Rivera-Brown, A. M. and Frontera, W. R. (2012) 'Principles of Exercise Physiology: Responses to Acute Exercise and Long-term Adaptations to Training', *PM and R*, 4(11), pp. 797–804.

Robergs, R. a, Ghiasvand, F. and Parker, D. (2004) 'Biochemistry of exercise-induced metabolic acidosis.', *American Journal of Physiology. Regulatory, Integrative and Comparative Physiology*, 287(3), pp. R502-16.

Roecker, K., Mayer, F., Striegel, H. and Dickhuth, H. H. (2000) 'Increase characteristics of the cumulated excess-CO_2 and the lactate concentration during exercise', *International Journal of Sports Medicine*, 21(6), pp. 419–423.

Roecker, K., Prettin, S. and Sorichter, S. (2005) 'Gas Exchange Measurements with High Temporal Resolution : The Breath-by-Breath Approach', *International Journal of Sports Medicine*, 26(Suppl 1), pp. S11–S18.

Roecker, K., Schotte, O., Niess, A. M., Horstmann, T. and Dickhuth, H. H. (1998) 'Predicting competition performance in long-distance running by means of a treadmill test.', *Medicine and Science in Sports and Exercise*, 30(10), pp. 1552–7.

Rossiter, H. B., Howe, F. A., Ward, S. A., Kowalchuk, J. M., Griffiths, J. R. and Whipp, B. J. (2000) 'Intersample fluctuations in phosphocreatine concentration determined by ^{31}P-magnetic resonance spectroscopy and parameter estimation of metabolic responses to exercise in humans.', *Journal of Physiology*, 528(2), pp. 359–369.

Rossiter, H. B., Ward, S. A., Doyle, V. L., Howe, F. A., Griffiths, J. R. and Whipp, B. J. (1999) 'Inferences from pulmonary O_2 uptake with respect to intramuscular [phosphocreatine] kinetics during moderate exercise in humans', *Journal of Physiology*, 518(3), pp. 921–932.

Rossiter, H. B., Ward, S. A., Howe, F. A., Kowalchuk, J. M., Griffiths, J. R. and Whipp, B. J. (2002) 'Dynamics of intramuscular ^{31}P-MRS P(i) peak splitting and the slow components of PCr and O_2 uptake during exercise.', *Journal of Applied Physiology*, 93(6), pp. 2059–69.

Rossiter, H. B., Ward, S. A., Howe, F. A., Wood, D. M., Kowalchuk, J. M., Griffiths, J. R. and Whipp, B. J. (2003) 'Effects of dichloroacetate on VO_2 and intramuscular ^{31}P metabolite kinetics during high-intensity exercise in humans.', *Journal of Applied Physiology*, 95(3), pp. 1105–15.

Rossiter, H. B., Ward, S. A., Kowalchuk, J. M., Howe, F. A., Griffiths, J. R. and Whipp, B. J. (2002) 'Dynamic asymmetry of phosphocreatine concentration and O(2) uptake between the on- and off-transients of moderate- and high-intensity exercise in humans.', *Journal of Physiology*, 541(Pt 3), pp. 991–1002.

Ryschon, T., Fowler, M. D., Arai, A., Balaban, S., Fowler, D., Wysong, R. E., Leighton, B. and Clem, R. (1995) 'A multimode dynamometer of human skeletal muscle for in vivo MRS studies', *Journal of Applied Physiology*, 79(6), pp. 2139–2147.

Rzanny, R., Grassme, R., Reichenbach, J. ., Rottenbach, M., Petrovitch, A., Kaiser, W. . and Scholle, H. . (2004) 'Simultaneous surface electromyography (SEMG) and -MR spectroscopy measurements of the lumbar back muscle during isometric exercise', *Journal of Neuroscience Methods*, 133(1–2), pp. 143–152.

Rzanny, R., Grassme, R., Reichenbach, J. R., Scholle, H.-C. and Kaiser, W. a (2006) 'Investigations of back muscle fatigue by simultaneous ^{31}P MRS and surface EMG measurements.', *Biomedical Engineering*, 51(5–6), pp. 305–13.

Rzanny, R., Stutzig, N., Gussew, A., Kaiser, W. A., Thorhauer, H.-A. and Reichenbach, J. R. (2009) 'Investigations of metabolic differences due to differences in the muscle fiber distribution by using ^{31}P-MRS at 3 . 0 T', in *Proceedings of the 16th Annual Meeting*. Honolulu.

Sahlin, K. (2014) 'Muscle Energetics During Explosive Activities and Potential Effects of Nutrition and Training', *Sports Medicine*, 44(S2), pp. 167–173.

Sahlin, K., Söderlund, K., Tonkonogi, M. and Hirakoba, K. (1997) 'Phosphocreatine content in single fibers of human muscle after sustained submaximal exercise.', *The American Journal of Physiology*, 273(1 Pt 1), pp. C172-8.

Sale, D., Quinlan, J., Marsh, E., McComas, a J. and Belanger, A. Y. (1982) 'Influence of joint position on ankle plantarflexion in humans.', *Journal of Applied Physiology. Respiratory, Environmental and Exercise Physiology*, 52(6), pp. 1636–42.

Sant'Ana Pereira, J. A., Sargeant, A. J., Rademaker, A. C., de Haan, A. and van Mechelen, W. (1996) 'Myosin heavy chain isoform expression and high energy phosphate content in human muscle fibres at rest and post-exercise.', *The Journal of Physiology*, 496 (Pt 2, pp. 583–8.

Scharhag-Rosenberger, F. (2010) 'Spiroergometrie zur Ausdauerleistungsdiagnostik', *Deutsche Zeitschrift fur Sportmedizin*, 61(6), pp. 146–147.

Scharhag-Rosenberger, F., Meyer, T., Walitzek, S. and Kindermann, W. (2009) 'Time course of changes in endurance capacity: A 1-yr training study', *Medicine and Science in Sports and Exercise*, 41(5), pp. 1130–1137.

Schiaffino, S. and Reggiani, C. (2011) 'Fiber types in mammalian skeletal muscles.', *Physiological Reviews*, 91(4), pp. 1447–531.

Schmid, A. I., Schewzow, K., Fiedler, G. B., Goluch, S., Laistler, E., Wolzt, M., Moser, E. and Meyerspeer, M. (2014) 'Exercising calf muscle T2 * changes correlate with pH, PCr recovery and maximum oxidative phosphorylation', *NMR in Biomedicine*, 27(5), pp. 553–560.

Schröder, L., Schmitz, C. and Bachert, P. (2005) 'Cumulative "roof effect" in high-resolution in vivo ^{31}P NMR spectra of human calf muscle and the Clebsch-Gordan coefficients of ATP at 1.5 T.', *Journal of Magnetic Resonance*, 174(1), pp. 68–77.

Seyri, K. M. and Maffiuletti, N. A. (2011) 'Effect of Electromyostimulation Training on Muscle Strength and Sports Performance', *Strength and Conditioning Journal*, 33(1), pp. 70–75.

Shanely, R. A., Zwetsloot, K. A., Triplett, N. T., Meaney, M. P., Farris, G. E. and Nieman, D. C. (2014) 'Human Skeletal Muscle Biopsy Procedures Using the Modified Bergström Technique', *Journal of Visualized Experiments*, (91), pp. 1–8.

Siebert, T., Leichsenring, K., Rode, C., Wick, C., Stutzig, N., Schubert, H., Blickhan, R. and Böl, M. (2015) 'Three-Dimensional Muscle Architecture and Comprehensive Dynamic Properties of Rabbit Gastrocnemius, Plantaris and Soleus: Input for Simulation Studies.', *PloS one*, 10(6), p. e0130985.

Siebert, T., Sust, M., Thaller, S., Tilp, M. and Wagner, H. (2007) 'An improved method to determine neuromuscular properties using force laws - From single muscle to applications in human movements.', *Human Movement Science*, 26(2), pp. 320–41.

Siebert, T., Till, O., Stutzig, N., Günther, M. and Blickhan, R. (2014) 'Muscle force depends on the amount of transversal muscle loading.', *Journal of Biomechanics*, 47(8), pp. 1822–8.

Sinha, S., Shin, D. D., Hodgson, J. a, Kinugasa, R. and Edgerton, V. R. (2012) 'Computer-controlled, MR-compatible foot-pedal device to study dynamics of the muscle tendon complex under isometric, concentric, and eccentric contractions.', *Journal of Magnet Resonace Imaging*, 36(2), pp. 498–504.

Sjöström, M., Lexell, J. and Downham, D. Y. (1992) 'Differences in fiber number and fiber type proportion within fascicles. A quantitative morphological study of whole vastus lateralis muscle from childhood to old age.', *The Anatomical Record*, 234(2), pp. 183–9.

Stegmann, H., Kindermann, W. and Schnabel, A. (1981) 'Lactate kinetics and individual anaerobic threshold.', *International Journal of Sports Medicine*, 2(3), pp. 160–5.

Steinacker, J. M., Wang, L., Lormes, W., Reißnecker, S. and Liu, Y. (2002) 'Strukturanpassungen des skelettmuskels auf Training', *Deutsche Zeitschrift fur Sportmedizin*, 53(12), pp. 354–360.

Street, D., Bangsbo, J. and Juel, C. (2001) 'Interstitial pH in human skeletal muscle during and after dynamic graded exercise.', *The Journal of Physiology*, 537(Pt 3), pp. 993–8.

Stubbs, M., Van den Boogaart, A., Bashford, C. L., Miranda, P. M., Rodrigues, L. M., Howe, F. a and Griffiths, J. R. (1996) '^{31}P-magnetic resonance spectroscopy studies of nucleated and non-nucleated erythrocytes; time domain data analysis (VARPRO) incorporating prior knowledge can give information on the binding of ADP.', *Biochimica et Biophysica Acta*, 1291(2), pp. 143–8.

Stutzig, N., Rzanny, R., Moll, K., Gussew, A., Reichenbach, J. R. and Siebert, T. (2017) 'The pH Heterogeneity in Human Calf Muscle During Neuromuscular Electrical Stimulation', *Magnetic Resonance in Medicine*, 77(6), pp. 2097–2106.

Stutzig, N. and Siebert, T. (2015a) 'Influence of joint position on synergistic muscle activity after fatigue of a single muscle head.', *Muscle & Nerve*, 51(2), pp. 259–67.

Stutzig, N. and Siebert, T. (2015b) 'Muscle force compensation among synergistic muscles after fatigue of a single muscle.', *Human movement science*, 42, pp. 273–87.

Takahashi, H., Kuno, S. Y., Katsuta, S., Shimojo, H., Masuda, K., Yoshioka, H., Anno, I. and Itai, Y. (1996) 'Relationships between fiber composition and NMR measurements in human skeletal muscle.', *NMR in Biomedicine*, 9(1), pp. 8–12.

Taylor, D. J., Styles, P., Matthews, P. M., Arnold, D. A., Gadian, D. G., Bore, P. and Radda, G. K. (1986) 'Energetics of human muscle: exercise-induced ATP depletion.', *Magnetic Resonance in Medicine*, 3(1), pp. 44–54.

Tesch, P. A., Thorsson, A. and Fujitsuka, N. (1989) 'Creatine phosphate in fiber types of skeletal muscle before and after exhaustive exercise.', *Journal of Applied Physiology*, 66(4), pp. 1756–9.

Tidow, G. and Wiemann, K. (1993) 'Zur Interpretation und Veränderbarkeit von Kraft-Zeit-Kurven bei Eexplosiv-Ballistischen Krafteinsätzen', *Deutsche Zeitschrift fur Sportmedizin*, 44(2), pp. 136–150.

Tonon, C., Gramegna, L. L. and Lodi, R. (2012) 'Magnetic resonance imaging and spectroscopy in the evaluation of neuromuscular disorders and fatigue.', *Neuromuscular Disorders*, 22 Suppl 3, pp. S187-91.

Tonson, A., Ratel, S., Le Fur, Y., Vilmen, C., Cozzone, P. J. and Bendahan, D. (2010) 'Muscle energetics changes throughout maturation: a quantitative ^{31}P-MRS analysis.', *Journal of Applied Physiology*, 109(6), pp. 1769–78.

Tschiesche, K., Gussew, A., Glöckner, M., Derlien, S. and Reichenbach, J. (2015) 'Multimodal determination of load changes in the muscle - A combination of ^{1}H MEGA-PRESS and blood sampling', in *Proceedings of the 23th Annual Meeting ISMRM*. Toronto.

Tschiesche, K., Rothamel, M., Rzanny, R., Gussew, A., Hiepe, P. and Reichenbach, J. R. (2014) 'MR-compatible pedal ergometer for reproducible exercising of the human calf muscle', *Medical Engineering & Physics*, 36(7), pp. 933–937.

Valkovič, L., Chmelík, M., Just Kukurová, I., Jakubová, M., Kipfelsberger, M. C., Krumpolec, P., Tušek Jelenc, M., Bogner, W., Meyerspeer, M., Ukropec, J., Frollo, I., Ukropcová, B., Trattnig, S. and Kršňák, M. (2014) 'Depth-resolved surface coil MRS (DRESS)-localized dynamic ^{31}P-MRS of the exercising human gastrocnemius muscle at 7 T', *NMR in Biomedicine*, 27(11), pp. 1346–1352.

Valkovič, L., Chmelík, M. and Kršňák, M. (2017) 'In-vivo(31)P-MRS of skeletal muscle and liver: A way for non-invasive assessment of their metabolism.', *Analytical Biochemistry*, 529, pp. 193–215.

Vandenborne, K., McCully, K., Kakihira, H., Prammer, M., Bolinger, L., Detre, J. a, De Meirlier, K., Walter, G., Chance, B. and Leigh, J. S. (1991) 'Metabolic heterogeneity in human calf muscle during maximal exercise.', *Proceedings of the National Academy of Sciences of the United States of America*, 88(13), pp. 5714–8.

Vandenborne, K., Walter, G., Leigh, J. S. and Goelman, G. (1993) 'pH heterogeneity during exercise in localized spectra from single human muscles.', *The American Journal of Physiology*, 265(5 Pt 1), pp. C1332–C1339.

Vanderthommen, M., Depresseux, J. C., Dauchat, L., Degueldre, C., Croisier, J. L. and Crielaard, J. M. (2000) 'Spatial distribution of blood flow in electrically stimulated human muscle: a positron emission tomography study.', *Muscle & Nerve*, 23(4), pp. 482–9.

Vanhamme, L., van den Boogaart A and Van Huffel S (1997) 'Improved method for accurate and efficient quantification of MRS data with use of prior knowledge', *Journal of Magnetic Resonance*, 129(1), pp. 35–43.

Vorgerd, M. and Zange, J. (2007) 'Treatment of glycogenosys type V (McArdle disease) with creatine and ketogenic diet with clinical scores and with ^{31}P-MRS on working leg muscle', *Acta Myologica*, 26(1), pp. 61–63.

Wahl, P., Bloch, W. and Mester, J. (2009) 'Moderne Betrachtungsweisen des Laktats: Laktat ein überschätztes und zugleich unterschätztes Molekül', *Schweiz Zeitschr Sportmed Sporttraum*, 57(3), pp. 100–107.

Wand, B. M. and O'Connell, N. E. (2008) 'Chronic non-specific low back pain - sub-groups or a single mechanism?', *BMC Musculoskeletal Disorders*, 9, p. 11.

Wasserman, K., Hansen, J. and Sue, D. (1991) 'Faciliation of Oxygen Consumption by Lactic Acidosis during Exercise', *Physiology*, 6(1), pp. 29–34.

Wasserman, K. and McIlroy, M. B. (1964) 'Detecting the Threshold of Anaerobic Metabolism in Cardiac Patients during Exercise', *The American Journal of Cardiology*, 14, pp. 844–52.

Weippert, M., Kreuzfeld, S., Arndt, D. and Stoll, R. (2008) 'Vergleich eines mobilen laktatmessgerätes mit einem laboranalysegerät - LactateScout vs. Miniphotometer 8', *Deutsche Zeitschrift fur Sportmedizin*, 59(2), pp. 46–49.

Westhoff, M., Rühle, K. H., Greiwing, A., Schomaker, R., Eschenbacher, H., Siepmann, M. and Lehnigk, B. (2013) 'Ventilatorische und metabolische (Laktat-)Schwellen', *DMW - Deutsche Medizinische Wochenschrift*, 138(6), pp. 275–280.

Whipp, B. J., Davis, J. A., Torres, F. and Wasserman, K. (1981) 'A test to determine parameters of aerobic function during exercise.', *Journal of Applied Physiology*, 50(1), pp. 217–21.

Whipp, B. J. and Rossiter, H. B. (2005) 'The Kinetics of Oxygen Uptake- Physiological Inferences from teh Parameters', in Jones, A. M. and Poole, D. C. (eds) *Oxygen Uptake kinetics in Sport, Exercise and Medicine*. London and New York: Routledge, pp. 62–94.

Whipp, B. J., Rossiter, H. B. and Ward, S. A. (2002) 'Exertional Oxygen Uptake Kinetics: A Stamen of Stamina?', *Biochem Soc Trans*, 30(2), pp. 237–47.

Whipp, B. J., Rossiter, H. B., Ward, S. A., Avery, D., Doyle, V. L., Howe, F. A. and Griffiths, J. R. (1999) 'Simultaneous determination of muscle ^{31}P and O_2 uptake kinetics during whole body NMR spectroscopy', *Journal of Applied Physiology*, 86(2), pp. 742–747.

Whittall, K. P., MacKay, A. L., Graeb, D. A., Nugent, R. A., Li, D. K. and Paty, D. W. (1997) 'In vivo measurement of T2 distributions and water contents in normal human brain.', *Magnetic resonance in medicine*, 37(1), pp. 34–43.

Widrick, J. J., Trappe, S. W., Blaser, C. A., Costill, D. L. and Fitts, R. H. (1996) 'Isometric force and maximal shortening velocity of single muscle fibers from elite master runners.', *The American journal of physiology*, 271(2 Pt 1), pp. C666-75.

Wilson, J. R., Mccully, K. K., Mancini, D. M., Boden, B., Chance, B. and Wilson, J. R. (1988) 'Relationship of muscular fatigue to pH and diprotonated Pi in humans : a ^{31}P-NMR study', *Journal of Applied Physiology*, 64(6), pp. 2333–2339.

Yoshida, T. (1988) 'The Rate of Phosphocreatine Hydrolysis and Resynthesis in Exercising Muscle in Humans using ^{31}P-MRS', *J Physiol Anthropol*, 21(5), pp. 247–255.

Yoshida, T., Abe, D. and Fukuoka, Y. (2013) 'Phosphocreatine resynthesis during recovery in different muscles of the exercising leg by ^{31}P-MRS', *Scandinavian Journal of Medicine and Science in Sports*, 23(5), pp. 313–319.

Yoshida, T. and Watari, H. (1993) 'Changes in intracellular pH during repeated exercise.', *European journal of applied physiology and occupational physiology*, 67(3), pp. 274–8.

Yoshida, T. and Watari, H. (1994) 'Exercise-induced splitting of the inorganic phosphate peak: investigation by time-resolved ^{31}P-nuclear magnetic resonance spectroscopy.', *European journal of applied physiology and occupational physiology*, 69(6), pp. 465–73.

Youdas, J. W., Krause, D. a, Egan, K. S., Therneau, T. M. and Laskowski, E. R. (2003) 'The effect of static stretching of the calf muscle-tendon unit on active ankle dorsiflexion range of motion.', *The Journal of Orthopaedic and Sports Physical Therapy*, 33(7), pp. 408–417.

List of Figures

List of Tables

Supplementary Material

Additional Figures for Chapter 4

Fig S4-1 PCr and pH time courses of all endurance-trained subjects in both muscles (left: *SOL*, right: *GM*) during rest, load (red dots) and recovery phase arranged according to their representative load duration. The blue dashed lines in the PCr kinetics indicate the fit results (cf. Eq [4-2]).

load duration	endurance-trained athletes	
	SOL	**GM**
180-200 s	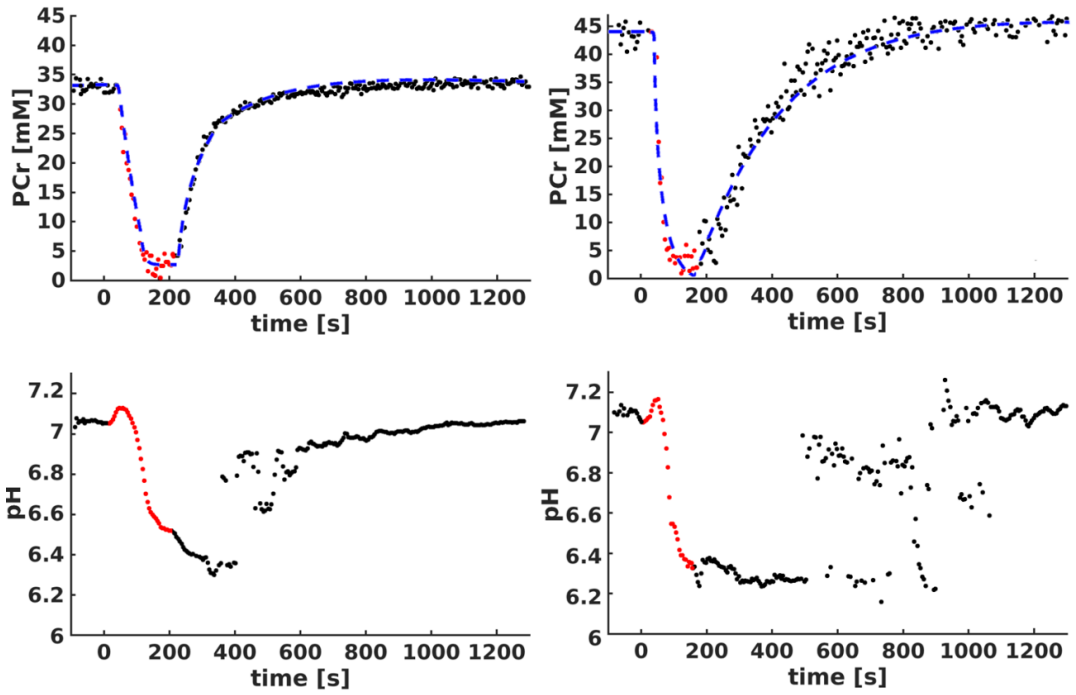	

	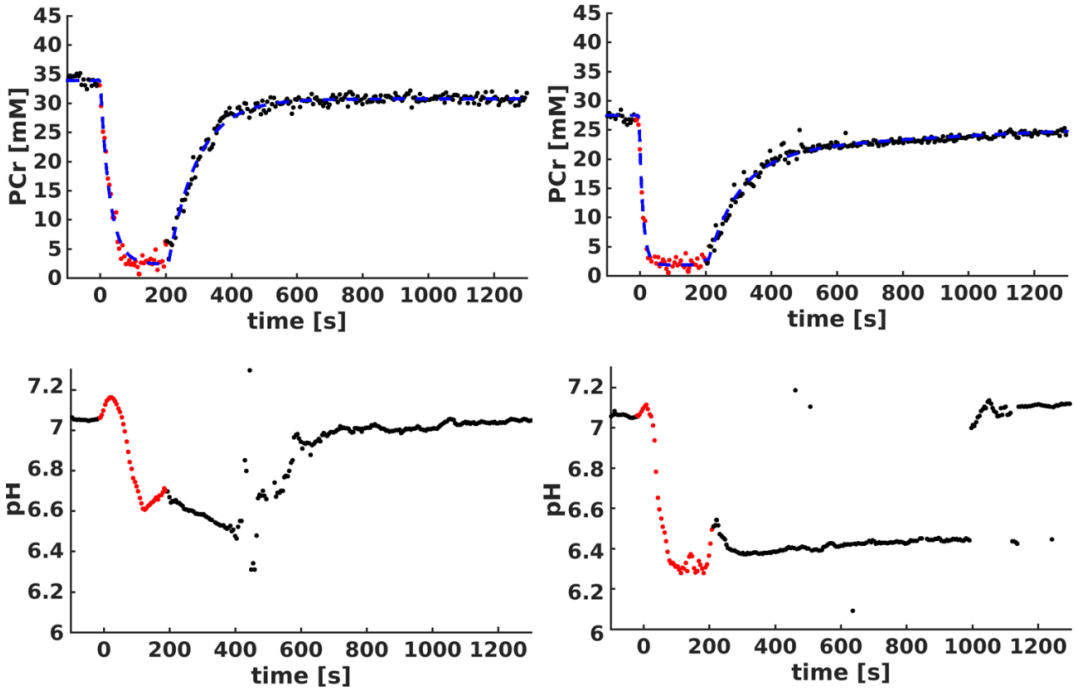
200-400 s	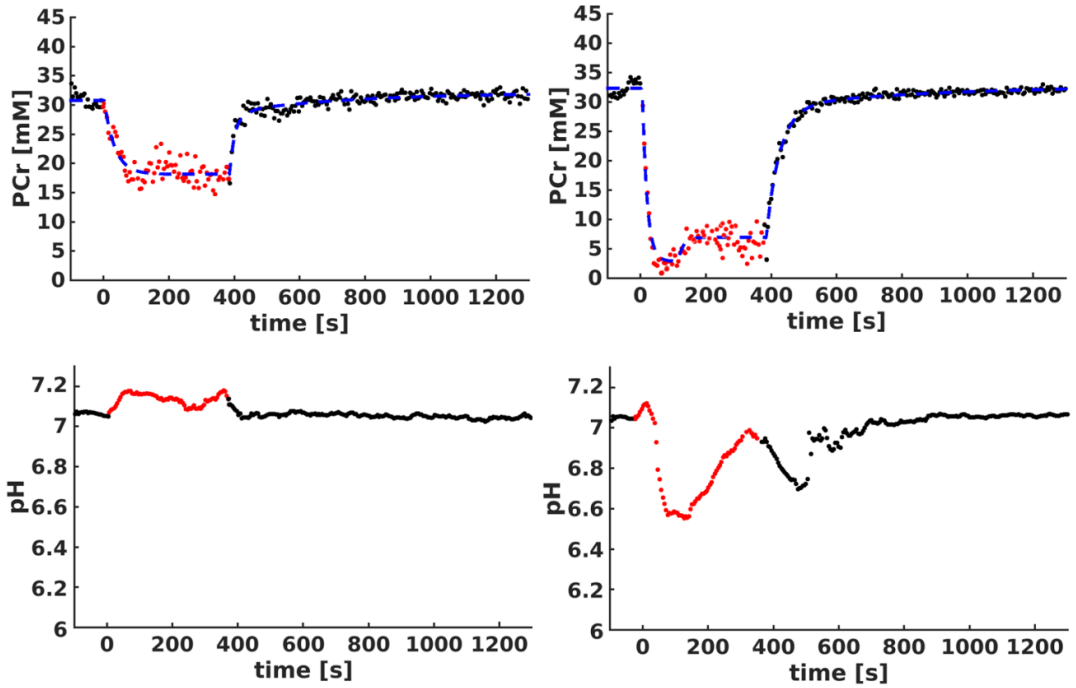

200- 400 s	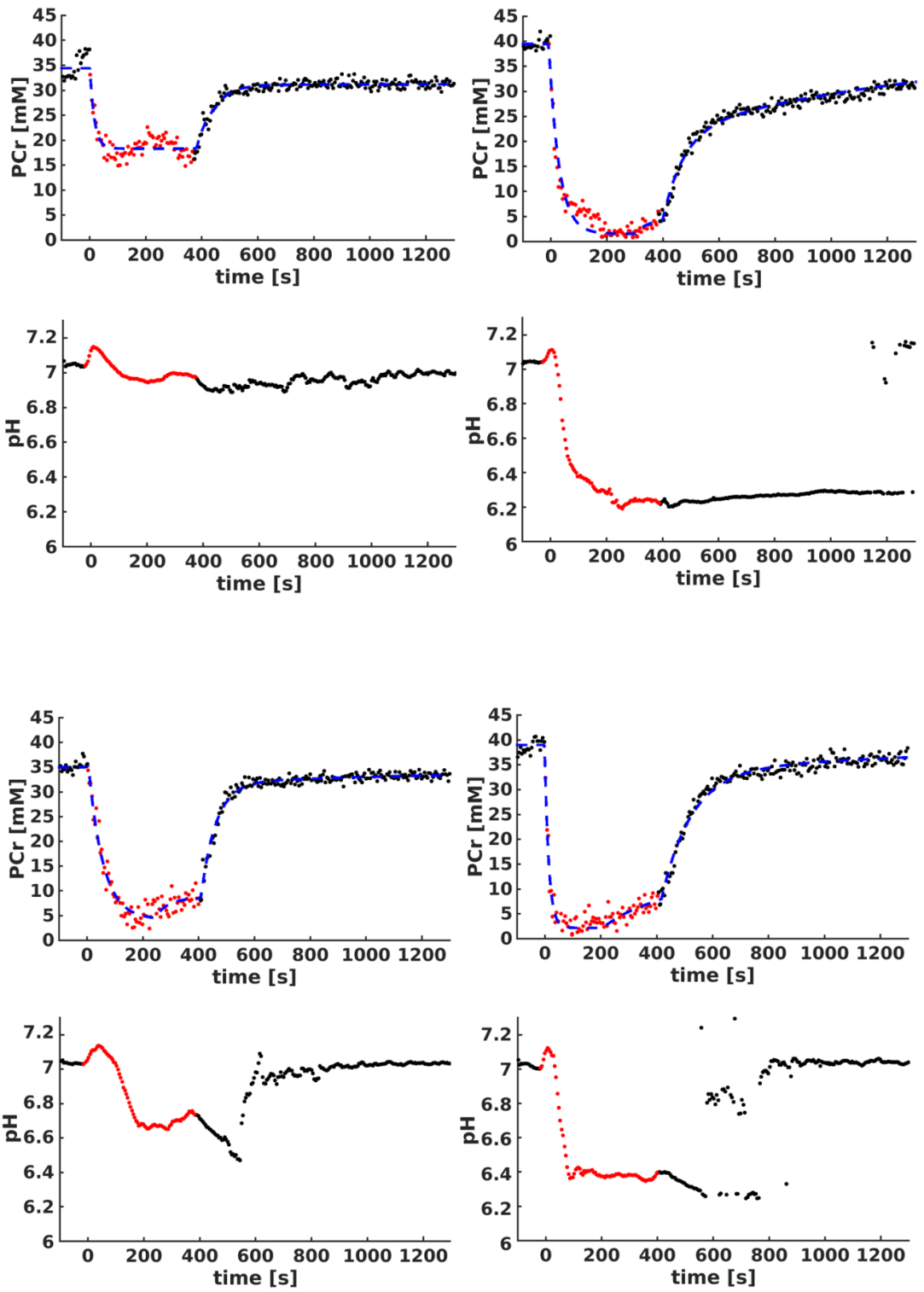 PCr [mM] time [s] pH time [s] PCr [mM] time [s] pH time [s] PCr [mM] time [s] pH time [s] PCr [mM] time [s] pH time [s]

400- 600 s	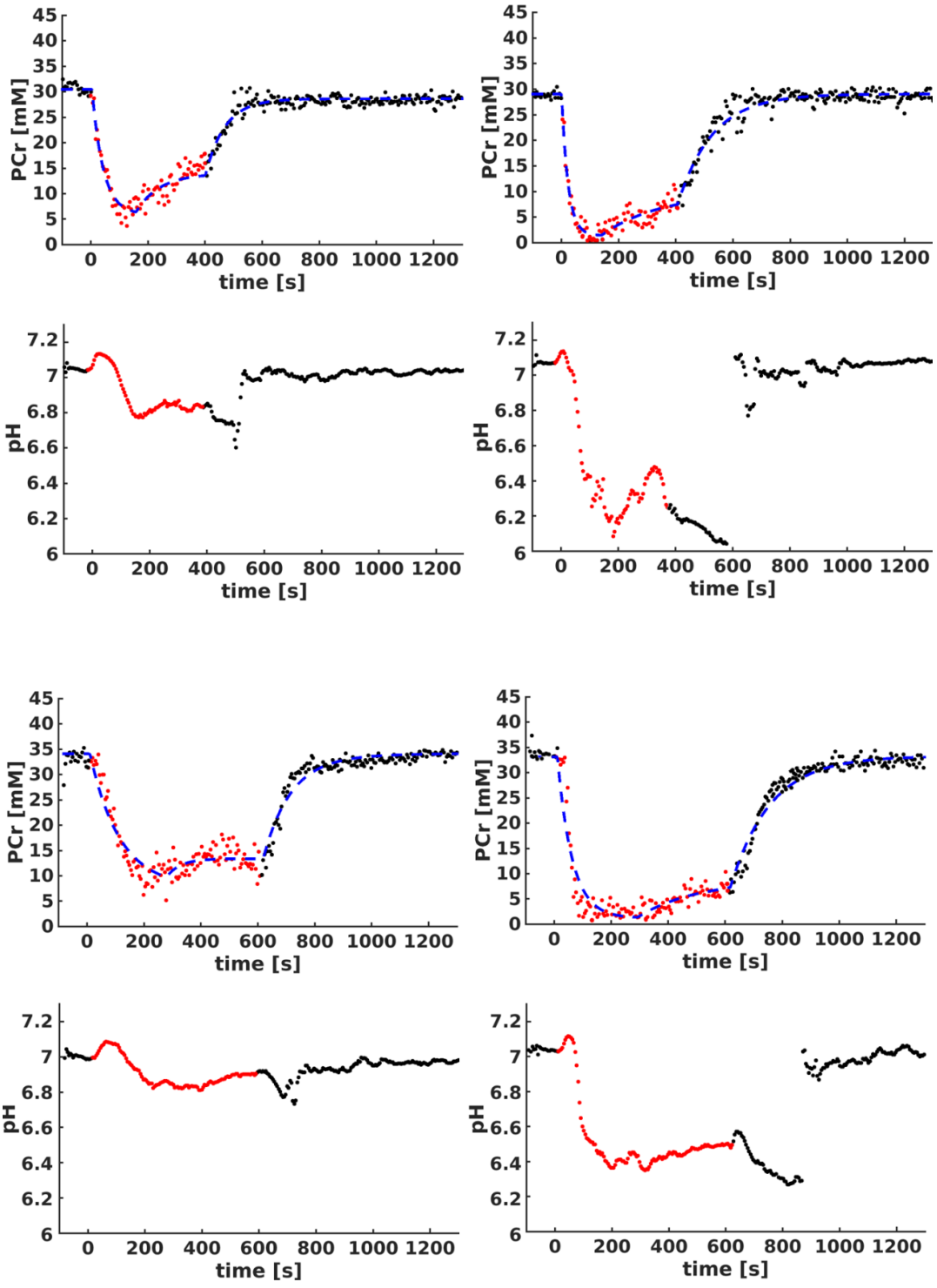

>600 s	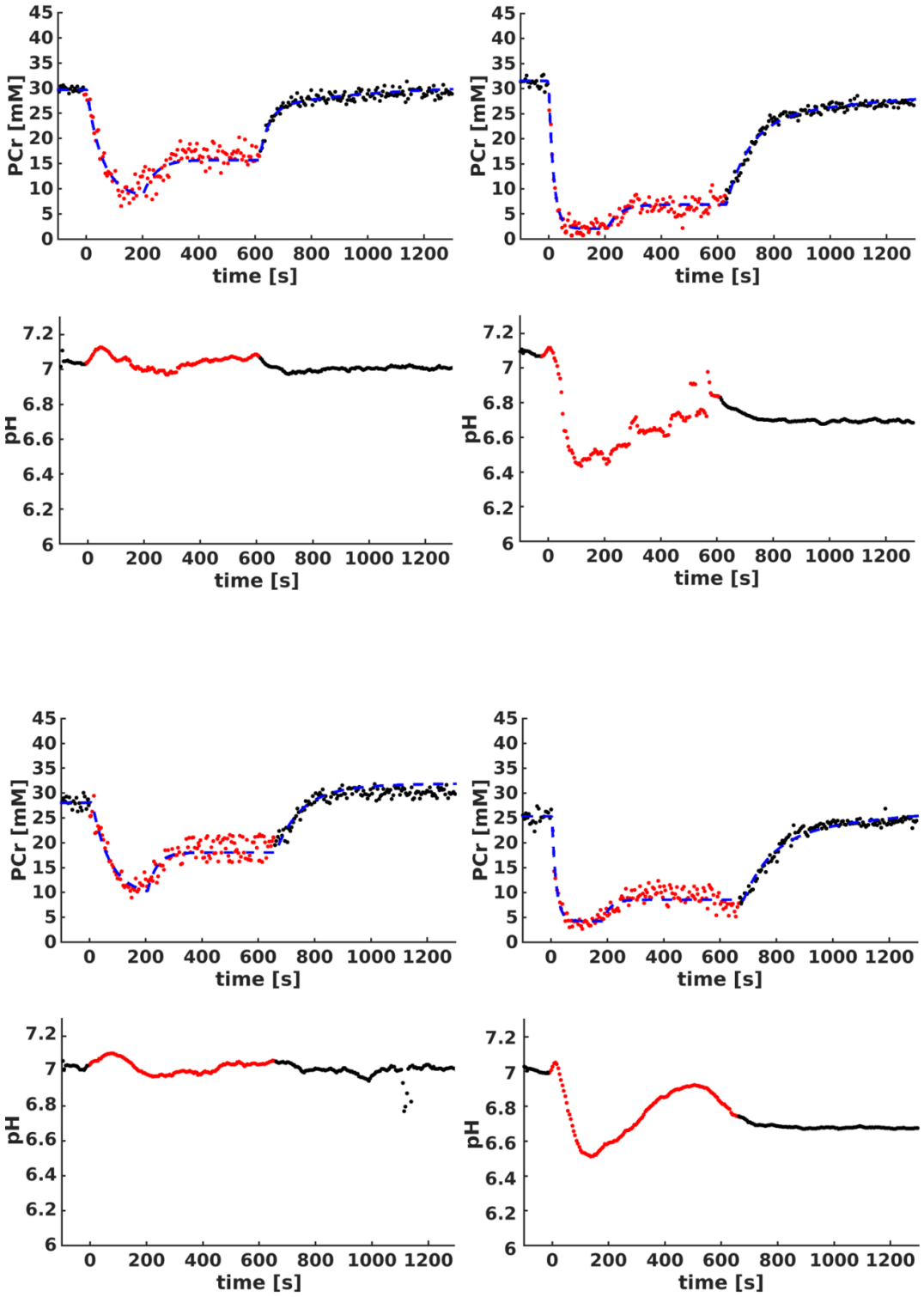

>600 s	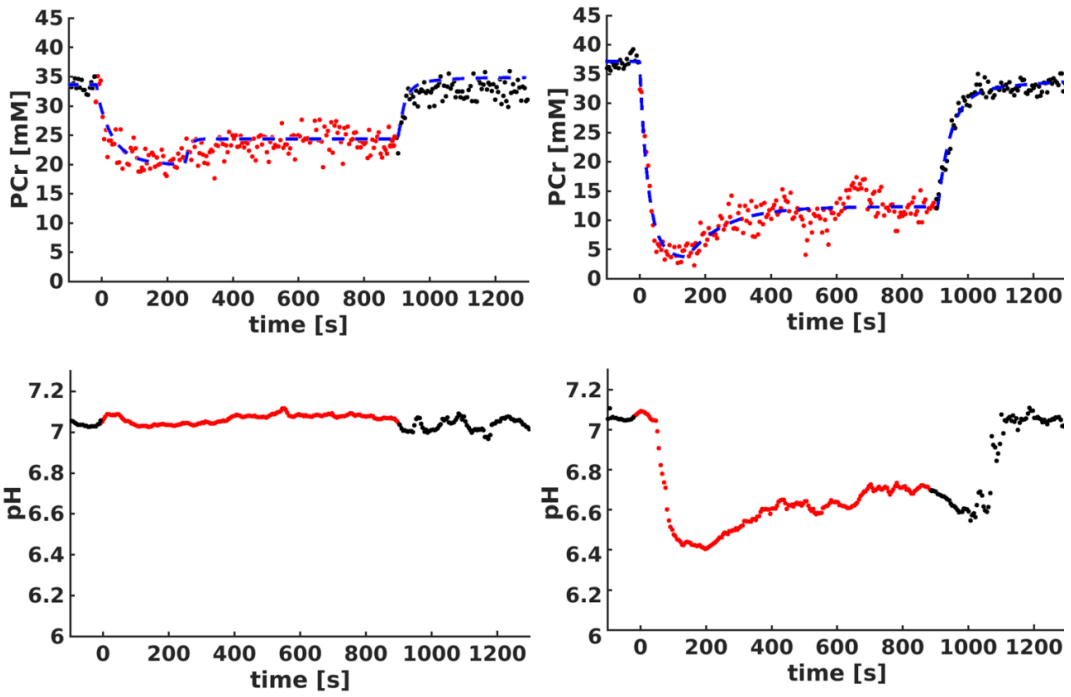

Fig S4-2 PCr and pH time courses of all sprint-trained subjects in both muscles (left: *SOL*, right: *GM*) during rest, load (red dots) and recovery phase arranged according to their representative load duration. The blue dashed lines in the PCr kinetics indicate the fit results (cf. Eq [4-2]).

load duration	sprint-trained athletes	
	SOL	**GM**
180-200 s	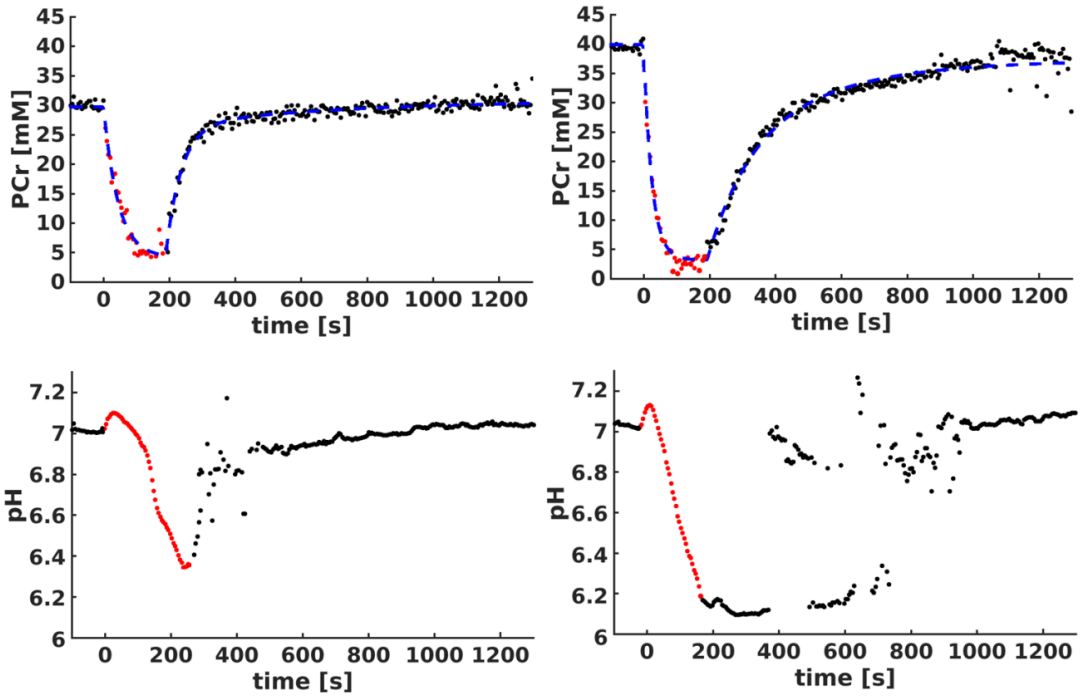	

200- 400 s	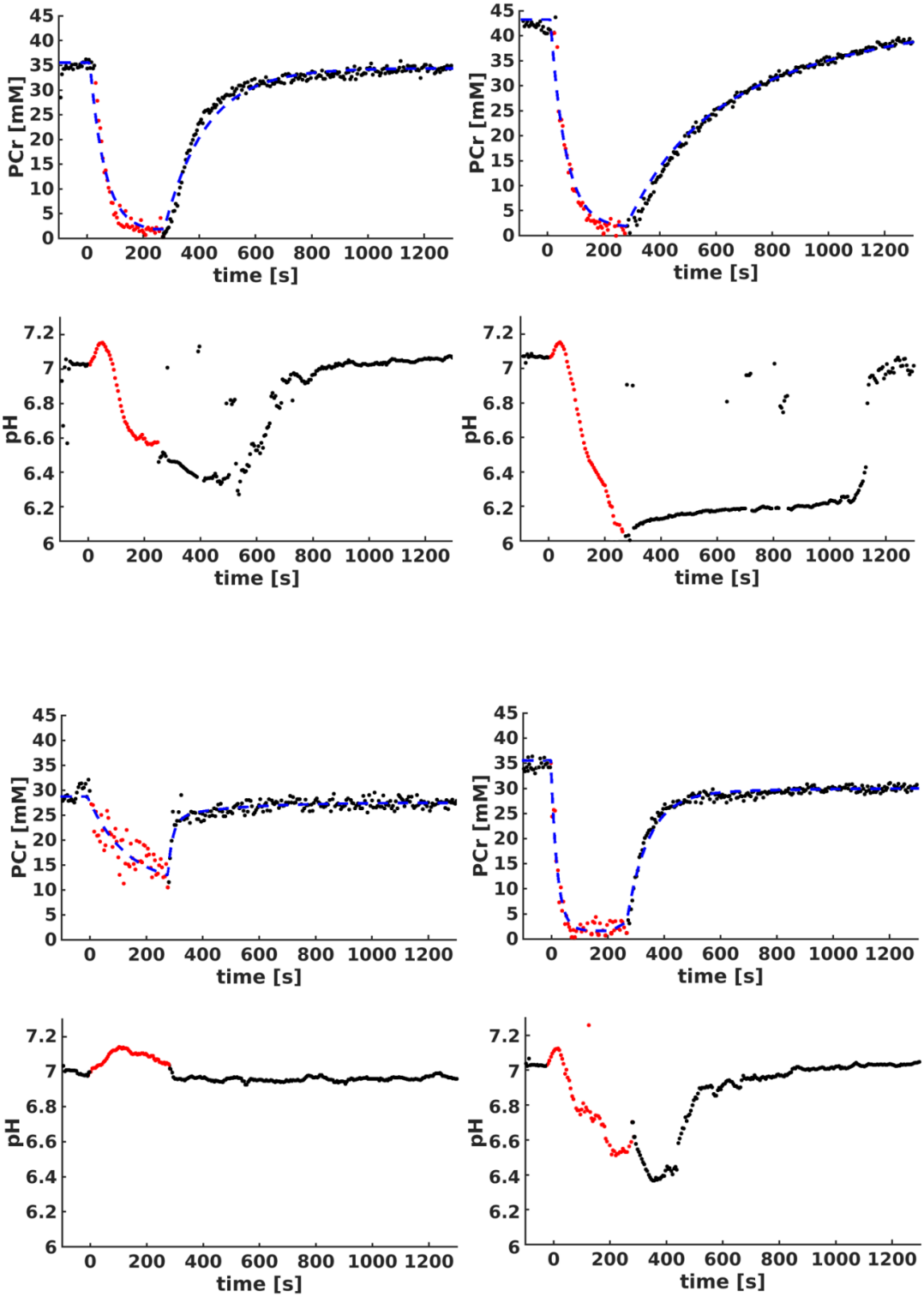

200- 400 s	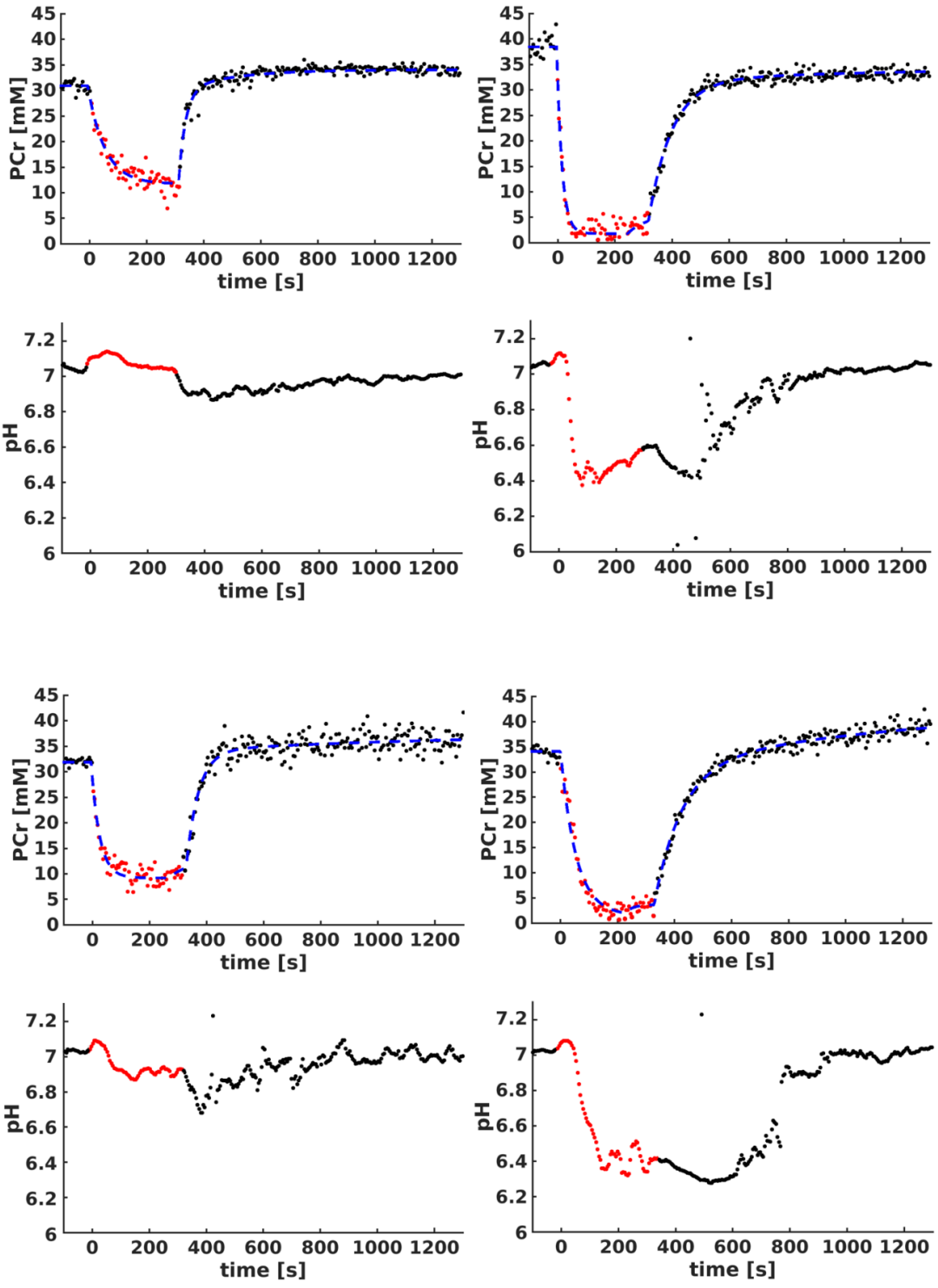 PCr [mM] time [s] pH time [s] PCr [mM] time [s] pH time [s] PCr [mM] time [s] pH time [s] PCr [mM] time [s] pH time [s]

400- 600 s	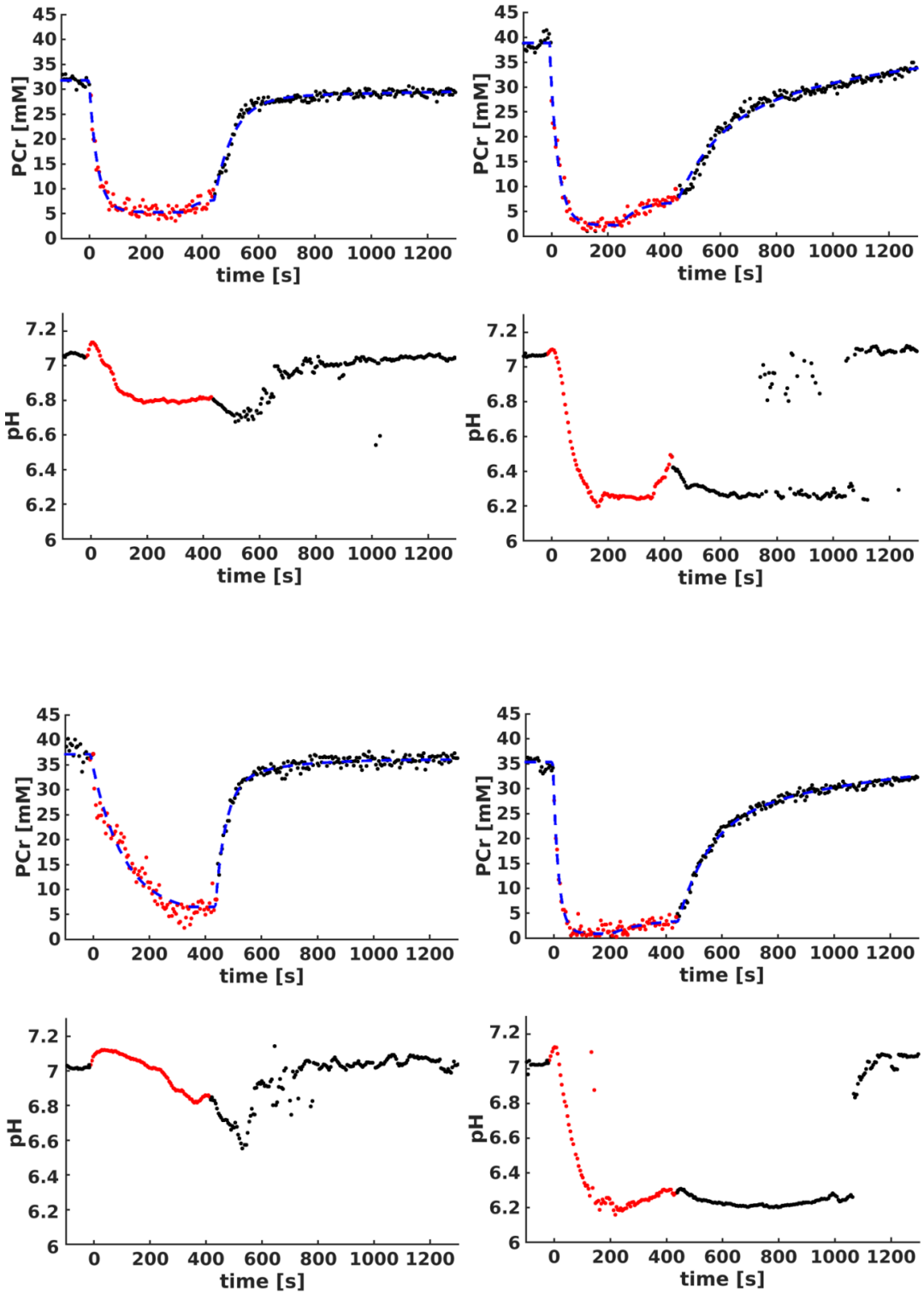 PCr [mM] time [s] pH time [s] PCr [mM] time [s] pH time [s] PCr [mM] time [s] pH time [s] PCr [mM] time [s] pH time [s]

400-600 s	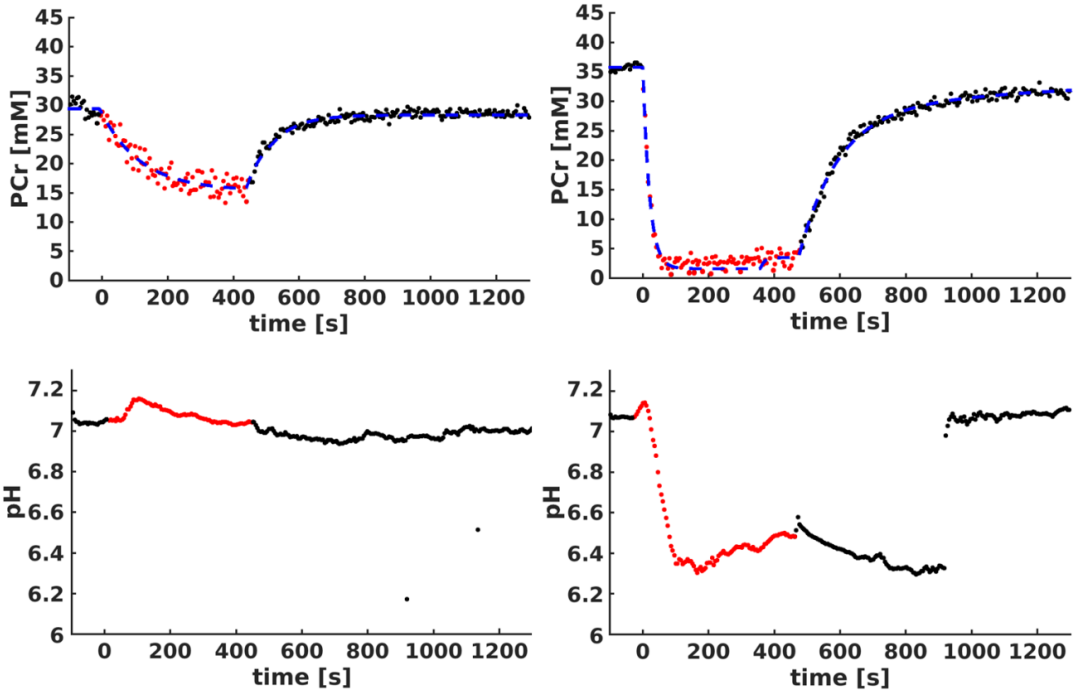
>600 s	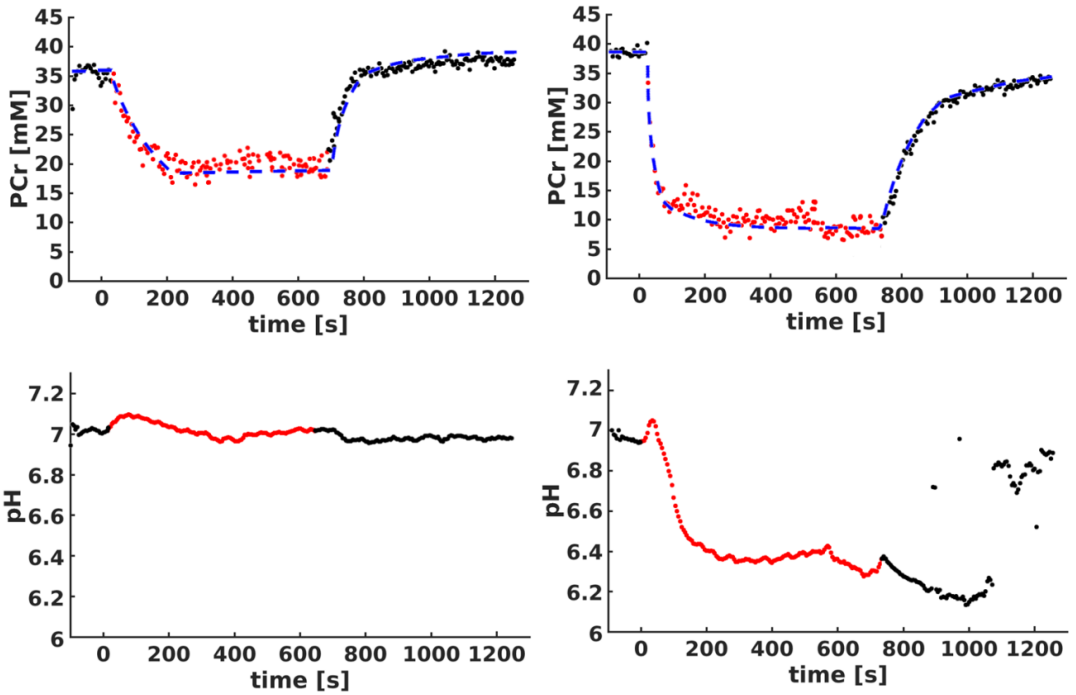

>600 s	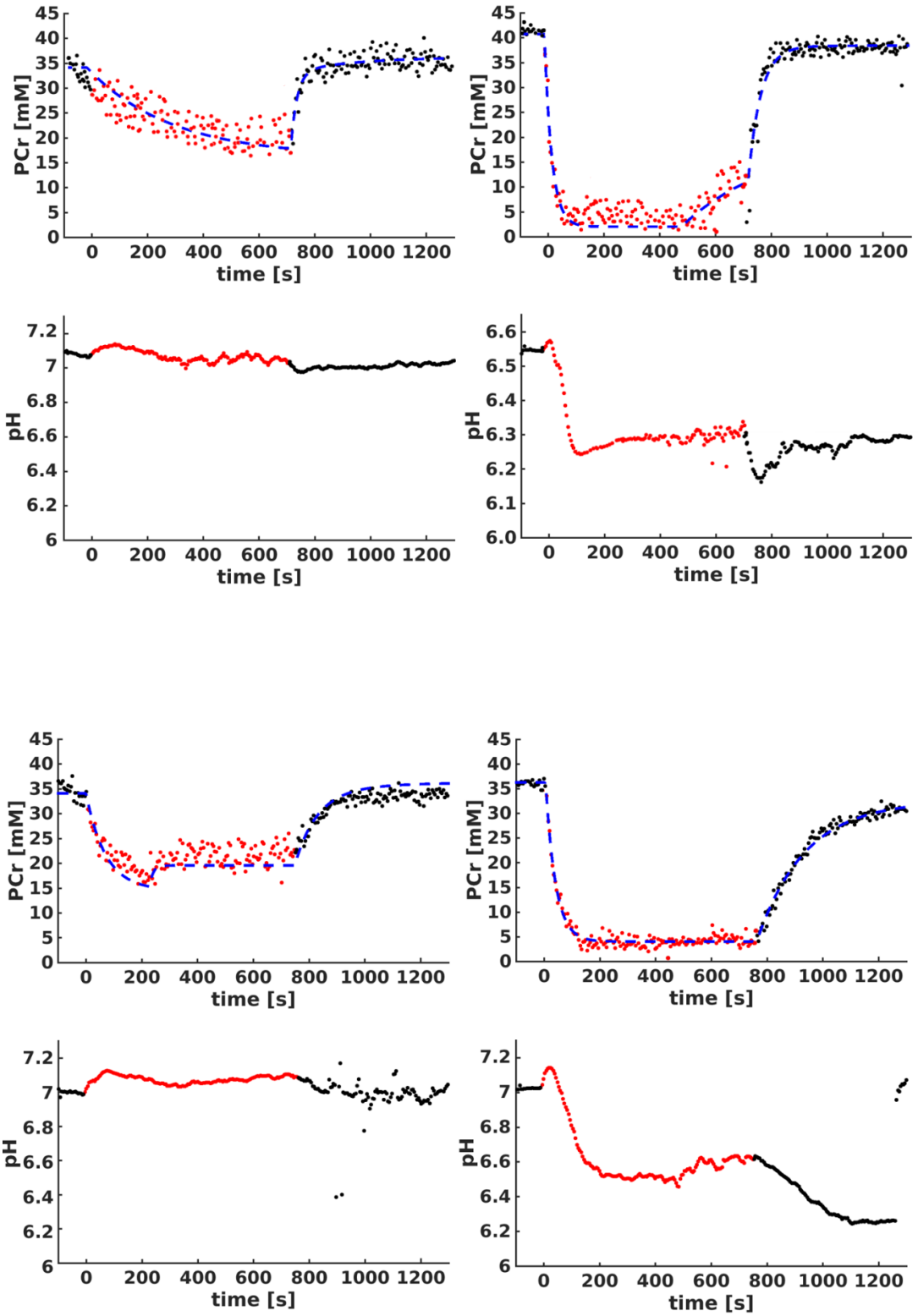 PCr [mM] time [s] pH time [s] PCr [mM] time [s] pH time [s] PCr [mM] time [s] pH time [s] PCr [mM] time [s] pH time [s]

Additional Figures for Chapter 5

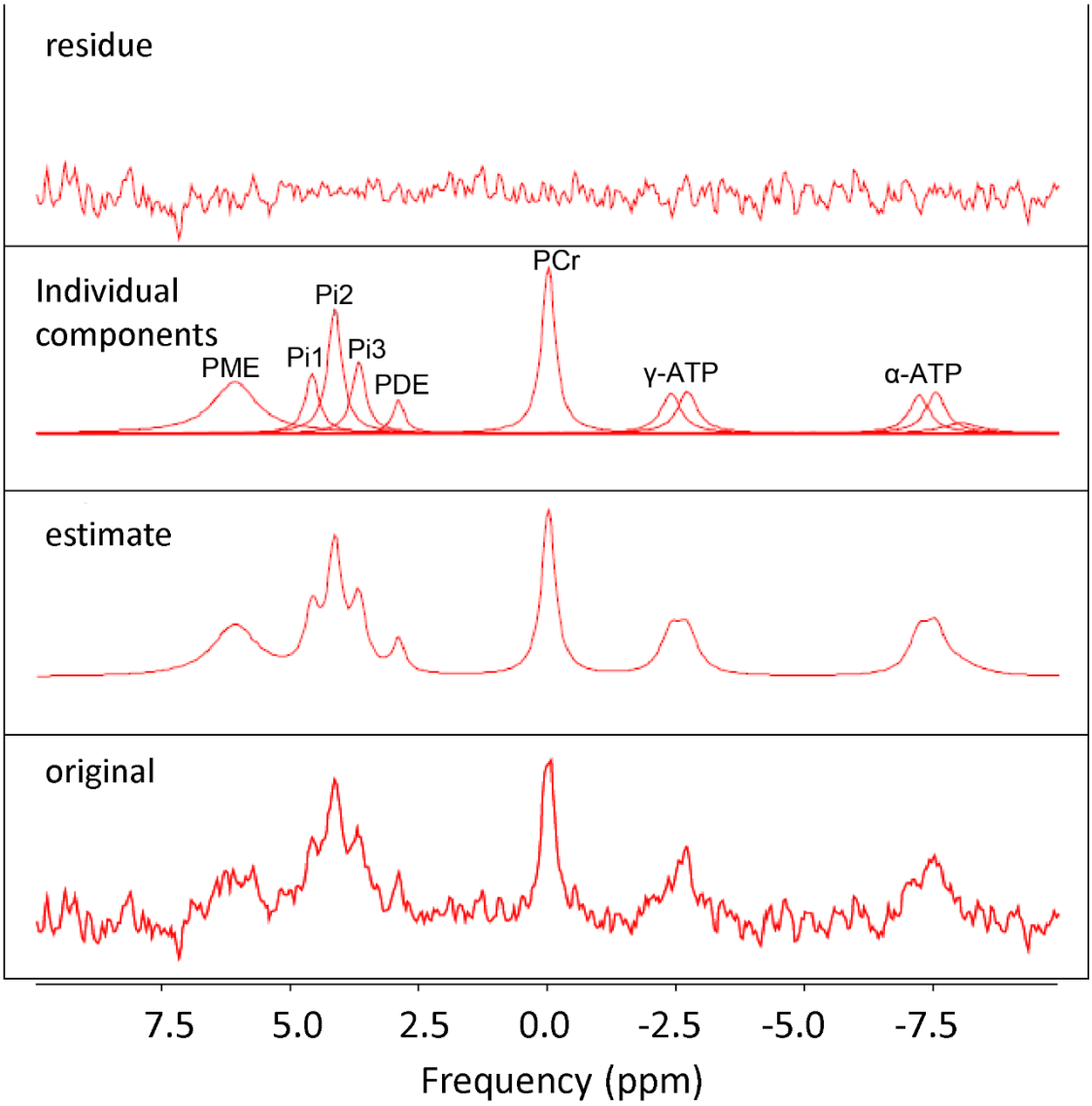

Fig S5-1 End-exercise spectrum of subject 1.

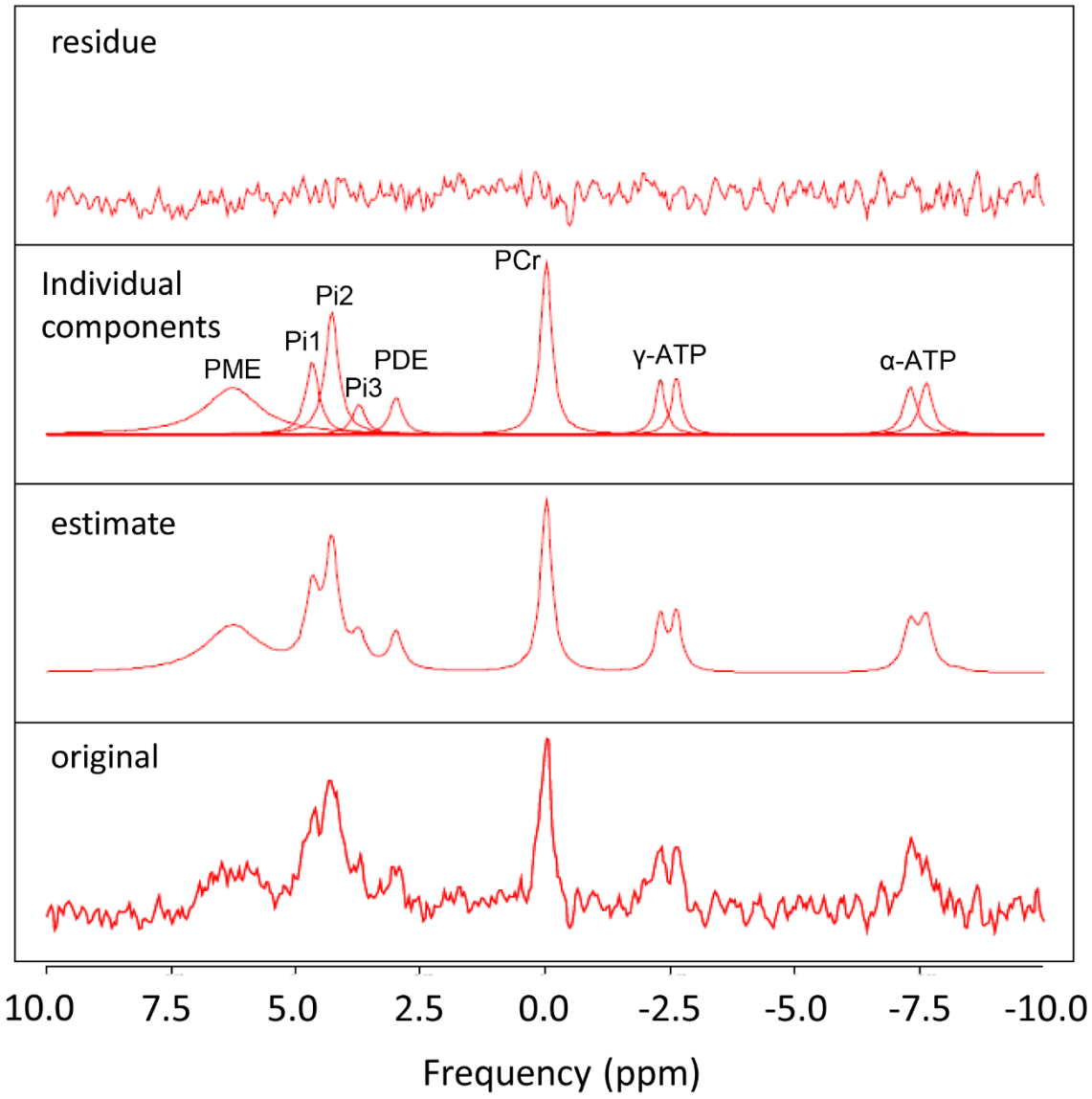

Fig S5-2 End-exercise spectrum of subject 2.

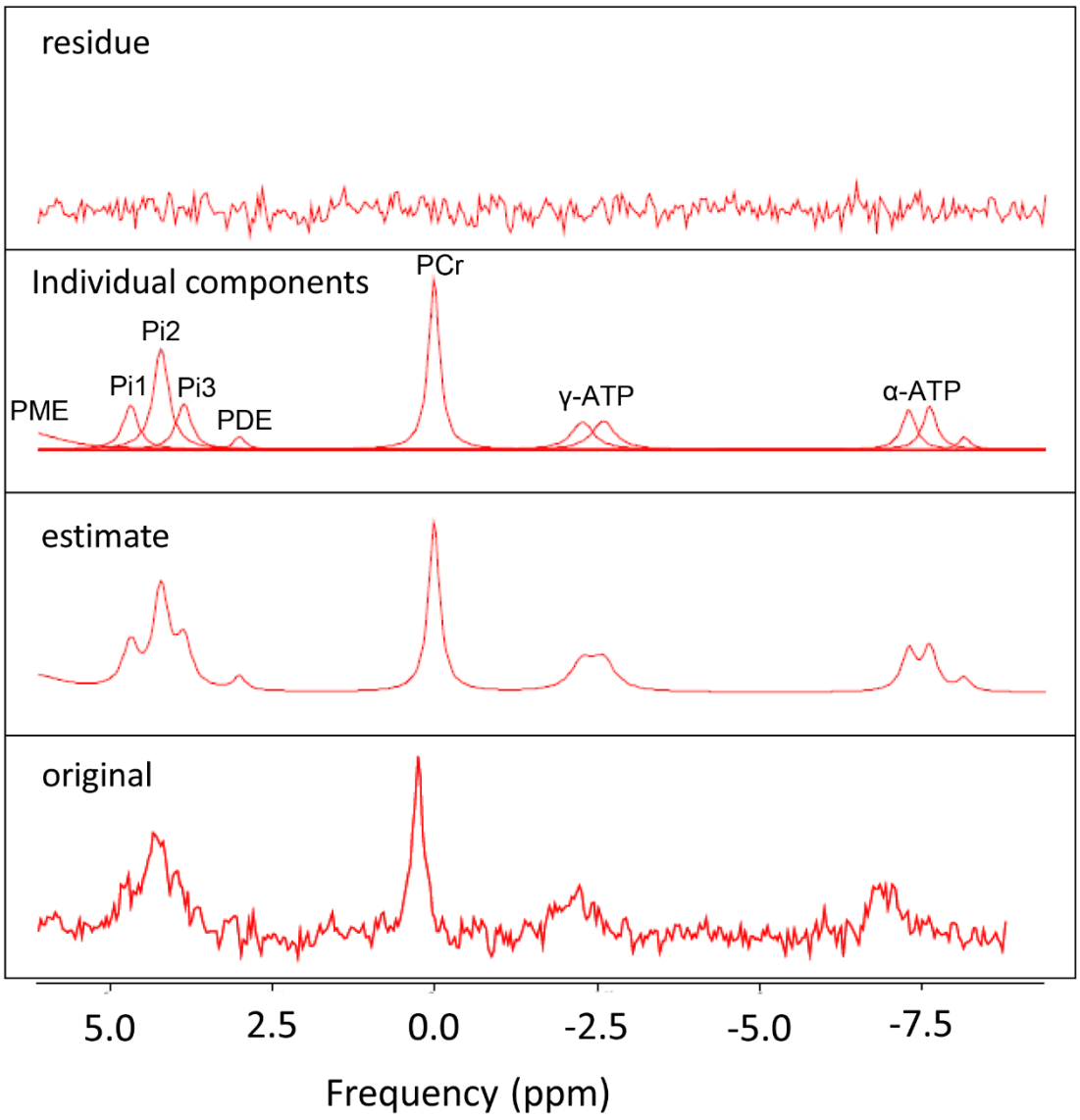

Fig S5-3 End-exercise spectrum of subject 3.

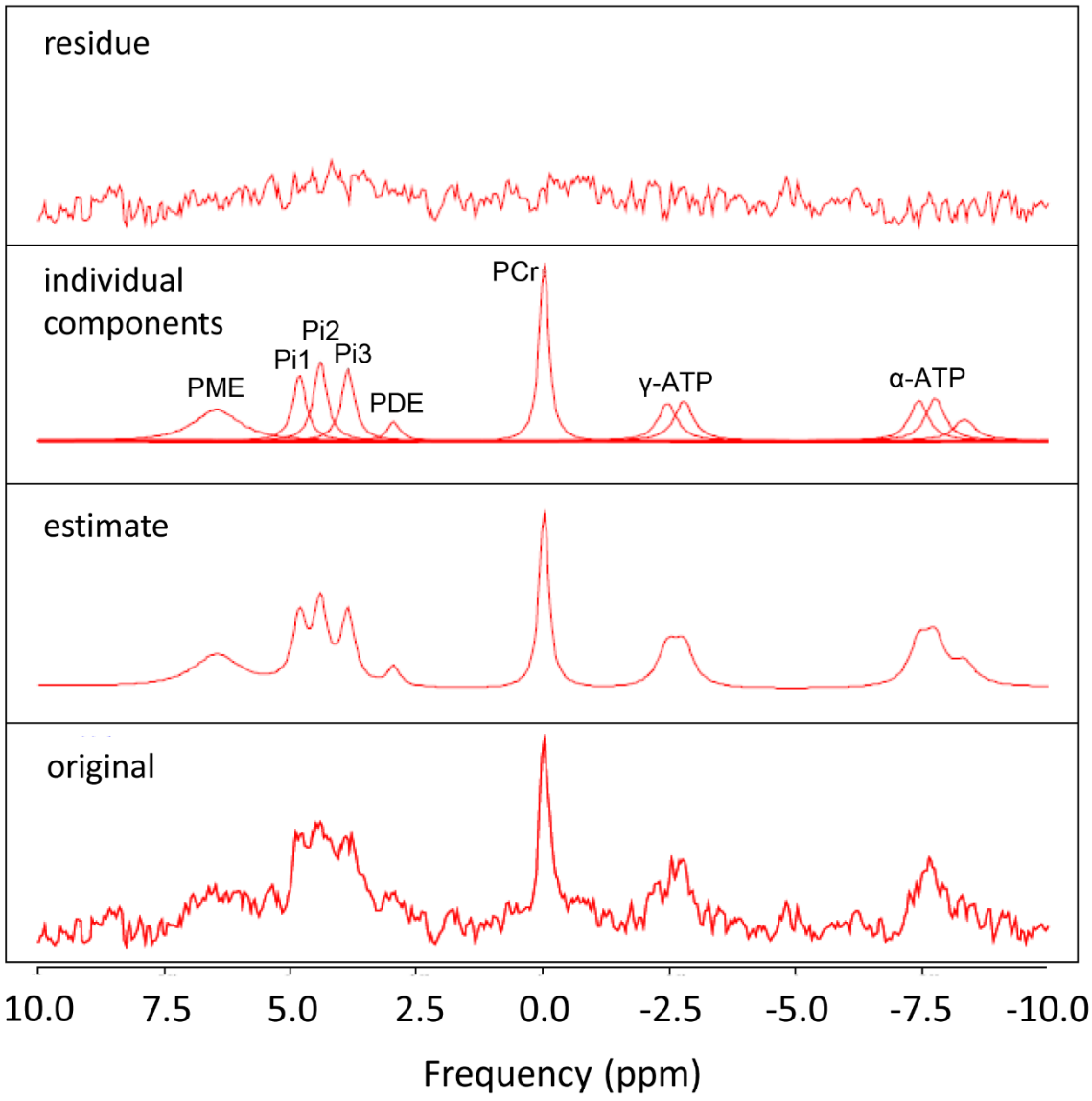

Fig S5-4 End-exercise spectrum of subject 4.

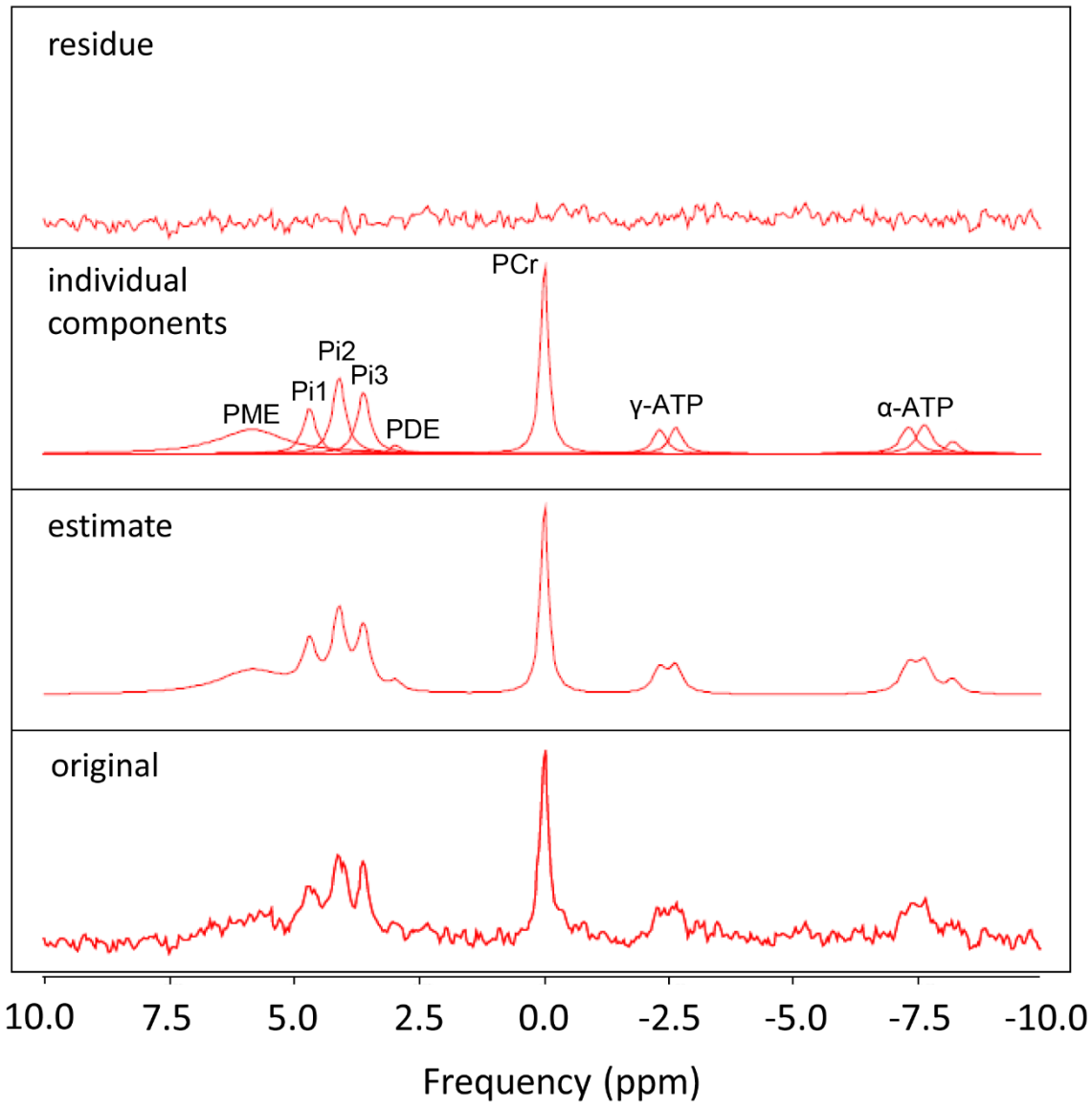

Fig S5-5 End-exercise spectrum of subject 5.

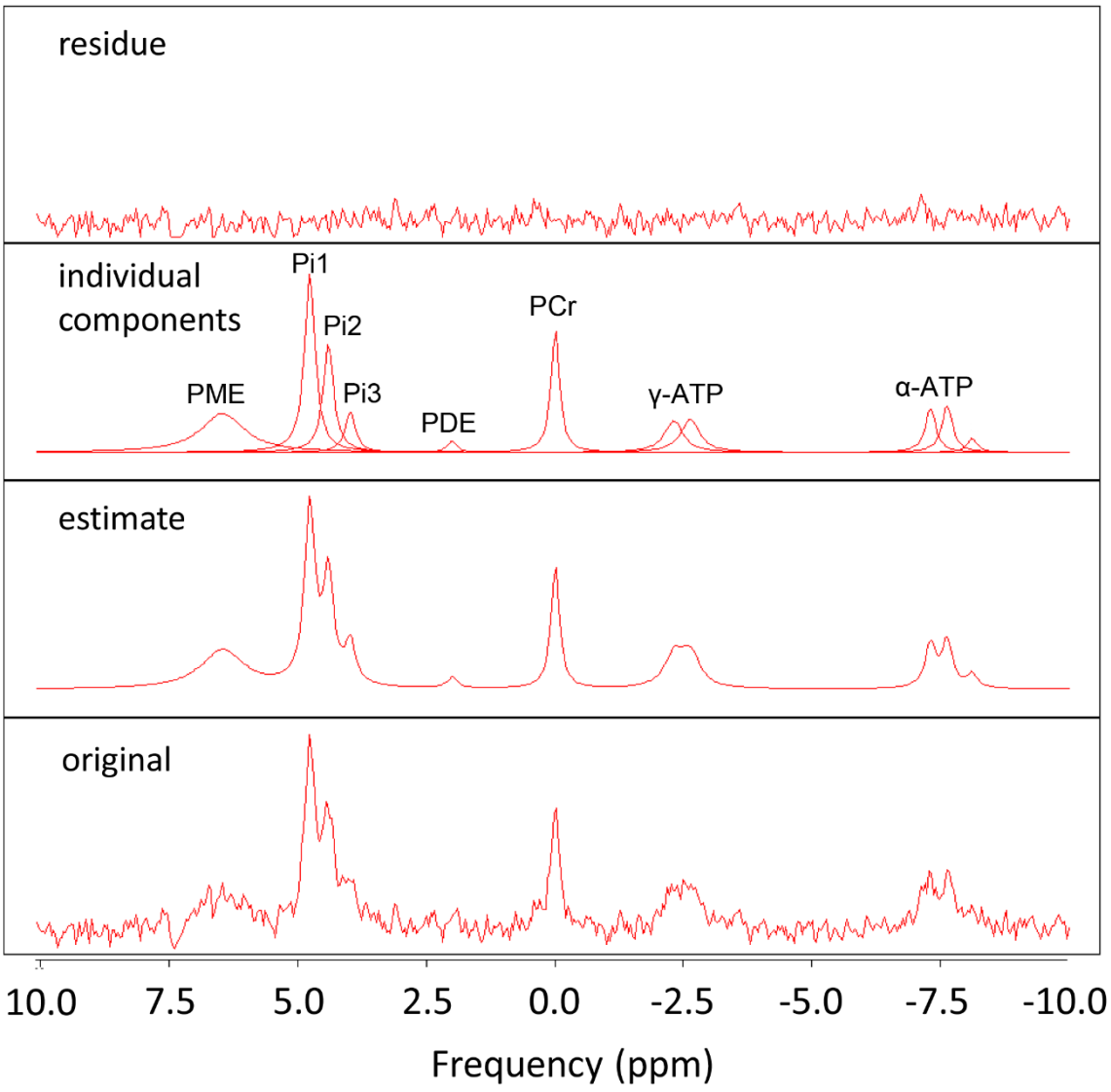

Fig S5-6 End-exercise spectrum of subject 6.

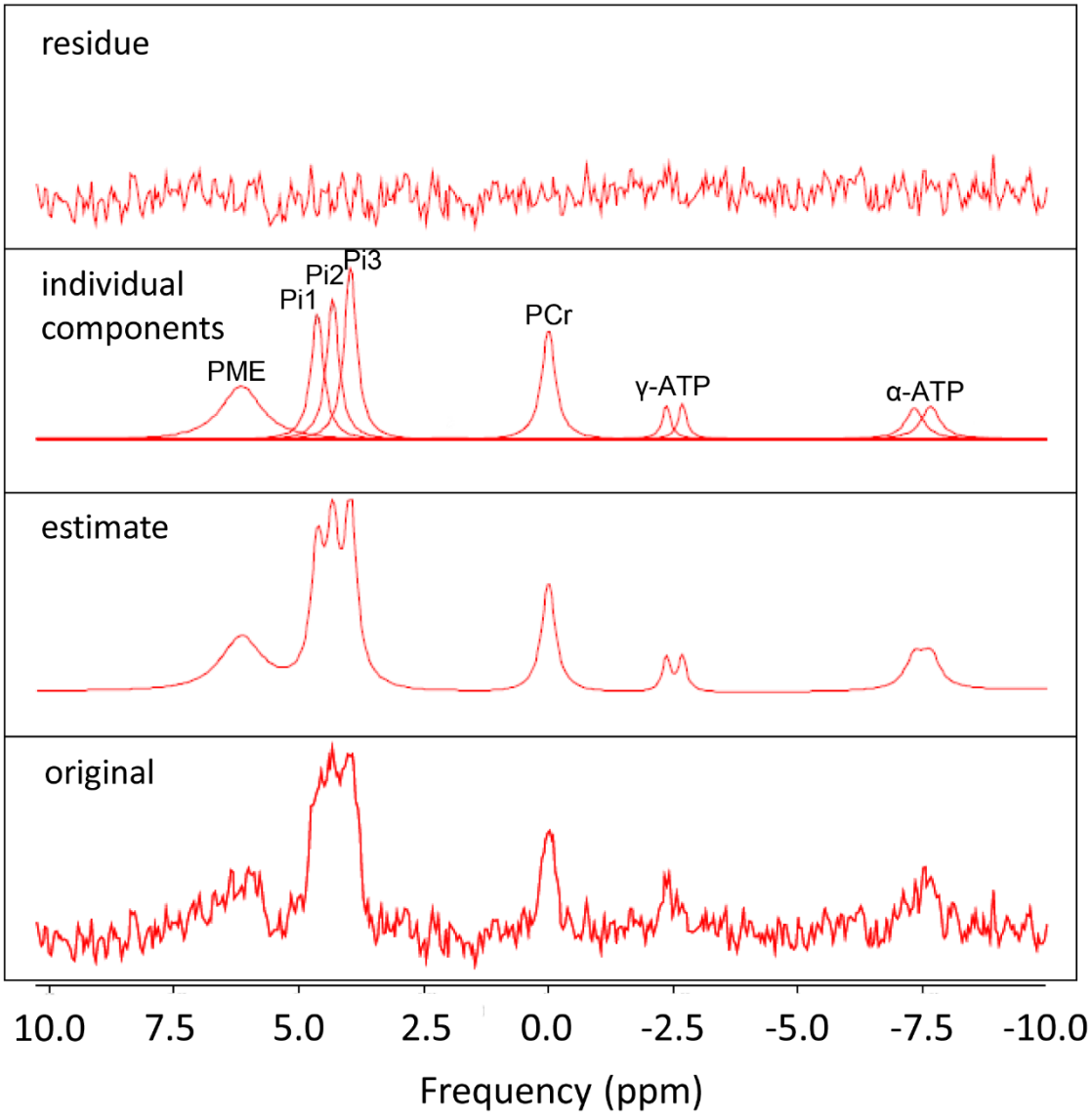

Fig S5-7 End-exercise spectrum of subject 7.

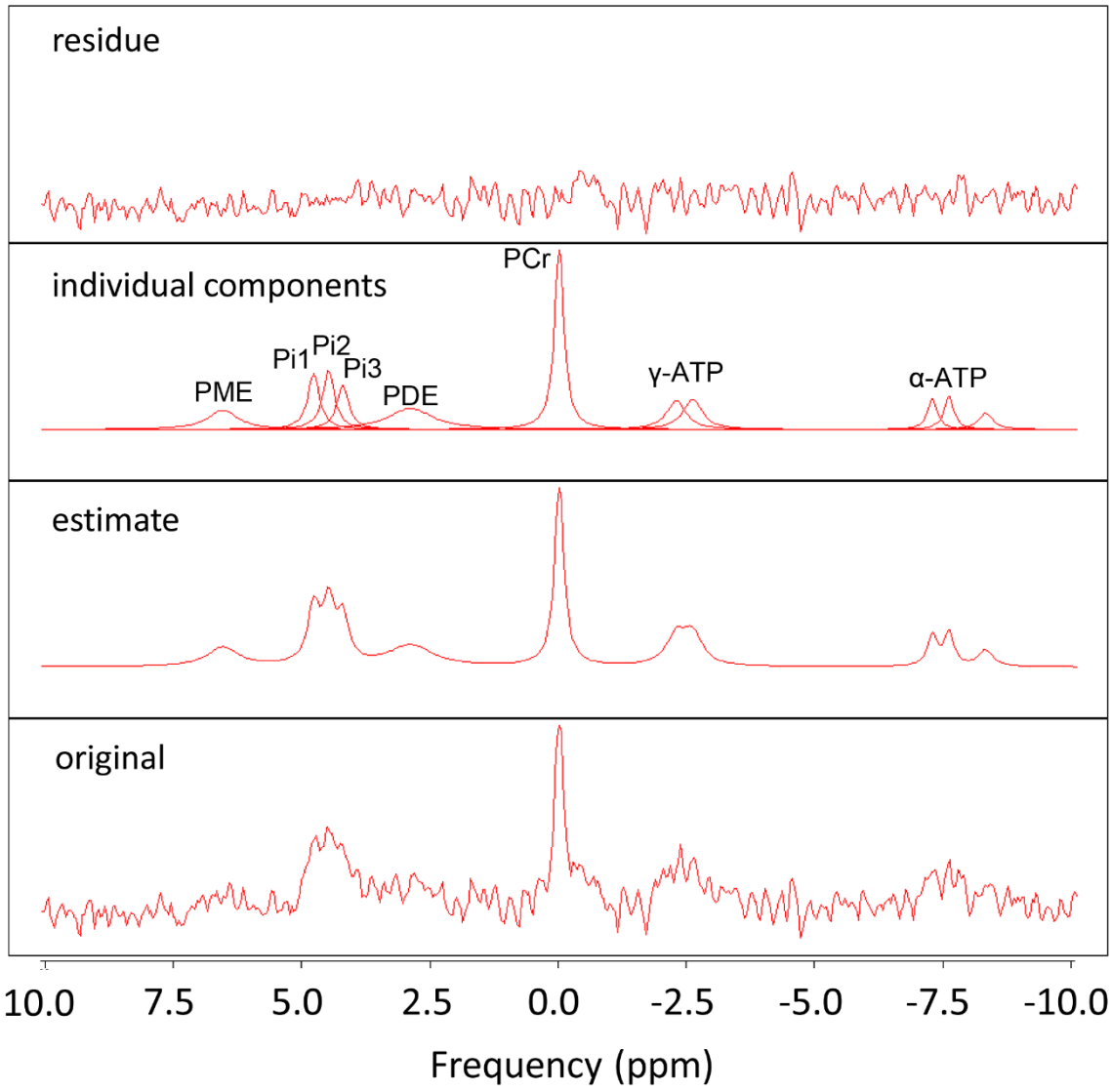

Fig S5-8 End-exercise spectrum of subject 8.

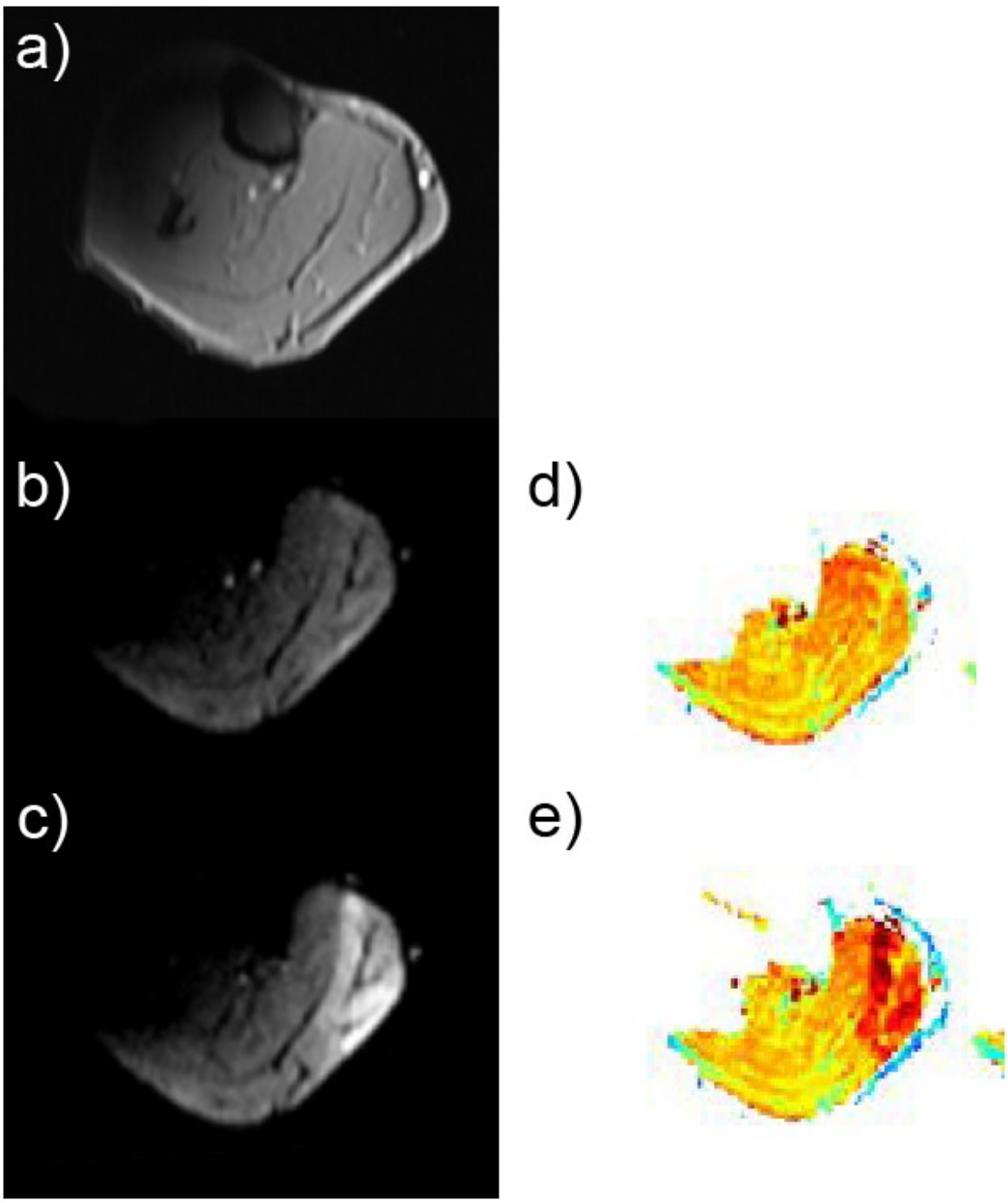

Fig S5-9 Visualization of the stimulated muscle area of subject 1 by signal changes between pre- and post-fatigue T2* weighted multiple gradient echo-planar images using the flex-coil (b, c) as well as by the T2*-differences in the calculated T2* maps (d, g). The morphological structures are visualized by a T1-image of the same slice (a).

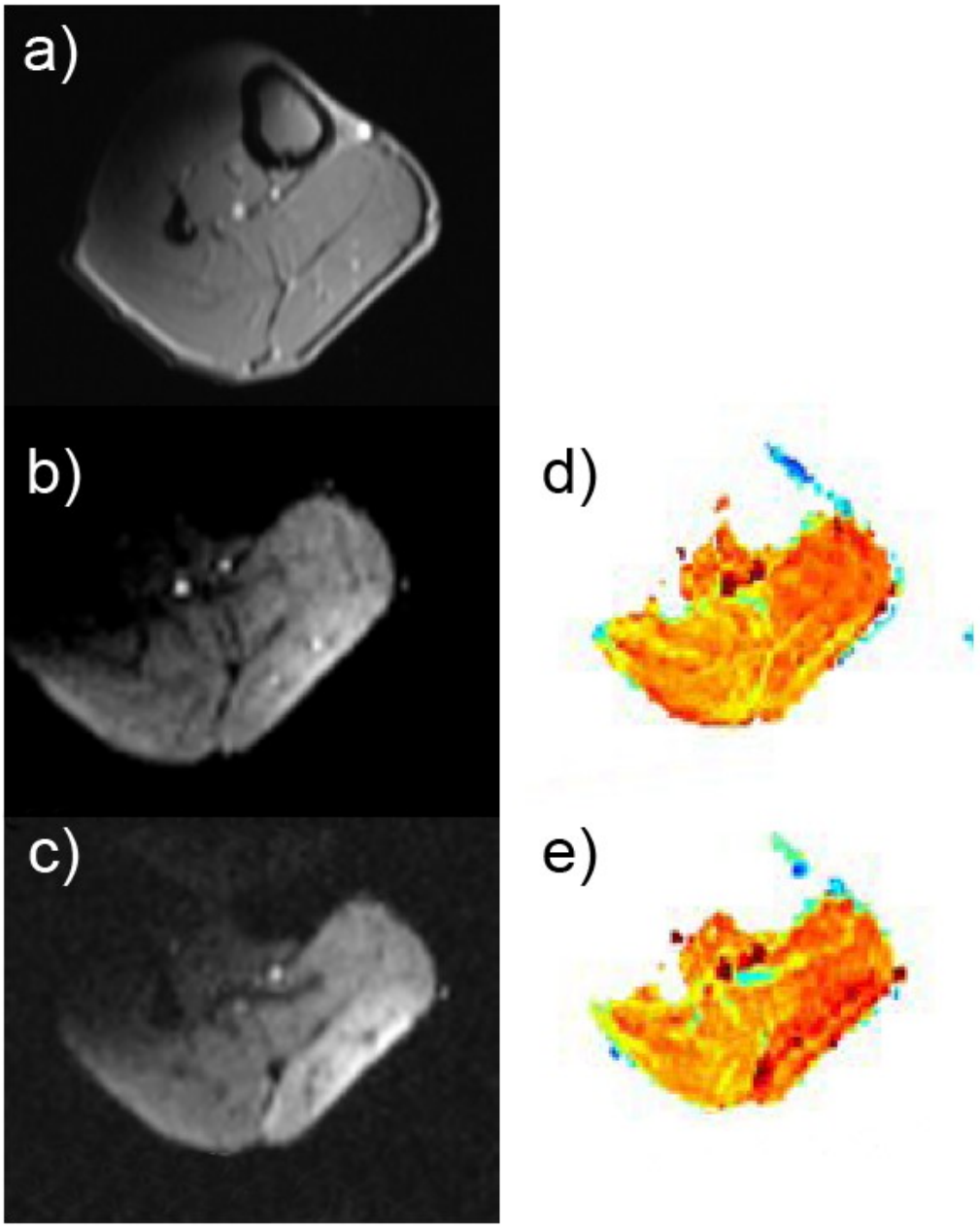

Fig S5-10 Visualization of the stimulated muscle area of subject 2 by signal changes between pre- and post-fatigue T2* weighted multiple gradient echo-planar images using the flex-coil (b, c) as well as by the T2*-differences in the calculated T2* maps (d, g). The morphological structures are visualized by a T1-image of the same slice (a).

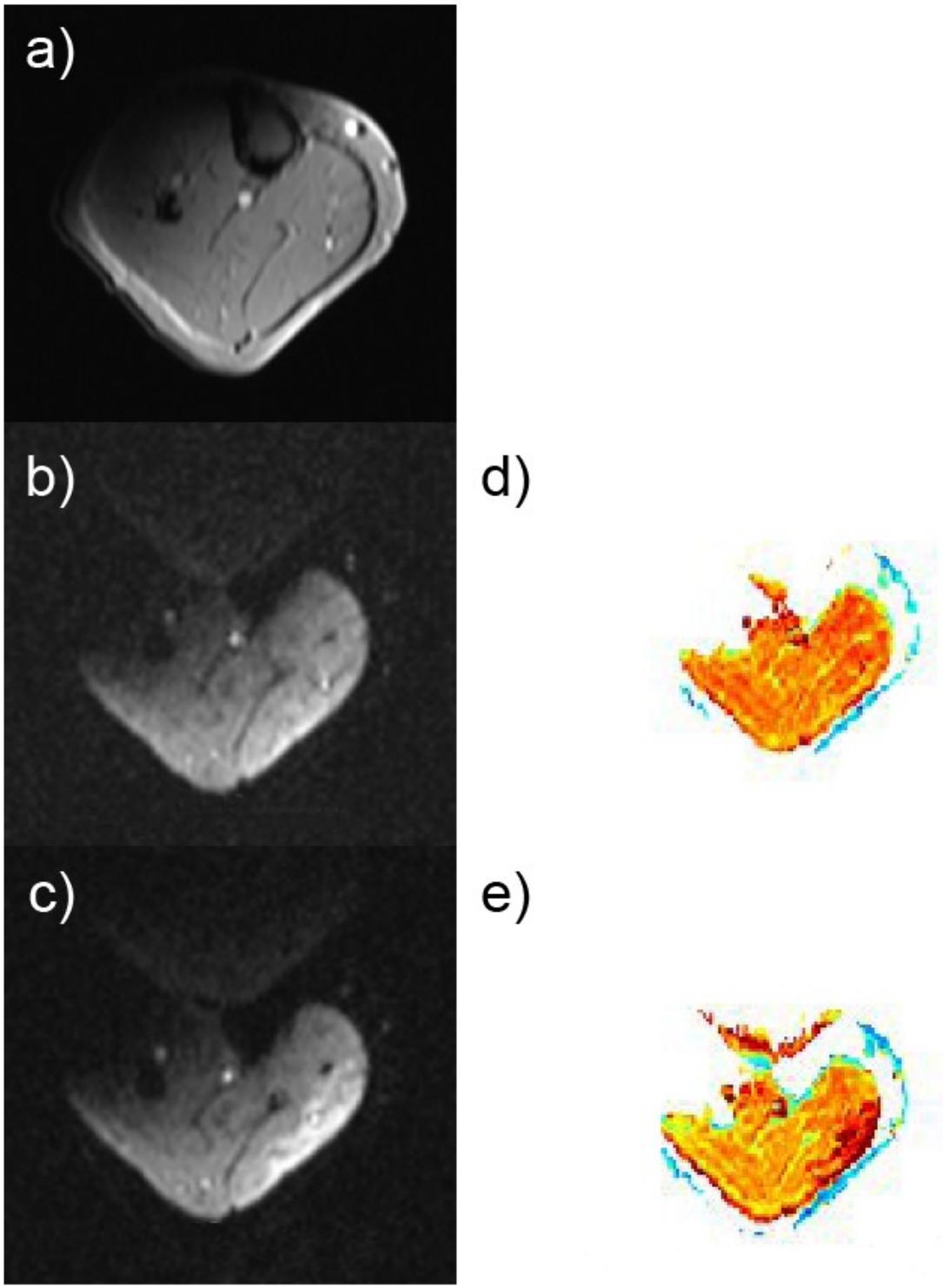

Fig S5-11 Visualization of the stimulated muscle area of subject 3 by signal changes between pre- and post-fatigue T2* weighted multiple gradient echo-planar images using the flex-coil (b, c) as well as by the T2*-differences in the calculated T2* maps (d, g). The morphological structures are visualized by a T1-image of the same slice (a).

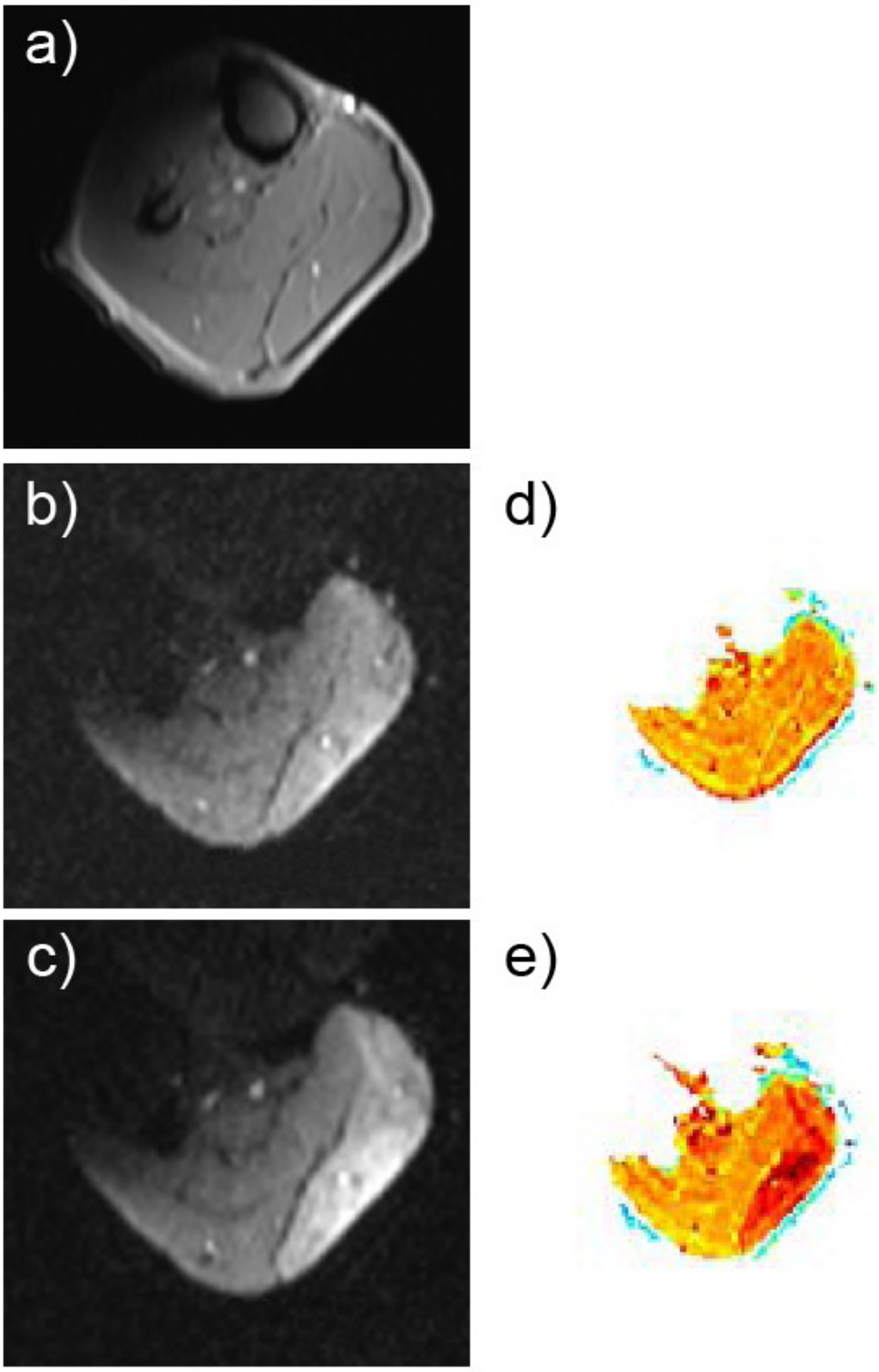

Fig S5-12 Visualization of the stimulated muscle area of subject 4 by signal changes between pre- and post-fatigue T2* weighted multiple gradient echo-planar images using the flex-coil (b, c) as well as by the T2*-differences in the calculated T2* maps (d, g). The morphological structures are visualized by a T1-image of the same slice (a).

Veröffentlichungen

Publikationen Zeitschriften (peer-reviewed)

- Müller R, **Tschiesche K**, Blickhan R. *Kinetic and kinematic adjustments during perturbed walking across visible and camouflaged drops in ground level.* Journal of Biomechanics, 2014; 47(10):2286-91.
- **Tschiesche K**, Rothamel M, Rzanny R, Gussew A, Hiepe P, Reichenbach JR. *MR-compatible pedal ergometer for reproducible exercising of the human calf muscle.* Medical Engineering & Physics. 2014; 36(7):933-7.
- Stutzig N, Rzanny R, **Moll K**, Gussew A, Reichenbach JR, Siebert T. *The pH heterogeneity in human calf muscle during neuromuscular electrical stimulation.* Magnetic Resonance in Medicine, 2016; 00:1-10.
- Stutzig N, Rzanny R, **Moll K**, Gussew A, Reichenbach JR, Siebert T. *Interpretation of pH-heterogeneity in human muscle induced by neuromuscular electrical stimulation.* Magnetic Resonance in Medicine, 2017; 77(2):466.
- **Moll K**, Gussew A, Hein C, Reichenbach JR. *Combined Spiroergometry and ^{31}P MRS of human calf muscle during high-intensity exercise.* NMR Biomedicine, 2017; 30(7):e3723.
- **Moll K**, Gussew A, Nisser M, Derlien S, Krämer M, Reichenbach JR. *Comparison of metabolic adaptions between endurance- and sprint-trained athletes in two different calf muscles using a multi-slice ^{31}P spectroscopic sequence.* NMR Biomedicine. Revision in process.

Buchartikel

- **Moll K**, Gussew A, Nisser M, Reichenbach JR. Ermüdungsbedingte Anpassungen im Energiestoffwechsel von unterschiedlich trainierten Athleten. In: Prävention von arbeitsbedingten Gesundheitsgefahren und Erkrankungen - 23. Erfurter Tage 2016. Grieshaber R, Stadeler M, Scholle HC (Publ), Verlag Bussert & Stadeler, Jena 2017, ISBN: 978-3-942115-45-2

Konferenzbeiträge

- **Tschiesche K**, Rothamel M, Gussew A, Hiepe P, Rzanny R, Reichenbach JR. Validierung eines Pedalergometers für standardisierte ^{31}P-MR spektroskopische Untersuchungen belastungsinduzierter Änderungen im Energiestoffwechsel der Wadenmuskulatur. 16. Jahrestagung der Deutschen Sektion der ISMRM, 19.-20. September 2013, Freiburg, Germany.
- **Tschiesche K**, Gussew, P, Rzanny R, Reichenbach JR. Simultane Bestimmung ventilatorischer und energiemetabolischer Parameter während der Belastung der Wadenmuskulatur im MRT. 17. Jahrestagung der Deutschen Sektion der ISMRM, 25.-26. September 2014, Jena, Germany.

- Rzanny R, Hiepe P, **Tschiesche K**, Gussew A, Stutzig N, Reichenbach JR. Effekte der EMS des Wadenmuskels auf Energiestoffwechsel, T2-Relaxation und die erzeugte Pedalkraft. Abstraktband der 17. Jahrestagung der Deutschen Sektion der ISMRM, 25.-26. September 2014, Jena, Germany.
- **Tschiesche K**, Gussew A, Glöckner M, Derlien S, Reichenbach JR. Multimodal determination of load changes in the muscle - A combination of ^{1}H MEGA-PRESS and blood sampling. 23th Annual Meeting of the International Society for Magnetic Resonance in Medicine, 30 May – 05 June 2015, Toronto, Canada. Posterpräsentation und eingeladener Vortrag zum Musculoskeletal Study Group Meeting
- **Tschiesche K**, Rothamel M, Rzanny R, Gussew A, Hiepe P, Reichenbach JR. Improvements in the reproducible exercising of the human calf muscle using a MR compatible pedal ergometer. 23th Annual Meeting of the International Society for Magnetic Resonance in Medicine, 30 May – 05 June 2015, Toronto, Canada.
- **Tschiesche K**. Simultane Bestimmung ventilatorischer und energiemetabolischer Parameter während der Belastung der Wadenmuskulatur im MRT. 6. Doktorandenkolloquium des Institutes für Sportwissenschaft J-DOKS 2015, 09.02.2015, Jena.
- **Tschiesche K**, Gussew A, Glöckner M, Derlien S, Reichenbach JR. Direkte Messung belastungsinduzierter Muskellaktatänderungen mit ^{1}H MR Spektroskopie. 21. Tagung der AKP, 02.-03.10.2015, Jena.
- **Tschiesche K**, Gussew A, Hein C, Reichenbach JR. Belastungsinduzierte Akquisition spirometrischer und ^{31}P MR spektroskopischer Parameter. 21. Tagung der AKP, 02.-03.10.2015, Jena.
- **Tschiesche K**, Gussew A, Hein C, Reichenbach JR. Belastungsinduzierte Akquisition spirometrischer und spektroskopischer Parameter. 46. Jahrestagung der DGMP, 09.-12.09.2015, Marburg.
- **Tschiesche K**. MR-Muskelspektroskopie und Spiroergometrie: Einfluss belastungsinduzierter, metabolischer Änderungen des Einzelmuskels auf die Gesamtkörperphysiologie. 7. Doktorandenkolloquium des Institutes für Sportwissenschaft J-DOKS 2015, 11.12.2015, Jena.
- **Tschiesche K**, Gussew A, Hein C, Reichenbach JR. Combined Spiroergometrie and ^{31}P MRS in human calf muscle during high intense exercise. 24th Annual Meeting of the International Society for Magnetic Resonance in Medicine, 07.–13.05.2016, Singapore. (Auszeichnung des Beitrages mit dem ISMRM Merit Award Summa cum Laude)
- **Moll K**, Gussew A, Stutzig N, Rzanny R, Reichenbach JR. Funktionelle Muskeluntersuchungen mit MR-Spektroskopie: Neue Sequenzen und Modelle. KIP-Konferenz, 27.06.2016, Jena.
- **Moll K**, Gussew A, Reichenbach JR. ^{31}P-MR spectroscopic investigation of effects of post exercise cramps on high energy metabolism in human calf muscle. 47. Jahrestagung der DMPG & 19. Jahrestagung der DS-ISMRM, Würzburg, 07.-10.09.2016, Würzburg.
- **Moll K**, Gussew A, Nisser M, Reichenbach JR. MR-Muskelspektroskopie und Spiroergometrie - Einfluss belastungsinduzierter, metabolischer Änderungen des Einzelmuskels auf die Gesamtkörperphysiologie. Forschungskolloquium des Institutes für Physiotherapie am Universitätsklinikum Jena, 04.10.2016, Jena.
- **Moll K**, Gussew A, Nisser M, Reichenbach JR. Ermüdungsbedingte Anpassungen im Energiestoffwechsel bei unterschiedlich trainierten Athleten. 23. Erfurter Tage, Erfurt, 01.12.2016, Erfurt.

- **Moll K**, Gussew A, Nisser M, Reichenbach JR. Vergleich metabolischer Anpassungen zwischen Ausdauerathleten und Sprintern anhand zweier Muskeln. 8. Doktorandenkolloquium des Institutes für Sportwissenschaft der FSU Jena - J-DOKS, Jena, 02.12.2016, Jena.
- **Moll K**. ^{31}P MR-spektroskopische Untersuchung des muskulären Energiestoffwechsels. CME Fortbildung im Institut für Diagnostische und Interventionelle Radiologie des UKJ, 15.03.2017, Jena.
- **Moll K**, Gussew A, Reichenbach JR. Influence of muscle fiber-tension on ^{31}P MRS recovery parameter after intense exercise. 25th Annual Meeting of the International Society for Magnetic Resonance in Medicine, 22.–27.04.2017, Honolulu, Hawaii.
- **Moll K**, Gussew A, Nisser, M, Derlien S, Reichenbach JR. Effects of Load-induced Metabolic Changes of a Single Muscle on Whole Body Physiology. 25th Annual Meeting of the International Society for Magnetic Resonance in Medicine, 22.–27.04.2017, Honolulu, Hawaii.
- **Moll K**, Gussew A, Nisser M, Krämer M, Reichenbach JR. Comparison of Metabolic Adaptions between Endurance- and Sprint-trained Athletes in Two Different Muscles using a ^{31}P Spectroscopic Multi-Slice Sequence. 25th Annual Meeting of the International Society for Magnetic Resonance in Medicine, 22.–27.04.2017, Honolulu, Hawaii.
- **Moll K**, Gussew A, Reichenbach JR. Belastungsinduzierte Anpassungen im Energiestoffwechsel bei Probanden unterschiedlicher Trainingsausrichtung. KIP-Konferenz, 26.06.2017, Jena.

Auszeichnungen

- Landesgraduiertenstipendium der Friedrich-Schiller Universität Jena zur Förderung eines Promotionsvorhabens mit dem Thema „MR-Muskelspektroskopie und Spiroergometrie: Einfluss belastungsinduzierter Stoffwechseländerungen im Einzelmuskel auf die Ganzkörperphysiologie – eine Gegenüberstellung globaler und lokaler physiologischer Parameter". Förderungszeitraum März 2014 - März 2017
- DAAD Auslandsstipendium für den Aufenthalt an der University of Liverpool – Department of Musculoskeletal Biology unter der Leitung von Prof. G. Kemp, März 2015 - Juni 2015.
- 2. Platz für den Vortrag auf dem Musculoskeletal Study Group Meeting mit dem Titel "Multimodal determination of load changes in the muscle - A combination of ^{1}H MEGA-PRESS and blood sampling" im Rahmen des 23th Annual Meeting of the International Society for Magnetic Resonance in Medicine, 30 Mai – 05 Juni 2015, Toronto, Kanada
- ISMRM Merit Award Magna cum Laude, " Multimodal determination of load changes in the muscle - A combination of ^{1}H MEGA-PRESS and blood sampling." im Rahmen des 23th Annual Meeting of the International Society for Magnetic Resonance in Medicine, 30 Mai – 05 Juni 2015, Toronto, Kanada
- ISMRM Merit Award Summa cum Laude, "Combined Spiroergometrie and ^{31}P MRS in human calf muscle during high intense exercise.." im Rahmen des 24th Annual Meeting of the International Society for Magnetic Resonance in Medicine, 07. – 13. Mai 2016, Singapur
- ISMRM Merit Award Summa cum Laude, „Effects of Load-Induced Metabolic Changes of a Single Muscle on Whole Body Physiology" im Rahmen des 25th Annual Meeting of the International Society for Magnetic Resonance in Medicine, 22. – 27. April 2017, Honolulu, Hawaii

Selbstständigkeitserklärung

Hiermit erkläre ich, dass mir die geltende Promotionsordnung der Fakultät für Sozial- und Verhaltenswissenschaft der Friedrich-Schiller Universität Jena bekannt ist und dass ich die Dissertation angefertigt und alle von mir benutzen Hilfsmittel, persönliche Mitteilungen und Quellen in meiner Arbeit angegeben habe. Weiterhin erkläre ich, dass mich keine Personen bei der Auswahl und Auswertung des Materials unterstützt haben.

Mit Ausnahme der Kapitel 1, 6 und 7 sind die Kapitel 2-5 der vorliegenden Dissertation in internationalen wissenschaftlichen Zeitschriften publiziert. Am publizierten Anteil waren die Autoren in folgender Weise beteiligt:

Kevin Moll, M.A. Sportwiss.
Medizinische Physik, Institut für Diagnostische und Interventionelle Radiologie Universitätsklinikum Jena
Initiierung, Durchführung, Auswertung und Interpretation der Ergebnisse sowie das Anfertigen des Manuskriptes (Kapitel 2-4).
Unterstützung bei der Durchführung, Auswertung, Interpretation von Ergebnissen und dem Anfertigen des Manuskriptes (Kapitel 5).

Alexander Gussew, Dr. Ing.
Medizinische Physik, Institut für Diagnostische und Interventionelle Radiologie Universitätsklinikum Jena
Unterstützung bei den MRT-Messungen (Kapitel 2-5), der Implementierung der genutzten MRT-Sequenzen, der Interpretation von Ergebnissen der gesamten Arbeit und dem Anfertigen der Manuskripte (Kapitel 2-5).

Reinhard Rzanny, Dr. rer. nat.
Medizinische Physik, Institut für Diagnostische und Interventionelle Radiologie Universitätsklinikum Jena
Unterstützung bei den MRT-Messungen mit dem Pedalergometer sowie dessen Verbesserung, der Interpretation von Ergebnissen und dem Anfertigen des Manuskriptes (Kapitel 2).
Unterstützung bei der Durchführung, Auswertung und Interpretation der Ergebnisse sowie das Anfertigen des Manuskriptes (Kapitel 5).

Patrick Hiepe, Dipl. Ing.
Medizinische Physik, Institut für Diagnostische und Interventionelle Radiologie Universitätsklinikum Jena
Unterstützung bei den MRT-Messungen mit dem Pedalergometer sowie dessen Verbesserung, der Interpretation von Ergebnissen und dem Anfertigen des Manuskriptes (Kapitel 2).

Markus Rothamel, B. Eng.
Medizinische Physik, Institut für Diagnostische und Interventionelle Radiologie Universitätsklinikum Jena
Unterstützung bei der Verbesserung des Pedalergometers und der Aufnahme und Auswertung mechanischer Parameter.

Christian Hein
Ganshorn Medizin Electronic GmbH, Niederlauer, Deutschland
Unterstützung bei der Anpassung der Spirometrie Einheit PowerCube (Kapitel 3).

Norman Stutzig, Dr. phil.
Abteilung für Bewegungs- und Trainingswissenschaft, Universität Stuttgart
Unterstützung bei der Verbesserung des Pedalergometers, der Interpretation von Ergebnissen und dem Anfertigen des Manuskriptes (Kapitel 3).
Initiierung, Durchführung der NMES Messungen, Auswertung und Interpretation der NMES Ergebnisse sowie das Anfertigen des Manuskriptes (Kapitel 5).

Maria Nisser, Dipl. Sportwiss.
Institut für Physiotherapie, Universitätsklinikum Jena
Unterstützung bei der Durchführung der Blutlaktatmessungen, Interpretation der Ergebnisse (Kapitel 4).

Steffen Derlien, Dr. phil.
Institut für Physiotherapie, Universitätsklinikum Jena
Unterstützung bei der Durchführung der Blutlaktatmessungen, Interpretation der Ergebnisse (Kapitel 4)

Martin Krämer, Dr. rer. nat.
Medizinische Physik, Institut für Diagnostische und Interventionelle Radiologie Universitätsklinikum Jena
Unterstützung bei der Entwicklung der MUSCLE Sequenz

Tobias Siebert, Prof. Dr. phil. habil.
Abteilung für Bewegungs- und Trainingswissenschaft, Universität Stuttgart
Unterstützung bei der Interpretation der Ergebnisse und dem Anfertigen des Manuskriptes (Kapitel 5).

Jürgen R. Reichenbach, Prof. Dr. rer. nat med. habil.
Medizinische Physik, Institut für Diagnostische und Interventionelle Radiologie Universitätsklinikum Jena
Unterstützung bei der Interpretation der Ergebnisse und dem Anfertigen aller Manuskripte (Kapitel 2-5)

Ferner erkläre ich, dass ich nicht die Hilfe eines Promotionsberaters in Anspruch genommen habe und dass Dritte weder unmittelbar noch mittelbar geldwerte Leistungen von mir für Arbeiten erhalten haben, die im Zusammenhang mit dem Inhalt der vorgelegten Dissertation stehen.

Die Dissertation wurde noch nicht als Prüfungsarbeit für eine staatliche oder andere wissenschaftliche Prüfung eingereicht und keiner gleiche, ähnliche oder andere Abhandlung bei einer anderen Hochschule als Dissertation eingereicht. Ich versichere, nach bestem Wissen die reine Wahrheit gesagt und nichts verschwiegen zu haben.

Jena, Oktober 2017 Kevin Moll